University of Salerno
Department of Chemistry and Biology "A. Zambelli"

and

University of Basilicata
Department of Science

Ph.D. in Chemistry

Cycle XXXI 2015-2018

Thesis on

PHARMACOLOGICAL POTENTIAL AND PHYTOCHEMICAL PROFILE OF THREE UNEXPLORED MEDICINAL PLANTS

Ph.D. Student: Immacolata Faraone
Matriculation number 8800100013

TUTOR
Prof. Lucia Chiummiento

CO-TUTOR
Prof. Luigi Milella

COORDINATOR
Prof. Gaetano Guerra

Academic Year 2017/2018

To my husband, my parents and my sister:
my strength, my daily encouragement, my everything

A mio marito, i miei genitori e mia sorella:
la mia forza, il mio incoraggiamento quotidiano, il mio tutto

Tieniti stretta la tua determinazione,
ti porterà lontano…
…ma non farla diventare a senso unico,
non far prevalere l'ambizione sugli affetti.
Le persone e i sentimenti sono le cose che contano davvero!
(*Anonimo*)

"I never am really satisfied that I understand anything;
because, understand it well as I may, my comprehension can only be an
infinitesimal fraction of all I want to understand"
Ada Lovelace

SUMMARY

LIST OF FIGURES

LIST OF TABLES

PERFORMED ACTIVITIES

COURSES FOLLOWED in 2015/2016:

1. Chimica delle sostanze organiche naturali - Prof. L. Chiummiento – University of Basilicata, Potenza, Italy.

COURSES FOLLOWED in 2016/2017:

1. Metodi Spettroscopici per lo Studio delle Molecole Bioattive – Prof. A. Pepe – University of Basilicata, Potenza, Italy;
2. Applicazione della spettrometria di massa per l'analisi di metaboliti di interesse alimentare e ambientale – Prof. F. Lelario – University of Basilicata, Potenza, Italy;
3. Trasferimento tecnologico: dalla ricerca alla creazione di impresa – Prof. P. Argoneto - University of Basilicata, Potenza, Italy;
4. English course B1 – Prof. Larry Adeyanju - University of Basilicata, Potenza, Italy;
5. Corso di formazione tecnico pratico per consulente per l'igiene degli alimenti e gestione del sistema H.A.C.C.P. - Napoli, Italy, 24-26 Maggio 2017.

COURSES FOLLOWED in 2017/2018:

1. Applicazione della spettrometria di massa per l'identificazione e la quantificazione di sostanze di interesse alimentare e ambientale – Prof. Sabino A. Bufo, Giuliana Bianco, Filomena Lelario, Raffaella Pascale - University of Basilicata, Potenza, Italy;

PARTICIPATION IN NATIONAL AND INTERNATIONAL CONGRESSES:

1. 24-29 November 2018. *"30th International Symposium on the Chemistry of Natural Products and the 10th International Congress on Biodiversity (ISCNP30 & ICOB10)"* Athens (Greece);

2. 12-13 November 2018. *"III Edition Green Extraction of Natural Products (GENP 2018)"* Bari (Italy);
3. 26-28 September 2018. *"2nd Conference on Food Bioactives & Health (FBHC 2018)"* Lisbon (Portugal);
4. 20-22 September 2018. *"Heroes 2018"* Maratea (Italy);
5. 12-15 September 2018. *"113° Congresso della Società Botanica Italiana and V International Plant Science Conference (IPSC)"* Fisciano (Italy);
6. 26-31 August 2018. *"XXII International Mass Spectrometry Conference (IMSC 2018)"* Firenze (Italy);
7. 30 June-1 July 2018. *"Botanicum, quando le erbe servono a curare e non solo… IX Convegno Filiera Lucana Piante Officinali, JuvenoLogia"* Castelluccio Superiore (Italy);
8. 21-23 June 2018. *"Valorizzazione della costa, protezione, governance ed ecoturismo, Gruppo Nazionale per la Ricerca sull'Ambiente Costiero (GNRAC)"* Matera (Italy);
9. 4-7 March 2018. *"Eco-Bio2018"* Dublin (Ireland);
10. 18-20 October 2017. *"3 MS BioPharma School, Practical training on applications of mass spectrometry in biopharma at TLS and GSK laboratories"* Siena (Italy);
11. 14-15 October 2017. *"Botanicum: Convegno di Botanica Farmaceutica e Fitoterapia, Corso di riconoscimento ed uso di piante officinali, Antiage & Longevità"* Potenza (Italy);
12. 03-07 July 2017. *"II International Summer School on Natural Products "Luigi Minale" and "Ernesto Fattorusso" (ISSNP)"* Napoli (Italy);
13. 28-30 June 2017. *"2nd MS-NatMed Day, Natural Molecules and Molecular Complexes: Characterization and Biomedical Effects"* Aboca, Sansepolcro (Italy);
14. 23 June 2017. *"Y-Rich Workshop"* Università La Sapienza, Roma (Italy);
15. 13 October 2016. *Workshop "Design your future"* Università degli Studi di Salerno, Salerno (Italy);
16. 4-5 April 2016. *"1st European Fourier Transform Mass Spectrometry School"* Matera (Italy)

ABROAD TRAINING:

From 09/12/2017 to 20/04/2018 at Teagasc Food Research Centre, Ashtown, Dublin, Ireland. Supervisor Dilip K. Rai.

DIDACTIC ASSISTANCE:

"Cultore della materia"in Parmaceutical botany and pharmacognosia from 2017 to 2018 at the University of Basilicata, Department of Sciences, Via dell'Ateneo lucano, 10, 85100 Potenza, Italy; referent Prof. Luigi Milella.

COMMUNICATIONS (*PRESENTING AUTHOR):

1. 24-29 November 2018. **Faraone I.***, Prinzo F., Kirke D., Chiummiento L., Fernandez E., Rai D.K., Milella L. Poster communication
   "Potential anti-hyperglycemic effects and chemical characterization of Senecio clivicolus" - 30th International Symposium on the Chemistry of Natural Products and the 10th International Congress on Biodiversity (ISCNP30 & ICOB10), Athens (Greece);
2. 12-13 November 2018. **Faraone I.***, Nolè M., Di Stefano M.R., Chiummiento L., Sinisgalli C., Saluzzi R., Gioia D., Vassallo A., Milella L. Oral communication
   "Green extractions of bioactives from Vitis vinifera L. (cv. Aglianico) leaves: phenolic profile, antioxidant and anti-cholinesterase activity of extracts" - III Edition Green Extraction of Natural Products (GENP 2018), University Aldo Moro Bari (Italy);
3. 26-28 September 2018. **Faraone I.***, Rai D.K., Choudhary A., Russo D., Chiummiento L., Fernandez E., Milella L. Poster communication
   "Antioxidant, antidiabetic, anti-cholinesterase activities and phytochemical profile of Minthostachys diffusa Epling" - 2nd Conference on Food Bioactives & Health (FBHC 2018), Lisbon (Portugal);
4. 26-28 September 2018. Birsan R., **Faraone I.**, Wilde P., Waldron K., Rai D.K. Poster communication
   "Anticholinesterase and antidiabetic activities of enriched polyphenolic extracts from brewers' spent grains" - 2nd Conference on Food Bioactives & Health (FBHC 2018), Lisbon (Portugal);
5. 20-22 September 2018. **Faraone I.*** Oral communication
   "Attività biologica di specie endemiche del Sud America" - Heroes 2018, Maratea (Italy);

6. 9-13 September 2018. Russo D., **Faraone I.**, Sinisgalli C., Di Stefano M.R., Saluzzi R., Bisaccia D., Milella L. Oral communication
   "Phytochemical composition and antioxidant activities of Melicoccus bijugatus Jacq fruit" - XXVII SILAE Congress, Milazzo (Italy);
7. 4-7 September 2018. Russo D., Miglionico R., Carmosino M., Bisaccia F., **Faraone I.**, Sinisgalli C., Milella L., Armentano M.F. Oral communication
   "Antioxidant and cytotoxic activities of methanol extract from Sclerocarya birrea [(A. Rich.) Hochst.] bark on HepG2 cell line" - 3rd International PSE Symposium on Natural Products in Cancer Prevention and Therapy. Trends in Methods and Modelling, Napoli (Italy);
8. 26-31 August 2018. **Faraone I.***, Ray D.K., Chiummiento L., Choudhary A., Russo D., Sinisgalli C., Fernandez E., Milella L. Oral communication
   "Antioxidant activities and phytochemical profile of Azorella glabra" - XXII International Mass Spectrometry Conference (IMSC 2018), Firenze (Italy);
9. 25-26 June 2018. D'Auria M., **Faraone I.**, Prasad P., Mecca M., Milella L., Sinisgalli C. Poster communication
   "Metbolite profile and biological activity of essential oils from Saussurea costus roots evaluated with GC-MS" - International proteomics & metabolomics conference and advanced proteomic school, Novara (Italy);
10. 21-23 June 2018. Milella L.*, **Faraone I.***, Esposito G., Sinisgalli C., Teta R., Russo D., Costantino V. Oral communication
    "New opportunities for research: marine sponges, source of antioxidant compounds to be protected and valorized" - Valorizzazione della costa, protezione, governance ed ecoturismo, Gruppo Nazionale per la Ricerca sull'Ambiente Costiero (GNRAC), Matera (Italy);
11. 7-9 June 2018. Russo D., **Faraone I.**, Bartolo M.A., Milella L. Oral communication
    "Development of extractive procedures and evaluation of the biological activity and chemical compositon of Echinacea angustifolia (DC.) Hell. root extracts" - Società Italiana di Fitochimica e delle Scienze delle Piante Medicinali, Alimentari e da Profumo. Scuola "Paolo Ceccherelli" Filiera corta in campo erboristico e medicinale: sviluppo tecnologico e programmazione comunitaria, Albenga (Italy);

12. 4-7 March 2018. **Faraone I.***, Russo D., Chiummiento L., Fernandez E., Milella L. Poster communication
    "In vitro biological assessment of Azorella glabra Wedd: antioxidant, antidiabetic and anti-cholinesterase properties" - Eco-Bio2018, Dublin (Ireland);
13. 16-17 November 2017. Lamorte D., Laurenzana I., Caivano A., De Luca L., Trino S., Russo D., **Faraone I.**, Armentano M. F., Milella L., Falco G., Del Vecchio L., Musto P. Poster communication
    "Azorella glabra extract induces apoptosis in multiple myeloma cells" - Under 40 in Hematology, Pacengo di Lazise (Italy);
14. 17-19 September 2017. Milella L., Nolè M., Hornedo-Ortega R., **Faraone I.**, Sinisgalli C., Gioia D., Vassallo A., García-Parrilla M.C. Oral communication
    "Phytochemical profiles, antioxidant and cholinesterase inhibition activity of Vitis vinifera L. cv. Aglianico leaf extracts" - New & old phytochemicals: their role in ecology, veterinary & welfare - Francavilla al Mare (Italy);
15. 3-7 July 2017. **Faraone I.***, Benedetto C., Tobia F., Vignola L., Russo D., Castronuovo D., Milella L. Poster communication
    "Arsicolo, Crovarese, Datterino and San Marzano: phytochemical composition and antioxidant activity of different tomato fruit cultivars" - II International Summer School on Natural Products "Luigi Minale" and "Ernesto Fattorusso" (ISSNP), Napoli (Italy);
16. 28-30 June 2017. **Faraone I.***, Prinzo F., Kirke D., Chiummiento L., Vignola L., Rai D. K. and Milella L. Oral communication
    "Antioxidant activity and phytochemical characterization of Senecio clivicolus" - 2nd MS-NatMed Day, Natural Molecules and Molecular Complexes: Characterization and Biomedical Effects, Sansepolcro (Italy);
17. 28-30 June 2017. Milella L., Da Pozzo E., De Leo M., **Faraone I.**, Cavallini C., Calderone V., Pistelli L., Braca A., Martini C. Poster communication
    "Antioxidant, cardiomyocyte anti-ageing properties and phytochemical profile of Citrus bergamia juices" - XV Congress of the Italian Society of Phytochemistry jointly with 1st International Congress on Edible, Medicinal and Aromatic Plants (ICEMAP 2017), Pisa (Italy);
18. 21-23 September 2016. Milella L., Russo D., **Faraone I.**, Vignola L., Andrade P., Fernandez E.C., De Tommasi N. Oral communication

"Biological activity and phytochemical profile of genetically different yacon genotypes" - 111° Congresso della Società Botanica Italiana onlus - III International plant science conference (IPSC), Roma, Tor Vergata (Italy);

19. 11-15 September 2016. Milella L., Bartolo M., **Faraone I.**, Benedetto C., Valentao P., Andrade P., Carmosino M., De Tommasi N. Oral communication *"Echinacea angustifolia DC. extract quali-quantitative analysis and fibroblast cell growth evaluation"* - XXV Italo-Latin American Congress of Ethnomedicine (SILAE), Modena (Italy);
20. 24-27 June 2016. Milella L., Milazzo S., De Leo M., Saltos M.B.V., **Faraone I.**, Tuccinardi T., Lapillo M., De Tommasi N., Braca A. Poster communication *"a-Glucosidase and a-amylase inhibitors from Arcytophyllum thymifolium"* - 9th Joint Natural Products Conference 2016 - Copenhagen (Denmark);
21. 9-10 June 2016. Russo D., **Faraone I.**, Vignola L., Valentão P., Andrade P., Fernandez E.C., Milella L. Oral communication *"Analisi genomica e metabolomica di cultivars di Smallanthus sonchifolius"* - XI Convegno Nazionale sulla Biodiversità, Matera (Italy);

INTERNATIONAL *PEER REVIEWED*:

1. Lamorte D.*, **Faraone I.** *, Laurenzana I., Milella L., Trino S., De Luca L., Del Vecchio L., Armentano M.F., Sinisgalli C., Chiummiento L., Russo D., Bisaccia F., Musto P., Caivano A. - Future in the past: *Azorella glabra* Wedd. as a source of new natural compounds with antiproliferative and cytotoxic activity on multiple myeloma cells" *Int. J. Mol. Sci.* 19(11):33483366, 2018;
2. **Faraone I.****, Rai D.K., Chiummiento L., Fernandez E., Choudhary A., Prinzo F., Milella L. - Antioxidant activity and phytochemical characterization of *Senecio clivicolus* Wedd. – *Molecules*, 23(10):2497-2514, 2018;
3. Da Pozzo E., De Leo M., **Faraone I.**, Milella L., Cavallini C., Piragine E., Testai L., Calderone V., Pistelli L., Braca A., Martini C. - Antioxidant and antisenescence effects of *Bergamot* juice - *Oxidative medicine and cellular longevity*, 2018:14pp, 2018;
4. Fidelis Q.C.*, **Faraone I.***, Russo D., Aragão Catunda-Jr F.E., Vignola L., de Carvalho M.G., de Tommasi N., Milella L. - Chemical and biological insights of *Ouratea hexasperma* (A. St.-Hil.) Baill.: a source of bioactive compounds with multifunctional properties - *Natural Product Research*, 2018:1-4, 2018;

5. Milella L., Milazzo S., De Leo M., Saltos V.M.B., **Faraone I.**, Tuccinardi T., Lapillo M., De Tommasi N., Braca A. - *a*-Glucosidase and *a*-Amylase Inhibitors from *Arcytophyllum thymifolium* - *Journal of Natural Products*, 79(8):2104-2112, 2016;
6. Saltos M.B.V., Puente B.F.N., **Faraone I.**, Milella L., De Tommasi N., Braca A. - Inhibitors of *a*-amylase and *a*-glucosidase from *Andromachia igniaria* Humb. & Bonpl. - *Phytochemistry Letters*, 14:45-50, 2015.

*Authors contributed equally to work

**Corresponding Author

NOTE:

Socio fondatore di maggioranza dello spinoff accademico BioActiPlant s.r.l. da Marzo 2018 ad oggi presso l'Università degli Studi della Basilicata, Via dell'Ateneo lucano, 10, 85100 Potenza, Italia

Acquisizione dei 24 crediti formativi universitari (CFU) relativi alle competenze di base nelle discipline antropo-psico-pedagogiche e nelle metodologie e tecnologie didattiche – Anno Accademico 2017/2018 presso Università degli Studi della Basilicata.

Esami sostenuti:

- Pedagogia generale - Ambito A - Cod. PF2401, S.S.D. M-PED/01, Votazione 30/30
- Psicologia generale - Ambito B - Cod. PF2402, S.S.D. M-PSI/01, Votazione 30/30
- Antropologia culturale - Ambito C - Cod. PF2403, S.S.D. M-DEA/01, Votazione 29/30
- Pedagogia e didattica speciale - Ambito D - Cod. PF2405, S.S.D. M-PED/03, Votazione 30/30

ACKNOWLEDGEMENTS

Many, many thanks to Professors Lucia Chiummiento and Luigi Milella for their support and their constructive criticism.

I would also like to thank to Professor Dilip Rai from Teagasc in Dublin and his lab team for their hospitality.

Many thanks to my husband, my parents, my sister, my all family, the "Milelliani" and everyone who supported me throughout my PhD.

Imma...

ABSTRACT

Nature is a wide source of biologically active compounds investigated with the purpose to be used as drugs due to their biological activity and also useful in pharmaceutical discovery and drug design. Nowadays, medicinal plants play a major role in primary health care as therapeutic remedies in many developing countries.

The aim of my PhD project was the phytochemical and biological investigation of three plant species, used in Bolivian traditional medicine, but few scientific studies were reported, such as: *Azorella glabra* Wedd., *Minthostachys diffusa* Epl. and *Senecio clivicolus* Wedd.

Samples were firstly analysed for their total content of polyphenols, flavonoids and terpenoids and for their *in vitro* antioxidant activity using different complementary assays. In particular, radical scavenging activity was tested against biological radicals such as nitric oxide (NO) and superoxide (SO) together with neutral or cationic (DPPH and ABTS) radicals; ferric reducing power and lipid peroxidation inhibitory capacity (FRAP and *Beta*-Carotene Bleaching tests) were also determined.

Oxidative stress is involved in different diseases, such as diabetes and neurodegenerative diseases. Then, the inhibitory ability of samples was investigated against *a*-amylase and *a*-glucosidase enzymes involved in diabetes and against acetylcholinesterase and butyrylcholinesterase enzymes considered as strategy for the treatment of Parkinson's or Alzheimer's diseases.

Moreover, cytotoxicity studies on cancer and non-cancer cell lines were carried out.

The antioxidant, antidiabetic, anticholinesterase and cytotoxic activities and the phytochemical profile were performed on aerial parts of *Azorella glabra*, *Minthostachys diffusa* and *Senecio clivicolus* for the first time.

Among all samples, the ethyl acetate fraction of *S. clivicolus* showed the highest antioxidant activity; instead, *M. diffusa* samples showed the highest antidiabetic potential and anti-cholinesterase activities. To confirm the inhibitory cholinesterase effects of the terpenes identified from *M. diffusa*, *in silico*, docking analysis were also carried out.

Moreover, the *A. glabra* samples were tested for the first time on Multiple Myeloma (MM) cell lines using several assays. The chloroform fraction of *A. glabra*

reduced the cell viability, and arrested the cell cycle on MM cells in G0/G1 phase, characteristic feature of apoptosis.

Instead, the ethyl acetate fraction of *S. clivicolus* was tested on hepatocellular carcinoma HepG2 cell line showed the ability to induct cell death via the mitochondrial apoptotic pathway.

In conclusion, this first report on *Azorella glabra*, *Minthostachys diffusa* and *Senecio clivicolus* phytochemical characterization and biological activity evaluation, demonstrates as these Bolivian plant species could be considered a source of health promoting compounds. Some of the results obtained during this study might partially explain their ethnobotanical use, evidencing a potential economic added value for extract future use in the field of biotechnology applied to environmental, agricultural, health, pharmaceutical and cosmeceutical development.

CHAPTER 1.

INTRODUCTION

1.1. Ethnobotany, phytochemistry and pharmacognosy

The use of plant species for the treatment of different disease is the oldest medicine used by man to find answers to the question of health; still today, many drugs used in clinical practice are made up of specie extracts or derivatives from these. Traditional herbal medicine is a complex system of methods, therapeutic techniques and products.

The American botanist Dr. John William Hershberger used for the first time the term "*ethnobotany*" in 1895 to describe his research. Ethnobotany is located between natural and social sciences and includes studies concerning the traditional uses of plant species in different populations and territories. In particular, the ethnobotany is the study of the relationship the "*ethno*" study of people and "*botany*" study of plant species. The use of the same or similar species in the same mode in different populations indicate that several and non-interacting human groups have independently acquired the same knowledge.

Papaverine, digoxin, cannabidiol, vinblastine and vincristine are among the most famous natural drugs developed from ethnobotanical studies and in 2015 Nobel Prize in Physiology or Medicine recognized the relevance of the artemisinin isolation from *Artemisia annua* L. as a powerful antimalarial drug (Cotton and Wilkie 1996; Garnatje, Peñuelas *et al.* 2017; Rahman, Afzal *et al.* 2018).

Ethnobotany has its roots in *botany* and in particular in *pharmaceutical botany* that allows us to understand the presence and distribution of chemical constituents and the function of the plant.

Pharmacognosy studies and recognizes plant drugs, plant parts used for pharmacological purposes. The term pharmacognosy derived from the Greek words "*pharmakon*" (drug) and "*gnosis*" (knowledge). For different years, pharmacognosy was focused on the authentication and quality of crude drugs of specie origin. The modern definition of pharmacognosy, instead, is the science of biogenic or naturally derived pharmaceuticals and poisons. In fact, it studies the medicinal plants used as crude herbs or extracts, pure natural compounds and foods with potential health benefits. This new definition reflects the changes that have taken place in the past 50 years, particularly with the focus on phytochemistry and biological activities of natural products. The scope of pharmacognosy is also defined as the study of physical,

chemical, biochemical and biological properties of drugs, drug substances, or potential drugs or drug substances of natural origin as well as the search for new drugs from natural sources. Then, research in pharmacognosy includes phytochemistry, microbial chemistry, biosynthesis, biotransformation, chemotaxonomy and other biological and chemical sciences (Phillipson 2007).

In particular, the *phytochemistry* studies and defines the chemical structure and biosynthesis of the single molecules present in the plant species.

1.2. Primary and secondary metabolites

The plant species are able to handle different organic compounds that are categorized as primary or secondary metabolites. These compounds are synthesized in plants using enzymatic systems during metabolic pathways.

The **primary metabolism** (**Fig. 1.1**) is involved in essential reactions in growth and development of plant species. The primary metabolites are produced from glycolysis and oxidative pentose phosphate pathway starting from photosynthesis. They are present in all plants and are nucleic acids, lipids, carbohydrates, and proteins.

The **secondary metabolism** (**Fig. 1.1**), instead, produces secondary metabolites or natural products starting from primary metabolites. These metabolites do not participate directly in the growth and development of plant species, but their production plays an important role in defence against predators and pathogens, in providing reproductive advantage as intraspecific and interspecific attracts towards the same or other species, in the adaptation of plants to their environment. These compounds are produced in small quantities and are very specific to each plant (Buchanan, Gruissem *et al.* 2000; Bourgaud, Gravot *et al.* 2001).

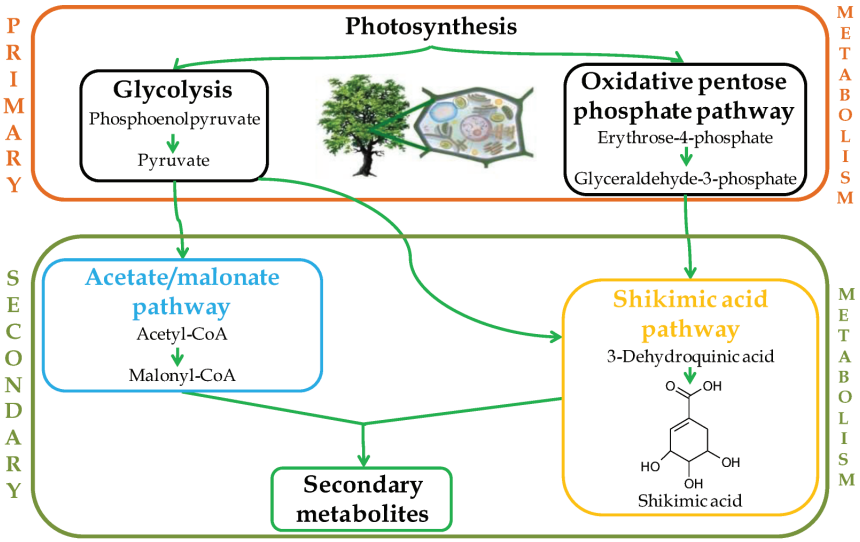

Figure 1.1. Primary and secondary metabolism

The secondary metabolites can be classificated in three main groups:

1. phenolic compounds (phenolic acids, flavonoids, tannins, lignins, lignans, coumarins, stilbenes);
2. terpenes (plant species volatiles, cardiac glycosides, carotenoids, sterols);
3. nitrogen containing compounds (alkaloids, glucosinolates) (Agostini-Costa, Vieira *et al.* 2012).

Phenolic compounds are widely distributed in nature. They include simple phenols (C_6), such as hydrobenzoic acid derivatives and catechols, as well as long chain polymers with high molecular weight, such as catechol melanins $(C_6)_6$, lignins $(C_6\text{-}C_3)_n$ and condensed tannins $(C_6\text{-}C_3\text{-}C_6)_n$.

Stilbenes ($C_6\text{-}C_2\text{-}C_6$) and flavonoids ($C_6\text{-}C_3\text{-}C_6$) are phenolic compounds with intermediate molecular weight that present many pharmacological and biological activities.

Flavonoids, including anthocyanins, flavonols (such as quercetin), isoflavones (such as genistein) and others are formed by multiple biosynthetic branches that originate from chalcone.

Terpenoids are the largest and most diverse family of natural products. Their structure ranging from linear to polycyclic molecules, and the size ranging from the five-carbon hemiterpenes to natural rubber, comprising thousands of isoprene units.

The condensation of isoprene units (C_5) is the first step for the synthesis of all terpenoids. They are classified by the number of five-carbon units present in the core structure.

Many aromatic molecules, as linalool, geraniol and menthol are formed by monoterpenes (C_{10}) with two isoprene units, and sesquiterpenes (C_{15}) with three isoprene units. Other bioactive compounds, as diterpenes (C_{20}), triterpenes (C_{30}) and tetraterpenes (C_{40}) show important activities.

Monoterpenes and sesquiterpenes (plant species volatiles) are typically lipophilic liquids than can cross membranes freely and evaporate into the atmosphere when there are no barriers to diffusion. The diterpene compounds derived from geranylgeranyl diphosphate; they have 20 carbon units in their basic skeletal. There are many types of diterpenoids derived from cyclization reactions of geranylgeranyl diphosphate and with a large range of polarity nature. Sesterterpenes (C_{25}) arise from cyclization of geranylfarnesyl diphosphate, and present different oxidation levels and several biological activities. Triterpenes (C_{30}) are a large class of compounds presenting interesting biological activities; they arise from the cyclization of squalene that lead to a large number of different triterpene skeletal types (with 30 carbons), such as lupane, oleane, and ursane types.

Steroids are triterpenoids modified, lacking the three methyl groups at C-4 and C-14. Sterols are characteristic of eukaryotes.

Saponins are a group of natural compounds presenting triterpenoidal or steroidal aglycone covalently linked to one or more sugar moieties.

Tetraterpenes, named also carotenoids, are isoprenoid compounds, biosynthesized by tail-to-tail linkage of two geranylgeranyl diphosphate molecules. This produces the parent C_{40} carbon skeleton from which all the individual variations are derived.

Nitrogen containing compounds as alkaloids, compounds synthesized by living organisms containing one or more heterocyclic nitrogen atom, derived from amino acids and pharmacologically active. The class name is directly related to the fact that nearly all alkaloids are basic (alkaline) compounds.

The secondary metabolites are very interesting for their biological activity. In fact, when they are giving into human or animal organism, they have different

activities, such as antioxidant, hypoglycaemic, hypolipidemic, antimicrobial, antifungal, antiviral, anti-inflammatory, and cytotoxic activities (Chen, Wu *et al.* 2016; Wu, Liu *et al.* 2016; Bouyahya, Bakri *et al.* 2017; Panda, Dash *et al.* 2018).

1.3. Oxidative stress and antioxidants

The formation of radical species is a physiological event within aerobic cells, which defend themselves due to the presence of enzymatic and non enzymatic systems (antioxidant defences) (Milella, Caruso *et al.* 2011).

Reactive oxygen and nitrogen species (ROS and RNS) are physiologically produced during metabolic processes and especially during electron transport chain reactions. The low concentration of these species is essential for several biochemical processes. Important endogenous antioxidant systems compensate the production of ROS, RNS, and other free radicals.

The imbalance between oxidants and antioxidants leads to a condition named *oxidative stress*. In fact, an overall increase in cellular levels of radical unstable molecules above the cells defences results in oxidative stress that can ultimately cause cell death (Faraone, Rai *et al.* 2018). The oxidative stress is responsible for toxicity and damage of cell components, including nucleic acids, proteins, and lipid. It has been recognized responsible in the aging process, for the onset of several chronic diseases, including liver diseases, diabetes, neurodegenerative diseases (Parkinson's and Alzheimer's diseases), cancer, and cardiovascular diseases (Melo, Monteiro *et al.* 2011).

In order to delete the oxidative stress, natural substances named antioxidant are used. An *antioxidant* has been defined by Halliwell as "*any substance that, when present at low concentrations compared with those of an oxidisable substrate, significantly delays or prevents oxidation of that substrate*".

A simplified definition is "*any substance that delays, prevents or removes oxidative damage to a target molecule*" (Halliwell 2007). The antioxidant defences are endogenous (antioxidants produced in the body) or exogenous (antioxidants derived from the diet) (Willcox, Ash *et al.* 2004).

The endogenous antioxidant defence mechanisms include different enzymatic system such as superoxide dismutase (SOD), catalase and glutathione peroxidases.

The exogenous antioxidants are radical traps and low molecular weight ROS scavengers can also overcome the deleterious effects of excessive generation of ROS/RNS. The protective effects of plant species secondary metabolites in our body can be attributed to direct scavenging activities against ROS, as well as to the induction of intracellular antioxidant effects. Many secondary metabolites are good antioxidants and it is possible to use them in several disorders.

1.4. Drug discovery

The drug discovery is the process by which new pharmacological active molecules are discovered. Most of drugs were discovered through identifying the active compound from traditional remedies or by serendipitous discovery.

Modern drug discovery involves in the optimization of those molecules to increase the affinity, selectivity (to reduce the potential of side effects), efficacy/potency, metabolic stability (to increase the half-life), and oral bioavailability. Once a compound that fulfils all of these requirements has been identified, it will begin the process of drug development prior to clinical trials.

The study of natural products involves the isolation in a pure form of these compounds and investigation of their structure, formation, use, and purpose in the organism. However, the drug discovery process, starting from natural substances, has been changed recently by the adoption of computational methods helping the design of new drug candidates more rapidly and at lower costs. *In silico* drug design consists of a collection of tools helping to make rational decisions in the different steps of the drug discovery process, such as the identification of a biomolecular target of therapeutic interest, the selection or the design of new lead compounds and their modification to obtain better affinities, as well as pharmacokinetic and pharmacodynamic properties (Shaikh, Jain *et al.* 2007; Zoete, Grosdidier *et al.* 2009). In particular, molecular docking has become an increasingly important tool for drug discovery. In fact, it tries to predict the structure of the intermolecular complex formed between two or more constituent molecules (Meng, Zhang *et al.* 2011). A variety of compounds from plant species sources have been reported to possess substantial biological properties; however, their modes of action have not been clearly defined.

CHAPTER 2.

BOLIVIAN INVESTIGATED PLANT SPECIES AND AIM OF THE RESEARCH

2.1. State of the art

Nature is a wide source of biologically active compounds used as medicines with a pharmacological or biological activity and useful in pharmaceutical discovery and drug design (Lahlou 2013). Natural products include plant, animal and microbial sources. Plants have been the origin and basis of pharmacy and pharmacology, constituting remedies in traditional medical systems and are still being used as a source of bioactive compounds. Nowadays, plant materials continue to play a major role in primary health care as therapeutic remedies in many developing or industrialized countries (Babu, Johnson *et al.* 2014). It has been reported that natural products (their derivatives and analogs) represent over 50% of all drugs in clinical use, in which natural products derived from higher plants represent about 25% of the total.

Throughout history, different cultures have developed knowledge about herbal remedies that have been passed from generation to generation constituting traditional medicine (Lawal, Uzokwe *et al.* 2010). South American plant species can be considered an important source for the discovery of new natural compounds for therapeutic applications, but they are poorly investigated, although are well known for their ethnomedicinal uses in literature (Mishra and Tiwari 2011).

After literature screening, my attention was focused on some species like *Azorella glabra* Wedd., *Minthostachys diffusa* Epl. and *Senecio clivicolus* Wedd. belonging to Apiaceae, Lamiaceae and Asteraceae families, respectively. These species are commonly used in ethnomedicine as carminative, digestive, antispasmodic, antimycotic, antiparasit and against muscle cramps, but few scientific studies were reported (Alkire, Tucker *et al.* 1994; Hilgert 2001; Schmidt-Lebuhn 2008).

The oxidative stress is the cause of most of these diseases. The antioxidant properties and content of flavonoids and terpenoids found in the aerial parts of other species belonging to *Azorella*, *Minthostachys* and *Senecio* genera, can explain, at least in part, the traditional use of the native plant species and health benefits of the infusions. In fact, flavonoids, among which isoflavones, and diterpenes, are promising antioxidants, which can be used in therapy (Bórquez, Kennelly *et al.* 2013). Moreover, terpenoid and flavonoid compounds have an antihyperglycemic action (Fuentes, Sagua *et al.* 2005) and several diterpenoid compounds are anticholinesterase inhibitors (Ren, Houghton *et al.* 2004). Further researches are needed to better explore the biological

activities of these species regarding phytochemical composition to support their potential effects on the human health. In fact, the study of these species may be useful to explain their ethnobotanical use, but it may also have economic implications in the field of biotechnology applied to environmental, agricultural, health, pharmaceutical and cosmeceutical development. The approach to new molecules through natural products has proved to be the most successful strategy for the discovery of new drugs and the relaunching of pharmaceutical industries (Rout, Choudary *et al.* 2009).

2.2. *Azorella glabra* Wedd.

Azorella glabra, also known as *Azorella diapensioides* or *yareta*, is an endemic species (**Fig. 2.1**) collected in Bolivia region belonging to the Apiaceae (Umbelliferae) family.

The genus *Azorella* includes about 70 species of flowering plant species, a native genus in South America, New Zealand and the islands of the Antarctic Ocean. They are dwarf mat-forming plants, usually less than 10 cm high, growing on mountains and sub Antarctic coasts.

Different species are ornamental plant species in rock gardens and are commonly used as a tea infusion in the Andean region of South America in folk medicine to treat various chronic diseases such as bronchitis, pneumonia, rheumatism and diabetes. Some of them are also used as diuretics, in gastric problems and as analgesics in case of cold. In addition, there was a previous study on *Azorella compacta* that reported an interesting effect of methanol extract on leukaemia cells (Sung, Kwon *et al.* 2015).

The *Azorella* genus is rich in diterpenoids, with mulinane and azorellane skeletal, compounds with a variety of important biological activities (Tůmová, Dučaiová *et al.* 2017).

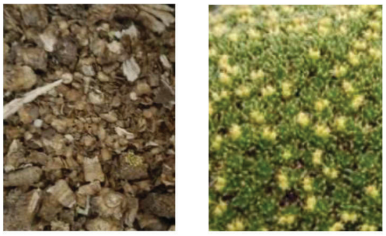

Figure 3.1. *Azorella glabra* Wedd.

2.3. *Minthostachys diffusa* Epl.

The genus *Minthostachys* is an important South American mint genus belonging to Lamiaceae family. It includes about twenty species used as medicinal, culinary, aromatic, and commercial essential oil. In the last years, this genus was of great ethnobotanical, pharmacological and commercial interest because contains important plant species commonly used in the folk medicine of the area.

The genus *Minthostachys* is known to the local population under differing names, the best known of these are "*muna*" in the area from central Peru to Bolivia and "*peperina*" in Argentina, where "*muna*" is more frequently used for species of *Clinopodium*. The use of plant species called "*muna*" has been reported as early as the 16th century. Ethno botanists have documented a wide array of traditional uses for *Minthostachys* plant species. These include use as carminative, digestive, antispasmodic, against colds and stomachache and for the production of liqueurs (*M. verticillata*), for antimycotic and antiparasitic purposes, as vermifuge or sedative, and against diarrhoea, colics, and respiratory illnesses (presumably *M. mollis* or *M. spicata*), against flea infestations, rheumatism, bronchitis, asthma and headache, to induce menstruation (*M. mollis*) and as a biopesticide. Moreover, different authors described the use of *Minthostachys* from southern Peru as a condiment for seasoning, tea, and especially for commercial production of aromatic oil. The application of water boiled containing *M. acris* leaves, or even of fresh plant parts, was traditionally used for the protection of stored potato and oca tubers from pests against aphids on crop plants, and was used in the house against flea infestations. Instead, an ethnobotanical study in Argentina characterized *M. verticillata* as a "hot" species used as an aphrodisiac and a digestive (Gayathiri, Sangeetha *et al.* 2016).

On the basis of this observation, the *Minthostachys* genus receives growing attention from modern pharmacology and medicine. Scientific interest in these species was concentrated on a few plant species, such as *M. verticillata*, *M. mollis*, *M. andina* or *M. glabrescens*. As in many Lamiaceae, the essential oils were tested for commercial and pharmaceutical interests. Pulegone and menthone are the main chemical components of *Minthostachys* plant's oil. Then, the ethnobotanical uses not surprising considering that other plant species containing the dominant essential oil components found in the

genus, like menthone, pulegone, carvone are likewise chiefly employed as digestives, carminatives, antispasmodics, and antitussives.

All these researches suggest that oil of *Minthostachys* species should be used also as a potential commercial source of natural mint flavouring with big pharmacological and commercial interest (Senatore 1995).

The aim of my PhD project was focused on *Minthostachys diffusa* Epl., also known as "*tusuwaya*", an endemic species (**Fig. 2.2**) collected in Bolivia region. Aerial parts of *Mintostachys diffusa* are used from the local population as antispasmodic, carminative and digestive tea (infusion) (Schmidt-Lebuhn 2008). However, its health-promoting properties have not been explored yet.

Figure 3.2. *Minthostachys diffusa* Epl.

2.4. *Senecio clivicolus* Wedd.

Senecio is one of the largest genus of the Asteraceae family, with a wide distribution in the world, consisting more than 1500 species of herbs, shrubs, vines, and trees. Many of these species grow in Bolivia, a central country of South America, with an extremely rich biodiversity of endemic species (Araujo, Mü Ller *et al.* 2005). The traditional use of medicinal plant species by various indigenous populations in Bolivia has been documented in literature (Muñoz, Sauvain *et al.* 2000; Deharo, Bourdy *et al.* 2001; Bourdy, Oporto *et al.* 2004; Macía, García *et al.* 2005; Thomas, Semo *et al.* 2011; Hajdu and Hohmann 2012). In particular, traditional medicine used extracts of leaves and roots of several *Senecio* species as a remedy for fever, cough, stomach pain, gastric ulcer, for the treatment of diabetes, skin wounds, and as vasodilator, antiemetic, and anti-inflammatory agents (Floegel, Kim *et al.* 2011).

Senecio clivicolus Wedd. (**Fig. 2.3**) grows in the mountain region of western Bolivia, where it is known as "*chiñi waycha*" or "*waycha negra*". The natives used this perennial shrub as a remedy for stomach pain and diarrhoea (Fournet, Barrios *et al.* 1994; Floegel, Kim *et al.* 2011). Moreover, this plant extract was used against fungal infections in the skin (Bustamante, Escalante *et al.* 2001).

Pyrrolizidine alkaloids, eremophilanes and furanoeremophilanes were reported in previous phytochemical studies on other species belonging to *Senecio* genus (Pelser, Nordenstam *et al.* 2007). These metabolites have several important properties as insect antifeedant, antifungal, cytotoxic, antioxidant, anti-inflammatory, and antimicrobial agents. Some furanoeremophilanes, such as cacalone compound, have a radical scavenging and antioxidant activity (Krasovskaya, Kulesh *et al.* 1989; Floegel, Kim *et al.* 2011).

These previous data are very interesting for future investigation of this specie, so there is a considerable scientific interest in the discovery of new compounds and biological activity from *Senecio clivicolus*.

Figure 3.3. *Senecio clivicolus* Wedd.

2.5. Objectives of the research

Natural products have been the major sources of chemical diversity of starting materials for driving pharmaceutical discovery over the past century. Pharmaceutical companies' utilized plant extracts to produce drugs, but with the advancement of antibiotics in the mid-twentieth century, drug formulations of fairly purified compounds have become more typical. Many natural products and synthetically modified natural product derivatives have been developed successfully for clinical use to treat human diseases in almost all therapeutic areas.

My research project aims to select the poorly investigated plant species that have an important involvement in traditional medicine such as *Azorella glabra* Wedd., *Minthostachys diffusa* Epl. and *Senecio clivicolus* Wedd.

These plant species are commonly used from local populations in several diseases based on oxidative stress. For these reasons, further researches are needed to better explore the biological activities of these species regarding phytochemical composition support their potential effects on the human health. In fact, the study of these species may be useful to explain their ethnobotanical use, but it may also have economic implications in the field of biotechnology applied to environmental, agricultural, health, pharmaceutical and cosmeceutical development. The approach to new molecules through natural products has proved to be the most successful strategy for the discovery of new drugs and the relaunching of pharmaceutical industries (Rout, Choudary *et al.* 2009).

Once selected the most promising species, the preparation of crude extracts from different species was the first step of this project.

Subsequently, these samples were fractionated on the basis of solvent polarity and tested to evaluate their biological activity with different tests.

At the first, the samples were tested to evaluate the total content of polyphenols, flavonoids and terpenoids and their *in vitro* antioxidant activity important in oxidative stress. In particular, the radical scavenging activity against biological radicals such as nitric oxide (NO) and superoxide (SO) together with neutral or cationic (DPPH and ABTS) radicals was tested to measure their antioxidant potential; the ferric reducing power and the inhibitory capacity of lipid peroxidation (FRAP and *Beta*-Carotene Bleaching tests) were also determined.

The oxidative stress is involved in different diseases, such as diabetes and neurodegenerative diseases. For these reasons, the inhibitory ability of samples against enzymes involved in diabetes (*e.g. a*-amylase and *a*-glucosidase enzymes) and in treatment of Parkinson's or Alzheimer's diseases (*e.g.* acetylcholinesterase and butyrylcholinesterase enzymes) was investigated.

Moreover, cytotoxicity studies on cancer and non-cancer cell lines were also carried out to evaluate the possible toxicity of selected samples.

The most active samples were further subjected to characterization of secondary metabolites responsible for their biological activities. Spectroscopic and spectrometric methodologies were used for their characterization and quantification (LC-MS/MS analysis). The characterization of the different classes of constituents and the identification of secondary metabolites allows us to increase the chemical knowledge of these species and identify the main responsible compounds of the shown biological activity. The identification of pure compounds is the first necessary step for developing new labelled drugs from natural products to be used in the pharmaceutical industry. The activities of bioactive compounds and their synergistic action make them ideal in alternative therapies.

To confirm the inhibitory effects of the plant-derived compounds against enzymes above mentioned, *in silico* docking analysis was also carried out. Molecular docking is an application, wherein molecular modelling techniques, used to predict how a protein could interact with small molecules (ligands). The concept of docking is important in the study of various properties associated with protein-ligand interactions. Elucidation of ligand binding mechanisms is the necessary step to obtain more selective and potent drug.

CHAPTER 3.

MATERIALS AND METHODS

3.1. Chemicals, reagents and equipments

Solvents as *n*-butanol, chloroform, *n*-hexane, hydrochloric acid, ethanol, ethyl acetate, glacial acetic acid, methanol, dimethyl sulfoxide (DMSO) and phosphoric acid were purchased from Carlo Erba (Milan-Italy). Acetonitrile and formic acid were purchased from Merck (Wicklow-Ireland).

Folin-Ciocalteu reagent 2 N, sodium carbonate, 2,2'-azino-bis(3-ethylbenzothiazoline-6-sulfonic acid) (ABTS), potassium persulfate, 2,2-diphenyl-1-picrylhydrazyl (DPPH), potassium phosphate monobasic, *β*-nicotinamide adenine dinucleotide reduced form (NADH), phenazine methosulfate (PMS), nitrotetrazolium blue chloride (NBT), sodium nitroprusside dehydrate (SNP), sulfanilamide, *N*-(1-naphthyl)ethylenediamine dihydrochloride, sodium acetate trihydrate, 2,4,6-tripyridyl-*s*-triazine (TPTZ), iron (III) chloride ($FeCl_3{*}6H_2O$), *β*-carotene, linoleic acid and Tween 20 were purchased from Sigma-Aldrich (Milan-Italy).

Hydroxymethyl aminomethane (Tris), 20,70-dichlorodihydrofluorescein diacetate (DCFH-DA), sodium chloride, tergitol™ solution (NP40), sodium dodecyl sulfate (SDS), non fat dry milk (NFM), sodium deoxycholate, *Dulbecco's Minimum Essential Medium* (DMEM), *N*-Acetyl-*L*-cysteine (NAC), Hoechst 33258 and anti-rabbit secondary antibody were purchased from Sigma-Aldrich (Milan-Italy) and Merck (Wicklow-Ireland).

Standard as 6-hydroxy-2,5,7,8-tetramethylchroman-2-carboxylic acid (Trolox), ascorbic acid, butylhydroxytoluen (BHT), gallic acid, leucine-enkephalin, 3,4-di-*O*-caffeoyl quinic acid, 3,5-di-*O*-caffeoyl quinic acid, 4-hydroxybenzoic acid, caffeic acid, chlorogenic acid, chlorogenic acid methyl ester, quercetin-3-*O*-glucoside, rutin and other standards mentioned in this work were purchased from Sigma-Aldrich (Milan-Italy) and Extrasynthese (Genay-France).

Fetal bovine serum (FBS), RPMI1640, phosphate-buffered saline (PBS), and penicillin/streptomycin were purchased from Gibco-BRL (Life technologies, Carlsbad, CA, USA).

A cell Titer 96 aqueous one solution assay kit (MTS) was purchased from Promega (Madison,WI, USA).

Nitrocellulose membrane was purchased from GE Healthcare (Chicago, IL, USA).

A FITC Annexin V Apoptosis Detection kit was purchased from Becton Dickinson (BD Pharmingen,San Jose, CA, USA).

24-well Millicell Hanging cell culture transwell inserts 8 m PET (Millipore Corporation, Billerica, MA, USA).

Tetramethyl rhodamine methyl ester (TMRM, Life Technologies, Carlsbad, CA, USA) was a kind gift from Dr. M. Lasorsa (IBBE, CNR, Bari).

Antibody anti-PARP-1 was purchased from CST (Danvers, MA, USA). Antibody anti-Bcl-2 and chemiluminescence (ECL plus) kit were purchased from Thermo Fisher (Rodano, Milano, Italy).

Water was deionised using a Milli-Q water purification system (Millipore, Bedford, MA, USA).

All spectrophotometric measurements were done in 96-well microplates or cuvettes on a UV/Vis spectrophotometer (SPECTROstar^{Nano} BMG Labtech, Ortenberg-Germany) and each reaction was performed in triplicate.

LC–MS/MS analyses were performed on a Q-Tof Premier mass spectrometer (Waters Corporation, Milford, MA, USA) coupled to an Alliance 2695 HPLC system (Waters Corporation, Milford, MA, USA). Mass spectrometry quantification of the compounds was performed by multiple reaction monitoring (MRM) experiments using Waters Acquity (Waters Corporation, Milford, MA) ultra-high performance liquid chromatography coupled with tandem mass spectrometry (UHPLC-MS/MS).

The fluorescence was measured by Glomax Multi Detection System (Promega, Madison, WI, USA).

The cellular morphology was observed using inverted phase contrast microscopy (Nikon Eclipse TS100) and fluorescence microscopy (Nikon Eclipse 80i).

The cells were analysed on a FACS Canto II flow cytometer and NAVIOS flow cytometer.

3.2. Preparation of specie samples

The aerial parts of *Azorella glabra* (Ag), *Minthostachys diffusa* (Md) and *Senecio clivicolus* (Sc) were collected in the 2014, near the Aymaya population/community (18.45°S to 66.46°W; 3750 msnm), Bustillo province, Potosí department, Bolivia (Province of Nor Yungas, GPS coordinates -16.190040, -67.884402). Voucher specimen

of each sample is stored in the herbal medicinal plants of the National University Siglo XX, Llallagua, Potosí, Bolivia at the University of La Paz. Samples were dried at room temperature, crushed and subsequently extracted by exhaustive dynamic maceration in a darkness shaker set at 25°C using 96% ethanol (four times for each sample). Extracts were filtered through a Buchner funnel (0.45 μm) and dried using a rotary evaporator equipped with a water bath set at 37°C.

A part of the reunited ethanol extract of each plant specie (Ag EtOH, Md EtOH and Sc EtOH) was solubilised in water and subjected to liquid/liquid partitioning in triplicate using an equal volume of *n*-hexane, chloroform, ethyl acetate and *n*-butanol in order to separate the compounds on the basis of increasing solvent polarity. Then, the *n*-hexane, chloroform, ethyl acetate, *n*-butanol and water fractions of each plant species were dried and stored in darkness at room temperature until further use (Faraone, Rai *et al.* 2018).

3.3. Total Polyphenolic Content (TPC)

The total polyphenolic content of the samples was determined by Folin-Ciocalteu assay as reported by Todaro *et al.* (Todaro, Russo *et al.* 2017) with slight modification.

The redox Folin-Ciocalteu reagent (**Fig. 3.1**) is a mixture of phosphomolybdate and phosphotungstate used to determine phenolic and polyphenolic antioxidants in colorimetric *in vitro* assay.

$$3H_2O - P_2O_5 - 13WO_3 - 5MoO_3 - 10H_2O$$

$$3H_2O - P_2O_5 - 14WO_3 - 4MoO_3 - 10H_2O$$

Figure 4.1. Folin Ciocalteu reagent

Polyphenols react with the Folin-Ciocalteu reagent to give a blue complex that can be quantified by spectrophotometry (Singleton and Rossi 1965; Schofield, Mbugua *et al.* 2001; Chun and Kim 2004). The reaction forms a blue chromophore of phosphotungstic-phosphomolybdenum complex (Schofield, Mbugua *et al.* 2001; Gülçin, Sat *et al.* 2004), where the maximum absorption of the chromophore depends on the alkaline solution and the concentration of phenolic compounds (**Fig. 3.2**).

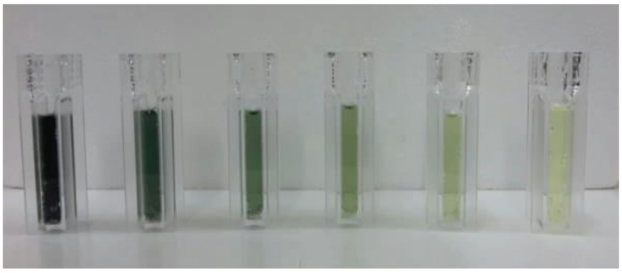

Figure 4.2. Folin Ciocalteu *in vitro* assay

Diluted sample (75 µL) and 425 µL of distilled water were added to 500 µL Folin Ciocalteu reagent and 500 µL of Na_2CO_3 (10% w/v). The mixture was mixed and incubated for 1 h in the dark at room temperature. After incubation, the mixture was measured at 723 nm using a UV-Vis spectrophotometer. Gallic acid (**Fig. 3.3**) was used as standard to make the calibration curve and the results were expressed as milligrams of Gallic Acid Equivalents per gram of dried sample (mg GAE/g).

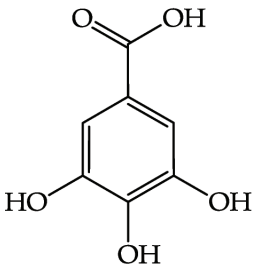

Figure 4.3. Gallic acid

3.4. Total Flavonoid Content (TFC)

Flavonoids are a group of polyphenolic compounds with recognized biological properties. The spectrophotometric *in vitro* assay determines the total flavonoid content by the aluminium complex. In fact, the aluminium chloride forms acid stable complexes with the C-4 keto group and either the C-3 or C-5 hydroxyl group of flavones and flavonols. Moreover, aluminium chloride forms acid labile complexes with the orthodihydroxyl groups in the A- or B-ring of flavonoids (Rajanandh and Kavitha 2010). In the test, diluted sample (150 µL) was added to 15 µL of $NaNO_3$ 5%. After 5 minutes at room temperature, 30 µL of $AlCl_3$ 10% were added and after another minute, 100 µL of 1 M NaOH solution were added and the total volume was made up

to 500 µL with distilled water. The solution was mixed and the absorbance was measured at 510 nm after 10 minutes of incubation at room temperature. Quercetin (**Fig. 3.4**) was used as standard to make the calibration curve and the results were expressed as milligrams of Quercetin Equivalents per gram of dried sample (mg QE/g) (Russo, Valentão *et al.* 2015).

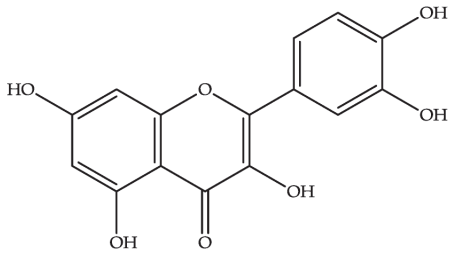

Figure 4.4. Quercetin

3.5. Total Terpenoid Content (TTeC)

Terpenes and terpenoids are primary constituents of essential oils of different type of plant species and flowers. The total terpenoid content was determined using the monoterpene linalool as standard reagent (**Fig. 3.5**). In this reaction, the primary alcohol geraniol ($C_{10}H_{18}O$) is produced from tertiary alcohol linalool ($C_{10}H_{18}O$). It is obscured to explain the exact chemical nature of the reaction in where a brick red precipitation has been formed and which is partially soluble in reaction mixture solution and chloroform but fully in methanol. In particular, 25 mg of sample were solubilised in 175 µL of 95% methanol. The mixture was sonicated for 5 minutes and centrifuged at 14000 rpm for 15 minutes. Then, the supernatant was collected. A part of supernatant (100 µL) was added to 750 µL of $CHCl_3$ and the mixture was vortexed and take 3 minutes to rest; then, 50 µL of H_2SO_4 were added and the mixture was incubated for 2 hours in the dark at room temperature. After that, the supernatant was removed and 750 µL of 95% MeOH were added on pellet. The absorbance was measured at 538 nm and the results were expressed as milligrams of Linalool Equivalents per gram of dried sample (mg LE/g) (Ghorai, Chakraborty *et al.* 2012).

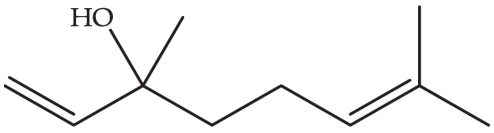

Figure 4.5. Linalool

3.6. Antioxidant activity

3.6.1. Radical-scavenging activity

The radical scavenging capacity of investigated plant species was evaluated by four different complementary *in vitro* assays. In particular, the synthetic coloured $ABTS^{\bullet+}$ and $DPPH^{\bullet}$ radicals, beside the use of biological super oxide anion ($O_2^{\bullet-}$) and nitric oxide ($^{\bullet}NO$) radicals. The electron transfer involves reduction of a coloured oxidant and the capacity of the samples to scavenge the radicals was monitored by spectrophotometer and quantified in Trolox Equivalents (**Fig. 3.6**), used as standard (Fournet, Barrios *et al.* 1994).

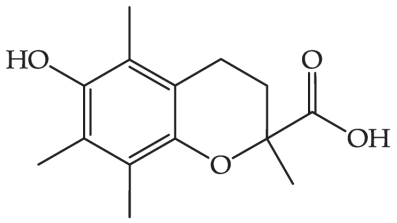

Figure 4.6. Trolox

3.6.1.1. ABTS Assay

The free radical-scavenging capacity of all samples was studied using the 2,2'-azinobis-(3-ethylbenzothiazoline-6-sulfonic acid) diammonium salt (ABTS) radical assay, by the procedure described by Armentano *et al.* (Armentano, Bisaccia *et al.* 2015) with slight modification. The reaction between ABTS salt (**Fig. 3.7 A**) dissolved in water to 7.00 mM concentration and 2.45 mM potassium persulfate (**Fig. 3.7 B**) generates the $ABTS^{\bullet+}$ radical after 16 h of incubation at room temperature.

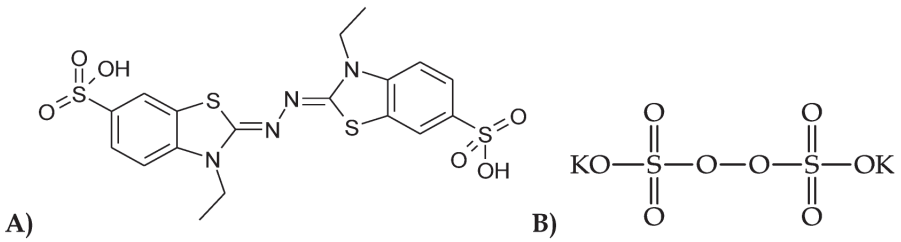

Figure 4.7. A) ABTS; **B)** Potassium persulfate

Each sample (15 μL) was added to 235 μL of ABTS solution and the reaction was incubated for 2 h in the dark. The reaction for scavenging the cationic radicals from the samples (**Fig. 3.8**) was monitored at 734 nm and the results were expressed as milligrams of Trolox Equivalents per gram of dried sample (mg TE/g) based on Trolox standard curve.

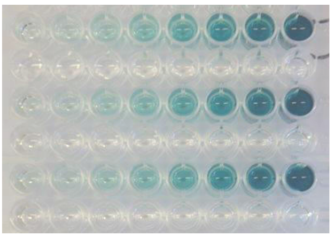

Figure 4.8. ABTS *in vitro* assay

3.6.1.2. DPPH assay

The radical-scavenging ability of the samples was also evaluated by *in vitro* 2,2-diphenyl-1-picrylhydrazyl (DPPH, **Fig. 3.9 A**) neutral radical and Trolox was used as standard. DPPH test is rapid, simple and inexpensive in comparison to other assays. The method is based on the reduction of the neutral DPPH solution in the presence of a hydrogen donating antioxidant, due to the formation of the non-radical form DPPH-H during the reaction (**Fig. 3.9 B**). The samples were able to reduce the radical DPPH to the yellow coloured diphenylpicrylhydrazine in a concentration dependent manner.

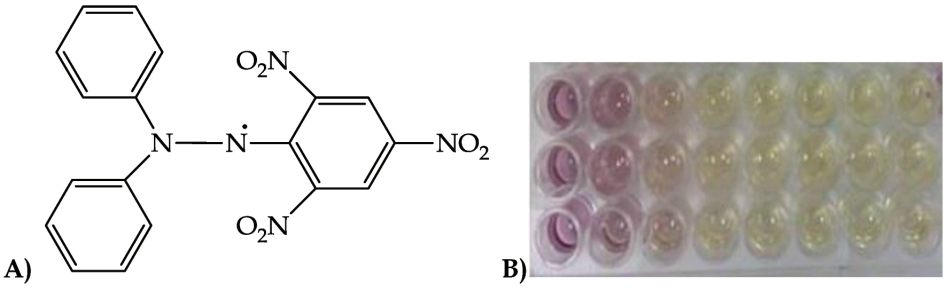

Figure 4.9. A) DPPH; **B)** DPPH *in vitro* assay

Different specie sample concentrations were added (50 µL of sample) in 200 µL of DPPH and left in the dark. The reaction was monitored at 515 nm after 30 minutes and the data were expressed as milligrams of Trolox Equivalents per gram of dried sample (mg TE/g) (Milella, Bader *et al.* 2014).

3.6.1.3. Super Oxide anion scavenging activity (SO)

Superoxide anion radicals ($O_2^{\cdot -}$) were generated *in vitro* by the NADH/PMS system as described by Russo *et al.* (Russo, Malafronte *et al.* 2015). The reduction of NBT by NADH is mediated through PMS under the aerobic conditions (**Fig. 3.10**). PMS is an electron acceptor and carrier in enzyme systems. The superoxide-scavenging ability of samples was quantified by their ability to inhibit NBT reduction. PMS oxidizes NADH and subsequently reduces O_2 to form $O_2^{\bullet -}$. The $O_2^{\bullet -}$, in turn, reduces NBT to a blue formazan, which can be quantified spectrophotometrically.

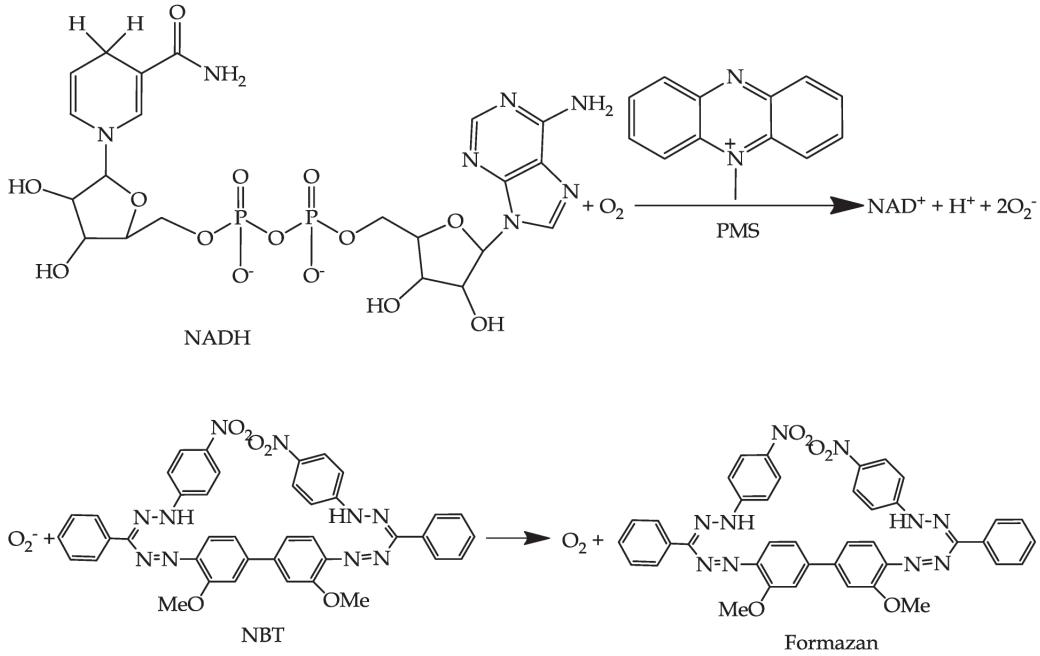

Figure 4.10. Reduction of NBT by NADH

Sample (40 µL) or phosphate buffer as negative control, NBT (130 µL) and NADH (40 µL) were put in the 96-well plate. The reaction was started by adding of PMS (40 µL) to the mixture. The scavenging activity of samples on the inhibition of formazan formation was monitored at 560 nm by spectrophotometer for 2 minutes and ascorbic acid (**Fig. 3.11**) was used as positive control. The results were expressed as the concentration inhibiting 25% of radical inhibition in mg/mL (IC_{25}), in case 50% IC_{50} was not reachable.

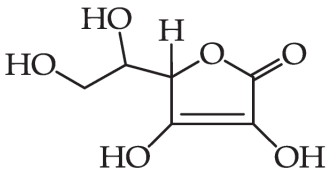

Figure 4.11. Ascorbic acid

3.6.1.4. Nitric Oxide radical scavenging activity (NO)

The nitric oxide ($^{\cdot}NO$) was spontaneously generated *in vitro* at physiological pH from nitroprusside (SNP). SNP solution (6 mg/mL, 80 µL) was prepared in phosphate buffer (KH_2PO_4 100 mM, pH 7.40) and mixed with 90 µL of different concentrations of sample, in a 96-wells plate. The mixture was further incubated at room temperature for 1 h under light. Then, the nitric oxide interacts with oxygen to give nitrite ions that can be determined spectrophotometrically by 80 µL Griess reagent (1:1 mixture (v/v) of 1% sulfanilamide and 0.10% *N*-(1-naphthyl) ethylenediamine in 2% H_3PO_4). The Griess reaction (**Fig. 3.12**) is based on the two-step diazotization reaction in which acidified NO_2^- produces a nitro sating agent, which reacts with sulfanilic acid to produce the diazonium ion. This ion is then coupled with *N*-(1-naphthyl) ethylenediamine to form the chromophoric azo-derivative which absorbs light at 560 nm. For this reason, the absorbance was read at 560 nm after 10 min of further incubation in the dark (Russo, Valentão *et al.* 2015).

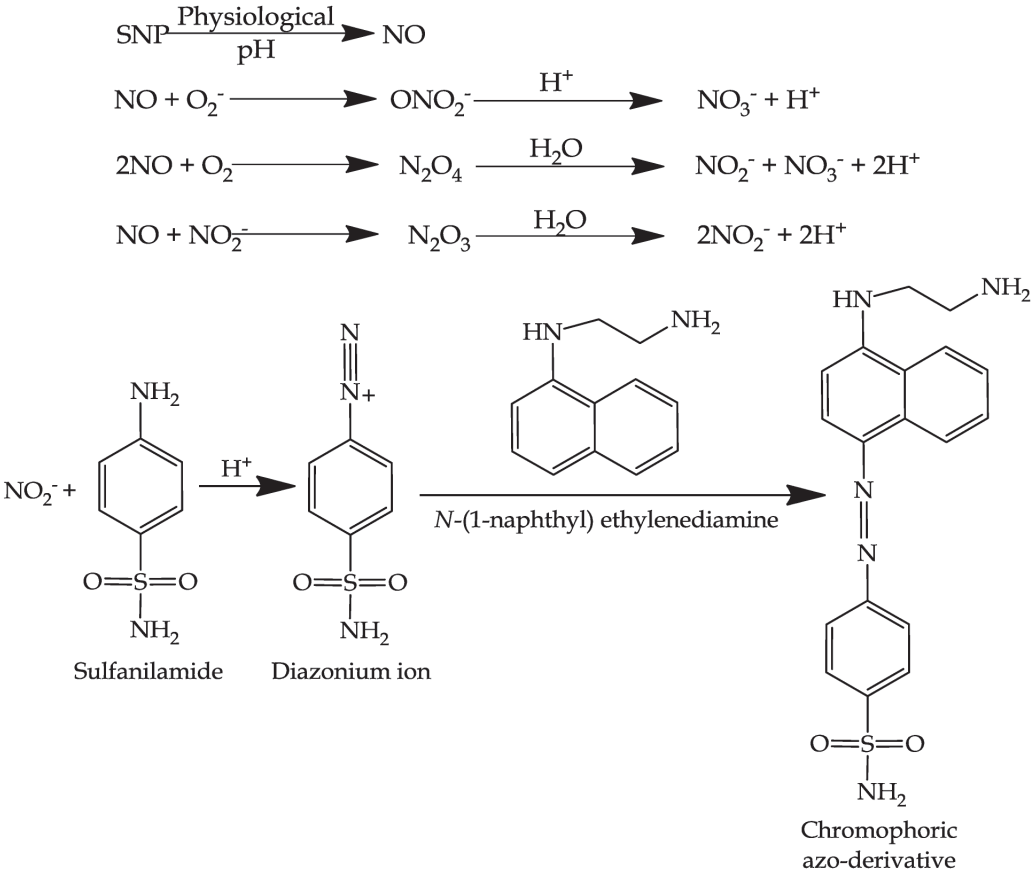

Figure 4.12. Griess reaction

Results were expressed as the concentration of the sample required to inhibit the activity of the radical by 25% (IC_{25}) in mg/mL (in case 50% IC_{50} was not reachable) and ascorbic acid was used as positive control.

3.6.2. Ferric Reducing Antioxidant Power assay (FRAP)

The FRAP assay is based on the reduction of the Fe^{3+} complex of tripyridyltriazine $[Fe(III)(TPTZ)_2]^{3+}$ to Fe^{2+} complex $[Fe(II)(TPTZ)_2]^{2+}$, intensely blue coloured by antioxidants present in acidic medium (**Fig. 3.13**).

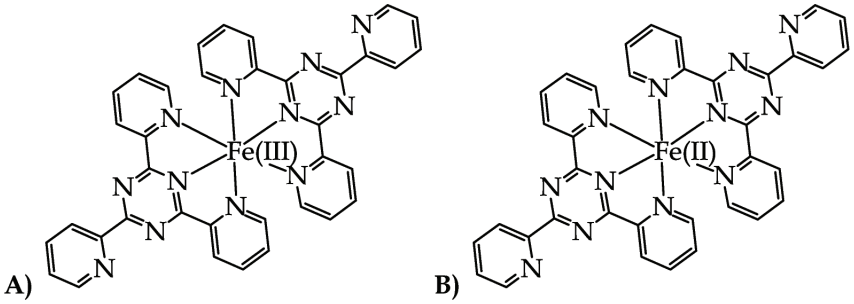

Figure 4.13. A) $[Fe(III)(TPTZ)_2]^{3+}$; **B)** $[Fe(II)(TPTZ)_2]^{2+}$

The FRAP reagent was prepared fresh before the experiment by mixing 300 mM sodium acetate buffer at pH 3.60, 20.00 mM $FeCl_3{*}6H_2O$ in distilled water and 10.00 mM TPTZ in 40.00 mM HCl in a ratio of 10:1:1.

Specie samples (25 µL) were allowed to react with 225 µL of the FRAP solution for 40 min at 37°C. The reaction (**Fig. 3.14**) was monitored at 593 nm and Trolox was used as reference antioxidant standard. The FRAP values were expressed as milligrams of Trolox Equivalents per gram of dried sample (mg TE/g) (Dekdouk, Malafronte *et al.* 2015).

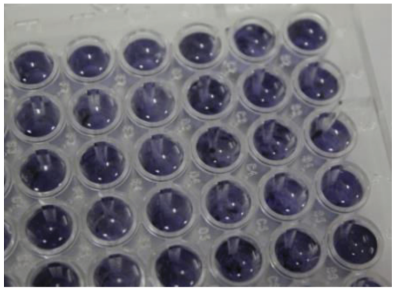

Figure 4.14. FRAP *in vitro* assay

3.6.3. *β*-Carotene Bleaching assay (BCB)

The inhibition of lipid peroxidation was evaluated by the *β*-Carotene Bleaching method (BCB) (Fidelis, Faraone *et al.* 2018). *β*-Carotene (0.20 mg) (**Fig. 3.15 A**) in 0.20 mL of chloroform), linoleic acid (20 mg, **Fig. 3.15 B**) and Tween 20 (200 mg) were mixed. Rotary evaporator at 37°C was used to remove the chloroform. Then, distilled water (50 mL) was added. The *β*-Carotene emulsion (950 µL) was mixed with 50 µL of sample at initial concentration of 1 mg/mL and BHT (**Fig. 3.15 C**) was used as positive control. The solution (250 µL) was transferred into a 96-well plate and outer wells were

filled with 250 µL of water to provide a large thermal mass because the reaction was temperature-sensitive and close temperature control throughout the plate was essential in this assay (MikaMi, YaMaguChi *et al.* 2009). Then, the microplate was placed at 50°C for 3 h and the absorbance was measured at 470 nm at 0′, 30′, 60′, 90′, 120′, 150′ and 180′. The results were expressed as percentage of *β*-Carotene Bleaching inhibition (% Antioxidant Activity, %AA). During the reaction, the present antioxidants transfer hydrogen atoms to the peroxyl radicals obtained from the oxidation of linoleic acid and convert them to hydroperoxides leaving *β*-carotene molecules intact.

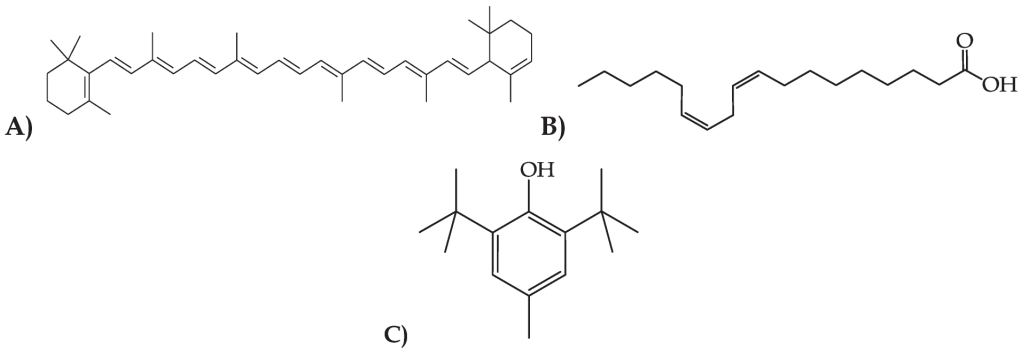

Figure 4.15. A) *β*-Carotene; **B) L**inoleic acid; **C)** BHT

3.6.4. Relative Antioxidant Capacity Index (RACI)

RACI is a statistic method for the integration of the results obtained from different *in vitro* antioxidant assays. This dimensionless index allows the comparison of the antioxidant capacity derived from different methods, but also provides a more comprehensive comparison. In fact, no single chemical test can give a total sample antioxidant capacity. However, it is impossible to get a mean value for the sample as the units and the scale of each chemical method is different. RACI is a standard score, derived by subtracting the mean (μ) from the raw data (χ) divided by the standard deviation (δ). The standard score is thus calculated as follows: $(\chi - \mu)/\delta$.

The standard score represents the distance between the raw data and the mean in units of the standard deviation, which is negative when the raw data are smaller than the mean and positive when larger.

RACI value was created by averaging the standard scores transformed from the raw data generated with different antioxidant methods. After data transformation, the standard scores (without any units) from various methods with different distributions

will have similar normal distributions with a mean of 0 and variance of 1. RACI calculation uses all data derived from *in vitro* assays to determine antioxidant activity. Also the total content of polyphenols was included because the principle involves an electron-transfer reaction between phenolic compounds and molybdenum under alkaline conditions, resulting in the formation of blue complexes that can be detected spectrophotometrically at 723 nm (Milella, Bader *et al.* 2014). Results of antioxidant activity expressed as IC_{25} or IC_{50} were converted in $1/IC_{25}$ and $1/IC_{50}$. The final data of RACI were represented into a histogram.

3.7. Potential antidiabetic activity

The deficiency in insulin secretion and/or action gives derangement in carbohydrate, fat and protein metabolism typical of the diabetes mellitus disease. In the pancreatic juice was prominent the *a*-amylase enzyme which breaks down large and insoluble starch molecules into absorbable molecules and then in maltose. Instead, the *a*-glucosidase enzyme is anchored in the mucosal brush border of the small intestine and catalyzes the end step of digestion of starch and disaccharides (**Fig. 3.16**).

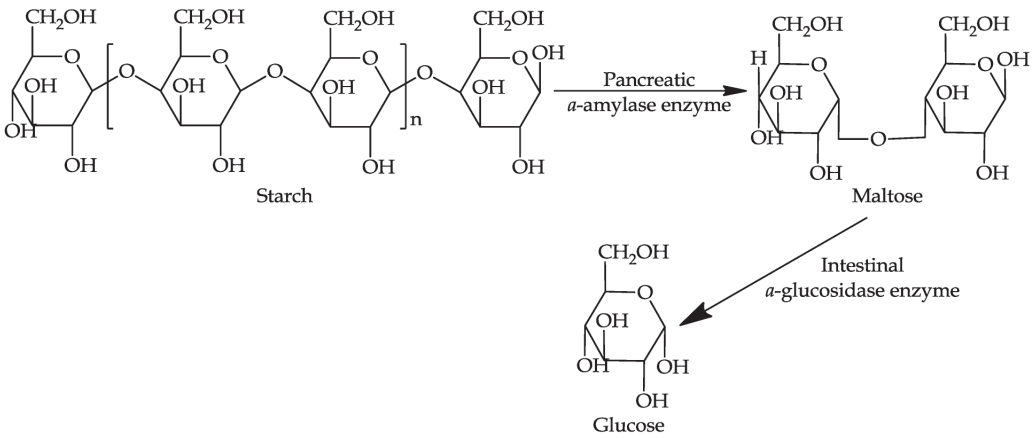

Figure 4.16. *a*-Amylase and *a*-glucosidase enzymes

For these reasons, the inhibitory ability of samples against *a*-amylase and *a*-glucosidase enzymes involved in diabetes were screened. In fact, the inhibitors of *a*-amylase and *a*-glucosidase enzymes were used in diabetes patients because delay the breakdown of carbohydrate in the small intestine and decrease the postprandial blood glucose excursion levels in diabetic patients. The inhibition of these enzymes has been

found as a useful and effective strategy to lower the levels of postprandial hyperglycaemia (Saltos, Puente *et al.* 2015).

3.7.1. *a*-Amylase inhibition

a-Amylase inhibition assay was performed using the method described by Milella *et al.* (Milella, Milazzo *et al.* 2016) with slight modifications (**Fig. 3.17**). Different concentrations of each sample (10 µL) and 10 µL of *a*-amylase enzyme from hog pancreas (50 units/mL of enzyme in 20.00 mM sodium phosphate buffer solution, pH 6.90 with 6.70 mM NaCl) were mixed in vials and incubated for 10 minutes at 25°C. After pre-incubation, 10 µL of substrate solution of 1% starch solution in sodium phosphate buffer were added to each vial, and the reaction mixture was again incubated for 10 minutes at 25°C. The yellow-orange 3,5-dinitrosalicylic acid colour reagent (20 µL) was added to stop the reaction. This reagent is an aromatic compound that reacts with reducing sugars released from starch hydrolysis and other reducing molecules to form 3-amino-5-nitrosalicylic acid, which absorbs strongly at 540 nm. Then, the vials were incubated for 10 minutes at 100°C. After cooling at room temperature, the reaction mixture was diluted with 300 µL of distilled water and the absorbance was measured. The absorbance of blank (the enzyme solution was added during the incubation at 100°C) and negative control (with the solvent used to solve the samples) was recorded. The final sample absorbance was determined at 540 nm by subtracting its corresponding blank reading. A widely used clinical antidiabetic drug, acarbose, was used as a positive control (**Fig. 3.18**). The results were expressed as IC_{50} in mg/mL on the basis of the concentration of the sample required to inhibit the activity of the enzyme by 50% calculated by nonlinear regression analysis.

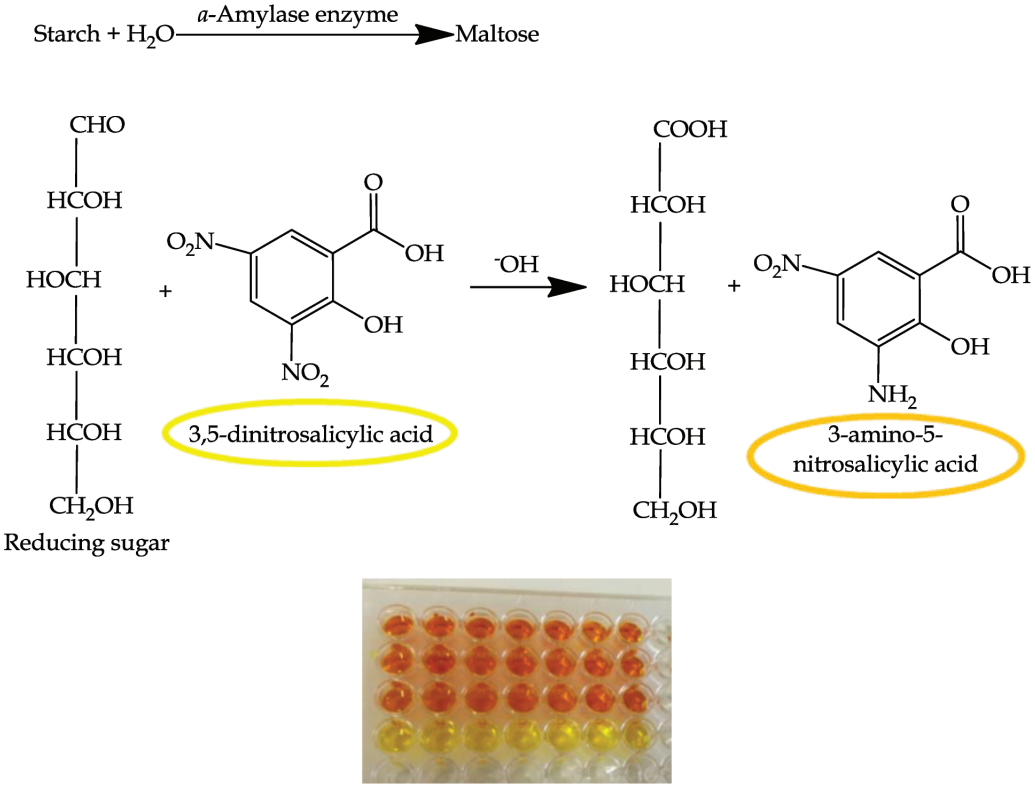

Figure 4.17. *a*-Amylase inhibition *in vitro* assay

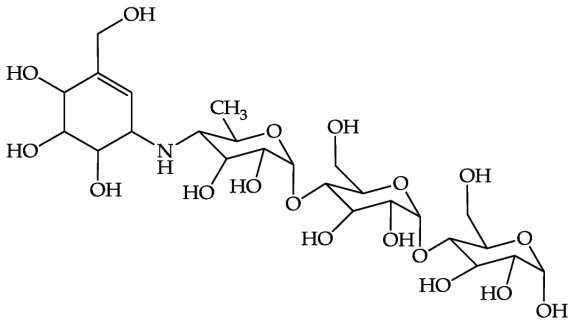

Figure 4.18. Acarbose

3.7.2. *a*-Glucosidase inhibition

The effect of samples on *a*-glucosidase enzyme was assessed in 96-well plates using a previously reported procedure (Saltos, Puente *et al.* 2015). In each well, different concentrations of sample (40 µL) were added to 130 µL of 10.00 mM phosphate buffer, pH 7.00, and 60 µL of 2.50 mM 4-*p*-nitrophenyl-*a*-D-glucopyranoside in 10.00 mM phosphate buffer. The addition of the 0.28 U/mL of enzyme (20 µL) initiated the reaction and the plates were incubated at 37ºC for 10 minutes.

The release of glucose and *p*-nitrophenol (yellow) by *a*-glucosidase enzyme (**Fig. 3.19**) is monitored spectrophotometrically by an absorbance increase measured at 405 nm after 10 minutes of incubation (T 10'), respect the absorbance measured before the addition of the enzyme (T 0'). Acarbose was used as positive control. The results were expressed as IC_{50} on the basis of the concentration of the sample required to inhibit the activity of the enzyme by 50% calculated by nonlinear regression analysis.

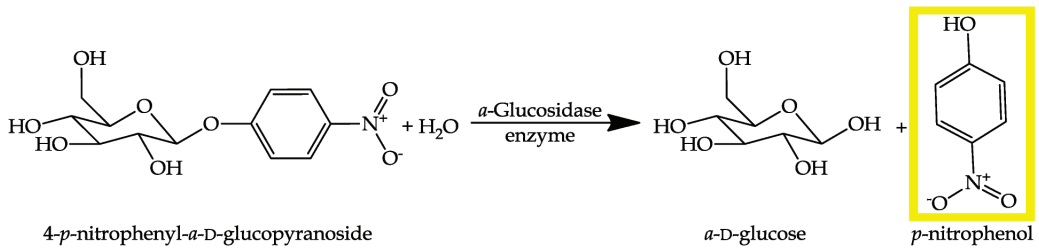

Figure 4.19. *a*-Glucosidase inhibition *in vitro* assay

3.8. Anticholinesterase activity

Parkinson's and Alzheimer's diseases (AD) are neurodegenerative disorders characterized by widespread loss of central cholinergic function. The central nervous system is vulnerable to free radical damage as a result of the brain's high oxygen consumption rate, its abundant lipid content, and the relative paucity of antioxidant enzymes compared with other tissues (Markesbery 1997; Markesbery 1999). In particular, the decrease of acetylcholine (ACh) in the brain brings the impossibility for the neuron to transmit nerve impulses and then death of the same, with a progressive atrophy of the brain.

The only symptomatic treatment proven effective to date is the use of cholinesterase (ChE) inhibitors to augment the surviving cholinergic activity. ChE inhibitors act on the enzymes that hydrolyse acetylcholine (ACh) following synaptic release. This results in increased acetylcholine in the synaptic cleft and increased availability of ACh for postsynaptic and presynaptic nicotinic (and muscarinic) ACh receptors.

There are two prevalent forms of ACh in a healthy brain:

- acetylcholinesterase (AChE) predominates (80%)

- butyrylcholinesterase (BChE) plays a minor role in regulating brain ACh levels, but it may have a role in the aetiology and progression of AD.

In the AD brain, BChE activity rises, while AChE activity remains unchanged or declines. Inhibiting AChE and BChE give elevate ACh level and this is one of the most effective treatment strategies suggested to AD. The most frequently used drugs to treat patients with mild to moderate AD are donepezil, rivastigmine, and galantamine.

Several methods for screening of ACh inhibitory activity from plant species resources has been reported based on Ellman's reactions (Russo, Valentão *et al.* 2015). The easy assay based on Ellman's method uses an alternative substrate of acetylcholine and 5,5'-dithio-bis-2-nitrobenzoic acid (DTNB). The DTNB is a versatile water-soluble compound used to quantitating free sulfhydryl groups in solution by the measurable yellow-colored product when it reacts with sulfhydryls. In fact, the DTNB reacts with a free sulfhydryl group to yield a mixed of disulfide and 2-nitro-5-thiobenzoic acid (TNB). DTNB target in this reaction is the conjugate base (R—S-) of a free sulfhydryl group. Therefore, the rate of this reaction is dependent on several factors: the reaction pH, the pKa of the sulfhydryl and steric and electrostatic effects. In the *in vitro* assays, acetylcholinesterase (AChE) and butyrylcholinesterase (BChE) efficiently catalyze the hydrolysis of acetyl- (**Fig. 3.20 A**) and butyryl-thiocholine (**Fig. 3.20 B**) -sulfur analogs of their respective natural substrate, acetylcholine.

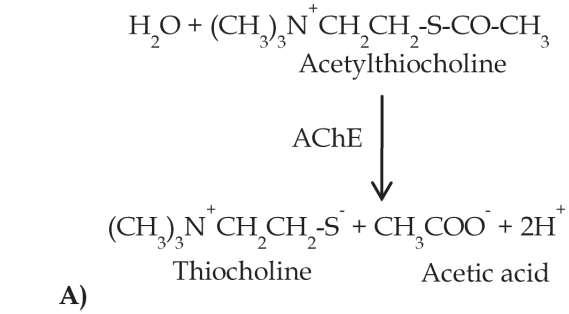

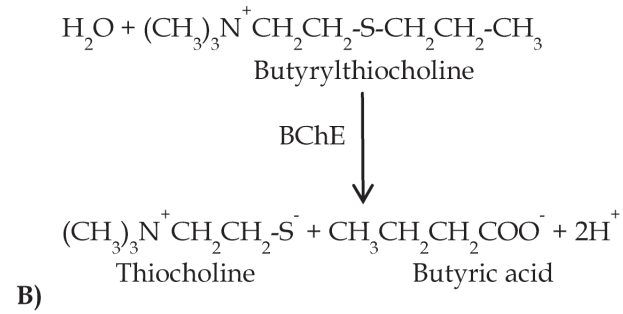

Figure 4.20. A) Hydrolysis of acetyl-thiocholine; **B)** Hydrolysis of butytyl-thiocholine

Upon hydrolysis, these substrate analogs produce acetate (or butyrate) and thiocholine. The thiocholine in the presence of the dithio-bis-nitro-benzoate (DTNB) ion reacts to generate the yellow 5-thio-2-nitrobenzoate anion (**Fig. 3.21**). The yellow colour can be quantified by its absorbance at 405 nm.

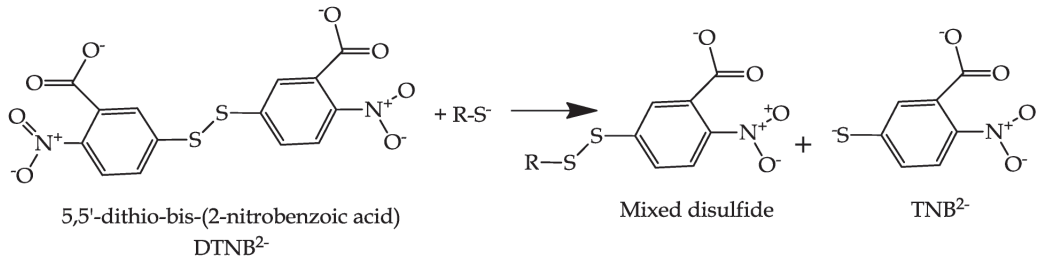

Figure 4.21. Reduction of Ellman's reagent

In particular in AChE inhibition *in vitro* assay, different concentrations of sample (25 µL), buffer B (50.00 mM Tris-HCl, pH 8.00 containing 0.10% BSA, 25 µL), 3.00 mM DTNB (125 µL) and 15.00 mM acetylthiocholine iodide (25 µL) were mixed.

The reaction was started by adding 0.18 U/mL of AChE enzyme (25 µL). The absorbance was measured at 405 nm for 2 minutes.

The BChE inhibition *in vitro* assay was performed in a similar way by using 25 µL of 15.00 mM butyrylthiocholine iodide as substrate and 0.10 U/mL of BChE enzyme.

Galantamine (**Fig. 3.22**) was used as standard for its capacity to inhibit both enzymes involved in the treatments of Parkinson's and Alzheimer's diseases. The results were expressed on the basis of the concentration of the sample required to inhibit the activity of the enzyme by 50% (IC_{50}) in mg/mL calculated by nonlinear regression analysis (Russo, Valentão *et al.* 2015).

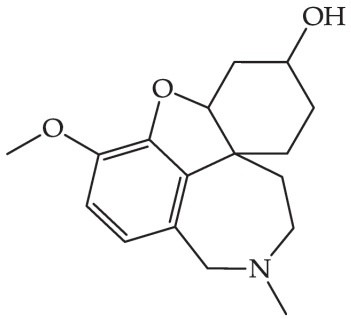

Figure 4.22. Galantamine

3.9. Identification and quantification by liquid chromatography mass spectrometry

This part of my PhD project was made during my abroad training in Teagasc Food Research Centre under the supervision of Professor Dilip K. Rai in Ashtown, Dublin, Ireland.

3.9.1. LC-MS/MS characterization of samples

LC-MS characterization was carried out on a Q-Tof Premier mass spectrometer (Waters Corporation, Milford, MA, USA) coupled to an Alliance 2695 HPLC system (Waters Corporation, Milford, MA, USA) as previously described (Rico, Diana *et al.* 2018). Accurate mass measurements of analytes were achieved through the use of an internal reference compound (Leucine-Enkephalin).

The separation of the compounds was performed on an Atlantis T3 C18 column (Waters Corporation, Milford, USA, 100 mm x 2.10 mm; 3 µm particle size) maintained at 40°C and using 0.10% aqueous formic acid (solvent A) and 0.10% formic acid in

acetonitrile (solvent B). A stepwise gradient from 10% to 90% solvent B was applied at a flow rate of 0.30 mL/min for 25 minutes. Electrospray mass spectra data were acquired on a negative ionization mode for a mass range *m/z* 100 to *m/z* 1000. Cone voltage and capillary voltage were set at 30 V and 3 kV, respectively. Collision induced fragmentation (CID) of the analytes was achieved using 12 eV to 30 eV energy with argon as the collision gas.

3.9.2. UHPLC-MS/MS quantification of compounds

For the quantification of the compounds in the selected samples, Waters Acquity (Waters Corporation, Milford, MA) ultra-high performance liquid chromatography coupled with tandem mass spectrometry (UHPLC-MS/MS) was used.

The compounds were separated on a Waters Acquity HSS T3 C18 column (2.10 x 100 mm; 1.80 µm particle size) using a binary solvent system (**Tab. 3.1**).

Table 4.1. Solvent gradient program used for elution during UHPLC-MS/MS analysis

Time (min.)	Flow rate (mL/min)	% Mobile phase A[a]	% Mobile phase B[b]
0-2.50	0.50	98	2
2.50-3.00	0.50	90	10
3.00-7.50	0.50	85	15
7.50-8.50	0.50	65	35
8.50-9.50	0.50	2	98
9.50-10.00	0.50	98	2

[a]Mobile phase A consisted of water containing 0.10% formic acid; [b]Mobile phase B consisted of acetonitrile containing 0.10% formic acid

The injection volume for all samples and standards was 3 µL. All standards in the concentration ranging from 0.01 to 50 µg/mL were dissolved in 80% methanol. Multiple reaction monitoring (MRM) quantification method was developed for each standard compound using the Waters Intellistart software, and the quantifications of the data were carried out using the Waters TargetLynx™ software. The ionization source conditions were as follows: capillary voltage 3 kV, cone voltage 35 V, source temperature 150°C, desolvation temperature 350°C, desolvation gas flow 200 L/h, cone gas flow 50 L/h, and collision gas flow 0.10 mL/min. The column temperature was maintained at 40°C.

3.10. Biological activity on cell lines

This part of my PhD project was made in collaboration with IRCCS "Referral Cancer Center of Basilicata" (CROB) under the supervision of Dr. Pellegrino Musto in Rionero in Vulture, Potenza, Italy and with laboratory of Professors Maria Francesca Armentano and Faustino Bisaccia.

3.10.1. Cell lines

3.10.1.1. Healthy donors and Multiple Myeloma (MM) cell lines

Peripheral blood was drawn from five healthy subjects gave informed consent. The blood samples were collected by Ficoll-hypaque gradient separation, and put into EDTA tubes and PBMCs.

Multiple Myeloma (MM) is the second most common hematologic malignancy and to date it remains incurable, although the development of novel agents has improved survival of patients.

MM cell lines, SKMM1, RPMI8226 and MM1S, were purchased from the American Type Culture Collection (ATCC) and cultured in RPMI1640 supplemented with 10% FBS and 1% of penicillin/streptomycin. All cells were grown at 37°C in 5% CO_2.

All selected samples of *Azorella glabra* were dissolved in DMSO at the stock solution of 30 mg/mL and then diluted in fetal bovine serum (FBS) for cell treatments. The final DMSO concentration in the cultures was no greater than 0.50% (Lamorte, Faraone *et al.* 2018).

3.10.1.2. The normal human dermal fibroblasts and HepG2 cell line cell lines

The normal human dermal fibroblasts (adult, HDFa, Life Technologies) were cultured in *Dulbecco's Minimum Essential Medium* (DMEM, supplemented with 10% FBS, 5% of glutamine, 5% of penicillin-streptomycin and 1% of nonessential amino acids (NEA)).

The human hepatocellular carcinoma cell line HepG2 cells were cultured in DMEM with 10% fetal bovine serum (FBS), 5% of glutamine, and 5% of penicillin-streptomycin.

Both the cell lines were maintained at 37°C in a humidified atmosphere containing 5% CO_2 (Armentano, Bisaccia *et al.* 2015).

The selected sample (*Senecio clivicolus* ethyl acetate fraction) was dissolved in DMSO at the stock solution of 110 mg/mL and then diluted in FBS for cell treatments. The final DMSO concentration in the cultures was no greater than 0.80%.

3.10.2. Cell viability assays

Cell-based assays (Riss Terry L. 2013) are used to determine if tested samples have effects on cell proliferation or show direct cytotoxic effects that lead to cell death. At the end of the experiment, it is very important to know how many viable cells are remaining. There are a variety of assay methods that can be used to estimate the number of viable eukaryotic cells. Under most standard culture conditions, the signal of incubated substrate is proportional to the number of present viable cells.

The viable cells were detected by different tetrazolium compounds, the most commonly used compounds are: MTT, MTS, XTT and WST-1.

In particular, it is possible divide these compounds into two basic categories:

1) the positively charged MTT, which readily penetrates viable eukaryotic cells;

2) the negatively charged MTS, XTT, and WST-1, which do not readily penetrate cells. They are used with an intermediate electron acceptor that can transfer electrons from the cytoplasm or plasma membrane to facilitate the reduction of the tetrazolium into the coloured formazan product.

3.10.2.1. MTT assay

The colorimetric MTT (3-(4,5-dimethylthiazol-2-yl)-2,5-diphenyltetrazolium bromide) assay (Laurenzana, Caivano *et al.* 2016; Laurenzana, Caivano *et al.* 2016) was used to assess cell viability.

This assay was the first cell viability assay developed for a 96-well format that was suitable for high throughput screening (HTS). The MTT substrate is added to cells in culture and incubated for 1 to 4 hours. Viable cells convert MTT into a purple

formazan product (**Fig. 3.23**). The quantity of formazan (presumably directly proportional to the number of viable cells) is measured by recording changes in absorbance at 570 nm using a plate reading spectrophotometer. The cells die lose the ability to convert MTT into formazan. In particular, the NAD(P)H-dependent cellular oxidoreductase enzymes reflect the present number of viable cells. These enzymes are capable of reducing the tetrazolium dye MTT to its insoluble purple formazan ((*E*,*Z*)-5-(4,5-dimethylthiazol-2-yl)-1,3-diphenyl formazan). The formazan product is an insoluble precipitate that accumulates in cells near the cell surface and in the culture medium. Prior to absorbance readings, the formazan must be solubilised (Riss Terry L. 2013).

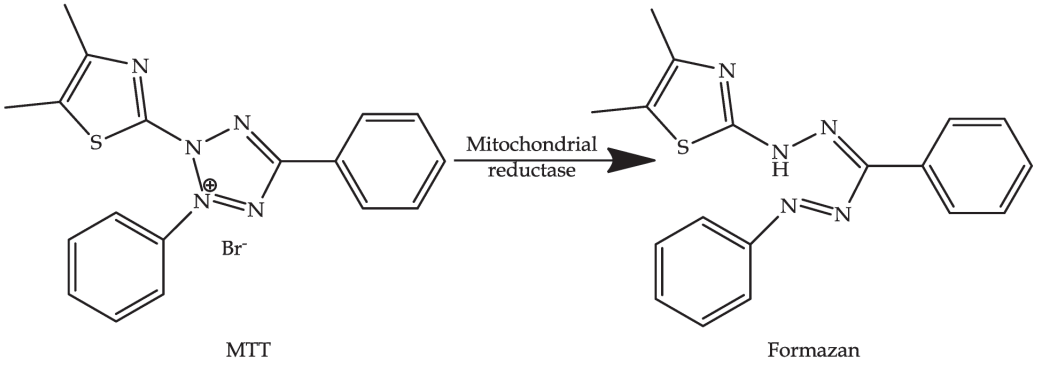

Figure 4.23. Mitochondrial reduction of MTT salt in formazan

In particular, HepG2 and normal human dermal fibroblast cell lines were seeded into 96-well plates (1500 cells/well). After 24 h of incubation at 37°C and 5% of CO_2, the cells were treated with sample (ethyl acetate fraction of *Senecio clivicolus*) at different concentrations (100, 200, 300, 400, 500, 600, 800 and 1000 µg/mL) and incubated for 24. The optical density was measured at 492 nm. All experiments were conducted in triplicate. Then, the phosphate buffered saline (PBS) was used to make two washes and 15 µL of MTT (5 mg/mL diluted in 85 µL of DMEM medium) were added in each well. The plate was incubated in the dark for 4 h at 37° C and 5% CO_2. Finally, the stop solution (100 µL of DMSO/isopropanol 1:1, Triton 1%) was added and the plate was incubated for another hour at 37°C and at 5% CO_2. The absorbance was determined at 560 nm, subtracting the value at 670 nm on Glomax Multi Detection System (Promega).

3.10.2.2. MTS assay

Cell viability was also assessed using the MTS (3-(4,5-dimethylthiazol-2-yl)-5-(3-carboxymethoxyphenyl)-2-(4-sulfophenyl)-2*H*-tetrazolium) assay (Riss Terry L. 2013; Laurenzana, Caivano et al. 2016; Laurenzana, Caivano et al. 2016). The tetrazolium reagents, in the presence of phenazine methosulfate (PMS), can be reduced by viable cells to generate formazan products which are directly soluble in cell culture medium. Tetrazolium compounds fitting this category include MTS, XTT, and the WST series (18-23). These reagents eliminate a step during the assay procedure because is not needed to solubilize formazan precipitates, thus making the protocols more convenient. Intermediate electron acceptor pheazine ethyl sylfate (PES) transfers electron from NADH in the cytoplasm to reduce MTS in the culture medium into an aqueous soluble formazan (**Fig. 3.24**).

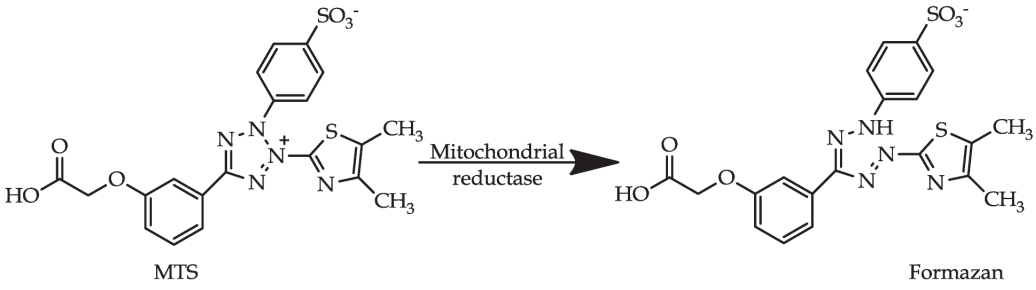

Figure 4.24. Mitochondrial reduction of MTS salt in formazan

In brief, cells were seeded into 96-well plates (3 x 10^4 cell/100 µL medium), treated with samples of *Azorella glabra* at different concentrations (10, 50, 100 and 150 µg/mL) and incubated for 24, 48 and 72 h. The optical density was measured at 492 nm. All experiments were conducted in triplicate. Cell viability was calculated as percentage of MM viable cells in samples *vs* DMSO treated cells. The EC_{50} was determined by GraphPad Prism (GraphPad Prism, San Diego, CA).

3.10.3. Apoptosis assays

Different methods are used for identification of apoptotic cells and the analysis of the morphological, biochemical and molecular changes that take place during this biological process. Apoptotic cells have reduced DNA content and morphological changes as nuclear condensation. The phosphatidyl serine on the plasma membrane

reacts with Annexin V-fluorochrome conjugates give changes in plasma membrane composition and function. The best-recognized biochemical hallmarks of apoptosis are the activation of cysteine proteases (caspases), condensation of chromatin and fragmentation of genomic DNA into nucleosomal fragments. Finally, the Bcl-2 family proteins and the mitochondria play an important role in apoptosis process that can be recognized by translocation of apoptogenic factors, such as Bax and cytochrome *c*, in and out of mitochondria (Oancea, Mazumder *et al.* 2006).

3.10.3.1. Annexin V/7-AAD staining assay

The percentage of cells undergoing apoptosis and necrosis after treatment with different concentrations of sample was quantified using FITC Annexin V-7-AAD kit (BD Pharmingen).

HepG2 cells were seeded at a density of 2×10^5 cells/well in 12-well plates and incubated for 24 h at 37°C and 5% CO_2. Then, they were treated with different concentrations of ethyl acetate fraction of *Senecio clivicolus* (100, 200, 300, 600 and 900 μg/mL) for 24 h. The cells were harvested and resuspended in binding buffer and finally 5 μL of AnnexinV-FIT C and 5 μL of 7-AAD were added. Each tube was incubated in the dark for 15 minutes at room temperature. The stained cells were analysed on a FACS Canto II flow cytometer (Armentano, Bisaccia *et al.* 2015).

Moreovers, MM cells were placed in a 6-well culture plate at density of 4×10^5 cell/well, treated with 50 µg/mL of *Azorella glabra* samples and incubated for 24 and 48 h. After treatment, cells were harvested, washed and resuspended in Annexin V binding buffer (Trino, Iacobucci *et al.* 2016). Next, cells were labeled with 5 µL of FITC Annexin V and 5 µL of propidium iodide (PI). Stained cells were incubated at dark for 15 minutes and 1×10^4 events were acquired using NAVIOS flow cytometer and analysed by Kaluza 2.0 software (Beckman Coulter, Life Sciences, Indianapolis, United States). Both single positive for Annexin V and double positive for Annexin V and propidium iodide (PI) cells were interpreted as signs of early and late phases of apoptosis, respectively.

3.10.3.2. Observation of morphological changes

The observation of morphological changes was done in two modes.

The HepG2 cells were cultured as above, seeded in 12-well plates at a density of 2 × 10^5 cells per well, and treated with *Senecio clivicolus* sample at different concentrations (100, 200, 300, 400, 500, 600, 800, 1000 μg/mL) for 24 h at 37°C and 5% CO_2. The cellular morphology was observed using inverted phase contrast microscopy (Nikon Eclipse TS100) (Armentano, Bisaccia *et al.* 2015).

Apoptosis was also determined by the assessment of nuclear morphology using Hoechst 33258 DNA staining. This fluorophore binds the minor groove of the double-stranded DNA. Its accumulation in cells highlights the morphological changes of apoptotic cells, such as condensation of chromatin and cellular fragmentation. The cells were seeded at a density of 2 × 10^5/well in 12-well plates and incubated for 24 h at 37°C and 5% CO_2. Then, they were treated for 24 h with different concentrations of the *S. clivicolus* sample (100, 200, 300, 400, 500, 600, 800 and 1000 µg/mL). After treatment, the cells were fixed with 4% *p*-formaldehyde for 20 minutes at room temperature, washed with PBS, and stained with 10 μg/mL Hoechst 33258 at room temperature for 10 min in the dark. The cells were washed with PBS for morphological observation by fluorescence microscopy (Nikon Eclipse 80i).

3.10.4. Cell cycle analysis

The cell cycle can be analysed by flow cytometry. One method is based on the analysis of cellular DNA content following cell staining with either propidium iodide (PI) and deconvolution of the cellular DNA content frequency histograms. This assay reveals distribution of cells in three major phases of the cycle (G_1 *vs* S *vs* G_2/M) and makes it possible to detect apoptotic cells with fractional DNA content.

In particular, after treatment with 50 µg/mL of *A. glabra* sample for 24 and 48 h, MM cells were harvested, washed and fixed in cold ethanol 70% for 1 h. Fixed cells were then labeled with PI/RNase staining solution for 30 min at room temperature in the dark (Russo, Malafronte *et al.* 2015; Trino, Iacobucci *et al.* 2016). A total of 1 x 10^4 events were acquired by Navios flow cytometer and analyzed by Kaluza 2.0 software (Beckman Coulter).

3.10.5. Cell migration assay

Migration is a key property of live cells and critical for normal development, immune response, and disease processes such as cancer metastasis and inflammation (Justus, Leffler *et al.* 2014).

In particular, for these migration studies were inserted trans well inserts with 8 µm pores into a 24-well plates. The cell Ts RPMI8226 (1 x 10^5) treated with 50 µg/mL of *A. glabra* sample and with DMSO control were seeded into the inserts in 300 µL of serum-free RPMI1640 medium. 500 µL of RPMI1640 medium with 10% FBS were placed in the single well of a 24 well plate. After 24 h of incubation, cells that migrated into the lower chamber were counted. Triplicates of each experiment were performed.

3.10.6. Measurement of Reactive Oxygen Species (ROS) generation and mitochondrial membrane potential ($\Delta\Psi_m$)

The carcinogenesis is associated with elevated levels of intracellular free radicals (ROS/RNS) and an increased basal oxidative stress (Armentano, Bisaccia *et al.* 2015). Proton pumps generate the mitochondrial membrane potential ($\Delta\Psi_m$) that is an essential component in the process of energy storage during oxidative phosphorylation. The levels of $\Delta\Psi_m$ and ATP in the cells are kept relatively stable and changes may be deleterious. A long-lasting drop or rise of $\Delta\Psi_m$ against normal levels may induce unwanted loss of cell viability and be a cause of various pathologies (Zorova, Popkov *et al.* 2018).

The 2.5 x 10^5 RPMI8226 cells were treated with with 50 µg/mL of *A. glabra* sample and used to measure ROS and $\Delta\Psi_m$ values, as reported in the following paragraphs.

3.10.6.1. ROS generation

The level of intracellular ROS was determined following the method reported by Armentano *et al.* with slight modification (Armentano, Bisaccia *et al.* 2015). The intracellular level of ROS was determined using the 2',7'-dichlorofluorescein diacetate (DCFH-DA), a cell permeable fluorogenic probe. This molecule is deacetylated by intracellular esterases and converted to nonfluorescent dichlorodihydrofluorescein

(DCFH), which is oxidized rapidly to the highly fluorescent compound dichlorofluorescein (DCF) in the presence of ROS (**Fig. 3.25**).

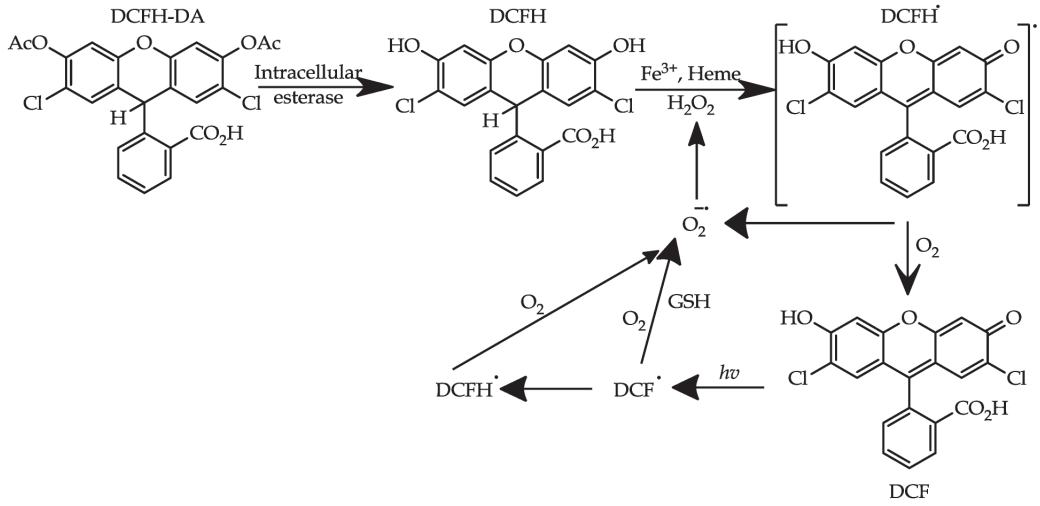

Figure 4.25. From DCFH-DA to DCF

HepG2 and fibroblast cells were seeded into dark 24-well tissue culture plates at a density of 2 × 10^5 cells/well and incubated for 24 h at 37°C and 5% of CO_2. Then, the cells were treated with different concentrations of *S. clivicolus* sample (100, 200, 300, 400, 500, 600, 800, 1000 μg/mL) for 3 h with and without incubation for 1 h with 10 mM *N*-acetylcysteine. Then, cells were stained with 10 μM DCFH-DA for 30 min at 37°C in the dark, added 150 µL of Trypsin-EDTA and 250 µL of DMEM medium. Then, they were washed three times with PBS. The fluorescence was measured by FACS Canto II flow cytometer and the data were analysed by DIVA software (BD Biosciences, San Jose, USA).

RPMI8226 cells were stained with 10 µM of DCFH-DA and incubated for 30 minutes at 37°C in the dark with *A. glabra* sample. The fluorescence was measured by FACS Canto II flow cytometer and the data were analysed by DIVA software (BD Biosciences, San Jose, USA).

3.10.6.2. $\Delta\Psi_m$ measurement

The levels of $\Delta\Psi_m$ were monitored by flow cytometry as reported by Armentano *et al.* (Armentano, Bisaccia *et al.* 2015). In brief, cells were incubated with 150 nM of tetra methyl rhodamine methyl ester (TMRM) in PBS for 20 min at 37°C in

the dark. The TMRM is a cationic fluorescent probe easily incorporated into the mitochondria of viable cells. Then, cells were analysed by FACS Canto II flow cytometer and data were analyzed by DIVA software.

3.10.7. Western blot analysis

Western blotting is used to identify specific proteins from a complex mixture of proteins extracted from cells. During the assay there is the proteins separation by size, transfer to a solid support and marking target protein using a proper primary and secondary antibody (Mahmood and Yang 2012).

A total of 2 x 10^6 of untreated, DMSO and 50 µg/mL of *A. glabra* sample treated RPMI8226 cells, were collected and lysed in buffer (50 mM Tris pH 7.40, 150 mM NaCl, 1% tergitol™ solution (NP40), 0.10% SDS, 0.50% sodium deoxycholate) supplemented with protease inhibitors cocktail (Sigma Aldrich, Milano-Italy), followed by centrifugation at 13000 g for 30 min at 4°C. The protein concentration in each sample was detected using the Bradford assay. Equal amount of sample lysate (80 µg) were separated by SDS-PAGE (4-8% for PARP and 4-15% for Bcl-2) and transferred to nitrocellulose membrane. Nonspecific binding sites were blocked with TBST buffer containing 5% non fat dry milk (NFM) at room temperature for 1 h. Subsequently, membranes were incubated with primary antibodies anti-PARP-1 (1:1000 in 5% NFM/TBST) and anti-Bcl-2 (1:200 in 5% NFM/TBST) overnight at 4°C. After incubation with HRP-conjugated anti-rabbit secondary antibody (1:10000), detection was performed using the enhanced chemiluminescence (ECL plus) kit.

HepG2 cells were seeded into 12-well plates at a density of 3 × 10^5 cells/well and then treated with 600 µg/mL of *S. clivicolus* sample (IC_{50} value at 24 h) for different time periods (3, 6 and 24 h). Cells were harvested, resuspended in ice-cold isotonic buffer (250 mM sucrose, 10 mM NaCl, 10 mM Tris-HCl, pH 7.50, and 1 mM EDTA), and homogenized using a glass Teflon homogenizer (35–40 times up and down). Unbroken cells and nuclei were sedimented by centrifugation at 1000 g for 10 minutes. Supernatants were centrifuged at 18000 g for 30 minutes. The supernatants (cytosolic fraction) were removed, and the mitochondrial pellets were resuspended in RIPA buffer (PBS pH 7.40, 1% NP-40, 0.50% sodium deoxycholate, and 0.10% sodium dodecyl sulfate) and supplemented with proteases and phosphatases inhibitor cocktail (*Protease Inhibitor Cocktail*, PIC Sigma). Protein concentration was measured using Bio-Rad Protein Assay (Bio-Rad, Hercules, CA, USA). Equal amounts of protein lysates were

resolved on 4–17% SDS PAGE and then blotted onto a nitrocellulose membrane (GE). The membrane was blocked with 5% non fat dry milk in TBST buffer (100 mM Tris-HCl pH 7.50, 150 mM NaCl, and 0.05% Tween 20) for 1 h and then incubated overnight at 4°C with primary antibody against cytochrome *c* (1:2000, Abcam). After that, the membrane was washed three times with TBST buffer and incubated at room temperature for 1 h with anti-mouse horseradish-peroxidase-conjugated secondary antibody (1:3000, Sigma). Detection was performed using the enhanced chemiluminescence (ECL) kit (GE).

3.11. *In Silico* methods (molecular modelling and docking calculations)

This part of my PhD project was made under the supervision of Professor Magnus Monné.

To understand inhibitory activities of identified terpenoids from *Minthostachys diffusa* on AChE and BChE, *in silico* molecular docking and conformational alignment studies were performed. In this mode, it is possible to rationalize and correlate the obtained experimental with the computational results, and to shed some lights into the various interactions between the ligands and the active sites of the enzymes. The molecular docking studies were performed by using Swiss-model and AutoDock 2 Vina.

Swiss-model is a bioinformatic structural program avaliable as a web server to create 3D structural homology models of proteins without known structures based on experimentally determined structures of homologs. On the web server, the protein sequences of the enzymes used *in vitro* assays were submitted and the program found possible structural templates, suggesting as top-hits (**Fig. 3.26**):

- AChE complexed with NAP from *Tetronarce californica* (PDBID: 1GQS) with 70% sequence identity with AChE used *in vitro* assay;

- BChE complexed with *N*-propargyliperidines from *Homo sapiens* (5LKR) with 91% sequence identity with BChE used *in vitro* assay.

In a second step, Swiss-model creates the coordinate files of the homology models by threading the proteins sequence of *Electrophorus electricus* AChE and equine BChE into the two top-hit templates listed above, followed by energy minimization.

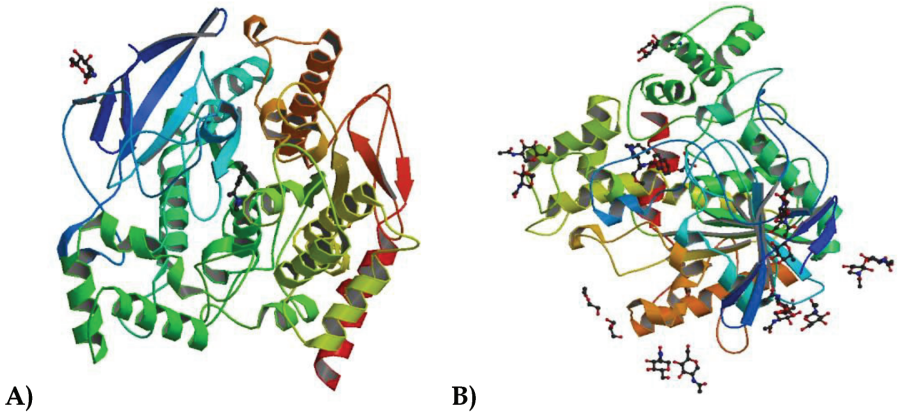

A) **B)**

Figure 4.26. A) Acetylcholinesterase (AChE) 1GQS; **B)** Butyrylcholinesterase (BChE) 5LKR

AutoDock 2 Vina was used to make a semi-rigid docking with full conformational flexibility of the freely rotatable bonds of the ligand and the partial flexibility of the protein, *i.e.* the side chains of the residues in the ligand-binding pocket. The program makes a search in conformational space with the ligand and the enzyme restricted to the ligand-binding pocket for 10 h.

The AChE and BChE complexes with various inhibitors provided valuable insights into the interactions that mediate the bonds with inhibitors. The docking procedure provides the treatment of ligand flexibility within the protein-binding site (Geromichalos, Lamari *et al.* 2012; Tripathi and Ayyannan 2018).

3.12. Statistical analysis

All data were expressed as mean ± standard deviation (SD) of three independent experiments performed in triplicate.

The R^2 values for all calibration curves were over 0.99.

To verify the correlation among used methods, the p value of 0.05 or less were analysed by one-way analysis of variance (ANOVA) and were considered statistically significant. Moreover, the statistical analysis was performed with the Student t-test.

Pearson coefficient was determined using GraphPad Prism 5 Software (San Diego, CA, USA).

CHAPTER 4. RESULTS AND DISCUSSIONS OF *AZORELLA GLABRA* WEDD.

4.1. The extraction yield of *A. glabra* samples

The aerial parts of *Azorella glabra* were dried at room temperature (140 g in triplicate) and extracted by dynamic maceration using 96% ethanol for 24 h at a solid to solvent ratio of 1:10 (w/v) per extraction for four times (Dávila, Sterner *et al.* 2013). The four extracts of each replicate extraction were combined. The ethanol extraction yield was calculated showing a value of 9.01 ± 0.81 %. To our knowledge, is the first time that *A. glabra* was extracted by 96% ethanol, usually other species of *Azorella* genus were extracted by petroleum ether (Loyola, Bórquez *et al.* 2004; Areche, Cejas *et al.* 2009).

Then, a part (32.00 g in 320 mL of water) of the reunited crude ethanol extract (Ag EtOH) was separated on the basis on the affinity solvent by liquid/liquid extraction using an increasing solvent polarity obtaining the following fractions: *n*-hexane (AgH), chloroform (AgC), ethyl acetate (AgEA), *n*-butanol (AgB) and water (AgW). The present compounds in Ag EtOH were separated on the basis of the solvent affinity (Saeed, Khan *et al.* 2012). The extraction's yield of dry fractions was reported in **Fig. 4.1**. The AgH and AgC fractions showed the highest extraction yield (31.52 ± 1.22 % and 44.50 ± 3.21 %, respectively); instead, the AgEA and AgB fractions demonstrated the lower extraction yields (2.23 ± 0.19 % and 5.66 ± 0.43 %, respectively) (Lamorte, Faraone *et al.* 2018).

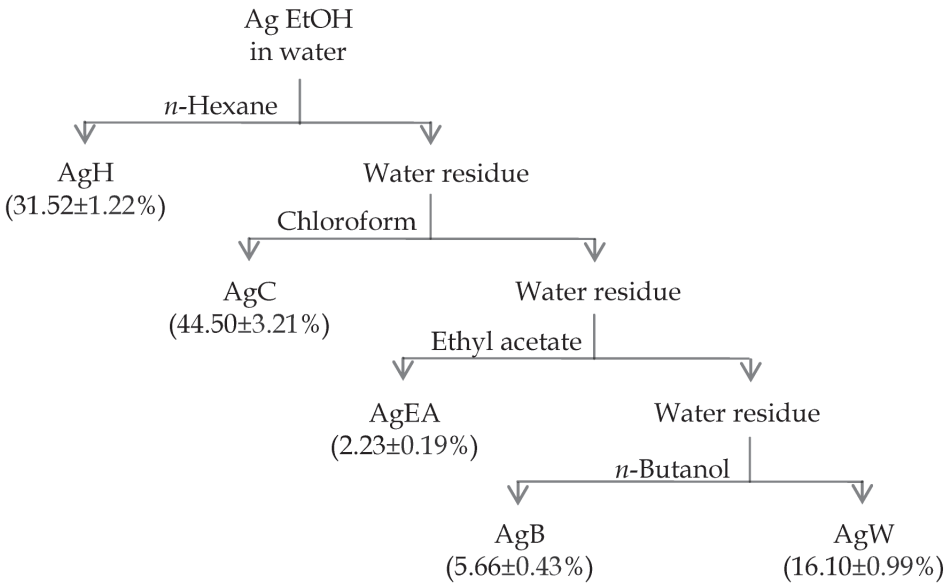

Figure 5.1. Extraction yields of *A. glabra* EtOH extract partitioned fractions
Results were expressed as mean ± standard deviation of the triplicate experiments. Samples are crude ethanol extract (Ag EtOH), *n*-hexane fraction (AgH), chloroform fraction (AgC), ethyl acetate fraction (AgEA), *n*-butanol fraction (AgB) and water fraction (AgW).

4.2. The influence of polarity solvents on total polyphenolic, flavonoid and terpenoid contents on *A. glabra* samples

Three different *in vitro* colorimetric assays were used for the determination of the phytochemical profiles of each sample in terms of total polyphenolic (TPC), flavonoid (TFC) and terpenoid (TTeC) content (**Fig. 4.2**).

The polyphenolic content (TPC) of Ag EtOH and its fractions was carried out based on the reaction of the samples with Folin-Ciocalteu reagent, which results in a blue colored solution whose intensity was directly proportional to the amount of phenolic compounds present. Gallic acid was used as a standard for the construction of calibration curve and the results were expressed as mg of Gallic Acid Equivalents per gram of dry sample (mg GAE/g). Samples displayed quantitative differences in TPC value (**Fig. 4.2**), with a mean value of 72.52 mg GAE/g. The AgEA and AgB fractions showed a higher TPC than other fractions (143.60 ± 0.40 and 128.14 ± 0.74 mg GAE/g, respectively).

In addition, flavonoids, a class of polyphenols with several biological properties (Russo, Valentão *et al.* 2015) have been measured in *Azorella* samples that presented a TPC value higher than the mean value. In particular, the TFC was carried out on AgEA and AgB fractions with TFC values of 354.97 ± 22.05 and 209.73 ± 5.56 mg of Quercetin Equivalents per gram of dried sample (mg QE/g), respectively.

Moreover, TTeC was also determined on all samples (**Fig. 4.2**). The AgC and AgH fractions and the Ag EtOH extract exhibited higher value (733.51 ± 9.42, 421.77 ± 41.46 and 405.44 ± 29.33 mg LE/g, respectively) than the mean value of 338.38 mg of Linalool Equivalents per gram of dried sample (mg LE/g).

There is a difference between TPC, TFC and TTeC tests; in fact, the total content of the polyphenols test involves in a redox reaction, whereas TFC and TTeC are tests based on the precipitation reaction of the flavonoids and terpenes, respectively.

Results demonstrated as the yield of phenolic, flavonoids and terpenoids extraction differs on the basis of used solvents. Fractions obtained by using solvents with high polarity reported the highest total polyphenols content, indicating that the majority of polyphenolic compounds in the aerial parts of *A. glabra* could be of polar nature (Nakamura, Ra *et al.* 2017).

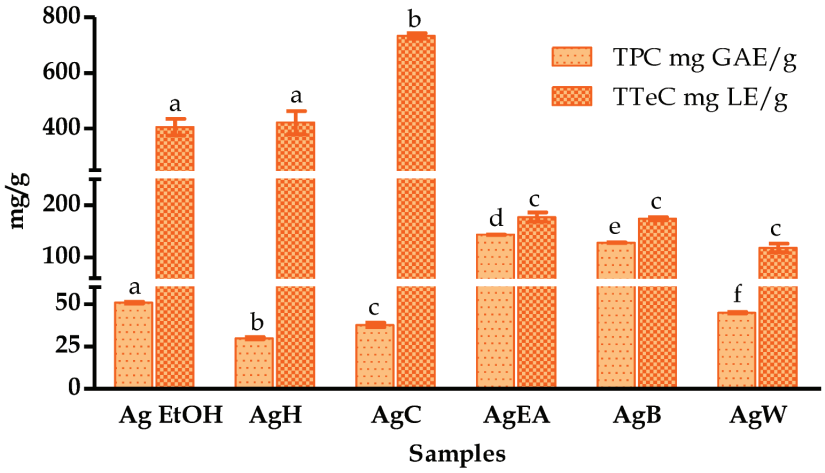

Figure 5.2. Total Polyphenol Content (TPC) and Total Terpenoid Content (TTeC) of *Azorella glabra* samples

Results were expressed as mean ± standard of triplicate determinations deviation in mg of Gallic Acid Equivalents per gram of dried sample (mg GAE/g) and in mg of Linalool Equivalents per gram of dried sample (mg LE/g). In each test, the values with the same letter are not significant different at the $p < 0.05$ level, 95% confidence limit, according to one-way analysis of variance (ANOVA). Samples are crude ethanol extract (Ag EtOH), *n*-hexane fraction (AgH), chloroform fraction (AgC), ethyl acetate fraction (AgEA), *n*-butanol fraction (AgB) and water fraction (AgW).

4.3. Antioxidant activity of *A. glabra* samples

Low concentrations of biological radicals are important in the human body; in fact, they are involved in biological functions as vascular homeostasis, neurotransmission, antimicrobial, antioxidant and antitumor activities. In contrast, the overproduction of biological radicals involves in redox imbalance associated with different diseases. For examples, the super oxide can form hydroxyl radical and singlet oxygen dangerous for human body (Patel Rajesh and Patel Natvar 2011). Phenolic compounds are gaining attention due to their significant antioxidant activities. Different *in vitro* assays were reported for the measurement of antioxidant activity on foods and plant species and it has been demonstrated as more than one method is necessary to elucidate the antioxidant capacity of samples because these assays differ in the principles and experimental conditions (Faraone, Rai *et al.* 2018).

In this study, the antioxidant activity of *A. glabra*, *M. diffusa* and *S. clivicolus* samples were tested using six different complementary *in vitro* antioxidant assays. In particular, the radical scavenging activity was evaluated by using synthetic cationic and neutral (ABTS and DPPH) and physiological (superoxide anion and nitric oxide) radicals.

The AgEA showed the highest radical scavenging-activity in all investigated tests (**Tab. 4.1**). In fact, the ethyl acetate fraction reported 282.26 ± 9.53 mg TE/g and 240.33 ± 10.73 mg TE/g values in ABTS and DPPH assays respectively, followed by AgB. Moreover, in both assays, the lowest activity was found in chloroform fraction. Instead, AgH was not active in ABTS, DPPH and SO assays. The ability of samples to scavenge superoxide anion and nitric oxide was expressed as IC_{25} and results were compared with ascorbic acid. The *A. glabra* samples caused a dose-dependent inhibition in the superoxide anion assay (SO). In particular, AgEA and AgB showed a higher activity than ascorbic acid (IC_{25} of 0.26 ± 0.02 mg/mL). The scavenging ability against the biological nitric oxide ($^{\cdot}NO$) was detectable only in AgB and AgW fractions, but their values were double than ascorbic acid (IC_{25} 9.13 ± 0.71, 8.94 ± 0.67 and 4.78 ± 0.09 mg/mL, respectively, data not shown in **table 4.1**).

Moreover, the ethyl acetate fraction presented the highest ferric reducing ability (410.29 ± 5.69 mg TE/g) followed by AgB fraction (318.57 ± 2.77 mg TE/g) assessed by FRAP test. AgC and AgH were again the least active.

To get a broader overview of the antioxidant potential of the plant complex of samples, the β-Carotene Bleaching test (BCB) was conducted. The antioxidant compounds compete with β-carotene for binding to the radical derived from linoleic acid and prevent the destruction of the conjugated system of the molecule responsible for colouring, for which, the higher is the antioxidant activity of the sample, the greater is the concentration of β-carotene in solution. The results were expressed as percentage of antioxidant activity (% AA) at the initial sample concentration of 1 mg/mL. The analysis evidenced that the most active sample in BCB test was the AgEA (34.93 ± 1.37 % AA), following to other fractions with very near values. While, there was no activity for the polar AgW fraction.

Table 5.1. Results of ABTS, DPPH and Super Oxide (SO) scavenging activity, Ferric Reducing Antioxidant Power (FRAP) and β-Carotene Bleaching (BCB) of *A. glabra* samples

Samples	ABTS (mgTE/g)	DPPH (mgTE/g)	SO (IC_{25} mg/mL)	FRAP (mgTE/g)	BCB %AA
Ag EtOH	76.83±1.23^{a}	28.17±2.32^{a}	2.59±0.11^{a}	73.58±0.71^{a}	26.70±0.61^{a}
AgH	nc	nc	nc	18.79±0.66^{b}	22.50±0.65^{b}
AgC	32.08±0.02^{b}	5.94±0.27^{b}	0.47±0.02^{b}	15.45±0.44^{b}	22.18±1.54^{b}
AgEA	282.26±9.53^{c}	240.33±10.73^{c}	0.12±0.01^{c}	410.29±5.69^{c}	34.93±1.37^{c}
AgB	206.65±7.28^{d}	224.91±4.84^{d}	0.20±0.01^{c}	318.57±2.77^{d}	21.68±0.57^{b}
AgW	65.09±0.40^{a}	43.12±1.23^{e}	0.37±0.02^{b}	95.33±3.86^{e}	nc

Samples are crude ethanol extract (Ag EtOH), *n*-hexane fraction (AgH), chloroform fraction (AgC), ethyl acetate fraction (AgEA), *n*-butanol fraction (AgB) and water fraction (AgW). Data are expressed as means ± standard deviation from three experiments; mg GAE/g = mg of Gallic Acid Equivalents per gram of dried sample; mg TE/g = mg of Trolox Equivalents per gram of dried sample; IC_{25} mg/mL = concentration of the sample required to inhibit the activity of the radical by 25%; % AA = percentage of Antioxidant Activity at initial sample concentration of 1 mg/mL; different superscripts in the same row indicate significant difference ($p < 0.05$); nc = not calculable.

Moreover, linear correlations were calculated based on the average of the results by the Pearson test (**Tab. 4.2**). This test calculates the linear correlation coefficient (r), a dimensionless number between -1 and 1, inclusive, reflecting the extent of a linear relationship between two data sets. The more the value of the coefficient comes close to the extremes, the more the correlation is present, in a positive or negative manner. The correlation value of 0 indicates no linear correlation.

The results showed a strong correlation between polyphenols and antioxidant activity. In fact, the highest correlation was found between the total polyphenol content and radical-scavenging activity ($r_{TPC/ABTS}$ = 0.99, $r_{TPC/DPPH}$ = 0.99 and $r_{TPC/SO}$ = 0.92) and

ferric reducing power ($r_{TPC/FRAP}$ = 0.99) demonstrating as the polyphenols are the compounds mostly involved in the antioxidant activity. The highest correlation was also observed between the ferric reducing power of the samples and the radical-scavenging activity by ABTS, DPPH and SO methods ($r_{FRAP/ABTS}$ = 0.99, $r_{FRAP/DPPH}$ = 0.99 and $r_{FRAP/SO}$ = 0.94). Polyphenols are less involved in the inhibition of radical-scavenging activity by NO assay and lipid peroxidation ($r_{TPC/NO}$ = 0.21 and $r_{TPC/BCB}$ = 0.48). Instead, terpenoids are less involved in testing activities ($r < 0$ for terpenoids against all assays, except for BCB test $r_{TTeC/BCB}$ = 0.24).

Table 5.2. Pearson correlation coefficient calculated among tested *Azorella glabra* extract and fractions

	TPC	**TTeC**	**ABTS**	**DPPH**	**SO**	**NO**	**FRAP**	**BCB**
TPC	1.00							
TTeC	-0.58	1.00						
ABTS	0.99	-0.60	1.00					
DPPH	0.99	-0.63	0.97	1.00				
SO	0.92	-0.53	0.94	0.92	1.00			
NO	0.21	-0.64	0.17	0.30	0.21	1.00		
FRAP	0.99	-0.65	0.99	0.99	0.94	0.23	1.00	
BCB	0.48	0.24	0.47	0.40	0.32	-0.71	0.42	0.42

Total Polyphenolic Content (TPC), Total Terpenoid Content (TTeC), ABTS Assay, DPPH assay, Super Oxide anion scavenging activity (SO), Nitric Oxide radical scavenging activity (NO), Ferric Reducing Antioxidant Power assay (FRAP) and β-Carotene Bleaching assay (BCB).

The results of the antioxidant activity obtained by the above-described chemical methods have been integrated by calculating the Relative Antioxidant Capacity Index (RACI). The RACI index allows the comparison of phytocomplex antioxidant capacity derived from different chemical methods (ABTS, DPPH, SO, NO, FRAP and BCB) even the TPC. It has been shown, that the results obtained with the method of Folin-Ciocalteu reagent can be interpreted to determine the total content of polyphenols, and as an alternative way to measure the total reducing capacity of the samples since the Folin reagent reacts with any reducing substance present in solution (Faraone, Rai *et al.* 2018). This index is dimensionless and measures the distance between the average of the results obtained and the raw data expressed in standard deviation units.

RACI values obtained agrees with the results obtained so far (**Fig. 4.3**) evidencing as the ethyl acetate fraction presented the highest value (1.15), followed by

the butanol fraction (0.88). The AgH fraction presented the lowest index (-0.72) and, therefore, a relative lack of antioxidant activity. In particular, the RACI values may be related to the high total polyphenol content of the ethyl acetate and butanol fractions.

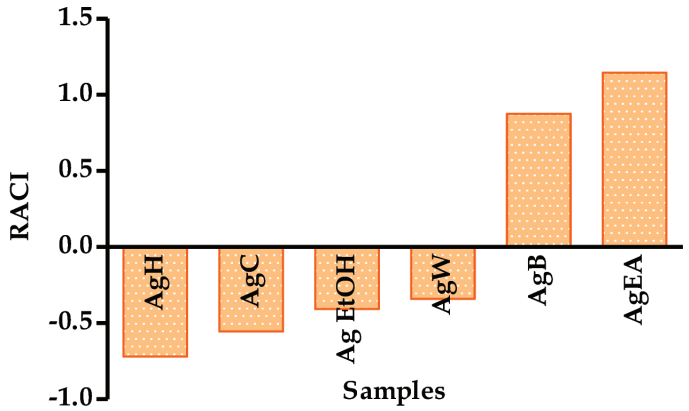

Figure 5.3. Relative Antioxidant Capacity Index (RACI) of *Azorella glabra* samples
Samples are crude ethanol extract (Ag EtOH), *n*-hexane fraction (AgH), chloroform fraction (AgC), ethyl acetate fraction (AgEA), *n*-butanol fraction (AgB) and water fraction (AgW).

Today, no study reported the antioxidant activity of *Azorella glabra*. There is only a paper that evaluated the antioxidant activity of *Azorella madreporica* aerial parts (Bórquez, Kennelly *et al.* 2013). In this study the specie aerial parts were extracted with petroleum ether and then with methanol. The methanol extract was subjected to TPC, TFC and DPPH assays. Compared with our results, is evident that Ag EtOH gave a greater total polyphenol and flavonoid content. Instead, *A. madreporica* had potent antioxidant property on DPPH radical and showed higher inhibition than that Ag EtOH obtained from us (**Tab. 4.3**). It is possible to explain these results with the different extraction solvent and *in vitro* methods used to determine the radical-scavenging activity.

Table 5.3. Results of Total Polyphenolic Content (TPC), Total Flavonoid Content (TFC) and DPPH scavenging activity of *A. madreporica* and *A. glabra* extracts

	TPC (mg gallic acid/100 g dry weight)	**TFC (mg quercetin/100 g dry weight)**	**DPPH (IC_{50} µg/mL)**
Methanol extract of *A. madreporica*	75.69±7.62	67.25±8.61	96.57±1.00
Ag EtOH	587.27±54.96	76486.08±1676.25	1109.04±33.84

Ag EtOH is the crude ethanol extract of *A. glabra* aerial parts. Data are expressed as means ± standard deviation from three experiments; IC_{50} mg/mL = concentration of the sample required to inhibit the activity of the radical by 50%.

4.4. Potential antidiabetic activity of *A. glabra* samples

Inhibitors of *a*-amylase and *a*-glucosidase enzymes can reduce postprandial hyperglycaemia through the retard the uptake of dietary carbohydrates. For this reason, the inhibition of these enzymes is an important strategy in the treatment of diabetes and/or obese patients. Thus, a part of my PhD project is searching for *a*-amylase and *a*-glucosidase enzymes sample inhibitors useful for the treatment of type 2 diabetes mellitus and all samples were screened biologically. Different concentrations of the *A. glabra* samples were assayed for both enzyme inhibitory activities.

Both the assays were concentration-dependent and acarbose was used as positive control (**Fig. 4.4**).

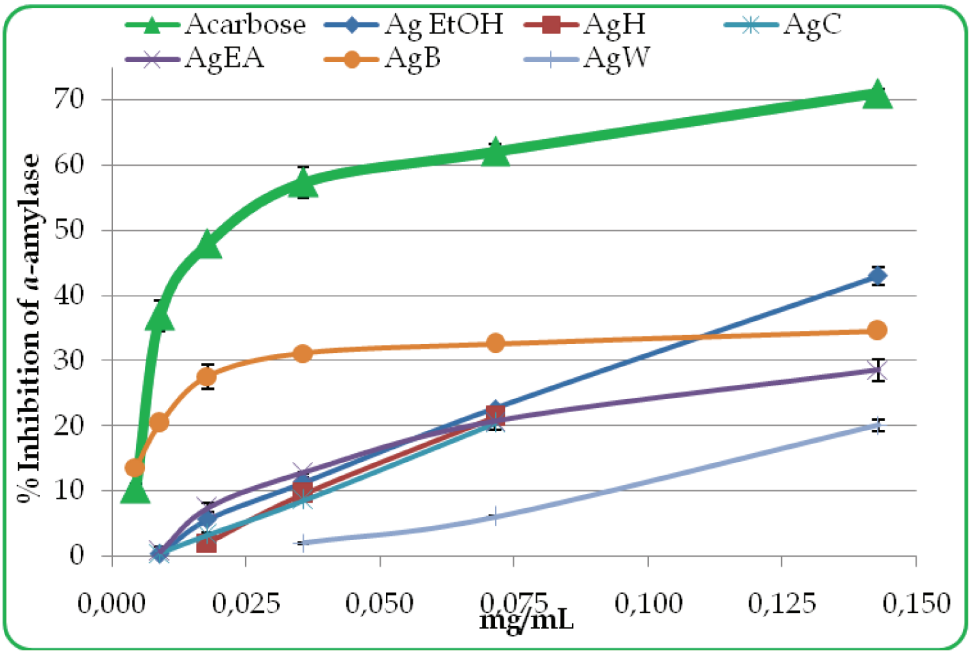

A)

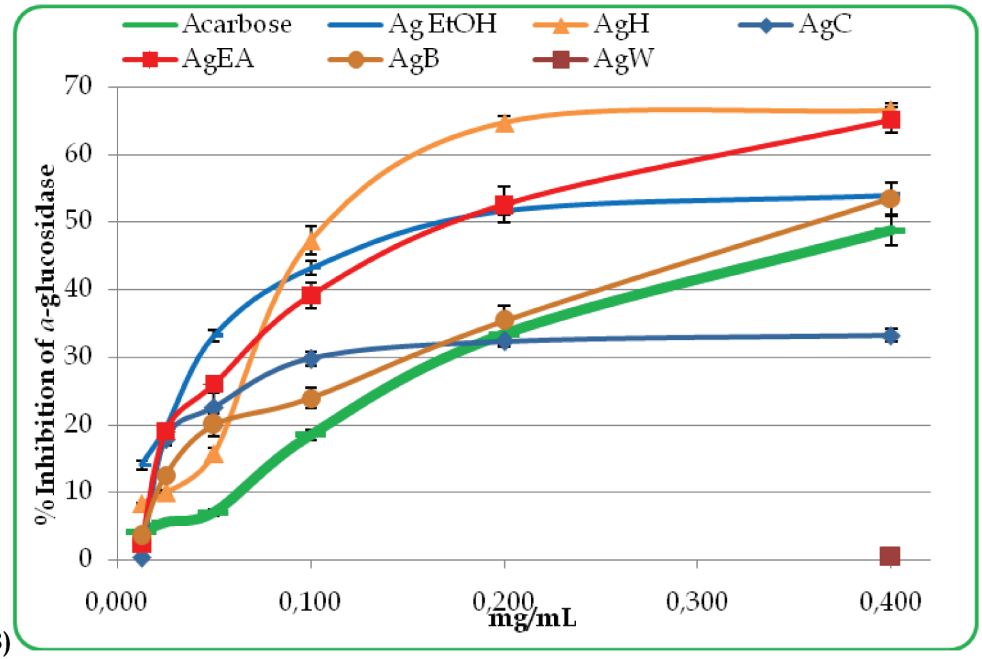

B)

Figure 5.4. *a*-Amylase (**A**) and *a*-glucosidase (**B**) inhibition activity of acarbose and *Azorella glabra* samples

Samples are acarbose, crude ethanol extract (Ag EtOH), *n*-hexane fraction (AgH), chloroform fraction (AgC), ethyl acetate fraction (AgEA), *n*-butanol fraction (AgB) and water fraction (AgW). Data are mean ± standard deviation from three experiments.

Usually the results are expressed as the concentration of the sample required to inhibit the activity of the enzyme by 50% (IC_{50}) in mg/mL calculated by nonlinear regression analysis. In this case, the IC_{50} was not reached for all samples at the tested concentrations. In particular, in *a*-amylase inhibition test was possible reached the IC_{50} only for the Ag EtOH. Instead, in *a*-glucosidase test was not possible reached the IC_{50} for the AgC and AgW fractions and the Ag EtOH showed an IC_{50} value of 0.17 ± 0.01 mg/mL higher than acarbose (IC_{50} of 0.02 ± 0.01 mg/mL, **Fig. 4.5**).

On the other hand, in the *a*-glucosidase inhibition test, the Ag EtOH and the AgH, AgEA and AgB fractions showed IC_{50} values lower than acarbose (IC_{50} of 0.40 ± 0.03 mg/mL). The best of all were the AgH and AgEA fractions (IC_{50} of 0.16 ± 0.01 and 0.16 ± 0.01 mg/mL, respectively).

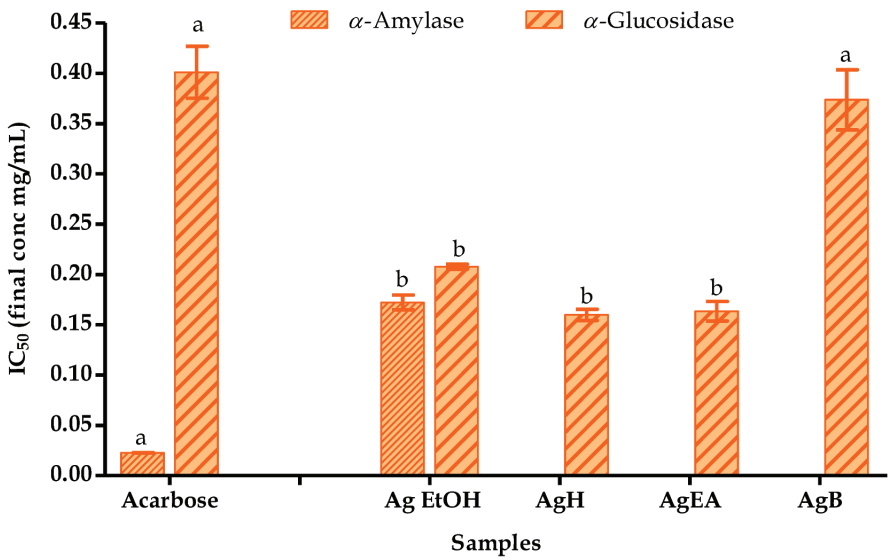

Figure 5.5. *a*-Amylase and *a*-glucosidase inhibition by acarbose and *Azorella glabra* samples expressed as IC_{50} values in mg/mL

Samples are acarbose, crude ethanol extract (Ag EtOH), *n*-hexane fraction (AgH), ethyl acetate fraction (AgEA) and *n*-butanol fraction (AgB). No enzymatic inhibition present for the missing samples. Data are means ± standard deviation from three experiments performed in triplicate. The concentration of the sample required to inhibit the activity of the enzyme by 50% (IC_{50}) in mg/mL was calculated by nonlinear regression analysis. In each test, the values with the same letter are not significant different at the $p < 0.05$ level, 95% confidence limit, according to one-way analysis of variance (ANOVA).

To compare all samples in both the assays, the results were expressed as percentage of inhibition at final concentration of 0.07 mg/mL in *a*-amylase test and 0.40 mg/mL in *a*-glucosidase test (**Fig. 4.6**). In particular, in *a*-amylase inhibition test, all tested samples of *A. glabra* showed percentage inhibition values at selected concentration lower than acarbose (62.14 ± 1.08 %). Among all, the butanol fraction presented the best value (32.62 ± 0.35 %) followed by ethanol extract (22.78 ± 0.19 %). Instead, in the *a*-glucosidase inhibition test, the Ag EtOH and the AgH, AgEA, and AgB fractions showed values higher than acarbose (48.69 ± 2.22 %).

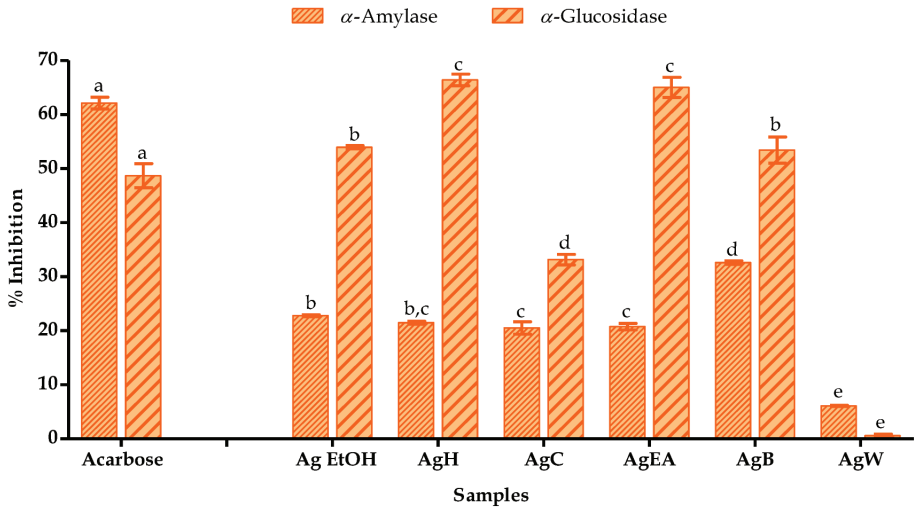

Figure 5.6. *a*-Amylase and *a*-glucosidase inhibition by acarbose and *Azorella glabra* samples expressed as percentage of inhibition at final concentration of 0.07 mg/mL in *a*-amylase test and 0.40 mg/mL in *a*-glucosidase test

Samples are acarbose, crude ethanol extract (Ag EtOH), *n*-hexane fraction (AgH), chloroform fraction (AgC), ethyl acetate fraction (AgEA), *n*-butanol fraction (AgB) and water fraction (AgW). Data are means ± standard deviation from three experiments performed in triplicate as a percentage of inhibition at final concentration of 0.07 mg/mL in *a*-amylase test and 0.40 mg/mL in *a*-glucosidase test. In each test, the values with the same letter are not significant different at the $p < 0.05$ level, 95% confidence limit, according to one-way analysis of variance (ANOVA).

To date, this is the first report on antidiabetic activity of *A. glabra*. Our promising results are supported by previous studies on *Azorella compacta*. This specie, such as many other plant species, has been used in the popular medicine as antidiabetic. In particular, Fuentes *et al.* in 2005 (Fuentes, Sagua *et al.* 2005) evidenced that the responsibility of the antidiabetic activity of *A. compacta* is of diterpenic compounds mulinolic acid, azorellanol, and mulin-11,13-dien-20-oic acid isolated from its. In fact, the glycemia of rats treated with the first two diterpenic compounds was decreased with values close to those reached by chlorpropamide injection used in controls. In conclusion, the antihyperglycemic effect of these compounds may explain the effectiveness of *A. compacta* in ethnomedicine. Then, in 2008 Prabhakar *et al.* (Prabhakar and Doble 2008) explained that the anti-diabetic properties of *A. compacta* is due to increase of insulin secretion.

4.5. Potential anticholinesterase activity of *A. glabra* samples

The inhibition of acetylcholinesterase and butyrylcholinesterase enzymes are considered as a strategy for the treatment of Alzheimer's disease, senile dementia, ataxia, and myasthenia gravis (Areche, Cejas *et al.* 2009; Fidelis, Faraone *et al.* 2018). The *A. glabra* samples had a concentration-dependent activity on both enzymes (**Fig. 4.7**).

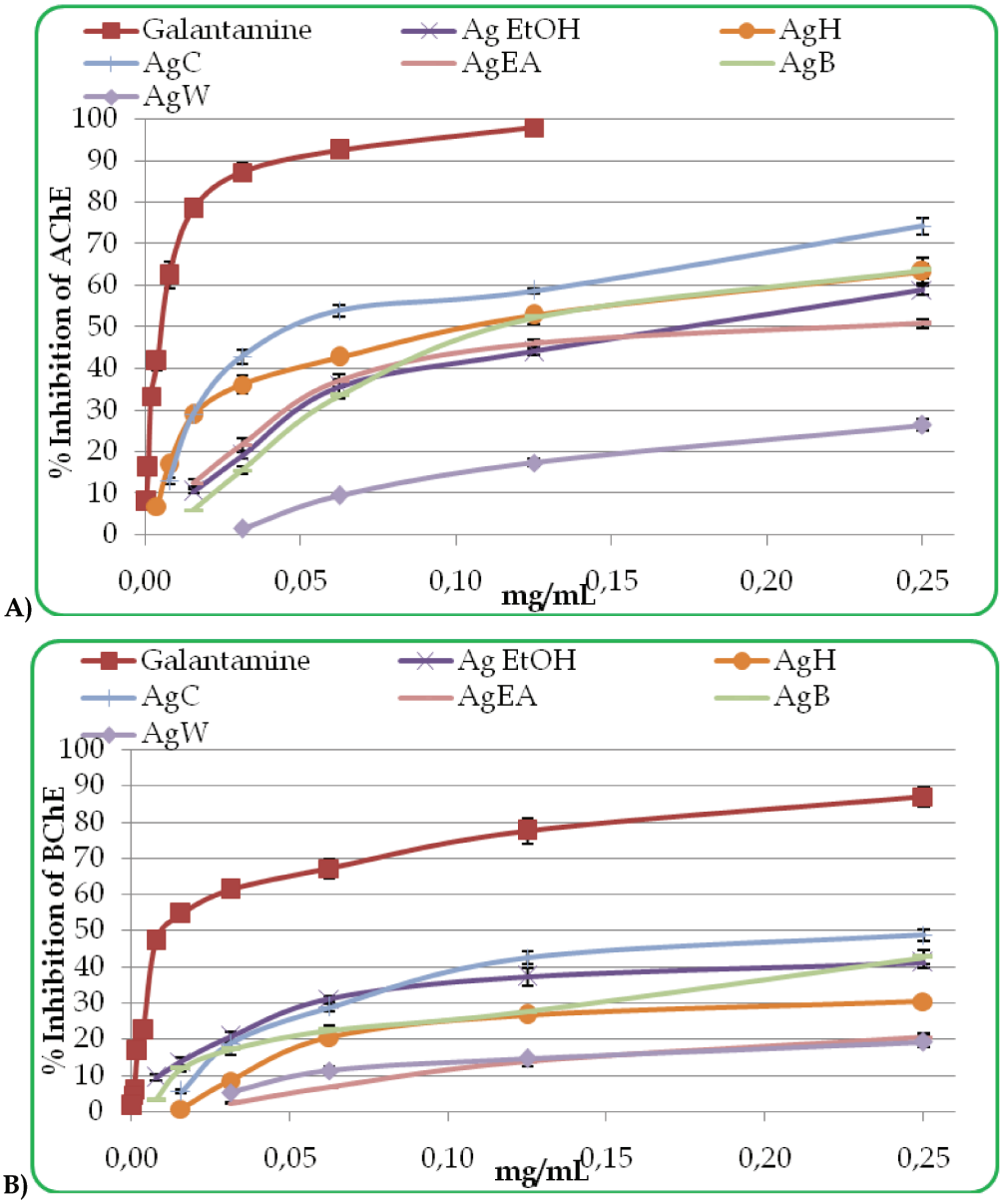

Figure 5.7. AChE (**A**) and BChE (**B**) inhibition activity of galantamine and *Azorella glabra* samples Samples are galantamine, crude ethanol extract (Ag EtOH), *n*-hexane fraction (AgH), chloroform fraction (AgC), ethyl acetate fraction (AgEA), *n*-butanol fraction (AgB) and water fraction (AgW). Data are mean ± standard deviation from three experiments.

The ability of samples to inhibit the AChE and BChE enzymes was expressed as IC_{50} and results were compared with galantamine (**Fig. 4.8**). In particular, in AChE *in vitro* assay the AgC, and AgH fractions showed a good activity (IC_{50} of 0.03 ± 0.01 and 0.10 ± 0.01 mg/mL), but lower than positive control galantamine (IC_{50} of 0.01 ± 0.00 mg/mL).

Instead, it was possible express the inhibition of BChE enzyme in IC_{50} only in Ag EtOH extract and in AgC and AgB fractions, but their activities were lower than galantamine (IC_{50} 0.02 ± 0.00 mg/mL). Again, the best value was in AgC fraction (IC_{50} 0.24 ± 0.01 mg/mL).

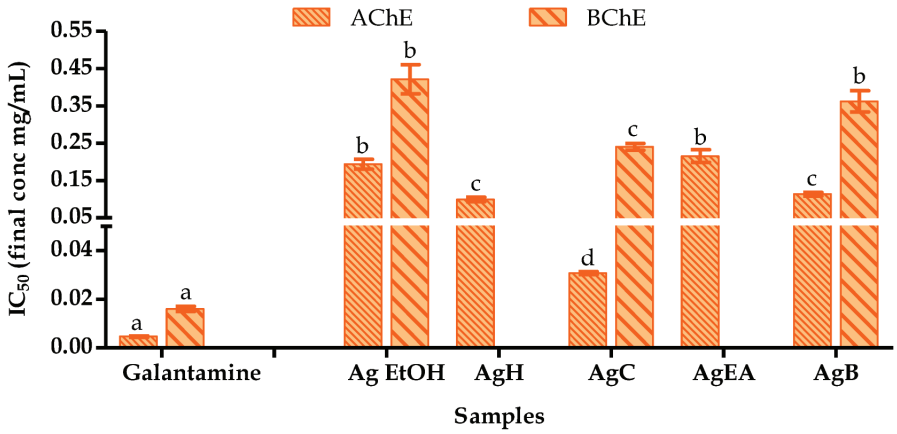

Figure 5.8. AChE and BChE inhibition by galantamine and *Azorella glabra* samples expressed as IC_{50} values in mg/mL
Samples are galantamine, crude ethanol extract (Ag EtOH), *n*-hexane fraction (AgH), chloroform fraction (AgC), ethyl acetate fraction (AgEA) and *n*-butanol fraction (AgB). No enzymatic inhibition present for the missing samples. Data are means ± standard deviation from three experiments performed in triplicate. The concentration of the sample required to inhibit the activity of the enzyme by 50% (IC_{50}) in mg/mL was calculated by nonlinear regression analysis. In each test, the values with the same letter are not significant different at the $p < 0.05$ level, 95% confidence limit, according to one-way analysis of variance (ANOVA).

Once again, this is the first report on anticholinesterase activity of *A. glabra*. There is only a study (Areche, Cejas *et al.* 2009) where was studying the effect of three lanostane-, two cycloartane-type triterpene and two mulinane-type diterpenes isolated from a petroleum ether extract of the whole shrub of *A. trifurcata* on the enzyme acetylcholinesterase. All compounds showed moderate inhibitory activity toward the enzyme AChE. The researchers gave the inhibitory activity of these compounds to the presence of acetate groups.

4.6. Identification and quantification of compounds by mass spectrometry in *A. glabra* samples

The phytochemical profile of *Azorella glabra* has never been studied before. The compounds previously identified in other species to *Azorella* genus belong mainly to the class of diterpenoids (Fuentes, Sagua *et al.* 2005; Areche, Cejas *et al.* 2009).

To evaluate the compounds responsible of the best measured antioxidant activity and the best enzymatic activity, were selected the samples with the best values. The AgEA was the sample with the best RACI value to indicate the best sample for the antioxidant activity. Instead, for antidiabetic activity did not show a high efficiency. For anticholinesterase activity, the best sample was the AgC fraction.

In conclusion, the ethyl acetate and chloroform fractions partitioned from the ethanol extract of *A. glabra* aerial parts were subject to mass spectrometry analysis in negative ionization (Hossain, Rai *et al.* 2010).

The LC–MS profile of AgEA is shown in **Fig. 4.9**. Different compounds (> 23) were detected and tentative identification of most of them have been reached through accurate mass and fragmentation pattern and aided by the existing literature (**Tab. 4.4**). Fifteen compounds have been identified for the first time in *Azorella glabra* by comparing their retention times with those of the available commercial standards.

These compounds belong to the classes of:

- cinnamic acid derivatives (cynarin (**2**), chlorogenic acid methyl ester (**6**), 3,5-di-*O*-caffeoyl quinic acid (**9b-10**), 3,4-di-*O*-caffeoyl quinic acid (**11a**), caffeic acid (**13b**) and chlorogenic acid (**17d**));
- flavones (iso-orientin (**4**), orientin (**5**), luteolin-7-*O*-glucoside (**11b**) and luteolin (**15a**));
- flavonols (rutin (**7**), quercetin-3-*O*-glucoside (**8**), kaempferol-3-*O*-glucoside (**9a**) and quercetin (**15b**));
- triterpene (oleanolic acid (**23**)).

The most abundant was orientin (104.22 ± 4.01 mg/g DW), followed by 3,5-di-*O*-caffeoyl quinic acid (89.40 ± 4.28 mg/g DW). These phenolic compounds are known for their antioxidant properties (Wang, Nair et al. 1999; McDonald, Prenzler *et al.* 2001; Hung, Na *et al.* 2006; Yang, Guo *et al.* 2008; Razavi, Zahri *et al.* 2009; Naveed, Hejazi *et al.* 2018). In particular, flavonoids are known to have more biological activity and in

particular anti-inflammatory properties. Luteolin, luteolin-glycosides and plant species containing these compounds have been reported to have anti-inflammatory and antioxidant activities. These effects dependent to the presence of ortho-dihydroxy groups at the B ring and OH substitution pattern at C-5 position of the A ring. The antioxidant abilities of flavonoids are widely acknowledged. The presence of a B-ring catechol group and the presence of a C2-C3 double bond in conjugation with an oxo group at C4 are the two antioxidant structural features of flavonoids; the first serves to donate hydrogen/electron to stabilize a radical species and the second serves to bind transition metal ions such as iron and copper. Luteolin (**15a**) and its glycosides isoorientin (luteolin 6-*C*-glucoside, **4**), orientin (luteolin 8-*C*-glucoside, **5**) and cynaroside (luteolin 7-*O*-glucoside, **11b**) fulfil these two structural requirements. For this reason, it is not surprising that many luteolin-containing plant species possess antioxidant properties. In particular, the antioxidant activity of luteolin and its glycosides has been related to their ability to scavenge reactive oxygen and nitrogen species, to chelate transition metals that may induce oxidative damage through the Fenton reaction, to inhibit prooxidant enzymes and to induce antioxidant enzymes. Moreover, luteolin could be developed as a cancer chemopreventive agent and be useful in cancer therapy to sensitize tumour cells to the cytotoxic effects of some chemotherapeutic drugs (Uma Devi, Ganasoundari *et al.* 2000; López-Lázaro 2009).

Moreover, four compounds were tentatively identified as feruloyl-caffeoyl quinic acid isomers with *m/z* 529.13 (**12**, **13a**, **14** and **16**). Upon fragmentation by CID, these compounds produced the ions at *m/z* 367, 349, 191, 179 and 161 (Clifford, Johnston *et al.* 2003; Han, Ye *et al.* 2008). In addition, one compound was tentatively identified as chlorogenic acid derivative (**1**) with *m/z* 409.11 and ion fragmentation at *m/z* 353, 191, 173, 135, 127, 93, 85.

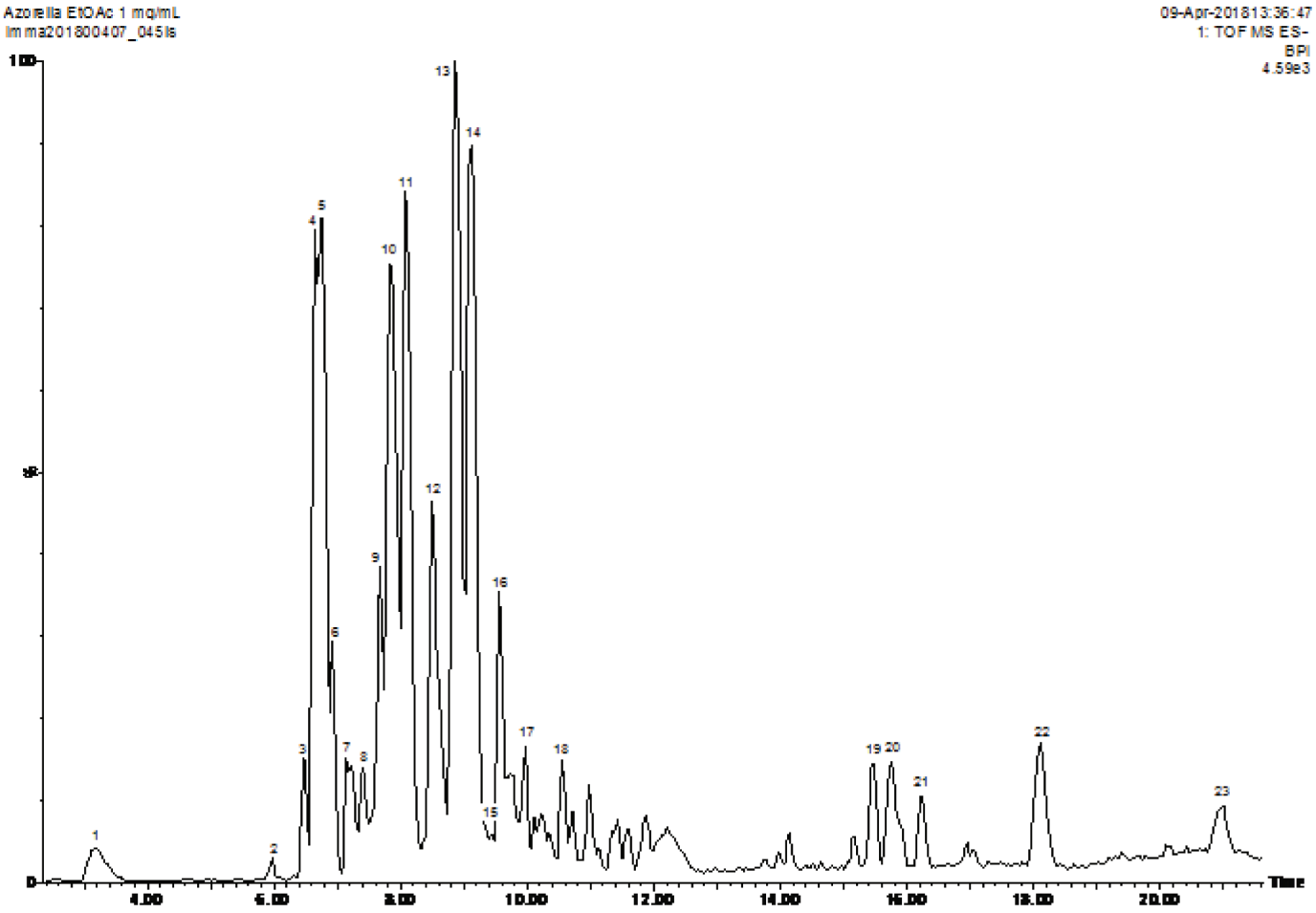

Figure 5.9. Ethyl acetate fraction of *Azorella glabra* base peak intensity chromatogram (BPI)

Table 5.4. Liquid chromatography-tandem mass spectrometry (LC–MS/MS) of ethyl acetate fraction of *Azorella glabra*

Peak no.	RT (min)	ESI (-) MS observed	ESI (-) MS Calc.	Molecular Formula	MS/MS	Tentative Identity	mg/g DW	References
1	3.17	409.1137	409.1140	$C_{19}H_{21}O_{10}$	353, 191, 173, 135, 127, 93, 85	Chlorogenic acid derivative	nq	(Araujo, Müller *et al.* 2005)
2	5.98	515.1180	515.1190	$C_{25}H_{23}O_{12}$	353, 179	Cynarin	0.15±0.03	(Ferracane, Graziani *et al.* 2010)
3	6.46	427.1980	427.1968	$C_{21}H_{31}O_{9}$	367, 327, 297, 285, 179, 161, 135, 101, 73, 61, 59	Unknown	nq	
4	6.64	447.0918	447.0927	$C_{21}H_{19}O_{11}$	357, 339, 327, 311, 299, 297, 285, 269, 253, 191, 175, 149, 133, 109	Iso-orientin	13.22±1.43	(Iswaldi, Arráez-Román *et al.* 2011)
5	6.84	447.0910	447.0927	$C_{21}H_{19}O_{11}$	357, 339, 327, 311, 299, 297, 285, 269, 253, 191, 175, 149, 133, 109	Orientin	104.22±4.01	(Iswaldi, Arráez-Román *et al.* 2011)
6	6.92	367.1038	367.1029	$C_{17}H_{19}O_{9}$	161, 85	Chlorogenic acid methyl ester	12.33±0.04	(Araujo, Müller *et al.* 2005)
7	7.14	609.1469	609.1456	$C_{27}H_{29}O_{16}$	300, 285, 271, 255, 179, 151	Rutin	0.02±0.00	(Araujo, Müller *et al.* 2005)
8	7.37	463.0859	463.0877	$C_{21}H_{19}O_{12}$	300, 271, 255, 179, 151	Quercetin-3-*O*-glucoside	0.07±0.00	(Araujo, Müller *et al.* 2005; Krzyzanowska-Kowalczyk,

								Pecio *et al.* 2018)
9	7.67/ 7.70	447.0921	447.0927	$C_{21}H_{19}O_{11}$	284, 255	Kaempferol-3-*O*-glucoside	0.01±0.00	(Downey and Rochfort 2008)
		515.1197	515.1190	$C_{25}H_{23}O_{12}$	179, 135	3,5-di-*O*-caffeoyl quinic acid	44.70±4.14	(Araujo, Mü Ller *et al.* 2005)
10	7.83	515.1197	515.1190	$C_{25}H_{23}O_{12}$	179, 135	3,5-di-*O*-caffeoyl quinic acid	44.70±4.14	(Araujo, Mü Ller *et al.* 2005)
11	8.07/ 8.20	515.1209	515.1190	$C_{25}H_{23}O_{12}$	179, 135	3,4-di-*O*-caffeoyl quinic acid	23.12±1.64	(Araujo, Mü Ller *et al.* 2005)
		447.0921	447.0927	$C_{21}H_{19}O_{11}$	285, 151	Luteolin-7-*O*-glucoside	0.65±0.10	(Ibrahim, El-Halawany *et al.* 2015)
12	8.53	529.1365	529.1346	$C_{26}H_{25}O_{12}$	367, 349, 191, 179, 161, 135, 133	Feruloyl-caffeoylquinic acid isomer	nq	(Han, Ye *et al.* 2008)
13	8.86/ 8.90	529.1365	529.1346	$C_{26}H_{25}O_{12}$	367, 349, 191, 179, 161, 135, 133	Feruloyl-caffeoylquinic acid isomer	nq	(Han, Ye *et al.* 2008)
		179.0339	179.0344	$C_9H_7O_4$	135, 79	Caffeic acid	2.82±0.29	(Araujo, Mü Ller *et al.* 2005)
14	9.12	529.1365	529.1346	$C_{26}H_{25}O_{12}$	367, 349, 191, 179, 161, 135, 133	Feruloyl-caffeoylquinic acid isomer	nq	(Han, Ye *et al.* 2008)
15	9.32	285.0380	285.0399	$C_{15}H_9O_6$	151, 133	Luteolin	0.39±0.01	(Ferracane, Graziani *et al.* 2010)
		301.0345	301.0348	$C_{15}H_9O_7$	179, 151	Quercetin	0.01±0.00	(Ferracane, Graziani *et*

								al. 2010)
16	9.55	529.1365	529.1346	$C_{26}H_{25}O_{12}$	367, 349, 191, 179, 161, 135, 133	Feruloyl-caffeoylquinic acid isomer	nq	(Han, Ye *et al.* 2008)
17	9.85/ 9.94	543.1498	543.1503	$C_{27}H_{27}O_{12}$	381, 367, 349, 335, 193, 179, 161, 149, 135	Unknown	nq	
		325.1651	325.1651	$C_{17}H_{25}O_6$	281, 263, 235, 219, 203, 191, 151, 111, 83, 59	Unknown	nq	
		689.2905	689.2903	$C_{46}H_{41}O_6$	627, 353, 325, 281, 235, 191, 179, 161, 135	Unknown	nq	
		353.0888	353.0873	$C_{16}H_{17}O_9$	191, 173, 135, 127, 93, 85	Chlorogenic acid	7.12±0.83	(Hossain, Rai *et al.* 2010)
18	10.55	853.4720	853.4738 853.4679	$C_{48}H_{69}O_{13}$ $C_{55}H_{65}O_8$	584, 513, 191, 179, 161, 135, 119, 113, 101, 89, 85, 71, 59	Unknown	nq	
18	10.97	649.4045	649.4046	$C_{47}H_{53}O_2$	407, 191, 129, 113, 85, 75	Unknown	nq	
19	15.46	504.3098	504.3087	$C_{29}H_{44}O_7$	279, 242, 224, 168, 153, 79, 59	Unknown	nq	
		564.3275	564.3298	$C_{31}H_{48}O_9$	279, 242, 224, 97, 79	Unknown	nq	
20	15.76	426.9764	426.9785	$C_{15}H_7O_{15}$	407, 387, 293, 283, 255, 217, 81, 79	Unknown	nq	
21	16.22	480.3083	480.3087	$C_{27}H_{44}O_7$	255, 242, 224, 168, 153, 79	Unknown	nq	
22	18.11	553.3193	553.3165	$C_{33}H_{45}O_7$	523, 345, 97, 84, 73	Unknown	nq	
23	21.00/ 21.16	418.9849	418.9828	$C_{24}H_3O_8$	353, 339, 311, 219, 205, 169, 119, 81	Unknown	nq	
		455.3539	455.3525	$C_{30}H_{47}O_3$	407, 377	Oleanolic acid	nq	(Kontogiani, Tomic *et al.* 2013)

Identification of compounds based on *m/z*, fragmentation pattern and retention time of standards. Quantities of the detected compounds were determined using commercial standards; nq = not quantified

Subsequently, the phytochemical profile of chloroform fraction of *Azorella glabra* was investigated due to its anticholinesterase activity. Then, the AgC was subject to mass spectrometry analysis in negative ionization (Hossain, Rai *et al.* 2010).

The LC–MS profile of AgC is shown in **Fig. 4.10**. Different compounds (> 14) were detected and tentative identification of most of them have not been reached through accurate mass and fragmentation pattern because not were present existing literature (**Tab. 4.5**). Moreover, not was possible to compare the retention times of compounds with those of the commercial standards because there were not available standards.

It is possible that the compounds present in AgC were terpenoids such as mulinic acid or azorellane and their derivatives isolated from *A. compacta* and other species belonging *Azorella* genus. As previously mentioned, the terpenes identified in other species of *Azorella* have a good activity against the AChE enzyme (Salgado, Areche *et al.* 2014; Bórquez, Bartolucci *et al.* 2016). If there were similar terpenes in the chloroform fraction of *A. glabra*, they would justify the anticholinesterase activity of the sample.

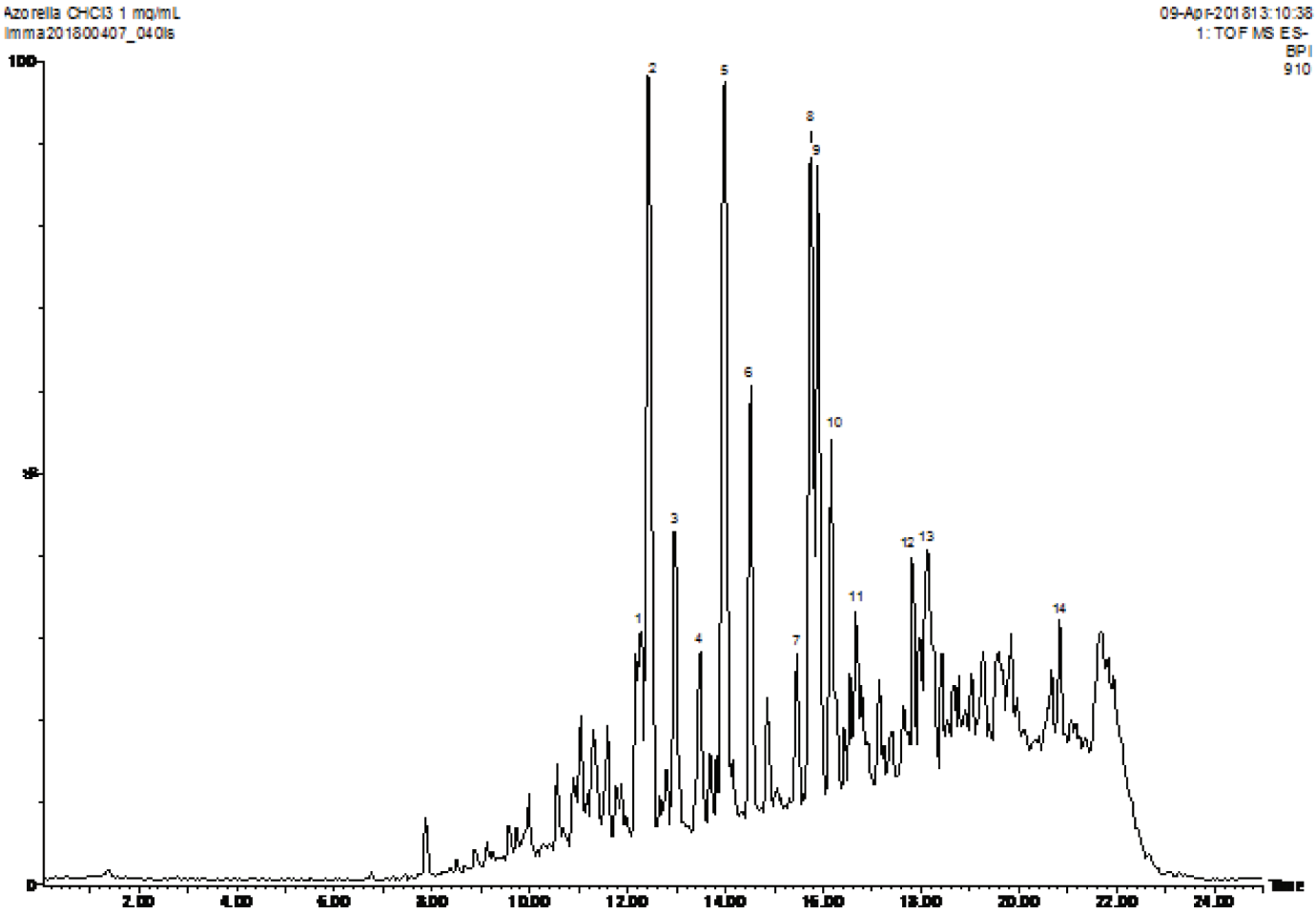

Figure 5.10. Chloroform fraction of *Azorella glabra* base peak intensity chromatogram (BPI)

Table 5.5. Liquid chromatography-tandem mass spectrometry (LC–MS/MS) of chloroform fraction of *Azorella glabra*

Peak no.	RT (min)	ESI (-) MS observed	ESI (-) MS Calc.	Molecular Formula	Δ ppm	MS/MS
1	12.25	393.2427	393.2430	$C_{26}H_{33}O_3$	-0.8	353, 335, 289, 273, 345, 235, 59
2	12.42	333.2072	333.2066	$C_{20}H_{29}O_4$	1.8	289, 287, 271, 253, 229, 135, 113, 95, 87, 83, 69, 57
3	12.91	333.2072	333.2066	$C_{20}H_{29}O_4$	1.8	271, 229, 135, 113, 95, 83, 69, 57
4	13.48	333.2072	333.2066	$C_{20}H_{29}O_4$	1.8	271, 229, 135, 113, 95, 83, 69, 57
5	13.98	331.1917	331.1909	$C_{20}H_{27}O_4$	2.4	287, 121, 111, 109, 96, 83
6	14.51	303.1940	303.1960	$C_{19}H_{27}O_3$	-6.6	259, 249, 243, 217, 189, 135, 123, 95, 81
7	15.46	505.3203	505.3224	$C_{22}H_{49}O_{12}$	-4.2	443, 375, 317, 273, 255, 187, 125, 97
8	15.76	333.2050	333.2066	$C_{20}H_{29}O_4$	-4.8	287, 121, 111, 109, 96, 83
9	15.89	657.4278	657.4308	$C_{46}H_{57}O_3$	-4.6	613, 335, 317, 307, 277, 273, 261, 235, 189, 187, 71
		317.2108	317.2117	$C_{20}H_{29}O_3$	-2.8	275, 273, 257, 255, 189, 187, 137, 97, 95, 83, 71
		402.2028	402.2042	$C_{23}H_{30}O_6$	-3.5	333, 317, 273, 187, 177, 111, 87, 71, 62
10	16.16	423.1459	423.1444	$C_{24}H_{23}O_7$	3.5	379, 367, 323, 320, 308, 305, 188, 176, 166
11	16.66	315.1962	315.1960	$C_{20}H_{27}O_3$	0.6	271, 253, 227, 187, 148, 135, 97
12	17.81	517.3687	517.3682	$C_{35}H_{49}O_3$	1.0	451, 405, 273, 201, 183, 169, 151, 125, 123, 107, 95, 73
13	18.14	553.2936	553.2954	$C_{36}H_{41}O_5$	-3.3	315, 187, 125
14	20.84	473.3442	473.3420	$C_{33}H_{45}O_2$	4.6	429, 411, 385, 357, 317, 271, 165, 109, 83, 69

4.7. Biological activity on cell lines of *A. glabra* samples

The phytochemical profiles of AgEA and AgC fractions of *A. glabra* were very interesting and suggest a further investigation. As previously mentioned, the identified compounds have antioxidant, anti-inflammatory, anti-tumoral activities (Uma Devi, Ganasoundari *et al.* 2000; López-Lázaro 2009).

In addition, it was previously reported that the methanolic extract of *Azorella compacta* induced apoptosis in leukaemia cells (Sung, Kwon *et al.* 2015).

The combination of specie extracts with anti-cancer drugs may offer a significant advantage for therapeutic efficacy by sensitizing malignant cells to drugs and overcoming drug-induced resistance in cancer. For these reasons, we focused our attention on the second most common hematologic malignancy, the Multiple Myeloma (MM) and we tested the *A. glabra* samples on MM cell lines, SKMM1, RPMI8226 and MM1S by different assays (Lamorte, Faraone *et al.* 2018).

4.7.1. Viability analysis of MM and healthy cells treated with *A. glabra* samples

The MM cell lines, RPMI8226, SKMM1 and MM1S, were treated with Ag EtOH extract and AgH, AgC, AgEA, AgB and AgW fractions and with DMSO, used as vehicle control at different concentrations (10 - 150 µg/mL) for 24, 48 and 72 h (**Fig. 4.11**). The viability test showed that most of samples, with the exception of the Ag EtOH extract and AgB and AgW fractions, exhibited a dose and time dependent anti-proliferative effect on MM cells.

In particular, the chloroform fraction (AgC) was the most active one on all MM cell lines and its effect was observed already at 24 h of treatment with the lowest concentration (10 µg/mL). Probably, its cytotoxic effect could be due to the greater content of terpenoids. In fact, AgC fraction contained more TTeC and, at the same time, showed a greater anti-proliferative effect compared to AgH fraction. This result is in accordance with other *in vitro* and *in vivo* studies that reported terpenoids as inhibitors of both cell proliferation and tumour growth in several tumours, including breast, prostate, pancreatic carcinomas, lung cancer and leukaemia. Moreover, the cytotoxic

activity of different azorellane diterpenoids isolated from *A. compacta* on a breast cancer cell line (MCF-7) was described (Lamorte, Faraone *et al.* 2018).

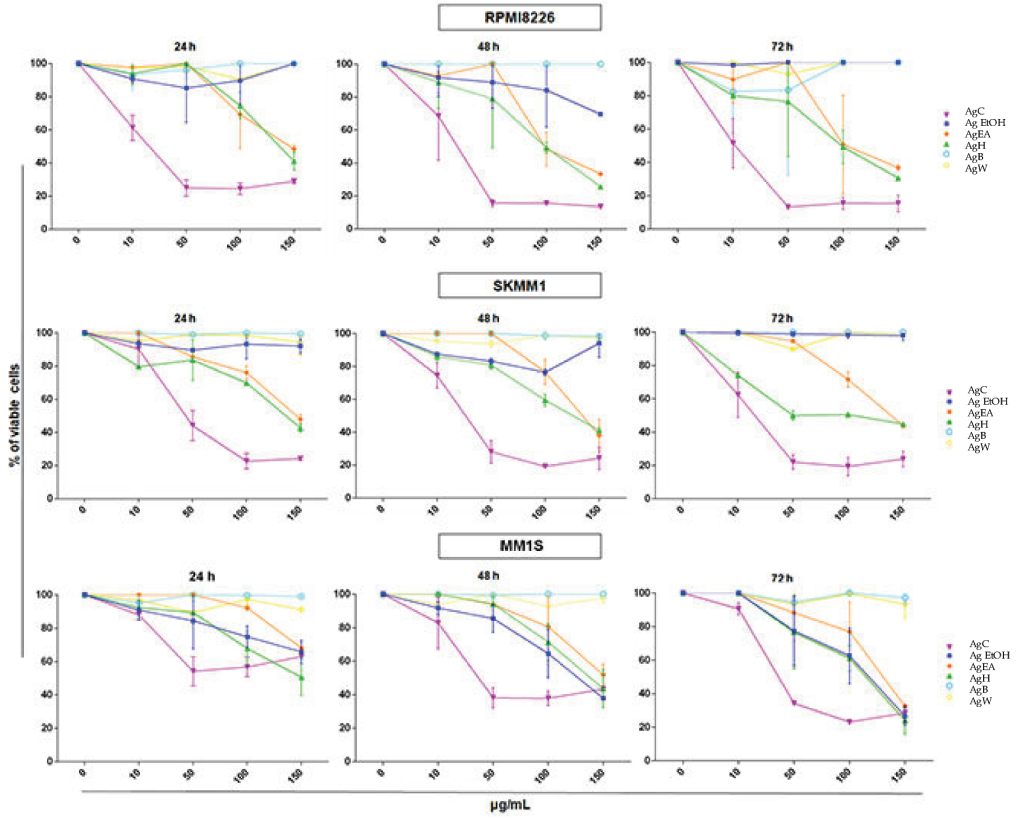

Figure 5.11. Viability assay of RPMI8226, SKMM1 and MM1S cells after treatment with *A. glabra* samples at different concentrations (10, 50, 100 and 150 µg/mL) for 24, 48 and 72 h
Results are expressed as percentage of cell viability normalized to DMSO-treated control cells. The line-graphs represent average with standard deviation from three independent experiments. Samples are crude ethanol extract (Ag EtOH), *n*-hexane fraction (AgH), chloroform fraction (AgC), ethyl acetate fraction (AgEA), *n*-butanol fraction (AgB) and water fraction (AgW).

The concentration of AgC fraction that inhibited MM cell growth of 50% (EC_{50}, **Tab. 4.6**) was also calculated. In all the MM tested lines, the EC_{50} value was reduced over the time. Already after 24 h of treatment, the EC_{50} value is 16.74, 44.76 and 165.90 µg/mL for RPMI8226, SKMM1 and MM1S cells, respectively.

Table 5.6. EC_{50} values of the chloroform fraction of *A. glabra* on Multiple Myeloma cells

MM Cell lines	24 h µg/mL	48 h µg/mL	72 h µg/mL
RPMI8226	16.74	17.38	10.03
SKMM1	44.76	25.75	16.52
MM1S	165.90	53.02	39.63

Furthermore, in order to exclude any toxic effects on healthy cells, the peripheral blood mononuclear cells isolated from five healthy donors (HD-PBMCs) were treated with different concentrations (10–150 µg/mL) of AgC fraction for 24 and 48 h. Interestingly, AgC fraction had negligible effect on HD-PBMCs (**Fig. 4.12**).

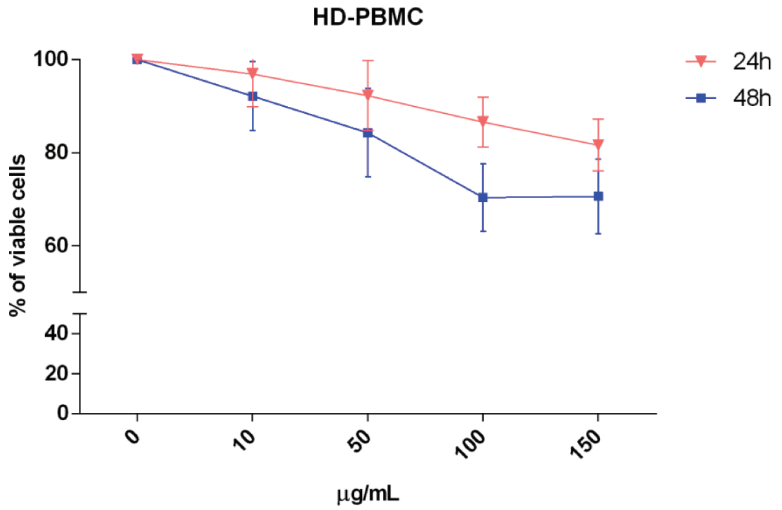

Figure 5.12. Analysis of five HD-PBMC viability after treatment with different concentrations (10, 50, 100 and 150 µg/mL) of chloroform fraction of *A. glabra* for 24 and 48 h
HD-PBMC = peripheral blood mononuclear cells isolated from five healthy donors. Results are expressed as percentage of cell viability normalized to DMSO-treated control cells. The line-graphs represent average with standard deviation from five healthy subjects.

4.7.2. Evaluation of apoptosis in MM cells treated with chloroform fraction of *A. glabra*

The apoptosis assay on MM cells was performed using a concentration of 50 µg/mL of the AgC fraction in order to investigate the anti-proliferative effect. The AgC fraction treatment for 24 and 48 h induced a significant increase of apoptosis in MM cells respect to their control in a time dependent manner (**Fig. 4.13 A-F**). In particular, the percentage of apoptotic cells increased:

- from 53.19 % at 24 h in the chloroform fraction of *A. glabra* treated cells, respect to DMSO control to 76.99 % at 48 h for RPMI8226 cells (**Fig. 4.13 A-B**);

- from 31.80 % at 24 h to 63.15 % at 48 h for SKMM1 cells (**Fig. 4.13 C-D**);

- from 64.35 % at 24 h to 86.25 % at 48 h for MM1S cells (**Fig. 4.13 E-F**).

Moreover, apoptosis was also evaluated by western blot analysis in RPMI8226 cells (**Fig. 4.13 G-I**). The presence of the cleaved form of the caspase-3 substrate, the poly-ADP ribose polymerase (cleaved PARP-1) and the expression level of Bcl-2 were examined. There was a significant activation of caspase-3 in MM cells treated for 24 h with 50 µg/mL of AgC fraction compared to the control, detectable by the increase of cleaved PARP-1 (**Fig. 4.13 G**). Instead, the expression of Bcl-2 was the same in MM treated and control cells (**Fig. 4.13 H**) (Lamorte, Faraone *et al.* 2018).

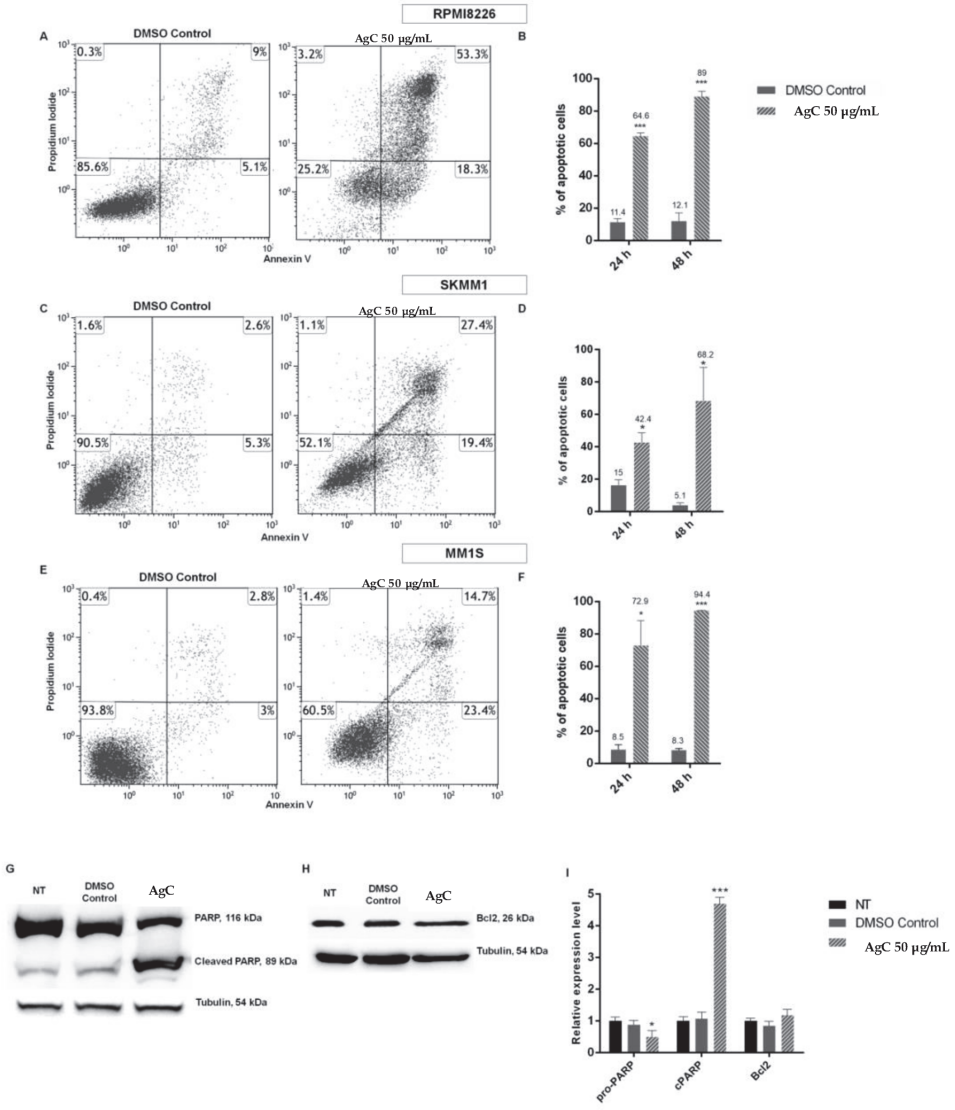

Figure 5.13. Cytofluorimetric evaluation of apoptosis/necrosis of RPMI8226 (**A-B**), SKMM1 (**C-D**) and MM1S (**E-F**) cell lines, after treatment with 50 µg/mL of chloroform fraction of *A. glabra* (AgC) for 24 and 48 h. Western blot analysis of AgC fraction on the expression of PARP-1 (**G**), and Bcl2 (**H**) in RPMI8226 cells treated with 50 µg/mL of AgC fraction for 24 h.

Dot plots (**A, C, E**) show a single representative experiment after 24 h of treatment; the bar-graphs (**B, D, F**) represent average of percent of apoptosis, obtained from the sum of early and late apoptosis, of three independent experiments with standard deviation (*$p < 0.05$, ***$p < 0.001$). Tubulin was used as a protein loading control. The bar-graphs (**I**) are representative of three independent experiments. Statistical analysis was carried out by a paired two-tailed Student's t-test (*$p < 0.05$, ***$p < 0.001$, n = 3). Data were represented as mean ± standard error of the mean.

4.7.3. Cell cycle analysis in MM cells treated with chloroform fraction of *A. glabra*

Cell cycle cytofluorimetric analysis of MM cells treated with 50 µg/mL of AgC fraction showed a G0/G1-phase arrest with respect to control in a time dependent manner (**Fig. 4.14 B, D, F**). In particular, the number of RPMI8226 treated cells in G0/G1 phase significantly increases from 34.50 % to 53.82 % and from 24.00 % to 60.00 % after 24 and 48 h, respectively.

Moreover, a significant decrease of RPMI8226 treated cells in S phase was observed at 24 and 48 h (28.10 % and 19.80%, respectively) (**Fig. 4.14 A-B**).

A similar result was observed for SKMM1 cells: the percentage of cells in G0/G1 phase increases from 48.46 % to 61.88 % and from 55.83 % to 73.55 % after 24 and 48 h of treatment, respectively. In addition, after 48 h of treatment, the number of cells at G2/M phase decreased from 15.10 % to 4.34 % for the control and SKMM1 cells, respectively (**Fig. 4.14 C-D**).

For MM1S was observed a significant increase of cells in G0/G1 phase from 47.08 % to 58.50 % ($p < 0.05$) after 48 h of treatment (**Fig. 4.14 E-F**).

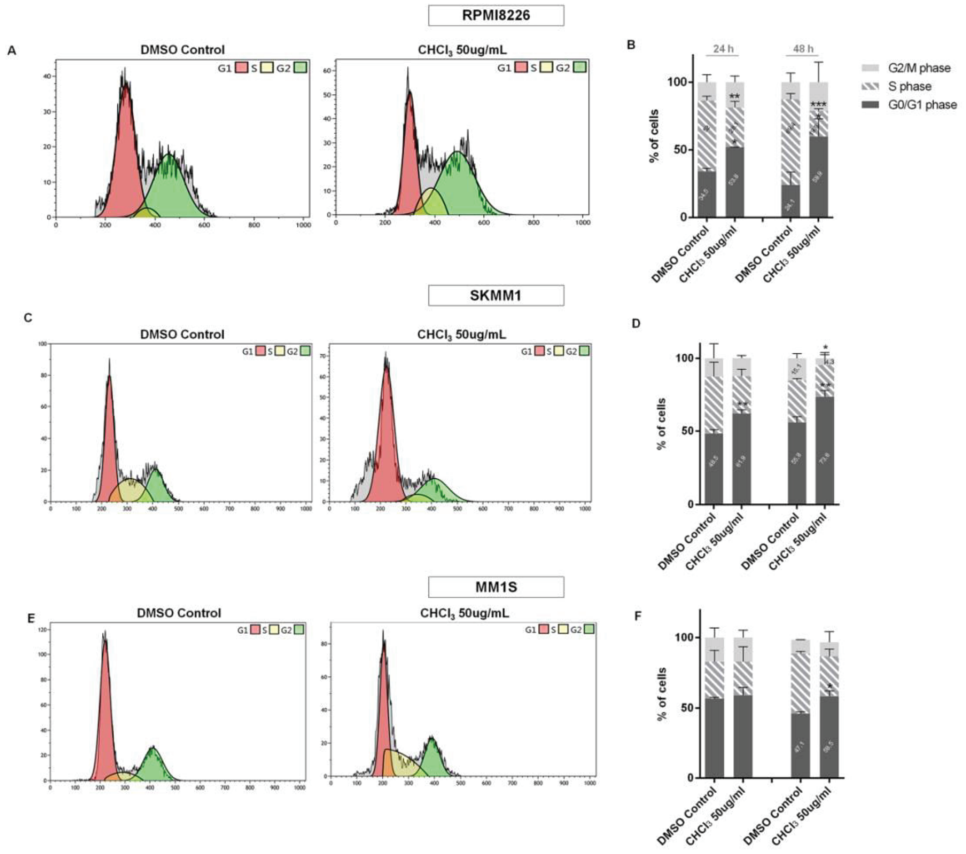

Figure 5.14. Cytofluorimetric evaluation of cell cycle on RPMI8226, SKMM1 and MM1S cell lines at 50 µg/mL of AgC fraction for 24 and 48 h
Cell cycle histograms (**A, C, E**) show a single representative experiment after 24 h of treatment; the bar-graphs (**B, D, F**) represent average of three independent experiments with standard deviation (*$p < 0.05$, **$p < 0.01$, ***$p < 0.001$).

4.7.4. Cell migration assay in RPMI8226 cells treated with chloroform fraction of *A. glabra*

The effects of the AgC fraction on the MM cell migration were investigated on RPMI8226 cells using a Transwell assay. Data showed that the chloroform fraction reduced cell migration rate. The percentage of migrated RPMI8226 treated cells was of 54.00 % respect to DMSO control, indicating that AgC induced a significant decrease of MM cell migration ($p = 0.01$) (**Fig. 4.15**).

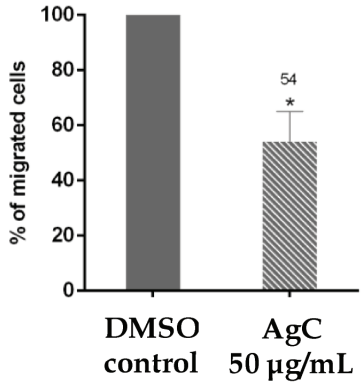

Figure 5.15. Transwell migration assays of RPMI8226 cells performed after treatment with 50 µg/mL of chloroform fraction of *A. glabra* and with DMSO control.
Migrated cells were counted after 24 h of incubation. The bar-graphs represent average of three independent experiments with standard deviation (*$p < 0.05$).

4.7.5. Measurement of Reactive Oxygen Species (ROS) generation and mitochondria membrane potential ($\Delta\Psi_m$)

The effects of the AgC fraction on the intracellular redox status were investigated in RPMI8226 cells by the determination of the levels of ROS production. Data showed that the fraction did not significantly affected ROS formation at 50 µg/mL as compared with control cells (**Fig. 4.16 A**).

The $\Delta\Psi_m$ was evaluated by the cation fluorescent probe tetramethyl rhodamine methyl ester (TMRM) in order to verify whether the ROS formation in RPMI8226 cells could be fit with changes or loss in $\Delta\Psi_m$. RPMI8226 cells exposed to 50 µg/mL of AgC fraction for 6 h did not show any significant difference compared to the control (**Fig. 4.17 B**) (Lamorte, Faraone *et al.* 2018).

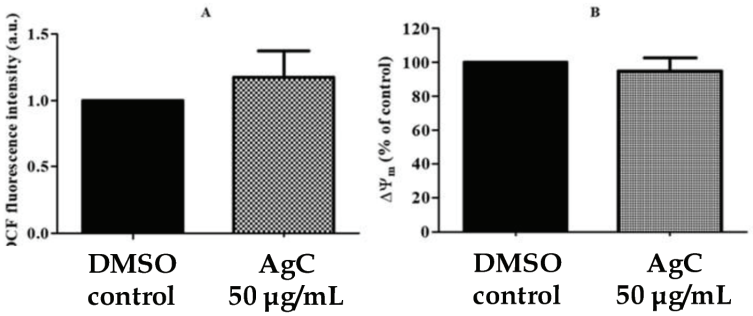

Figure 5.16. Evaluation of the intracellular ROS levels (**A**) and of $\Delta\Psi_m$ depolarization (**B**) of RPMI8226 cells treated with 50 µg/mL of AgC fraction.
The values are means ± standard error of mean of three replicates from three independent experiments.

In conclusion, the anti-proliferative effect of AgC on three MM cell lines that harbour different chromosomal translocations [t(16;22), t(14;20) and t(14;16) for RPMI8226, SKMM1 and MM1S, respectively]. In particular, the translocation t(14;16) represents a high-risk cytogenetic marker. Our data are in agreement with previous studies that described the cytotoxic activity on solid and haematological malignancies of other *Azorella* extracts. Sung *et al.* reported the cytotoxic activity of methanolic extract of *A. compacta* and its ability to induce apoptosis on leukemic HL60 cells (Sung, Kwon *et al.* 2015). Previously, another work described the antiproliferative activity of a new chalcone from *A. madreporica* on colon, breast and prostate cancer cells. All these data candidate *Azorella* genus as a possible source of natural agent against different cancer types, including hematologic malignancies (Lamorte, Faraone *et al.* 2018). The main criterion for an "ideal" anti-tumour agent is the specificity of the action on tumour cells with no or minimal toxicity on healthy ones. For this reason, in addition to efficacy, the safety profile for the development of a new anti-tumour agent should be taken into consideration. To our knowledge, few studies verified specie extracts toxicity on healthy cells in a preliminary step. Interestingly, in the present work it showed that AgC fraction did not show toxicity towards the normal cells like PBMCs.

Wong *et al.* reported that EC_{50} values are widely used to assess the potency of a compound (Wong, Woo *et al.* 2013). Our data indicated that the EC_{50} value was reduced over the time in all the MM cells with a mean of 22.06 ± 15.56 µg/mL after 72 h of treatment. These data are in agreement with a report demonstrating that a natural extracts possessing an EC_{50} value of about 20.00 µg/mL are considered to have anti-cancer therapeutic value. Thus, the fact that the AgC fraction showed an EC_{50} value around 20.00 µg/mL encourages further investigation for its possible therapeutic application.

Another essential characteristic of an antitumor drug is the ability to induce tumour cell apoptosis. In fact, the simultaneous ability of a substance to inhibit cell growth and to induce apoptosis allows discriminating between anti-tumour agents and toxic ones. Our data showed a significant increase of apoptotic cells during treatment with the AgC fraction. Several works have demonstrated that the block in the G0/G1 phase is a characteristic feature of apoptosis. Our data showed an increase of treated cells in the G0/G1 phase in a time depended manner with a corresponding decline of cells in the S and G2/M phases, confirming apoptosis. In addition, the AgC fraction

induced a strong inhibition of migration in myeloma cells, however, apoptosis was promoted.

Furthermore, to get a preliminary indication of the cellular mechanisms by which the AgC fraction induced cell death, the expression level of apoptosis-related proteins was detected by western blot analysis. The chloroform fraction-treated cells showed an increase of PARP-1 cleavage, but no reduction of the Bcl-2 protein level was observed. These results indicated that, probably, the death process was not regulated through a mitochondrial damage characteristic of the intrinsic pathway. In fact, both the extrinsic and intrinsic apoptotic pathways may be involved in caspase-3 cleavage, but Bcl-2 is implicated only in the intrinsic pathways. Bcl-2 blocks the release of cytochrome c from the mitochondria into the cytosol inhibiting changes in mitochondrial membrane potential and mitochondrial permeability.

Accumulation of ROS and the disruption of $\Delta\Psi_m$ represent an early event in the intrinsic pathway of apoptosis. In our setting, the AgC fraction did not significantly stimulate ROS formation in treating MM cells as compared with control. ROS concentration was even not reduced. These results were the same that have been shown using *in vitro* assays in which we did not observe a strong radical scavenging activity of AgC fraction. In addition, no loss of $\Delta\Psi_m$ was detected in MM cells treated with AgC fraction, pointing out that AgC fraction-induced apoptosis could be not regulated through a mitochondrial damage.

In summary, our data strongly show that the AgC fraction has *in vitro* potential anti-MM effects compared to HD-PBMCs, giving an additional advantage over other fractions. Considering the lack of literature knowledge on the anticancer effects of *Azorella glabra* samples, this study represents a pioneer research in this area. Further investigations are ongoing in order to identify specific bioactive compounds. Altogether, our data indicate that *A. glabra* samples could represent a promising source of natural anti-MM compounds.

These data are reported in our recent paper (Lamorte, Faraone *et al.* 2018).

4.8. *Azorella glabra* study conclusions

The ethanol extract of *A. glabra* aerial parts was subjected to liquid/liquid fractionation using solvent with increasing polarity.

The antioxidant activity, determined by six complementary *in vitro* assays, showed different values among fractions. Relative Antioxidant Capacity Index (RACI) evidenced as the *A. glabra* ethyl acetate fraction is the most active sample. More in detail, fraction reported activity was: *n*-hexane < chloroform < water < *n*-butanol < ethyl acetate.

Furthermore, the antidiabetic and anticholinesterase activities were performed on the samples and the phytochemical profile in *A. glabra* ethyl acetate and chloroform fractions was analyzed with the identification or tentative identification of more than 20 compounds for the first time in this specie.

Then, the biological activity on MM cell lines was investigated. In particular, some fractions showed a dose and time dependent anti-proliferative activity on MM cells. The chloroform fraction showed major effects in terms of reduction of cell viability, induction of apoptosis, and cell cycle arrest on MM cells. The apoptosis induction was also confirmed by the activation of caspase-3. Importantly, the chloroform fraction exhibited a negligible effect on the viability of healthy cells.

In conclusion, this first report on *A. glabra* characterization and biological activity demonstrated as it could be considered a rich source of potential nutraceuticals that is promising for the development of safe food products, natural additives and cosmetics.

CHAPTER 5. RESULTS AND DISCUSSIONS OF *MINTHOSTACHYS DIFFUSA* EPL.

5.1. The extraction yield of *M. diffusa* samples

The aerial parts of *Minthostachys diffusa* were dried at room temperature (95 g in triplicate) and extracted by dynamic maceration using 96% ethanol for 24 h at a solid to solvent ratio of 1:15 (w/v) per extraction for four times (Dávila, Sterner *et al.* 2013). The four extracts of each replicate extraction were combined.

The ethanol extraction yield was about 12.30 ± 1.07 %. This is the first time that aerial parts of *M. diffusa* were extracted with 96% ethanol.

In bibliography are reported studies on other species of *Minthostachys* genus. For example, the aerial parts of *M. verticillata* were extracted with ethanol obtained an extraction yield of 3.60 %, considerably lower than values obtained in our study (Palacios, del Corral *et al.* 2010). Instead, *M. molli* and *M. verticillata* extracts were obtained from infusing with an extraction yield of 20.80 % in the first case (Vaquero, Serravalle *et al.* 2010; Solis-Quispe, Tomaylla-Cruz *et al.* 2016). Often the *Minthostachys* species were extracted to obtain the essential oil, for example the leaves of *M. spicata*, were extracted using hydrodistillation to have the essential oil to study its chemical composition and antioxidant and antiproliferative activities by Solis-Quispe *et al.* (Solis-Quispe, Tomaylla-Cruz *et al.* 2016).

Then, a part (7.00 g in 100 mL of water) of the reunited crude ethanol extract (Md EtOH) was subjected to liquid/liquid extraction using an increasing solvent polarity to make a separation of compounds present in the initial sample. The obtaining fractions were the following: *n*-hexane (MdH), chloroform (MdC), ethyl acetate (MdEA), *n*-butanol (MdB) and water (MdW) (Saeed, Khan *et al.* 2012). The extraction's yield of dry fractions was reported in **Fig. 5.1**.

The water and chloroform fractions showed the highest extraction yield (28.46 ± 1.87 % and 23.06 ± 2.19 %, respectively); instead, the butanol fraction demonstrated the lower extraction yield (12.36 ± 1.01 %).

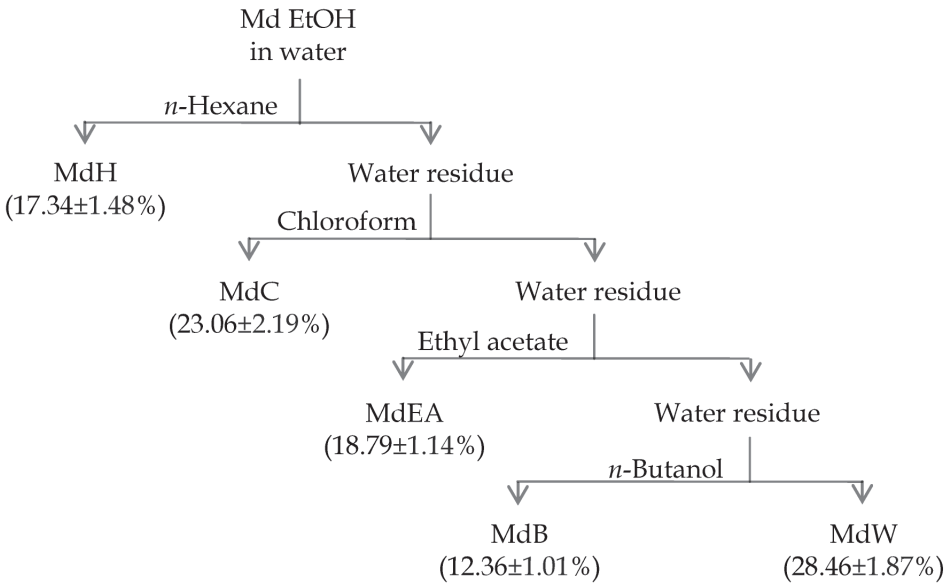

Figure 6.1. Extraction yields of *M. diffusa* EtOH extract partitioned fractions
Results were expressed as mean ± standard deviation of the triplicate experiments. Samples are crude ethanol extract (Md EtOH), *n*-hexane fraction (MdH), chloroform fraction (MdC), ethyl acetate fraction (MdEA), *n*-butanol fraction (MdB) and water fraction (MdW).

5.2. The influence of polarity solvents on total polyphenolic, flavonoid and terpenoid content on *M. diffusa* samples

The phytochemical profiles of each sample in terms of total polyphenolic (TPC), flavonoid (TFC) and terpenoid (TTeC) content were determined by three different *in vitro* assays.

The total polyphenolic content (TPC) of Md EtOH and its fractions was carried out and the samples showed quantitative differences in TPC value (**Fig. 5.2**), with a mean value of 79.29 mg of Gallic Acid Equivalents per gram of dried sample (mg GAE/g). The MdEA and MdB fractions showed the higher TPC values than other samples (169.74 ± 3.10 and 135.11 ± 5.22 mg GAE/g, respectively).

The total flavonoid content assay on *M. diffusa* samples that presented a TPC value higher than the mean value was carried out (Md EtOH, MdEA and MdB). In particular, Md EtOH extract showed the higher TFC value (400.84 ± 26.94 mg QE/g), followed by MdEA and MdB (177.33 ± 14.05 and 114.23 ± 6.03 mg QE/g, respectively).

Again, the total terpenoid content (**Fig. 5.2**) determined in *M. diffusa* samples showed the Md EtOH extract as the best sample with the highest value (1590.31 ± 32.33 mg LE/g) than the mean value of 577.80 mg of Linalool Equivalents per gram of dried sample (mg LE/g).

Results demonstrated again as the phenolic, flavonoid and terpenoid contents depends from using solvents during the extraction (Nakamura, Ra *et al.* 2017).

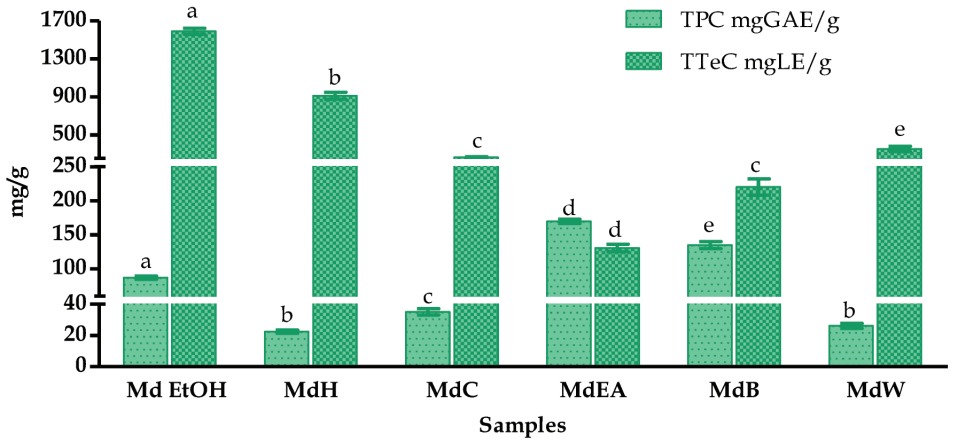

Figure 6.2. Total Polyphenol Content (TPC) and Total Terpenoid Content (TTeC) of *Minthostachys diffusa* samples
Results were expressed as mean ± standard deviation of triplicate determinations in mg of Gallic Acid Equivalents per gram of dried sample (mg GAE/g) and in mg of Linalool Equivalents per gram of dried sample (mg LE/g). In each test, the values with the same letter are not significant different at the $p < 0.05$ level, 95% confidence limit, according to one-way analysis of variance (ANOVA). Samples are crude ethanol extract (Md EtOH), *n*-hexane fraction (MdH), chloroform fraction (MdC), ethyl acetate fraction (MdEA), *n*-butanol fraction (MdB) and water fraction (MdW).

5.3. Antioxidant activity of *M. diffusa* samples

The antioxidant activity of *M. diffusa* aerial parts was determined by six different complementary *in vitro* antioxidant assays (ABTS, DPPH, SO, NO, FRAP and BCB). The radical scavenging activity was evaluated by synthetic cationic and neutral (ABTS and DPPH) and physiological (superoxide anion and nitric oxide) radicals.

The ethyl acetate fraction of *M. diffusa* showed the highest radical scavenging-activity (**Tab. 5.1**). In fact, the MdEA reported 444.76 ± 28.24 mg TE/g and 281.64 ± 7.93

mg TE/g in ABTS and DPPH, respectively, followed by MdB (218.56 ± 9.38 and 122.30 ± 2.77 mg TE/g in ABTS and DPPH, respectively). The MdC followed by MdW showed the lowest activity in both assays.

The ability of samples to scavenge superoxide anion and nitric oxide was expressed as IC_{25} and results were compared with ascorbic acid. In the superoxide anion assay (SO), all samples caused a dose-dependent inhibition. In particular, the butanol fraction of *M. diffusa* showed an IC_{25} of 0.26 ± 0.01 mg/mL, very similar to ascorbic acid (IC_{25} of 0.26 ± 0.02 mg/mL). The MdW and MdC fractions presented the lowest activity.

The MdH was not active in ABTS, DPPH and SO assays.

The scavenging ability against the biological nitric oxide ($^{\cdot}NO$) was detectable only in MdB fraction with an ability higher than ascorbic acid (IC_{25} of 2.50 ± 0.15 and 4.78 ± 0.09 mg/mL, respectively; data not shown in **table 5.1**).

The ferric reducing antioxidant power was determined and the ethyl acetate and butanol fractions of *M. diffusa* presented the higher values (574.86 ± 9.14 and 297.75 ± 5.71 mg TE/g, respectively). Instead, the MdC and MdH fractions were the least active.

The ability of *M. diffusa* samples to inhibit the lipid peroxidation was determined by *β*-Carotene Bleaching test (BCB) and the results were expressed as percentage of antioxidant activity (% AA) at the initial sample concentration of 1 mg/mL. The samples presented values very similar. Among all, the most active sample was the MdEA fraction (19.13 ± 0.93 % AA); while, there was no activity for the MdB and MdW fractions.

Table 6.1. Results of ABTS, DPPH and Super Oxide (SO) scavenging activity, Ferric Reducing Antioxidant Power (FRAP) and *β*-Carotene Bleaching (BCB) of *Minthostachys diffusa* samples

Samples	ABTS (mgTE/g)	DPPH (mgTE/g)	SO (IC_{25} mg/mL)	FRAP (mgTE/g)	BCB %AA
Md EtOH	146.07±4.20^{a}	113.05±3.51^{a}	0.92±0.08^{a}	224.67±3.37^{a}	10.12±0.52^{a}
MdH	nc	nc	nc	27.27±0.99^{b}	11.01±0.33^{a}
MdC	29.61±0.74^{b}	17.64±0.03^{b}	1.03±0.08^{a,b}	22.18±0.90^{b}	13.03±0.49^{b}
MdEA	444.76±28.24^{c}	281.64±7.93^{c}	0.62±0.04^{c}	574.86±9.14^{c}	19.13±0.93^{c}
MdB	218.56±9.38^{d}	122.30±2.77^{a}	0.26±0.01^{d}	297.75±5.71^{d}	nc
MdW	45.85±0.42^{b}	37.01±1.63^{d}	1.14±0.09^{b}	64.67±1.63^{e}	nc

Samples are crude ethanol extract (Md EtOH), *n*-hexane fraction (MdH), chloroform fraction (MdC), ethyl acetate fraction (MdEA), *n*-butanol fraction (MdB) and water fraction (MdW). Data are expressed as means ± standard deviation from three experiments; mg GAE/g = mg of Gallic Acid Equivalents per gram of dried sample; mg TE/g = mg of Trolox Equivalents per gram of dried sample; IC_{25} mg/mL = concentration of the sample required to inhibit the activity of the radical by 25%; % AA = percentage of Antioxidant Activity at initial sample concentration of 1 mg/mL; different superscripts in the same row indicate significant difference ($p < 0.05$); nc = not calculable.

Moreover, the Pearson correlation coefficient was calculated (**Tab. 5.2**). Results showed a good correlation between polyphenols and antioxidant activity. The highest correlations were found between the total polyphenol content and radical-scavenging activity ($r_{TPC/ABTS}$ = 0.96 and $r_{TPC/DPPH}$ = 0.94) and ferric reducing power ($r_{TPC/FRAP}$ = 0.96). The highest correlation was also observed between the ferric reducing power of the samples and the radical-scavenging activity by ABTS and DPPH assays ($r_{FRAP/ABTS}$ = 1.00 and $r_{FRAP/DPPH}$ = 0.99). There were good correlations between ABTS and DPPH assays ($r_{ABTS/DPPH}$ = 0.99) and between NO and SO tests ($r_{NO/SO}$ = 0.91).

Terpenoids are less involved in testing activities (r < 0 for terpenoids against all assays, except for BCB test $r_{TTeC/BCB}$ = 0.06).

Table 6.2. Pearson correlation coefficient calculated among tested *M. diffusa* extract and fractions

	TPC	TTeC	ABTS	DPPH	SO	NO	FRAP	BCB
TPC	1.00							
TTeC	-0.26	1.00						
ABTS	0.96	-0.31	1.00					
DPPH	0.94	-0.23	0.99	1.00				
SO	0.69	-0.40	0.50	0.44	1.00			
NO	0.44	-0.31	0.21	0.13	0.91	1.00		
FRAP	0.96	-0.24	1.00	0.99	0.50	0.22	1.00	
BCB	0.26	0.06	0.40	0.43	-0.40	-0.58	0.38	1.00

Total Polyphenolic Content (TPC), Total Terpenoid Content (TTeC), ABTS assay, DPPH assay, Super Oxide anion scavenging activity (SO), Nitric Oxide radical scavenging activity (NO), Ferric Reducing Antioxidant Power assay (FRAP) and β-Carotene Bleaching assay (BCB).

The Relative Antioxidant Capacity Index (RACI) was calculated on the results of TPC, ABTS, DPPH, SO, NO, FRAP and BCB assays. The values confirmed the results obtained so far (**Fig. 5.3**) evidencing as the ethyl acetate fraction of *M. diffusa* presented the highest value (1.12), followed by the butanol fraction (0.68). The MdW and MdH fractions presented the lowest index (-0.66 and -0.68, respectively) and, therefore, a relative lack of antioxidant activity. Also in this case, the RACI values may be related to the high total polyphenol content of the ethyl acetate and butanol fractions.

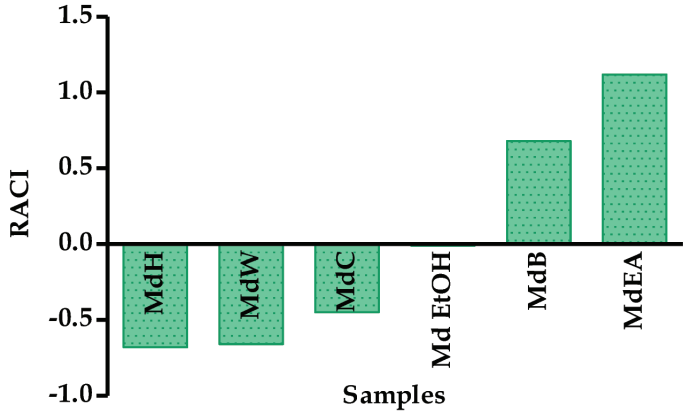

Figure 6.3. Relative Antioxidant Capacity Index (RACI) of *Minthostachys diffusa* samples. Samples are crude ethanol extract (Md EtOH), *n*-hexane fraction (MdH), chloroform fraction (MdC), ethyl acetate fraction (MdEA), *n*-butanol fraction (MdB) and water fraction (MdW).

To the best of our knowledge, this is the first study of antioxidant activity of *Minthostachys diffusa*. Other studies are reported on species belonging *Minthostachys* genus.

Vaquero *et al.* reported a low radical scavenging activity in infusion extract of *M. verticillata* determined by DPPH assay (Vaquero, Serravalle *et al.* 2010).

Instead, the essential oil obtained from leaves of *M. spicata* exhibited the maximum radical scavenging effect on DPPH radical at 76.05 ± 2.40 % at 500 µg/mL with an IC_{50} value of 82.19 ± 6.70 µg/mL (Solis-Quispe, Tomaylla-Cruz *et al.* 2016). Comparing our results, the ethanol extract presented in DPPH assay an IC_{50} value of 269.45 ± 8.24 µg/mL significantly higher than that of essential oil of *M. spicata*. Instead, the ethyl acetate fraction, the most active sample of *M. diffusa*, showed an IC_{50} value of 108.14 ± 3.07 µg/mL after 30 minutes of incubation and IC_{50} of 90.04 ± 3.44 µg/mL after 90 minutes. This value is very close to that of *M. spicata*.

5.4. Potential antidiabetic activity of *M. diffusa* samples

The ability of *M. diffusa* samples to inhibit the *a*-amylase and *a*-glucosidase enzymes was tested. In both assays results were concentration-dependent and acarbose was used as standard (**Fig. 5.4**). In *a*-amylase test the MdH and MdB fractions were not active and in both assays the MdW fraction was not active.

A)

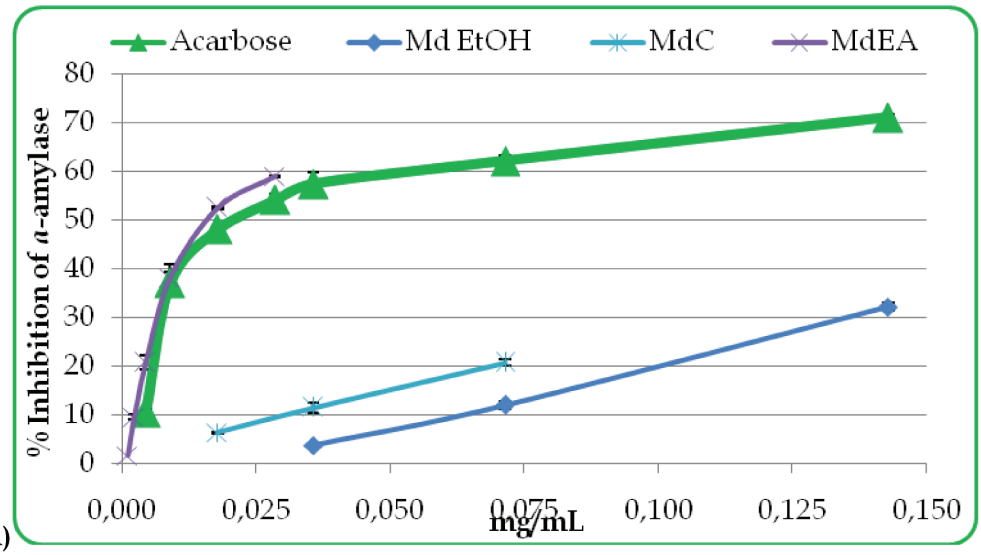

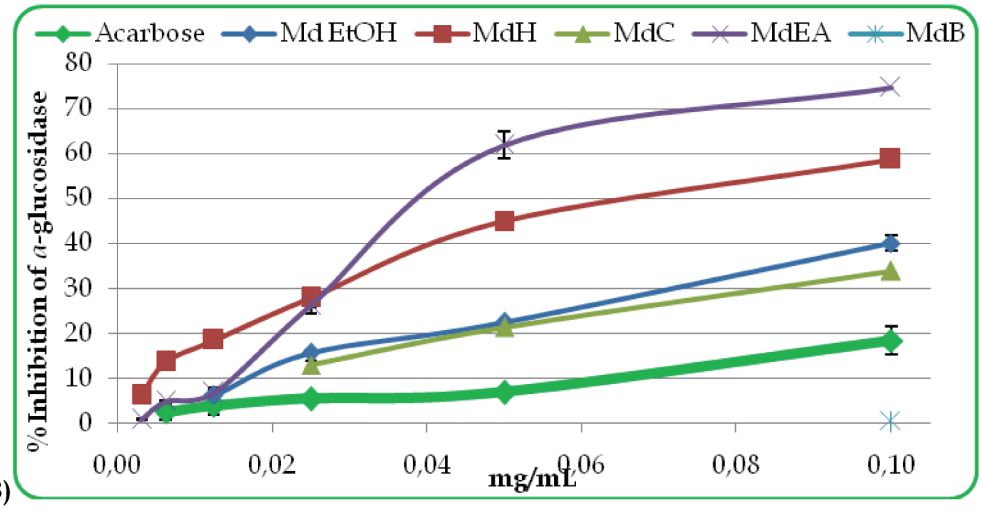

B)

Figure 6.4. *a*-Amylase (**A**) and *a*-glucosidase (**B**) inhibition activity of acarbose and *Minthostachys diffusa* samples

Samples are acarbose, crude ethanol extract (Md EtOH), *n*-hexane fraction (MdH), chloroform fraction (MdC), ethyl acetate fraction (MdEA) and *n*-butanol fraction (MdB). No enzymatic inhibition present for the missing samples. Data are mean ± standard deviation from three experiments.

In *a*-amylase inhibition test was possible reached the inhibition percentage of 50% only in the ethyl acetate fraction of *Minthostachys diffusa* with an IC_{50} value of 0.02 ± 0.00 mg/mL lower than acarbose (IC_{50} of 0.02 ± 0.00 mg/mL) (**Fig. 5.5** and **5.6**).

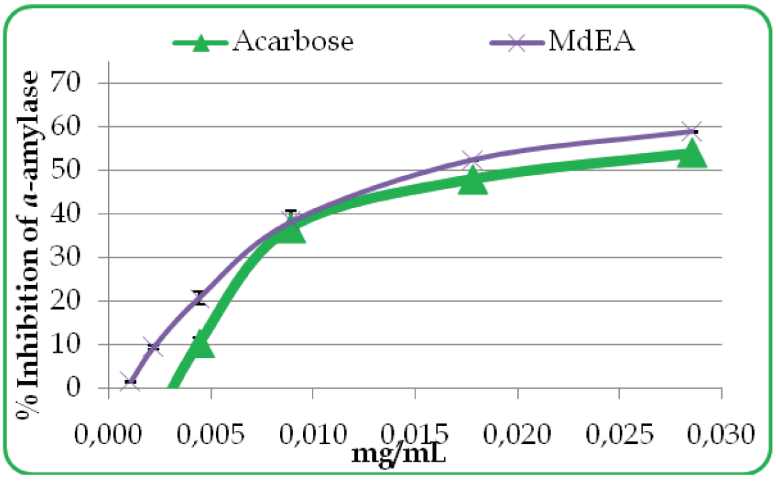

Figure 6.5. *a*-Amylase inhibition activity of acarbose and ethyl acetate fraction of *Minthostachys diffusa*

Samples are acarbose and ethyl acetate fraction (MdEA). Data are mean ± standard deviation from three experiments performed in triplicate.

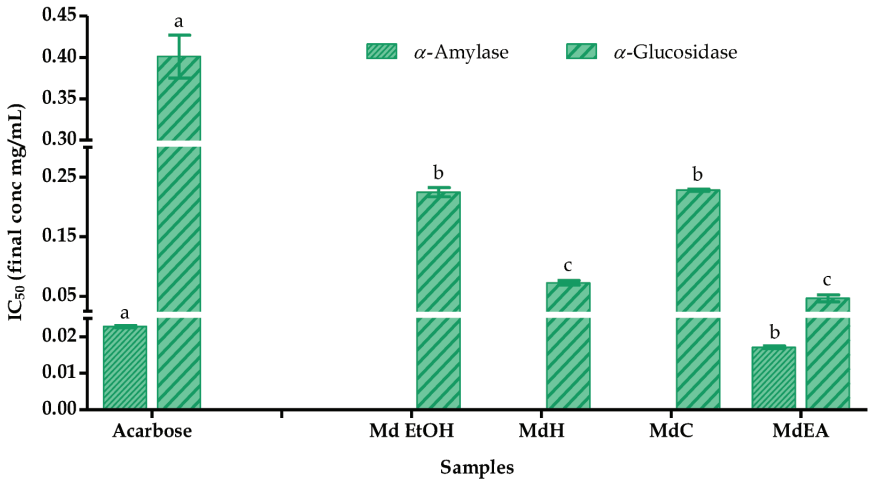

Figure 6.6. *a*-Amylase and *a*-glucosidase inhibition by acarbose and *Minthostachys diffusa* samples expressed as IC_{50} values in mg/mL

Samples are acarbose, crude ethanol extract (Mg EtOH), *n*-hexane fraction (MdH), chloroform fraction (MdC) and ethyl acetate fraction (MdEA). No enzymatic inhibition present for the missing samples. Data are means ± standard deviation from three experiments performed in triplicate. The concentration of the sample required to inhibit the activity of the enzyme by 50% (IC_{50}) in mg/mL was calculated by nonlinear regression analysis. In each test, the values with the same letter are not significant different at the $p < 0.05$ level, 95% confidence limit, according to one-way analysis of variance (ANOVA).

In *a*-glucosidase test it was not possible to reach IC_{50} for the MdB and MdW fractions (**Fig. 5.6**). The other samples showed values lower than acarbose (IC_{50} of 0.40 ± 0.03 mg/mL). Among all, the best samples were the MdEA and MdH fractions (IC_{50} of 0.04 ± 0.00 mg/mL and 0.07 ± 0.00 mg/mL, respectively).

To date, this is the first report on antidiabetic activity of *Minthostachys diffusa* and in general in *Minthostachys* genus. The results are very interesting and in particular, the ethyl acetate fraction inhibitory activity against both tested enzymes and the *n*-hexane fraction inhibitory activity against *a*-glucosidase enzyme.

5.5. Potential anticholinesterase activity of *M. diffusa* samples

The *Minthostachys diffusa* samples had a concentration-dependent activity on both enzymes (**Fig. 5.7**).

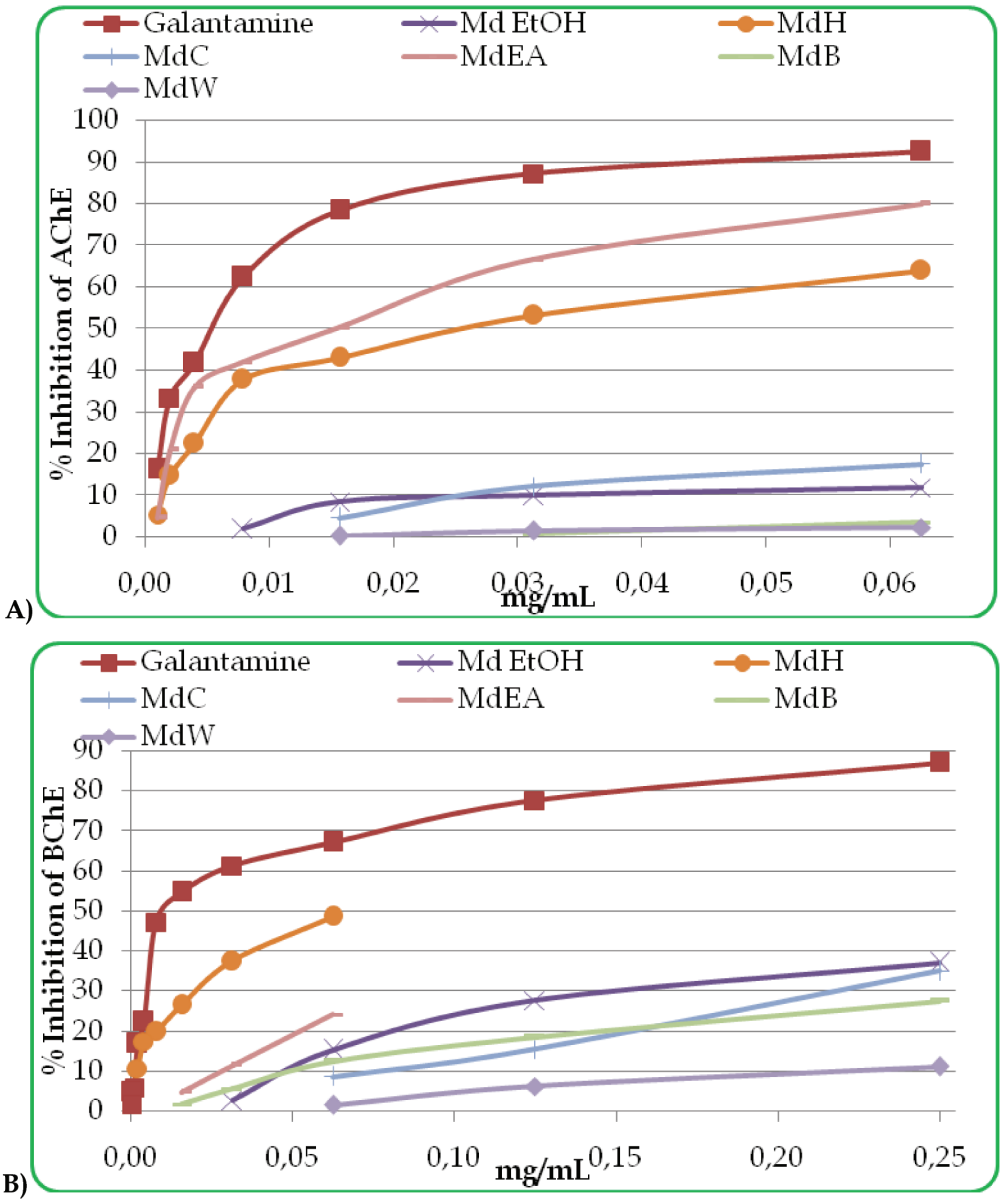

Figure 6.7. AChE **(A)** and BChE **(B)** inhibition activity of galantamine and *Minthostachys diffusa* samples

Samples are galantamine, crude ethanol extract (Mg EtOH), *n*-hexane fraction (MdH), chloroform fraction (MdC), ethyl acetate fraction (MdEA), *n*-butanol fraction (MdB) and water fraction (MdW) Data are mean ± standard deviation from three experiments.

The ability of samples to inhibit the AChE and BChE enzymes was expressed as IC_{50} and results were compared with galantamine (**Fig. 5.8**). In particular, in AChE assay only the MdEA and MdH fractions showed a good activity (IC_{50} of 0.01 ± 0.00 and 0.03 ± 0.00 mg/mL) but lower than positive control galantamine (IC_{50} of 0.01 ± 0.00 mg/mL).

Instead, it was possible to express the inhibition of BChE enzyme in IC_{50} only for MdH fraction, even if its activity was lower than galantamine (IC_{50} 0.02 ± 0.00 mg/mL).

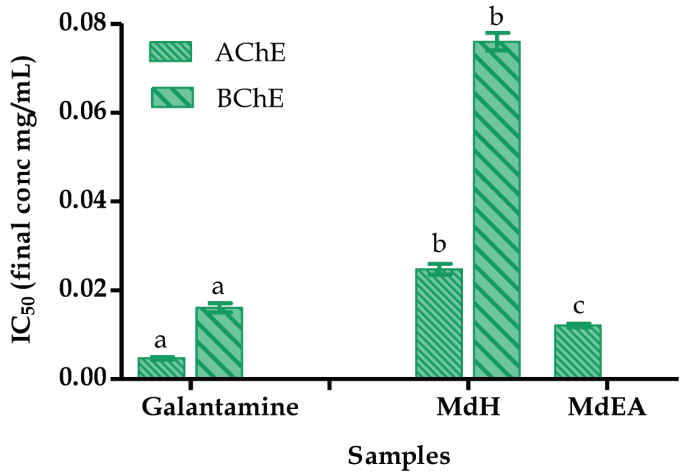

Figure 6.8. AChE and BChE inhibition by galantamine and *Minthostachys diffusa* samples expressed as IC_{50} values in mg/mL

Samples are galantamine, *n*-hexane fraction (MdH) and ethyl acetate fraction (MdEA). No enzymatic inhibition present for the missing samples. Data are means ± standard deviation from three experiments performed in triplicate. The concentration of the sample required to inhibit the activity of the enzyme by 50% (IC_{50}) in mg/mL was calculated by nonlinear regression analysis. In each test, the values with the same letter are not significant different at the $p < 0.05$ level, 95% confidence limit, according to one-way analysis of variance (ANOVA).

To compare all samples in both assays, the results were expressed as percentage of inhibition at final concentration of 0.06 mg/mL (**Fig. 5.9**).

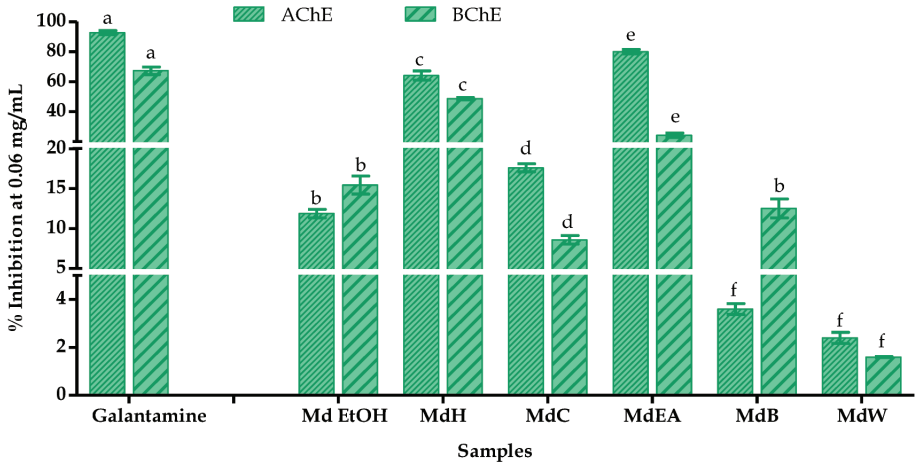

Figure 6.9. AChE and BChE inhibition by galantamine and *Minthostachys diffusa* samples expressed as percentage of inhibition at final sample concentrations of 0.06 mg/mL
Samples are galantamine, crude ethanol extract (Md EtOH), *n*-hexane fraction (MdH), chloroform fraction (MdC), ethyl acetate fraction (MdEA), *n*-butanol fraction (MdB) and water fraction (MdW). Data are mean ± standard deviation from three experiments as a percentage of inhibition at final sample concentrations of 0.06 mg/mL. In each test, the values with the same letter are not significant different at the $p < 0.05$ level, 95% confidence limit, according to one-way analysis of variance (ANOVA).

In particular, in AChE inhibition test, all tested samples of *M. diffusa* showed percentage inhibition values at selected concentration lower than galantamine (92.61 ± 1.41 %). Among all, the MdEA and MdH fractions presented the best values (80.00 ± 1.49 and 64.11 ± 3.11 %). Similar results in the BChE inhibition test. In fact, the MdH and MdEA fractions showed the best values (48.65 ± 0.82 and 24.20 ± 1.57 %), but their values were lower than galantamine (67.26 ± 2.61 %).

Once again, this is the first report on anticholinesterase activity of *Minthostachys diffusa*. The *M. verticillata* was the only *Minthostachys* specie studied for its anticholinesterase activity (Carpinella, Andrione *et al.* 2010). In particular, the ethanol extract of this specie was partitioned in CH_2Cl_2/H_2O to obtain an organic and an aqueous fraction, respectively. Then the organic and aqueous fractions were investigated for their acetylcholinesterase inhibitory activity, presenting at the concentration of 10.00 mg/mL the AChE inhibition of 5.10 ± 5.10 % and 0.00 % in organic and aqueous fractions, respectively. Other species belonging Lamiaceae family were investigated for their anticholinesterase activity with good results. For example, the *Salvia* genus, within the Lamiaceae family, causes the inhibition of AChE as well as nicotinic activity (Savelev, Okello *et al.* 2004; Mukherjee, Kumar *et al.* 2007).

5.6. Identification and quantification of compounds by mass spectrometry in *M. diffusa* samples

This is the first phytochemical study on *Minthostachys diffusa*. The compounds previously identified in other species belonging to *Minthostachys* genus belong mainly to the class of monoterpenes (Alkire, Tucker *et al.* 1994; Schmidt-Lebuhn 2008).

To evaluate the compounds responsible of the measured antioxidant and enzymatic activities, the samples with the highest values were selected. The ethyl acetate fraction of *M. diffusa* was the sample with the highest RACI and, also it demonstrated the highest activity for antidiabetic and anticholinesterase activities, together the MdH fraction. For these reasons, the ethyl acetate and *n*-hexane fractions of *M. diffusa* were selected for mass spectrometry analysis in negative ionization (Hossain, Rai *et al.* 2010).

The LC–MS profile of MdEA is shown in **Fig. 5.10**. Different compounds (> 30) were detected and tentative identification for the first time in *Minthostachys diffusa* and in general in *Minthostachys* genus have been performed. Most of these compound structures have been reached through accurate mass and fragmentation pattern and aided by the existing literature (**Tab. 5.3**).

Twenty compounds have been identified for the first time in the ethyl acetate fraction of *Minthostachys diffusa* by comparing their retention times with those of the available commercial standards.

These compounds belong to the classes of:

- phenolic acids (protocatechuic acid (**1**));
- flavonols (quercetin-3,4'-di-glucoside (**2**), rutin (**4**), quercetin-3-*O*-glucoside (**5a**), quercetin-3-*O*-arabinoside (**6b**), kaempferol-3-*O*-glucoside (**6c**) and quercetin (**13b**));
- flavones (orientin (**3**), apigenin-7-*O*-glycoside (**8a**), luteolin-7-*O*-glucoside (**9b**) and luteolin (**13a**));
- flavanones (hesperidin (**8b**) and naringenin-7-*O*-glucoside (**8c**));
- cinnamic acid derivatives (3,4-di-*O*-caffeoyl quinic acid (**7**), rosmarinic acid (**9a**), 4-coumaric acid (**10d**) and caffeic acid (**11**));
- triterpenes (corosolic acid (**26**), betulinic acid (**28**) and oleanolic acid (**29**)).

The most abundant was rosmarinic acid (69.64 ± 1.53 mg/g DW), followed by the quercetin-3-*O*-glucoside (22.87 ± 0.25 mg/g DW). These phenolic compounds are known for their antioxidant properties. Luteolin, luteolin-glycosides and plant species containing these compounds have been reported to be extremely active. Luteolin (**13a**) and its glycosides cynaroside (luteolin 7-*O*-glucoside, **9b**) fulfil the structural requirements to have anti-inflammatory and antioxidant activities characteristic of flavonoid compounds (Uma Devi, Ganasoundari *et al.* 2000; López-Lázaro 2009).

Moreover, other compounds tentatively identified were quercetin derivatives (**5b** and **10a**), rutin derivative (**6a**), coumaric acid derivative (**10b**), luteolin derivative (**12b**), rosmarinic acid methyl ester (**14a**), caffeic acid derivative (**17**), asiatic acid types (**15**, **16**, **24d** and **25d**), maslinic/corosolic acid types (**18**, **19**, **23**, **24b** and **25b**), betulinic/oleanolic/ursolic acid type (**21**), oleane type triterpenoids (**22**, **24** and **25**) and oleanonic acid type (**27**).

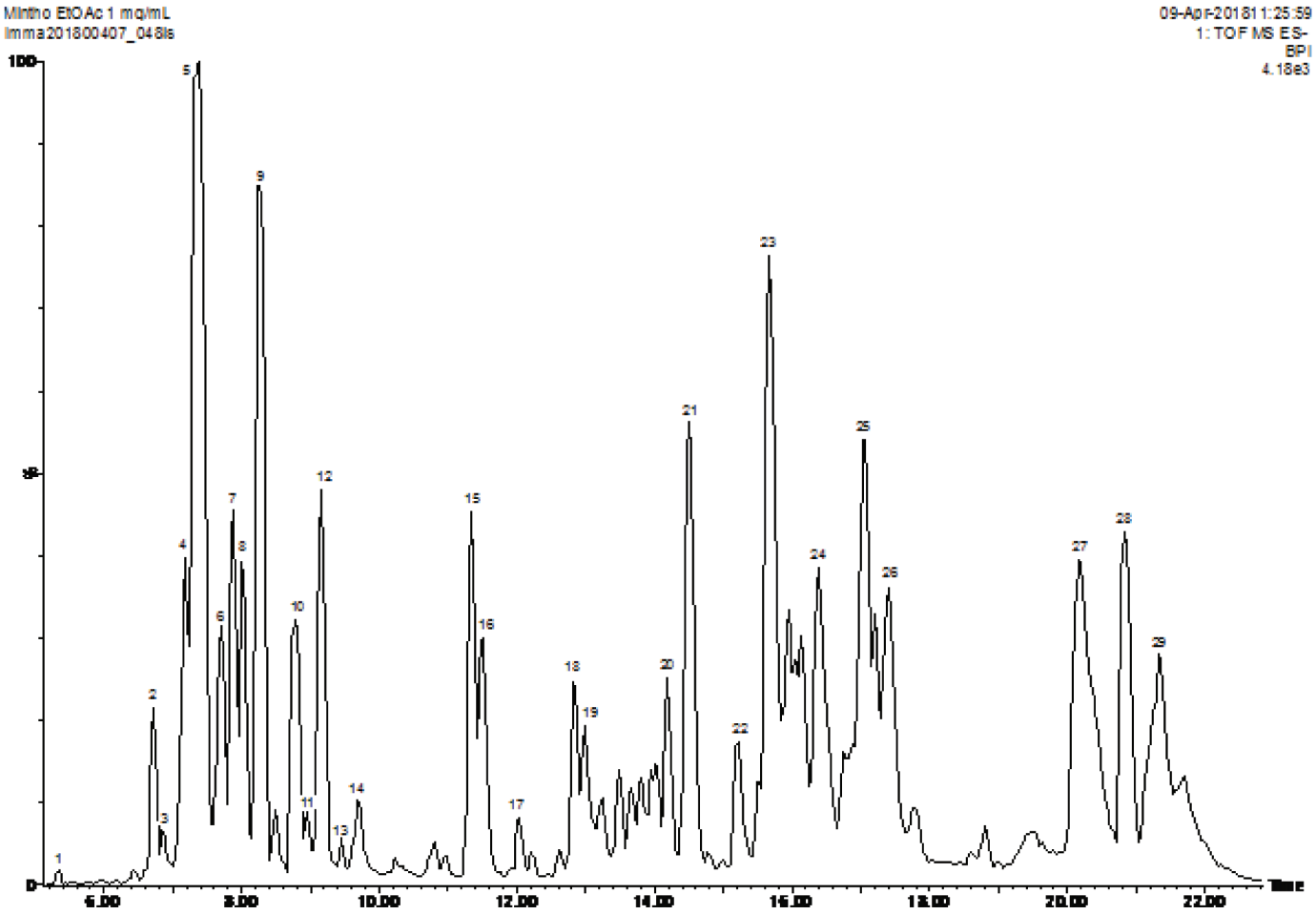

Figure 6.10. Ethyl acetate fraction of *Minthostachys diffusa* base peak intensity chromatogram (BPI)

Table 6.3. Liquid chromatography-tandem mass spectrometry (LC–MS/MS) of ethyl acetate fraction of *Minthostachys diffusa*

Peak no.	RT (min)	ESI (-) MS observed	ESI (-) MS Calc.	Molecular Formula	MS/MS	Tentative Identity	mg/g DW	References
1	5.39	153.0177	153.0188	$C_7H_5O_4$	109, 81	Protocatechuic acid	0.39±0.12	(Sánchez-Rabaneda, Jáuregui *et al.* 2003)
2	6.71	625.1441	625.1405	$C_{27}H_{29}O_{17}$	343, 301, 271, 255, 179, 151	Quercetin-3,4′-di-glucoside	0.03±0.02	(Bonaccorsi, Caristi *et al.* 2008)
3	6.75	447.0921	447.0927	$C_{21}H_{19}O_{11}$	357, 339, 327, 311, 299, 297, 285, 284, 269, 253, 191, 175, 149, 133, 109	Orientin	0.13±0.00	(Iswaldi, Arráez-Román *et al.* 2011)
4	7.21	609.1473	609.1456	$C_{27}H_{29}O_{16}$	300, 285, 271, 255, 179, 151	Rutin	1.63±0.07	(Araujo, Mü Ller *et al.* 2005)
5	7.25/ 7.30	463.0876	463.0877	$C_{21}H_{18}O_{12}$	300, 271, 255, 179, 151	Quercetin-3-*O*-glucoside	22.87±0.25	(Araujo, Mü Ller *et al.* 2005; Krzyzanowska-Kowalczyk, Pecio *et al.* 2018)
		927.1961	927.1925	$C_{53}H_{35}O_{16}$	463, 343, 301, 271, 179, 151, 125	Quercetin-*O*-glucoside derivative	nq	(Araujo, Mü Ller *et al.* 2005; Krzyzanowska-Kowalczyk, Pecio *et al.* 2018)
6	7.70	505.0982	503.098	$C_{23}H_{21}O_{13}$	300, 271, 255, 179, 161, 151	Rutin derivative	nq	(Araujo, Mü Ller *et al.* 2005)
		433.0742	433.0771	$C_{20}H_{17}O_{11}$	300, 271, 255, 179,151	Quercetin-3-*O*-arabinoside	1.92±0.02	(Zhu, Wu *et al.* 2015)
		447.0921	447.0927	$C_{21}H_{19}O_{11}$	284, 255	Kaempferol-3-*O*-glucoside	2.07±0.15	(Downey and Rochfort 2008)
7	7.87	515.1174	515.1190	$C_{25}H_{23}O_{12}$	179, 135	3,4-di-*O*-caffeoyl quinic acid	0.01±0.00	(Araujo, Mü Ller *et al.* 2005)
8	8.00/ 8.03	431.0981	431.0978	$C_{21}H_{20}O_{10}$	269, 239, 224	Apigenin-7-*O*-glycoside	0.54±0.05	(Petkovskaa, Gjamovskic *et al.*)
		609.1848	609.1819	$C_{28}H_{33}O_{15}$	325, 301, 286, 242, 199, 164, 125	Hesperidin	1.10±0.09	(Shi, He *et al.* 2007)

		433.1125	433.1135	$C_{21}H_{21}O_{10}$	151, 107	Naringenin-7-*O*-glucoside	0.17±0.01	(Pereira, Peres *et al.* 2013)
9	8.20/ 8.23	359.0766	359.0767	$C_{18}H_{15}O_8$	197, 179, 161, 135, 133, 123, 73	Rosmarinic acid	69.64±1.53	(Barros, Dueñas *et al.* 2013)
		447.0921	447.0927	$C_{21}H_{19}O_{11}$	285, 151	Luteolin-7-*O*-glucoside	0.86±0.01	(Ibrahim, El-Halawany *et al.* 2015)
10	8.73/ 8.79	609.1457	609.1456	$C_{27}H_{29}O_{16}$	463, 323, 300, 285, 271, 255, 179, 161, 151, 125	Quercetin-*O*-glucoside-rhamnoside	nq	(Cha, Zhang *et al.* 2008)
		533.1882	533.1870	$C_{23}H_{33}O_{14}$	387, 374, 207, 163, 145, 119, 101	Coumaric acid derivative	nq	(Gruz, Novák *et al.* 2008)
		471.1216	471.1232	$C_{31}H_{19}O_5$	307, 205, 163, 145, 119, 101	Unknown	nq	
		163.0392	163.0395	$C_9H_7O_3$	119, 93	4-Coumaric acid	0.23±0.02	(Gruz, Novák *et al.* 2008)
11	8.95	179.0367	179.0344	$C_9H_7O_4$	135, 79	Caffeic acid	2.49±0.01	(Araujo, Mü Ller *et al.* 2005)
12	9.15/ 9.19	469.1855	469.1862	$C_{26}H_{29}O_8$	307, 247, 179, 163, 145, 125, 119, 99, 71, 57	Unknown	nq	
		593.1697	593.1506	$C_{27}H_{29}O_{15}$	327, 309, 285, 270, 241, 164, 151	Luteolin-rutinoside	nq	(Dalar, Uzun *et al.* 2015)
13	9.36/ 9.39	285.0384	285.0399	$C_{15}H_9O_6$	151, 133	Luteolin	1.00±0.00	(Ferracane, Graziani *et al.* 2010)
		301.0362	301.0348	$C_{15}H_9O_7$	179, 151	Quercetin	2.07±0.09	(Ferracane, Graziani *et al.* 2010)
14	9.72	373.0908	373.0923	$C_{19}H_{17}O_8$	197, 179, 161, 135, 117, 107	Rosmarinic acid methyl ester	nq	(Parejo, Caprai *et al.* 2004)
		582.2838	582.2829	$C_{33}H_{42}O_9$	462, 436, 419, 342, 316, 299, 179, 145, 119	Unknown	nq	
15/ 16	11.34/ 11.50	487.3447	487.3424	$C_{30}H_{47}O_5$	469, 441, 405, 397,389, 85, 73	Asiatic acid type	nq	(Müller, Lankes *et al.* 2013)
17	12.00	829.41568	829.4163	$C_{48}H_{61}O_{12}$	811, 789, 667, 649, 553, 359, 341, 279, 241, 197, 179, 161, 135	Caffeic acid derivative	nq	(Hossain, Rai *et al.* 2010)
18/ 19	12.82/ 12.99	471.3475	471.3474	$C_{30}H_{47}O_4$	427, 425, 409, 353, 337, 57	Maslinic/Corosolic acid type	nq	(Tchivounda, Koudogbo *et al.*

								1991)
20	14.18	813.4201	813.4214	$C_{48}H_{61}O_{11}$	651, 453, 359, 197, 179, 161, 135, 73	Unknown	nq	
21	14.57	455.3527	455.3525	$C_{30}H_{47}O_3$	411, 393, 381, 351, 83, 71, 57	Betulinic/Oleanolic/Ursolic acid type	nq	(Kontogianni, Tomic *et al.* 2013)
22	15.26	469.3342	469.3318	$C_{30}H_{45}O_4$	451, 425, 421, 407, 391, 377, 353, 337, 137, 97, 71, 57	Oleane type triterpenoid	nq	(Kontogianni, Tomic *et al.* 2013)
23	15.79	471.3453	471.3474	$C_{30}H_{47}O_4$	453, 411, 353, 337, 121, 113, 97, 71, 57	Maslinic/Corosolic acid type	nq	(Tchivounda, Koudogbo *et al.* 1991)
24/ 25	16.33/ 17.04	469.3342	469.3318	$C_{30}H_{45}O_4$	453, 423, 411, 409, 407, 405, 391, 353, 337, 113, 97, 71, 57	Oleane type triterpenoid	nq	(Kontogianni, Tomic *et al.* 2013)
		471.3470	471.3474	$C_{30}H_{47}O_4$	453, 424, 407, 391, 377, 353, 290, 97, 83, 71	Maslinic/Corosolic acid type	nq	(Tchivounda, Koudogbo *et al.* 1991)
		453.3434	453.3427	$C_{23}H_{49}O_8$	423, 407, 405, 391, 377, 97, 71	Unknown	nq	
		487.3429	487.3424	$C_{30}H_{47}O_5$	471, 469, 467, 453, 451, 423, 409, 407, 405, 391, 389, 97, 81, 71	Asiatic acid type	nq	(Müller, Lankes *et al.* 2013)
26	17.48	471.3453	471.3474	$C_{30}H_{47}O_4$	453, 424, 411, 407, 393, 375, 205, 97, 71, 58	Corosolic acid	nq	
27	20.18	453.3460	453.3369	$C_{30}H_{45}O_3$	405, 391, 389, 371, 337, 97	Oleanonic acid type	nq	(Kontogianni, Tomic *et al.* 2013)
28	20.88	455.3521	455.3525	$C_{30}H_{47}O_3$	452, 407, 391, 389, 375, 373, 189, 183, 137, 97	Betulinic acid	nq	(Kontogianni, Tomic *et al.* 2013)
29	21.00/ 21.16	455.3539	455.3525	$C_{30}H_{47}O_3$	407, 391, 389, 375, 373, 189, 183, 137, 97	Oleanolic acid	nq	(Kontogianni, Tomic *et al.* 2013)

Identification of compounds based on *m/z*, fragmentation pattern and retention time of standards. Quantities of the detected compounds were determined using commercial standards; nq = not quantified

Subsequently, the phytochemical profile of *n*-hexane fraction of *Minthostachys diffusa* has been analyzed by mass spectrometry in negative ionization (Hossain, Rai *et al.* 2010).

The LC–MS profile of MdH is shown in **Fig. 5.11**. Different compounds (> 20) were detected and tentative identification of most of them have not been reached through accurate mass and fragmentation pattern because not were present existing literature (**Tab. 5.4**).

These compounds were triterpene and in particular, maslinic acid (**10**), betulinic acid (**17**), oleanolic acid (**18**) and ursolic acid (**19**) with several biological activities as antioxidant, anti-cholinesterase and *a*-glucosidase inhibition activities (Sultana 2011; Leal 2012) that can explain the *in vitro* activity of MdH and MdEA.

Moreover, other compounds tentatively identified were asiatic acid types (**1**, **3** and **6**), maslinic/corosolic acid types (**2**, **4** and **5**), oleane triterpenoid types (**8**, **9**, **11** and **20**), maslinic acid type (**12**) oleanonic acid types (**15** and **16**) and betulinic/oleanolic/ursolic types (**15** and **16**).

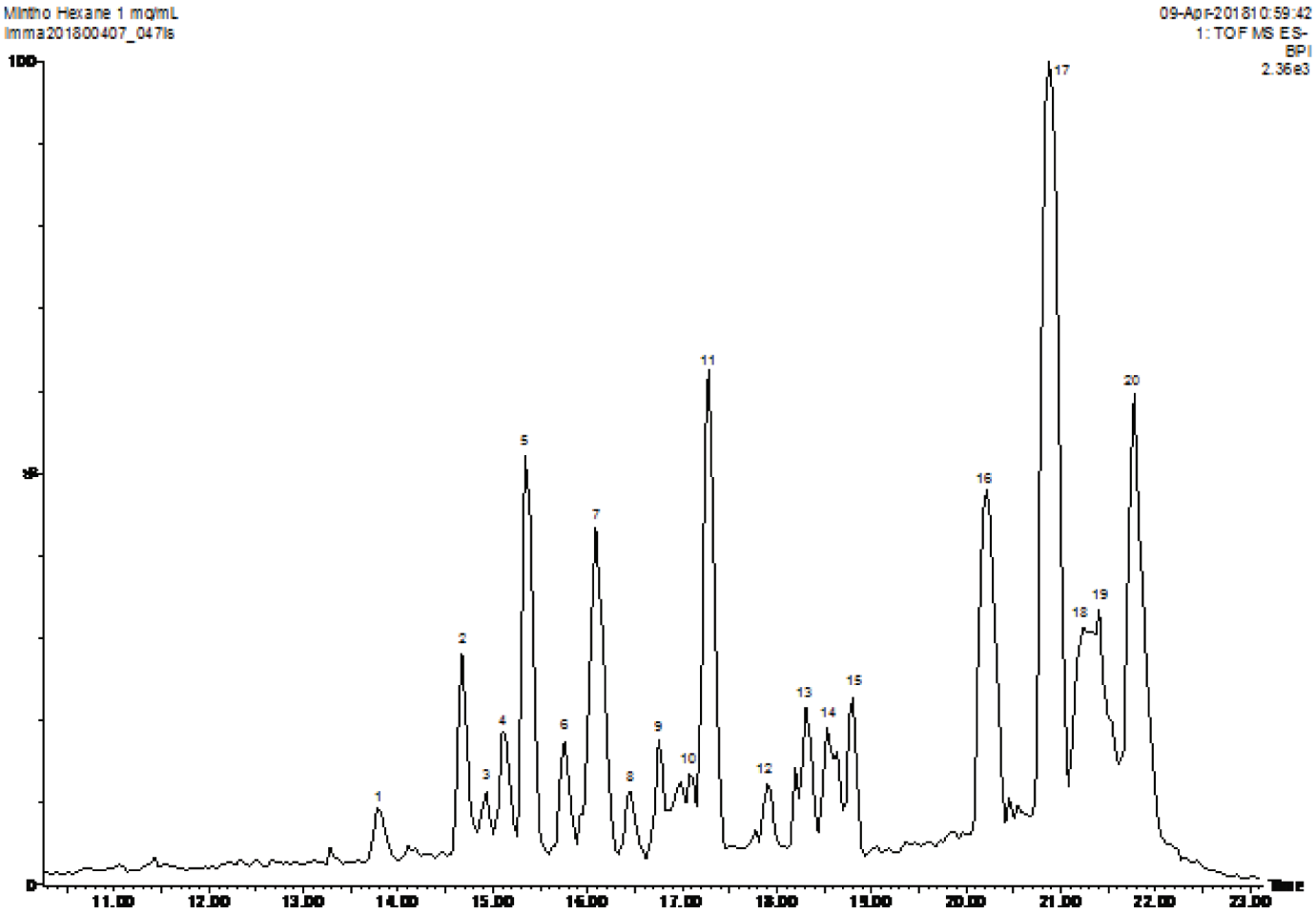

Figure 6.11. *n*-Hexane fraction of *Minthostachys diffusa* base peak intensity chromatogram (BPI)

Table 6.4. Liquid chromatography-tandem mass spectrometry (LC–MS/MS) of *n*-hexane fraction of *Minthostachys diffusa*

Peak no.	RT (min)	ESI (-) MS observed	ESI (-) MS Calc.	Molecular Formula	Δ ppm	MS/MS	Tentative Identity	References
1	13.78	487.3445	487.3424	$C_{30}H_{47}O_5$	4.3	469, 443, 441, 425, 221, 141, 97	Asiatic acid type	(Müller, Lankes *et al.* 2013)
2	14.68	471.3453	471.3474	$C_{30}H_{47}O_4$	-4.5	453, 427, 407, 391, 358, 329, 125, 97, 83, 62	Maslinic/Corosolic acid type	(Tchivounda, Koudogbo *et al.* 1991)
3	14.93	487.3445	487.3424	$C_{30}H_{47}O_5$	4.3	469, 443, 425, 237, 191, 171, 125, 97	Asiatic acid type	(Müller, Lankes *et al.* 2013)
4	15.10	473.3606	473.3631	$C_{30}H_{49}O_4$	-5.3	455, 429, 411, 306,62	Maslinic/Corosolic acid type	(Tchivounda, Koudogbo *et al.* 1991)
5	15.34	471.3453	471.3474	$C_{30}H_{47}O_4$	-4.5	455, 426, 407, 339, 62	Maslinic/Corosolic acid type	(Tchivounda, Koudogbo *et al.* 1991)
6	15.76	487.3445	487.3424	$C_{30}H_{47}O_5$	4.3	469, 443, 425, 237, 191, 171, 125, 97	Asiatic acid type	(Müller, Lankes *et al.* 2013)
7	16.09	426.9622	426.9632	$C_{11}H_7O_{18}$	-2.3	407, 387, 217, 83, 81	Unknown	
8/ 9	16.45/ 16.75	469.3342	469.3318	$C_{30}H_{45}0_4$	5.1	453, 425, 423, 409, 407, 393, 179, 97, 83	Oleane triterpenoid type	(Kontogianni, Tomic *et al.* 2013)
10	17.09	471.3453	471.3474	$C_{30}H_{47}O_4$	-4.5	425, 405, 397, 83, 57	Maslinic acid	(Tchivounda, Koudogbo *et al.* 1991)
11	17.28	469.3342	469.3318	$C_{30}H_{45}0_4$	5.1	453, 425, 423, 409, 407, 393, 179, 97, 83	Oleane triterpenoid type	(Kontogianni, Tomic *et al.* 2013)
12	17.90	471.3467	471.3474	$C_{30}H_{47}O_4$	-1.5	425, 405, 397, 83, 57	Maslinic acid type	(Tchivounda, Koudogbo *et al.* 1991)
13/ 14	18.31/ 18.47	475.3401	475.3424	$C_{29}H_{47}O_5$	-4.8	457, 413, 359, 164, 138, 97, 61	Unknown	
15/ 16	18.80/ 20.21	453.3382	453.3369	$C_{30}H_{45}O_3$	2.9	407, 391, 303, 255, 149, 109, 97, 93	Oleanonic acid type	(Kontogianni, Tomic *et al.* 2013)
		485.3770	485.3783	$C_{35}H_{49}O_1$	-2.7	453, 451, 431, 407, 391, 279, 187, 125, 97	Betulinic/Oleanolic/Ursolic type	(Kontogianni, Tomic *et al.* 2013)
17	20.91	455.3543	455.3525	$C_{30}H_{47}O_3$	4.0	452, 443, 425, 413, 407, 399, 345, 83	Betulinic acid	(Kontogianni, Tomic *et*

								al. 2013)
18	21.24	455.3543	455.3525	$C_{30}H_{47}O_3$	4.0	407	Oleanolic acid	(Kontogianni, Tomic *et al.* 2013)
19	21.41	455.3543	455.3525	$C_{30}H_{47}O_3$	4.0	453	Ursolic acid	(Kontogianni, Tomic *et al.* 2013)
20	21.74	455.3543	455.3525	$C_{30}H_{47}O_3$	4.0	407, 371	Oleane type triterpenoid	(Kontogianni, Tomic *et al.* 2013)

Identification of compounds based on *m/z*, fragmentation pattern and retention time of standards. Quantities of the detected compounds were determined using commercial standards; nq = not quantified

5.7. Potential anticholinesterase activity of identified terpenes from *M. diffusa* samples

Chemical investigation of MdEA and MdH led to the identification of five triterpenes and in particular, betulinic, corosolic and oleanolic acids from MdEA and betulinic, maslinic, oleanolic and ursolic acids from MdH.

Moreover, other compounds tentatively identified were asiatic acid types, but there was not the asiatic acid in the samples.

Several investigations were reported in the literature on terpenoids as potential leads for the development of cholinesterase inhibitors (Jamila, Khairuddean *et al.* 2015; Bahadori, Dinparast *et al.* 2016; Ruhal and Dhingra 2018). Thus, as a part of my project was focused on potential new cholinesterase inhibitors useful for the neudegenerative deaeases. For these reasons, *in vitro* assays were performed to test the activities of the following triterpenes: betulinic, corosolic, maslinic, oleanolic and ursolic acids identified for the first time in *Minthostachys diffusa*.

All terpenoids were screened for their *in vitro* inhibitory activities against the AChE and BChE enzymes. The results were expressed as IC_{50} in mg/mL and compared with galantamine, used as a positive control and with MdEA and MdH fractions they come from. The samples inhibited the AChE and BChE enzymes with different potencies.

All samples inhibited the AChE enzyme less than the galantamine, but betulinic, maslinic and oleanolic acids (IC_{50} of 0.009 ± 0.001 mg/mL, 0.022 ± 0.001 mg/mL and 0.020 ± 0.002 mg/mL) were more active than the MdH fraction they come from (IC_{50} of 0.025 ± 0.001 mg/mL, **Fig. 5.12**).

In BChE assay, only the maslinic acid (IC_{50} of 0.005 ± 0.001 mg/mL) inhibited the enzyme more than the galantamine (IC_{50} of 0.016 ± 0.001 mg/mL). Instead, all identified terpenes from MdH inhibited the BChE enzyme more than the fraction they come from.

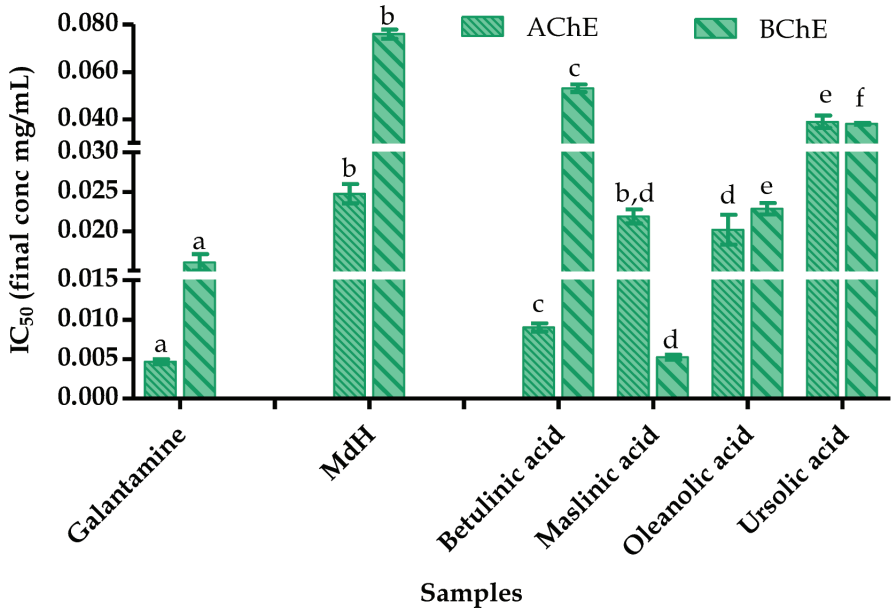

Figure 6.12. AChE and BChE inhibition by galantamine and *n*-hexane fraction of *Minthostachys diffusa* and identified terpenes expressed as IC_{50} values in mg/mL
Samples are galantamine, *n*-hexane fraction (MdH) of *M. diffusa*, betulinic, maslinic, oleanolic and ursolic acids. Data are means ± standard deviation from three experiments performed in triplicate. The concentration of the sample required to inhibit the activity of the enzyme by 50% (IC_{50}) in mg/mL was calculated by nonlinear regression analysis. In each test, the values with the same letter are not significant different at the $p < 0.05$ level, 95% confidence limit, according to one-way analysis of variance (ANOVA).

On the other hand, among all identified terpenes from MdEA, only the betulinic acid was more active than the MdEA fraction it come from (IC_{50} of 0.012 ± 0.001 mg/mL, **Fig. 5.13**) in AChE inhibition test.

In BChE assay, the MdEA fraction was not active, and also the identified terpenes were less active than the galantamine.

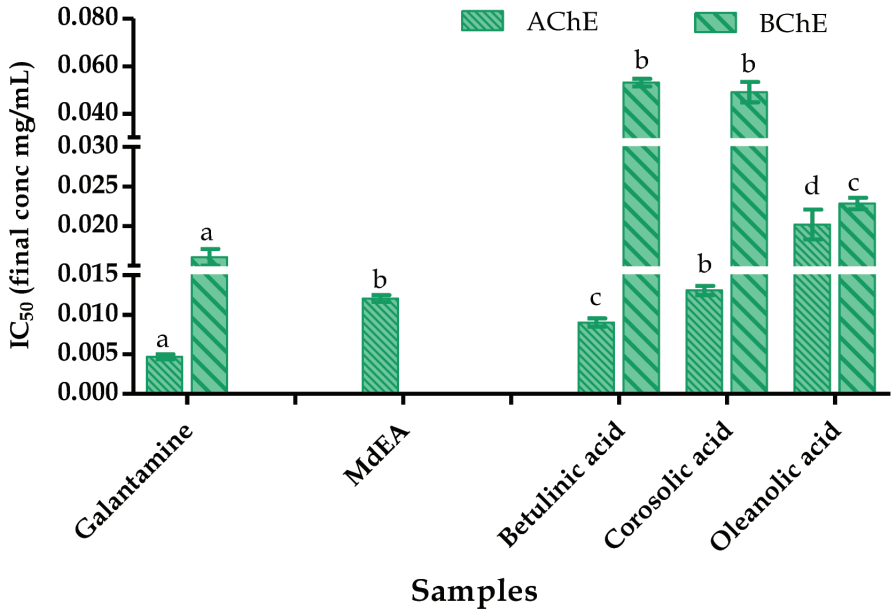

Figure 6.13. AChE and BChE inhibition by galantamine and ethyl acetate fraction of *Minthostachys diffusa* and identified terpenes expressed as IC_{50} values in mg/mL
Samples are galantamine, ethyl acetate fraction (MdEA) of *M. diffusa*, betulinic, corosolic and oleanolic acids. No enzymatic inhibition present for the missing samples. Data are means ± standard deviation from three experiments performed in triplicate. The concentration of the sample required to inhibit the activity of the enzyme by 50% (IC_{50}) in mg/mL was calculated by nonlinear regression analysis. In each test, the values with the same letter are not significant different at the $p < 0.05$ level, 95% confidence limit, according to one-way analysis of variance (ANOVA).

Then, the results of terpenoids were expressed also as IC_{50} in µM and compared with galantamine (**Fig. 5.14**).

All identified terpenes were less active than galantamine (IC_{50} of 16.30 ± 1.08 µM) in AChE inhibition assay.

In BChE assay, instead, the maslinic and olenolic acids were more active than galantamine (IC_{50} of 11.10 ± 0.07 µM, 50.09 ± 1.57 µM and 55.92 ± 3.62 µM, respectively).

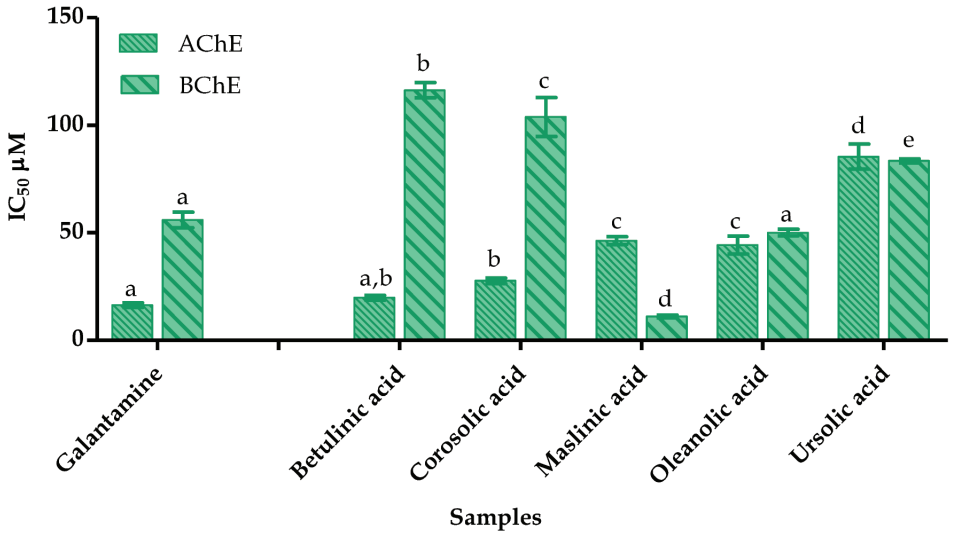

Figure 6.14. AChE and BChE inhibition by galantamine and five terpenoids identified from *Minthostachys diffusa* expressed as IC_{50} values in µM

Samples are galantamine and betulinic, corosolic, maslinic, oleanolic and ursolic acids. Data are means ± standard deviation from three experiments performed in triplicate. The concentration of the sample required to inhibit the activity of the enzyme by 50% (IC_{50}) in µM was calculated by nonlinear regression analysis. In each test, the values with the same letter are not significant different at the $p < 0.05$ level, 95% confidence limit, according to one-way analysis of variance (ANOVA).

Triterpenoids present in medicinal plant species, such as betulinic acid, corosolic, maslinic acid, oleanolic acid, and ursolic acid, have several biological activities, including anticancer, cytotoxic, antitumor, antioxidant, anti-inflammatory, anti-HIV, anti-cholinesterase, *a*-glucosidase inhibition, antimicrobial, and hepatoprotective activities (Ovesna, Vachalkova *et al.* 2004; Sultana 2011; Leal 2012).

It was demonstrated that betulinic acid improves learning and memory of aged as well as scopolamine-induced amnesic rats. Moreover, it decreases lipid peroxidation and nitrite level and increases the levels of reduced glutathione and superoxide dismutase. Then, betulinic acid gives neuroprotective and memory enhancing effect in aged possibly through its anti-acetylcholinesterase and antioxidant activities (Ruhal and Dhingra 2018).

Moreover, oleanolic and ursolic acids are known for their hepatoprotective, anti-inflammatory, antihyperlipidemic, antioxidant, and antitumor activities (Ali, Muhammad *et al.* 2017). The pentacyclic triterpene ursolic acid was reported to inhibit cholinesterases with contradicting IC_{50} values in different research. In particular, the ursolic acid isolated from *Micromeria cilicica* reported IC_{50} of 93.80 and 41.10 µM against

AChE and BChE, respectively (Jamila, Khairuddean *et al.* 2015). In our assays, it showed similar IC_{50} of 85.35 ± 5.85 against AChE enzyme and IC_{50} of 83.50 ± 0.94 in BChE inhibition test.

5.8. *In Silico* methods (molecular modelling and docking calculations) of identified terpenes from *M. diffusa* samples

The interesting results of inhibitory activity obtained from *in vitro* assays of terpenoids identified for the first time in *Minthostachys diffusa* suggest following the study of these compounds.

Corosolic, oleanolic and ursolic acids were docked into the active site of the AChE enzyme in previous studies (Bahadori, Dinparast *et al.* 2016) to confirm their acetylcholinesterase inhibitory activity.

In our research, molecular modelling studies on AChE and BChE enzymes were performed for the first time with the lead triterpene betulinic, corosolic, maslinic, oleanolic and ursolic acids, and also on asiatic acid being there many tentatively compounds maslinic acid types.

The first step was to draw the compound structures (**Fig. 5.15**).

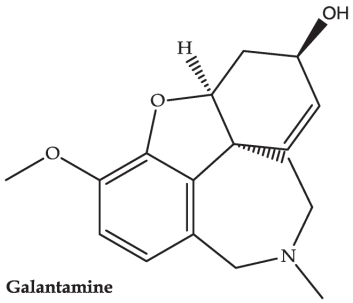

Galantamine
Chemical Formula: $C_{17}H_{21}NO_3$
Exact Mass: 287.15
Molecular Weight: 287.35
m/z: 287.15 (100.0%), 288.16 (18.7%), 289.16 (2.3%)
Elemental Analysis: C, 71.06; H, 7.37; N, 4.87; O, 16.70

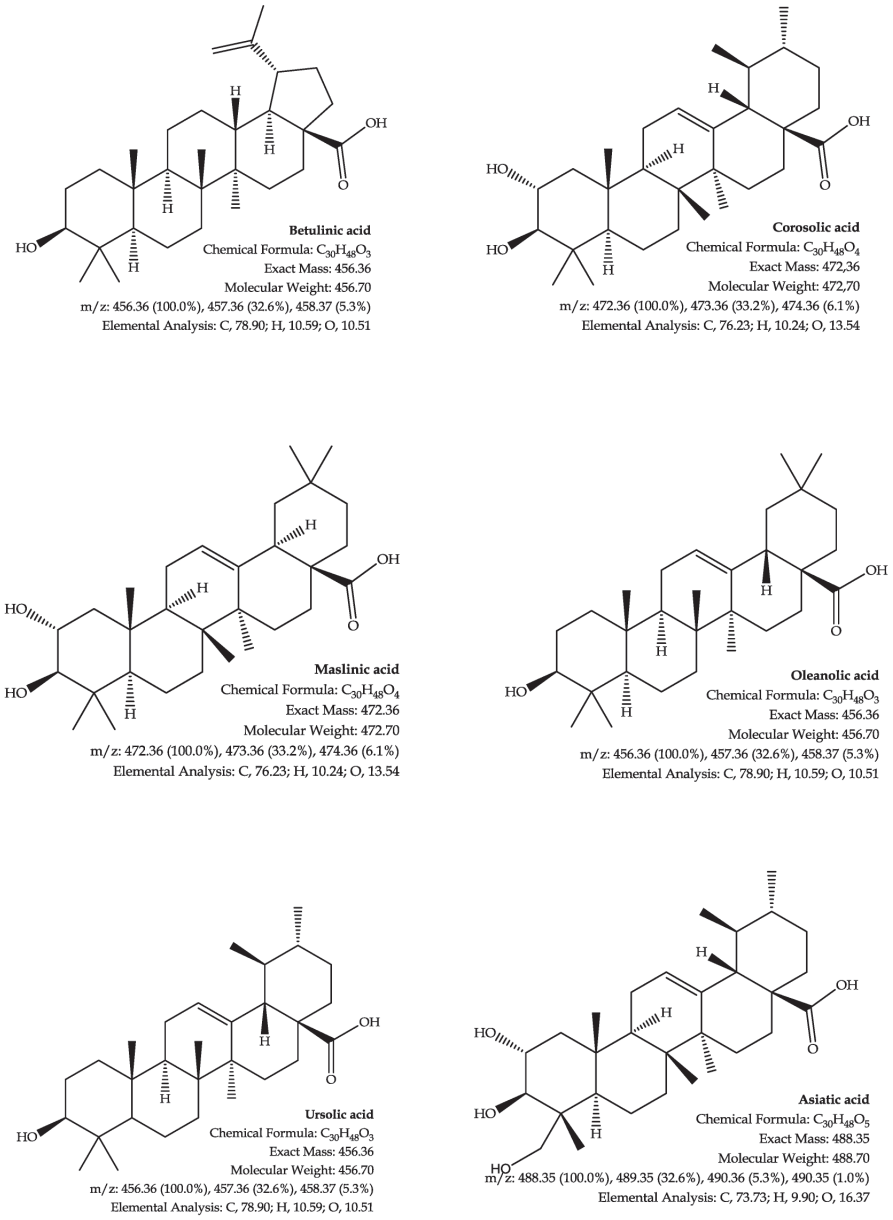

Figure 6.15. Structure of galantamine and betulinic, corosolic, maslinic, oleanolic, ursolic and asiatic acids

Then, 3D protein structures of AChE and BChE enzymes were create in Swiss-model software and was make the semi-rigid Docking for 10 h in AutoDock 2. Molecular modelling studies were carried out in order to propose a possible binding mode for terpenoids inside the catalytic site of the AChE enzyme (**Fig. 5.16**) and BChE enzyme (**Fig. 5.17**).

Modelling studies suggest that all samples interact in both enzyme active sites.

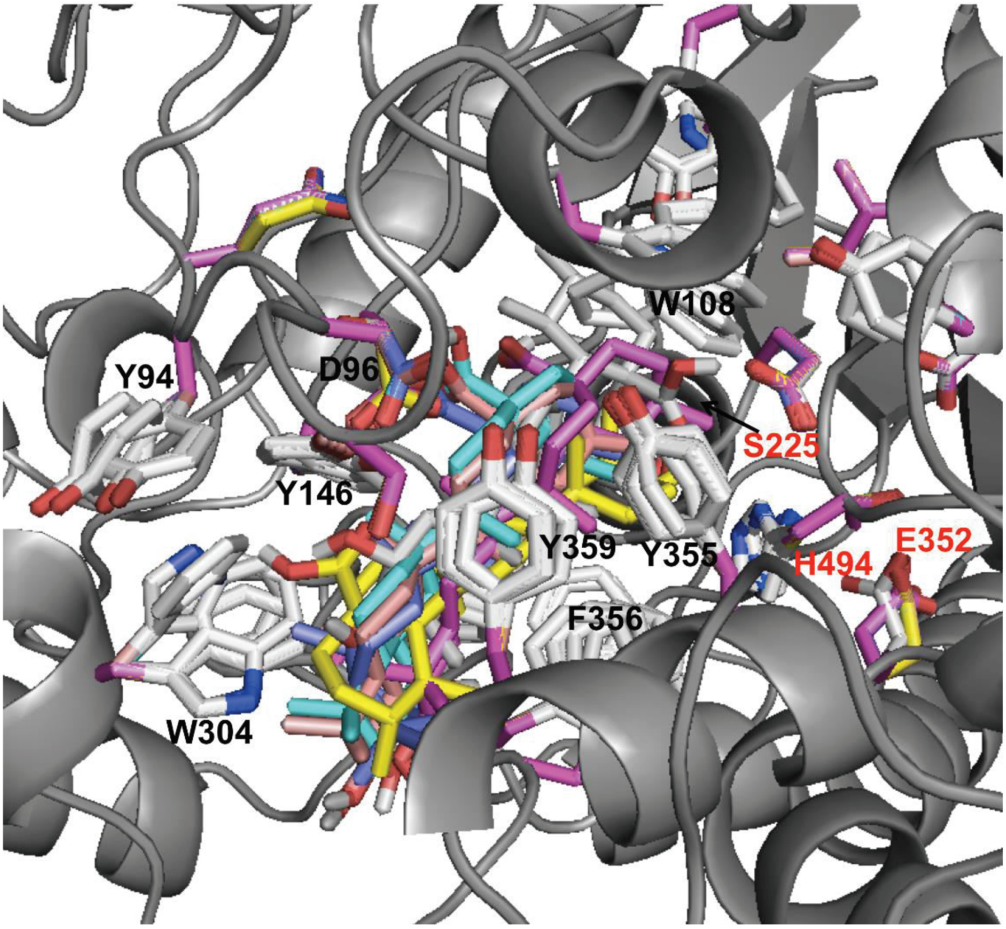

Figure 6.16. Docking results of betulinic acid (cyan), corosolic acid (light gray), maslinic acid (salmon), oleanoic acid (magenta), ursolic acid (yellow), and asiatic acid (blue) in the homology model of *Electrophorus electricus* acetylcholinesterase (AChE enzyme). Residues interacting with the ligands are indicated in black and the residues of the catalytic triad in red.

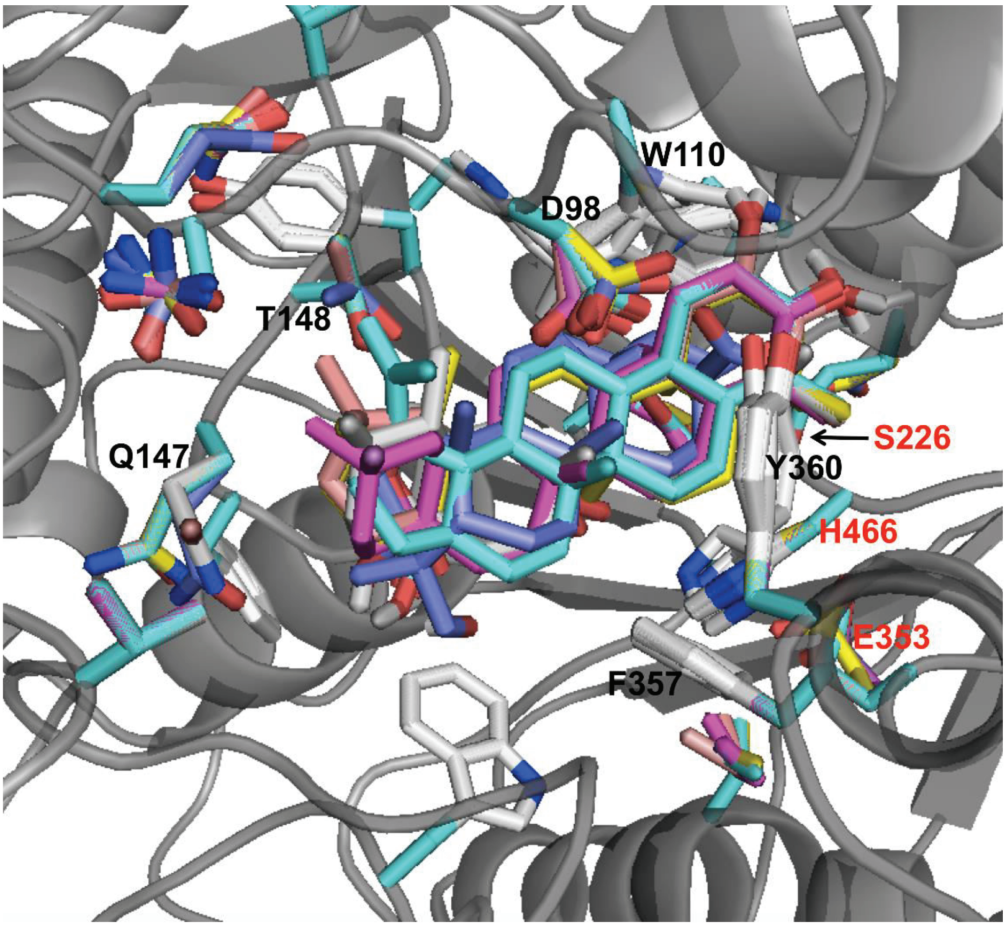

Figure 6.17. Docking results of betulinic acid (cyan), corosolic acid (light gray), maslinic acid (salmon), oleanoic acid (magenta), ursolic acid (yellow), and asiatic acid (blue) in the homology model of horse butyrylcholinesterase (BChE enzyme)
Residues interacting with the ligands are indicated in black and the residues of the catalytic triad in red.

In particular, betulinic acid and maslinic acid were the most active compounds in AChE and BChE assays, respectively. In **Fig. 5.18** is shown the betulinic acid and galantamine docked in AChE enzyme and in **Fig. 5.19** the maslinic acid and galantamine docked in BChE enzyme.

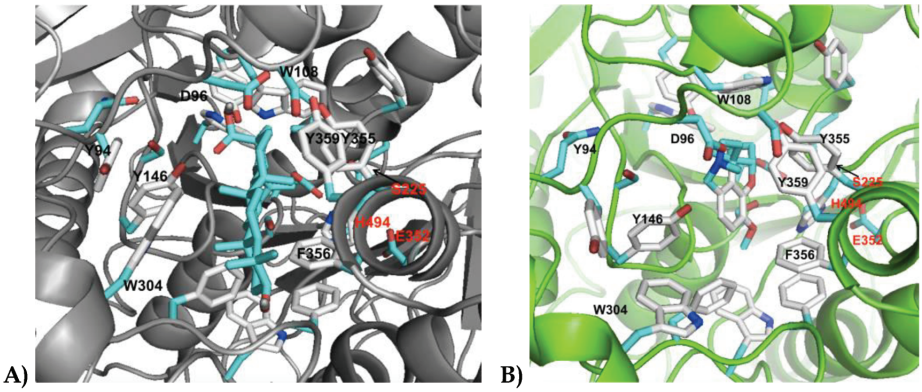

Figure 6.18. Docking results of betulinic acid (**A**) and galantamine (**B**) in the homology model of *Electrophorus electricus* acetylcholinesterase (AChE enzyme)
Residues interacting with the ligands are indicated in black and the residues of the catalytic triad in red.

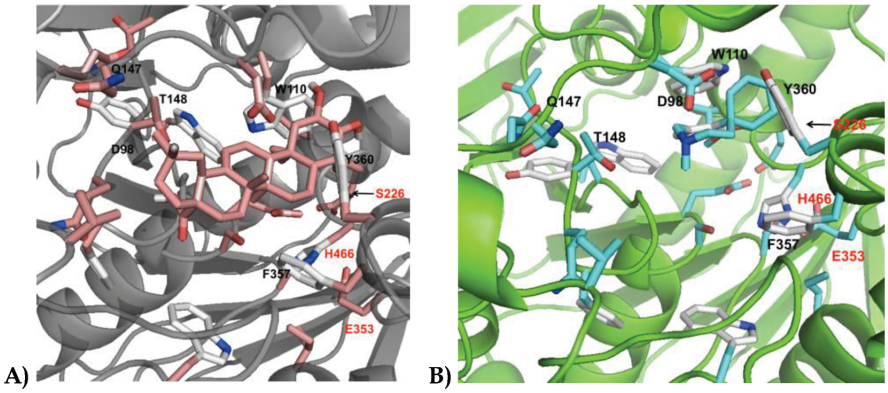

Figure 6.19. Docking results of maslinic acid (**A**) and galantamine (**B**) in the homology model of horse butyrylcholinesterase (BChE enzyme)
Residues interacting with the ligands are indicated in black and the residues of the catalytic triad in red.

5.9. *Minthostachys diffusa* study conclusions

The ethanol extract of *M. diffusa* aerial parts was subjected to liquid/liquid fractionation using solvent with increasing polarity.

The antioxidant activity, determined by six complementary *in vitro* assays, showed different values among fractions. Relative Antioxidant Capacity Index (RACI) evidenced as the ethyl acetate fraction of *M. diffusa* is the most active. More in detail, fraction reported activity was: *n*-hexane < water < chloroform < *n*-butanol < ethyl acetate.

Furthermore, the antidiabetic and anticholinesterase activities were performed on the samples with interesting results in particular mode in *n*-hexane and ethyl acetate fractions.

For these reasons the phytochemical profile in *M. diffusa* ethyl acetate and *n*-hexane fractions was analyzed with the identification or tentative identification of more than 50 compounds for the first time in this specie.

In conclusion, this first report on *M. diffusa* characterization and biological activity demonstrated as it could be considered a rich source of potential nutraceuticals that is promising for the development of safe food products, natural additives and cosmetics.

CHAPTER 6. RESULTS AND DISCUSSIONS OF *SENECIO CLIVICOLUS* WEDD.

6.1. The extraction yield of *S. clivicolus* samples

The dried aerial parts of *Senecio clivicolus* (110 g in triplicate) were extracted by dynamic maceration using 96% ethanol for 24 h at a solid to solvent ratio of 1:10 (w/v) per extraction for four times (Dávila, Sterner *et al.* 2013; Faraone, Rai *et al.* 2018).

The four extracts of each replicate extraction were combined.

The extraction yield was calculated showing a value of 27.06 ± 2.51 %, higher than other reports. In fact, it has been reported that the extraction yield of the aerial parts of other species of *Senecio* with 95% ethanol (yield of 5.60 % in *S. biafrae* (Lienou, Telefo *et al.* 2010) and 12.57 % in *S. aegyptius* (Hassan, Gendy *et al.* 2012)), methanol (yield of 13.85 % in *S. gibbosus* (Conforti, Marrelli *et al.* 2006)) or water (yield of 13.60 % in *S. candicans* (Hariprasath, Raman *et al.* 2012)) was considerably lower than values obtained in this study.

Then, the liquid/liquid partition of a part of the crude ethanol extract (20.00 g in 400 mL of water) was performed using increasing polarity solvents (*n*-hexane, chloroform, ethyl acetate and *n*-butanol); thus, a separation of the compounds was obtained based on the affinity with the solvent used (Saeed, Khan *et al.* 2012).

The extraction's yield of dry *n*-hexane, chloroform, ethyl acetate, *n*-butanol and water fractions (ScH, ScC, ScEA, ScB and ScW fractions) was reported in **Fig. 6.1**. The chloroform fraction (ScC) showed the highest extraction yield (63.39 ± 5.23 %); instead, the water and ethyl acetate fractions demonstrated the lower extraction yields (7.60 ± 0.42 % and 6.87 ± 0.39 %, respectively) (Faraone, Rai *et al.* 2018).

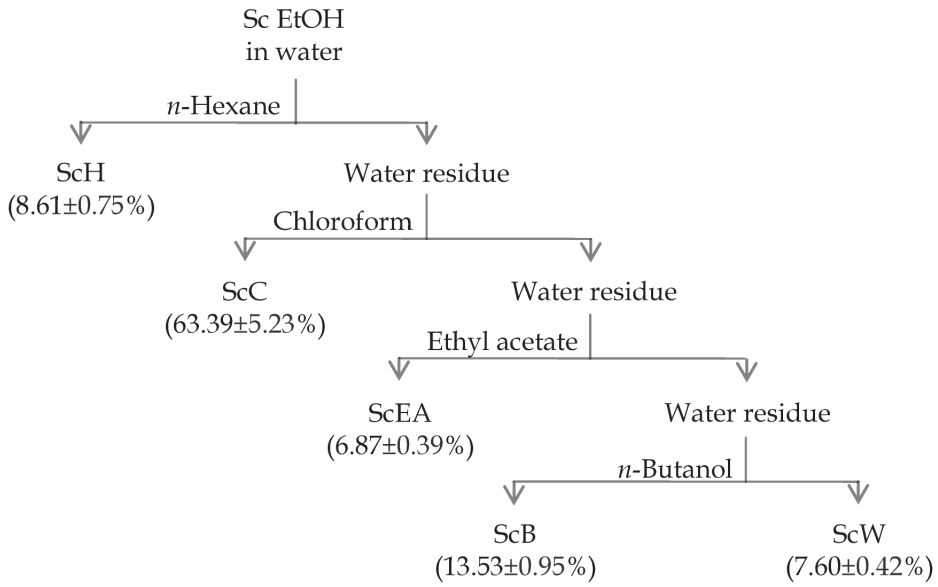

Figure 7.1. Extraction yields of *S. clivicolus* EtOH extract partitioned fractions
Results were expressed as mean ± standard deviation of the triplicate experiments. Samples are crude ethanol extract (Sc EtOH), *n*-hexane fraction (ScH), chloroform fraction (ScC), ethyl acetate fraction (ScEA), *n*-butanol fraction (ScB) and water fraction (ScW).

6.2. The influence of polarity solvents on total polyphenolic, flavonoid and terpenoid content on *S. clivicolus* samples

The polarity of solvents used during liquid/liquid extraction make an important influence on content of polyphenols, flavonoids and terpenoids in the different samples.

The total polyphenolic content (TPC) ranged from 24.32 ± 0.43 to 170.11 ± 1.49 mg of Gallic Acid Equivalents per gram of dry sample (mg GAE/g) in ScW and ScEA fractions, respectively. Out of all samples, ScEA had the highest value, followed by ScB and Sc EtOH (82.50 ± 1.94 and 48.31 ± 1.32 mg GAE/g, respectively, **Fig. 6.2**).

Instead, the Total Flavonoid Content (TFC) has been measured in *S. clivicolus* that presented a TPC value higher than the mean value (ScEA and ScB). The tested fractions ScEA and ScB showed TFC values of 311.92 ± 5.23 and 51.45 ± 3.70 mg of Quercetin Equivalents per gram of dried sample (mg QE/g), respectively.

Moreover, the total terpenoid content (TTeC) was evaluated for their characteristic reddish brown colour at 538 nm. The linalool, a monoterpene, was used as standard reagent and the results (**Fig. 6.2**) were expressed as mg of Linalool Equivalents per gram of dry sample (mg LE/g). The terpenoids content in *S. clivicolus* ranged from 470.77 ± 3.61 to 2074.24 ± 12.76 mg LE/g in ScEA and ScC fractions, respectively. ScC, followed by ScB, ScW and Sc EtOH, exhibited higher values.

Results demonstrated again as yield of phenolic, flavonoids and terpenoids extraction differs on the basis of used solvents (Nakamura, Ra *et al.* 2017; Faraone, Rai *et al.* 2018).

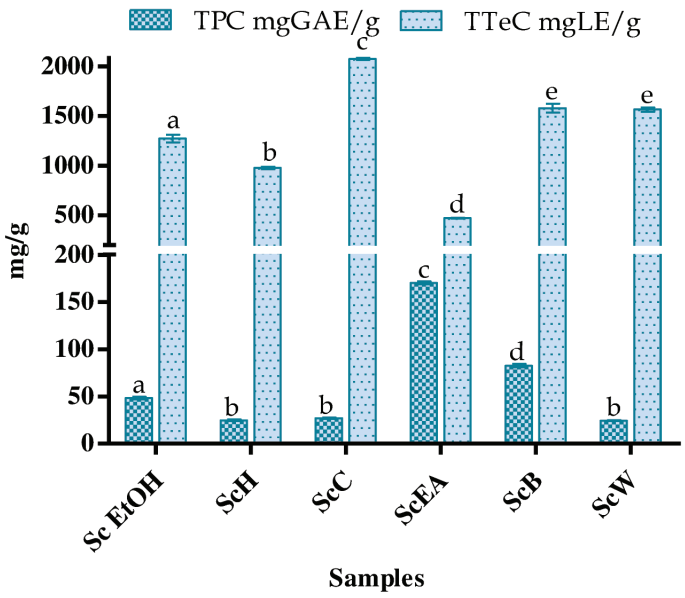

Figure 7.2. Total Polyphenolic Content (TPC) and Total Terpenoid Content (TTeC) of *S. clivicolus* samples

Results were expressed as mean ± standard of triplicate determinations deviation in mg of Gallic Acid Equivalents per gram of dried sample (mg GAE/g) and in mg of Linalool Equivalents per gram of dried sample (mg LE/g). In each tests, the values with the same letter are not significant different at the $p < 0.05$ level, 95% confidence limit, according to one-way analysis of variance (ANOVA). Samples are crude ethanol extract (Sc EtOH), *n*-hexane fraction (ScH), chloroform fraction (ScC), ethyl acetate fraction (ScEA), *n*-butanol fraction (ScB) and water fraction (ScW).

6.3. Antioxidant activity of *S. clivicolus* samples

The antioxidant activity of *S. clivicolus* aerial parts were tested using six different complementary *in vitro* antioxidant assays to evaluate the radical scavenging activity, the ferric relative antioxidant power and the inhibition of lipid peroxidation.

The ScEA showed the highest radical scavenging-activity in all investigated tests (**Tab. 6.1**). In particular, the ScEA reported 409.53 ± 9.53 mg TE/g and 317.53 ± 5.81 mg Trolox Equivalents per gram of dry sample (mg TE/g) values in ABTS and DPPH assays respectively, followed by ScB and Sc EtOH. Instead, in both assays, the lowest activity was found in ScH and ScC fractions.

The ability of samples to scavenge superoxide anion and nitric oxide was expressed as IC_{25} and results were compared with ascorbic acid. The *S. clivicolus* extract and fractions caused a dose-dependent inhibition in the superoxide anion assay (SO) and ScEA fraction showed the highest inhibition, that means the lowest IC_{25} value (IC_{25} of 0.08 ± 0.00 mg/mL), followed by ScC, ScH and ScB (**Tab. 6.1**). These samples showed a higher activity than that measured for ascorbic acid (IC_{25} of 0.26 ± 0.02 mg/mL).

The scavenging ability against the biological nitric oxide (·NO) was not detectable in any fraction, but ScEA showed a dose-dependent inhibition ability (IC_{25} of 1.11 ± 0.05 mg/mL, data not show in **table 6.1**); its value was four times lower than ascorbic acid (IC_{25} 4.78 ± 0.09), demonstrating its effectiveness.

The ferric reducing ability of samples in a redox reaction was assessed using the FRAP test. The ScEA fraction also in this case showed the highest activity (507.66 ± 5.26 mg TE/g) followed by ScB fraction (184.18 ± 4.59 mg TE/g). ScC and ScH were again the less active (**Tab. 6.1**).

The inhibition of lipid peroxidation tested by *β*-Carotene Bleaching test (BCB) evidenced that the most active sample is the ScEA, followed by Sc EtOH and ScB (55.82 ± 2.22, 53.11 ± 0.45 and 51.70 ± 1.97 %AA, respectively). While, there was a low activity for the apolar ScH fraction.

Table 7.1. Results of ABTS, DPPH and Super Oxide (SO) scavenging activity, Ferric Reducing Antioxidant Power (FRAP) and *β*-Carotene Bleaching (BCB) of *S. clivicolus* samples

Samples	ABTS (mgTE/g)	DPPH (mgTE/g)	SO (IC_{25} mg/mL)	FRAP (mgTE/g)	BCB %AA
Sc EtOH	137.87±1.45^{a}	63.42±0.78^{a}	0.37±0.02^{a}	93.08±1.12^{a}	53.11±0.45^{a,e}
ScH	28.94±2.50^{b}	nc	0.16±0.01^{b,c}	12.98±1.04^{b}	4.75±0.23^{b}
ScC	55.93±2.24^{c}	12.70±0.94^{b}	0.14±0.01^{b}	23.90±1.32^{c}	44.58±0.96^{c}
ScEA	409.53±9.53^{d}	317.53±5.81^{c}	0.08±0.001^{d}	507.66±5.26^{d}	55.82±2.22^{a}
ScB	208.37±3.21^{e}	119.54±6.71^{d}	0.20±0.01^{c}	184.18±4.59^{e}	51.70±1.97^{e}
ScW	107.01±0.94^{f}	55.58±1.07^{a}	0.64±0.04^{e}	53.41±2.55^{f}	23.28±0.70^{d}

Samples are crude ethanol extract (Sc EtOH), *n*-hexane fraction (ScH), chloroform fraction (ScC), ethyl acetate fraction (ScEA), *n*-butanol fraction (ScB) and water fraction (ScW). Data are expressed as means ± standard deviation from three experiments; mg GAE/g = mg of Gallic Acid Equivalents per gram of dried sample; mg TE/g = mg of Trolox Equivalents per gram of dried sample; IC_{25} mg/mL = concentration of the sample required to inhibit the activity of the radical by 25%; % AA = percentage of Antioxidant Activity at initial sample concentration of 1 mg/mL; different superscripts in the same row indicate significant difference ($p < 0.05$); nc = not calculable

Moreover, linear correlation coefficient was calculated based on the average of the results by the Pearson test (**Tab. 6.2**). A high correlation was found between the total polyphenol content and radical-scavenging activity ($r_{TPC/ABTS}$ = 0.98; $r_{TPC/DPPH}$ = 0.98; $r_{TPC/NO}$ = 0.92; $r_{TPC/SO}$ = 0.77) and reducing power ($r_{TPC/FRAP}$ = 0.99) demonstrating as the polyphenols are the compounds mostly involved in the antioxidant activity. The highest correlation was observed between the reducing power of the samples and the radical-scavenging activity by ABTS and DPPH methods ($r_{FRAP/ABTS}$ = 0.99 and $r_{FRAP/DPPH}$ = 1.00). Polyphenols are less involved in the inhibition of lipid peroxidation ($r_{TPC/BCB}$ = 0.61). The antioxidant activity determined with the BCB method, a lipophilic system constituted by the emulsion *β*-carotene-linoleic acid, generally has a low correlation with the phenolic compounds and the other methods tested because of the effectiveness of lipophilic compounds (Mariod and Matthaeus 2008). Instead, terpenoids are less involved in testing activities.

Table 7.2. Pearson correlation coefficient calculated among tested *Senecio clivicolus* extract and fractions

	TPC	TTeC	ABTS	DPPH	SO	NO	FRAP	BCB
TPC	1.00							
TTeC	-0.69	1.00						
ABTS	0.98	-0.64	1.00					
DPPH	0.98	-0.68	0.99	1.00				
SO	0.77	-0.56	0.65	0.70	1.00			
NO	0.92	-0.75	0.89	0.93	0.84	1.00		
FRAP	0.99	-0.70	0.99	1.00	0.75	0.94	1.00	
BCB	0.61	0.01	0.65	0.59	0.29	0.41	0.58	1.00

Total Polyphenolic Content (TPC), Total Terpenoid Content (TTeC), ABTS assay, DPPH assay, Super Oxide anion scavenging activity (SO), Nitric Oxide radical scavenging activity (NO), Ferric Reducing Antioxidant Power assay (FRAP) and β-Carotene Bleaching assay (BCB).

The results of the antioxidant activity obtained by ABTS, DPPH, SO, NO, FRAP and BCB and even the TPC have been integrated by calculating the Relative Antioxidant Capacity Index (RACI, **Fig. 6.3**) evidencing as ScEA fraction presented the highest value (1.73), followed by the ScB (0.16). The ScH fraction presented the lowest index (-0.73) and, therefore, a relative lack of antioxidant activity. In particular, the RACI values may be related to the high total polyphenol content of the ethyl acetate fraction.

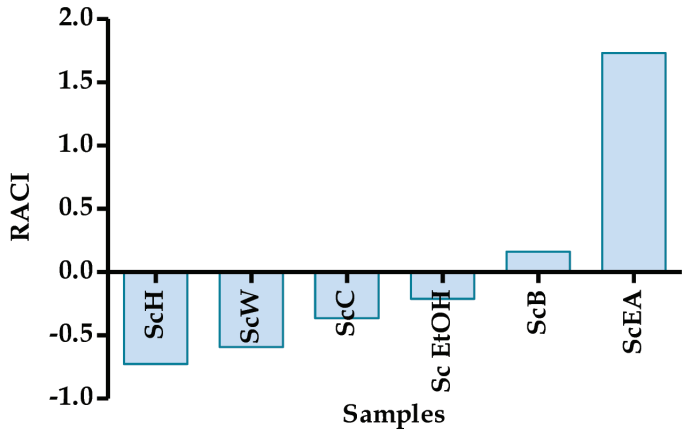

Figure 7.3. Relative Antioxidant Capacity Index (RACI) of *Senecio clivicolus* samples
Samples are crude ethanol extract (Sc EtOH), *n*-hexane fraction (ScH), chloroform fraction (ScC), ethyl acetate fraction (ScEA), *n*-butanol fraction (ScB) and water fraction (ScW).

To date, no study reported the antioxidant activity of *Senecio clivicolus* extracts, but Conforti *et al.* (Conforti, Marrelli *et al.* 2006) evaluated the antioxidant activity of

Senecio gibbosus aerial parts. This study reported as the methanol extract and ethyl acetate fraction had potent antioxidant property on DPPH radical as well as on lipid peroxidation. In particular, the paper reported an IC_{50} of 0.01 mg/mL for the ethyl acetate fraction of *S. gibbosus* on DPPH and showed higher inhibition than that ScEA (IC_{50} of 0.10 ± 0.00 mg/mL) obtained from us. It is possible to explain these results with the different methods used to obtain the ethyl acetate fraction. In fact, Conforti *et al.* extracted the specie materials with methanol; then, the methanolic extract was acidified with 2.50 % H_2SO_4 and partitioned with *n*-hexane, dichloromethane and ethyl acetate. Moreover, in this paper the *n*-hexane fraction tested by DPPH assay was inactive, such as our ScH.

Similarly, the *in vitro* antioxidant activity of *Senecio inaequidens* and *Senecio vulgaris* by the DPPH assay showed that the ethyl acetate fraction gave the 61.60 % and 44.57 % of inhibition, respectively, at a concentration of 0.31 mg/mL (Conforti, Loizzo *et al.* 2006). In our case, ScEA gave a greater inhibition compared to both species tested by Conforti *et al.* (90.55 ± 0.61 % of inhibition at 0.31 mg/mL).

These data are reported in our recent paper (Faraone, Rai *et al.* 2018).

6.4. Potential antidiabetic activity of *S. clivicolus* samples

Different concentrations of the *S. clivicolus* samples were tested for their antidiabetic activity testing the enzyme inhibitory activities against *a*-amylase and *a*-glucosidase enzymes.

Both the *in vitro* tests were concentration-dependent and acarbose was used as standard (**Fig. 6.4**).The ScW fraction was no activity in both assays.

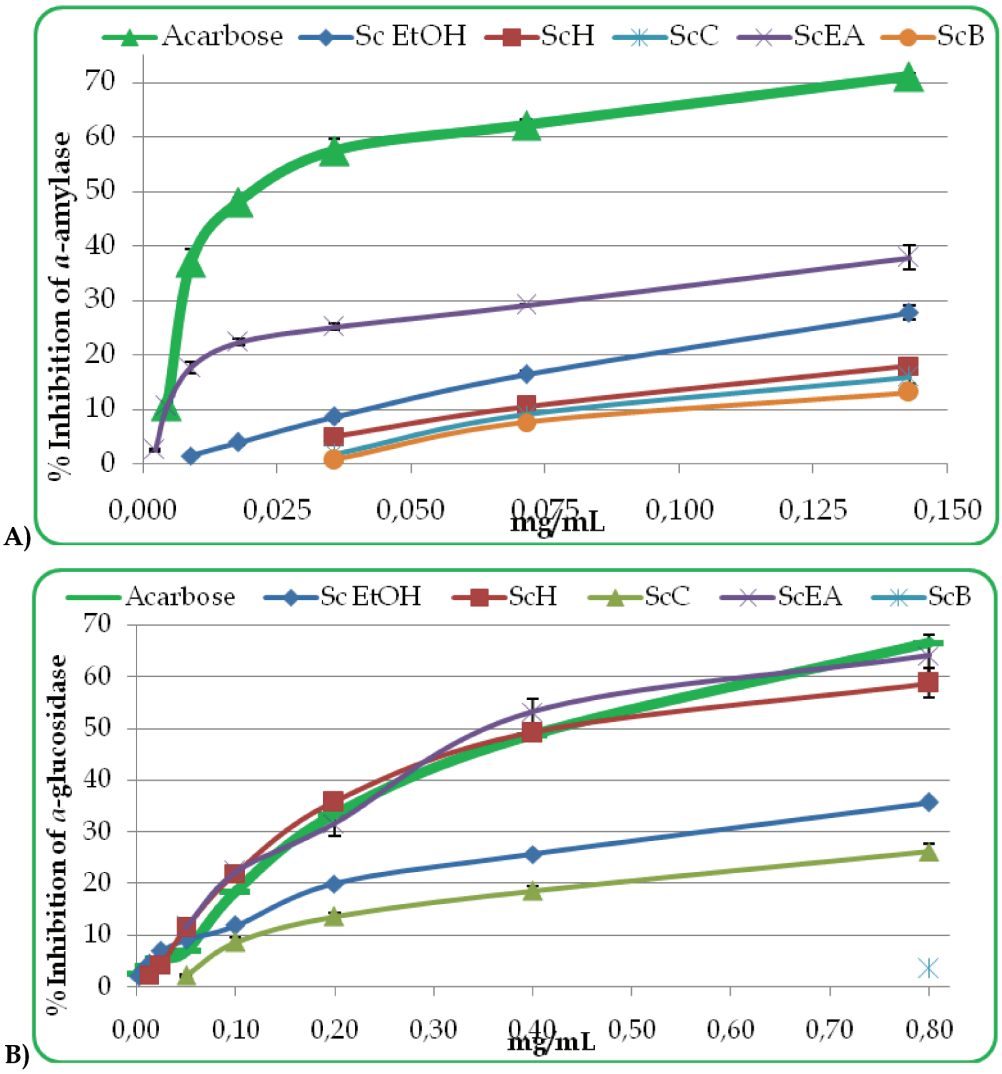

Figure 7.4. *a*-Amylase (**A**) and *a*-glucosidase (**B**) inhibition activity of acarbose and *Senecio clivicolus* samples

Samples are acarbose, crude ethanol extract (Sc EtOH), *n*-hexane fraction (ScH), chloroform fraction (ScC), ethyl acetate fraction (ScEA) and *n*-butanol fraction (ScB). No enzymatic inhibition present for the missing samples. Data are mean ± standard deviation from three experiments.

In *a*-amylase inhibition test was not possible to reach the IC_{50} for samples at the tested concentrations. Instead, in *a*-glucosidase test was IC_{50} values closed to that of acarbose have been recorded for the ScH and ScEA fractions (**Fig. 6.5**) (IC_{50} of 0.40 ± 0.03 mg/mL, 0.45 ± 0.03 and 0.41 ± 0.04, respectively).

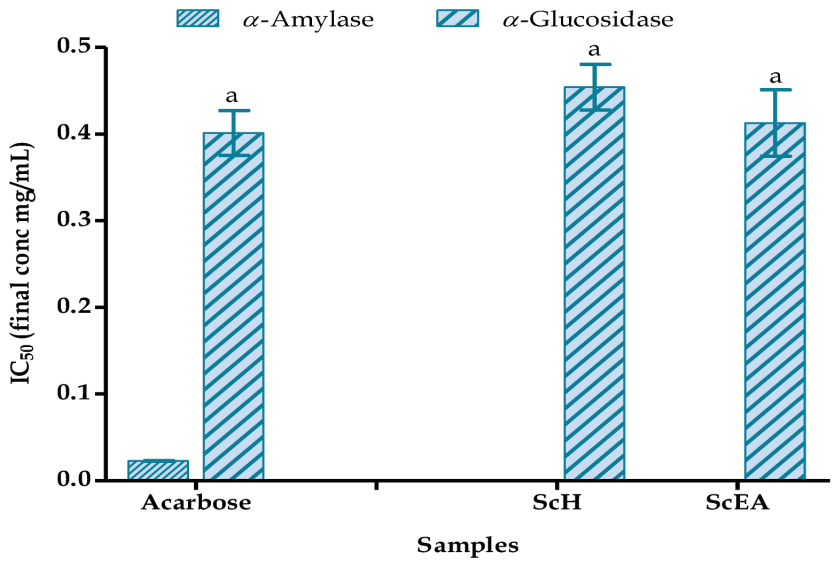

Figure 7.5. *a*-Amylase and *a*-glucosidase inhibition by acarbose and *Senecio clivicolus* samples expressed as IC_{50} values in mg/mL

Samples are acarbose, *n*-hexane fraction (ScH) and ethyl acetate fraction (ScEA). No enzymatic inhibition present for the missing samples. Data are means ± standard deviation from three experiments performed in triplicate. The concentration of the sample required to inhibit the activity of the enzyme by 50% (IC_{50}) in mg/mL was calculated by nonlinear regression analysis. In each test, the values with the same letter are not significant different at the $p < 0.05$ level, 95% confidence limit, according to one-way analysis of variance (ANOVA).

To compare all samples in both assays, results were expressed as percentage of inhibition at final concentration of 0.07 mg/mL in *a*-amylase test and 0.40 mg/mL in *a*-glucosidase test (**Fig. 6.6**). In particular, in *a*-amylase inhibition test, all tested samples of *S. clivicolus* showed percentage inhibition values at selected concentration lower than acarbose (62.14 ± 1.08 %). Among all, the ethyl acetate fraction presented the highest value (29.07 ± 0.11 %).

Instead, in the *a*-glucosidase inhibition test, the ScEA and ScH fractions showed values higher than acarbose (53.26 ± 2.55, 49.19 ± 0.85 and 48.69 ± 2.22 %, respectively). Moreover, ScB was inactive at 0.40 mg/mL in *a*-glucosidase assay and ScW in both tests.

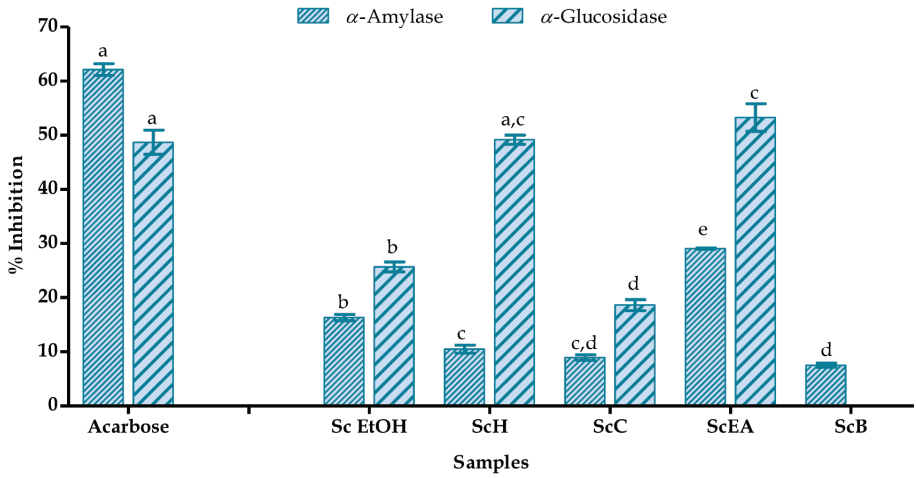

Figure 7.6. *a*-Amylase and *a*-glucosidase inhibition by acarbose and *Senecio clivicolus* samples expressed as percentage of inhibition at final concentration of 0.07 mg/mL in *a*-amylase test and 0.40 mg/mL in *a*-glucosidase test

Samples are acarbose, crude ethanol extract (Sc EtOH), *n*-hexane fraction (ScH), chloroform fraction (ScC), ethyl acetate fraction (ScEA) and *n*-butanol fraction (ScB). No enzymatic inhibition present for the missing samples. Data are means ± standard deviation from three experiments as a percentage of inhibition at final concentration of 0.07 mg/mL in *a*-amylase test and 0.40 mg/mL in *a*-glucosidase test. In each test, the values with the same letter are not significant different at the $p < 0.05$ level, 95% confidence limit, according to one-way analysis of variance (ANOVA).

In conclusion, the sample with the highest potential antidiabetic activity from the *S. clivicolus* samples is the ethyl acetate fraction.

To date, this is the first report on antidiabetic activity of *S. clivicolus*. In bibliography are present other studies present on different *Senecio* species.

Andrade-Cetto *et al.* (Andrade-Cetto and Heinrich 2005) reported *S. albo-lutescens*, *S. palmeri* and *S. peltiferus* as species commonly used in Mexico in the treatment of diabetes.

The dichloromethane and *n*-butanol extracts of *S. leucanthemifolius* inhibited *a*-amylase enzyme with a value of 56.60 % at 0.05 mg/mL and 89.20 % at 1.00 mg/mL, respectively (Tundis, Loizzo *et al.* 2007).

Moreover, the methanolic and dichloromethane extracts of *S. vulgaris* and *S. inaequidens* showed appreciable *a*-amylase inhibition (Conforti, Loizzo *et al.* 2006) and the 80% acetone extract of *S. biafrae* showed good activities in *a*-amylase (IC_{50} = 126.90 µg/mL) and *a*-glucosidase (IC_{50} = 139.66 µg/mL) inhibition assays (Ajiboye, Ojo *et al.* 2018).

6.5. Potential anticholinesterase activity of *S. clivicolus* samples

The *S. clivicolus* samples were analysed for their ability to inhibit the acetylcholinesterase and butyrylcholinesterase enzymes. They had a concentration-dependent activity on both enzymes (**Fig. 6.7**).

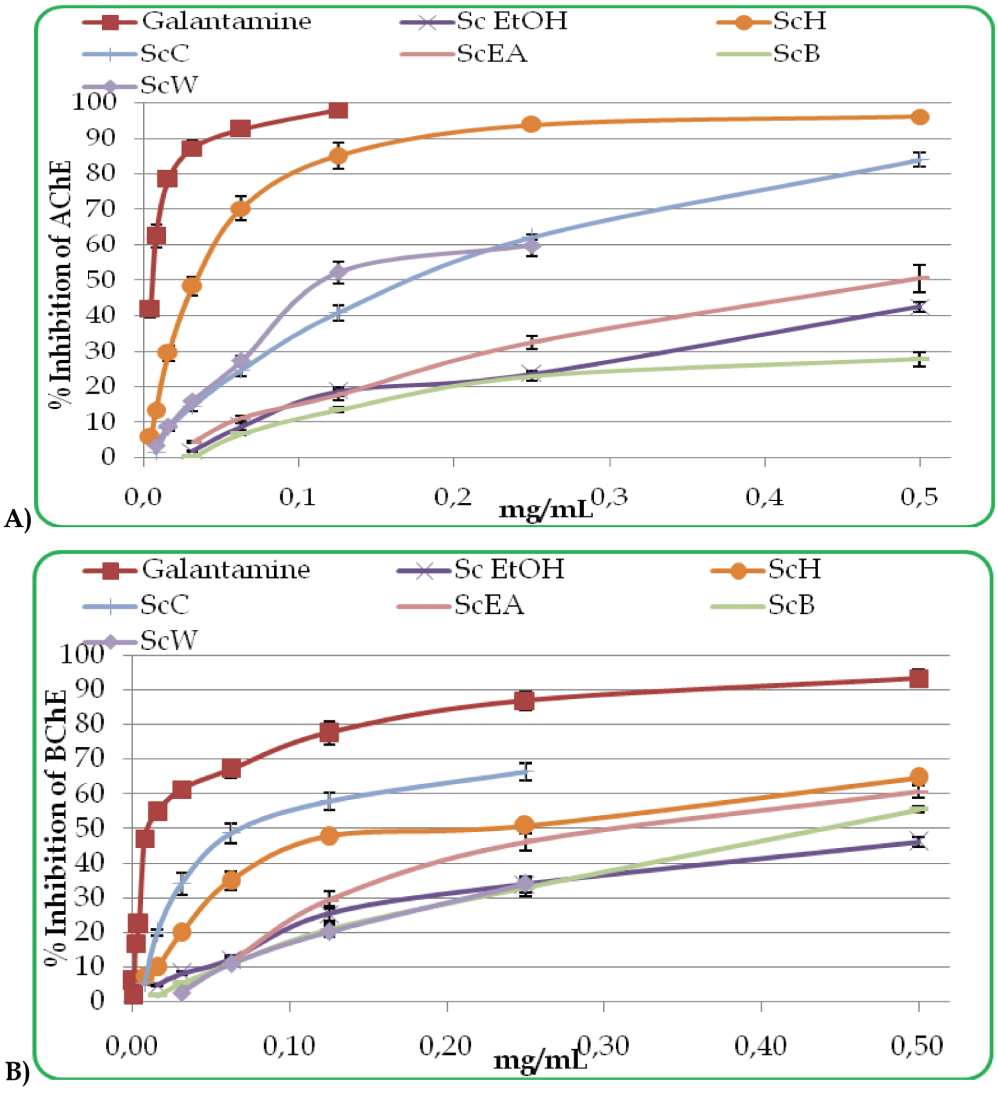

Figure 7.7. AChE **(A)** and BChE **(B)** inhibition activity of galantamine and *Senecio clivicolus* samples

Samples are galantamine, crude ethanol extract (Sc EtOH), *n*-hexane fraction (ScH), chloroform fraction (ScC), ethyl acetate fraction (ScEA), *n*-butanol fraction (ScB) and water fraction (ScW). Data are mean ± standard deviation from three experiments.

The ability of samples to inhibit the AChE and BChE enzymes was expressed as IC_{50} and results were compared with galantamine (**Fig. 6.8**).

In AChE *in vitro* assay the ScH, ScW, and ScC fractions showed a good activity (IC_{50} of 0.03 ± 0.01, 0.12 ± 0.01, and 0.16 ± 0.01 mg/mL, respectively) but lower than positive control galantamine (IC_{50} of 0.01 ± 0.00 mg/mL).

Instead, in BChE assay the ScC and ScH fractions presented the highest IC_{50} values among all samples (0.08 ± 0.01 and 0.19 ± 0.01 mg/mL, respectively) but their activities were lower than galantamine IC_{50} 0.02 ± 0.00 mg/mL).

Instead, the fraction ScB in AChE and the ScW fraction in BChE did not reach the IC_{50}.

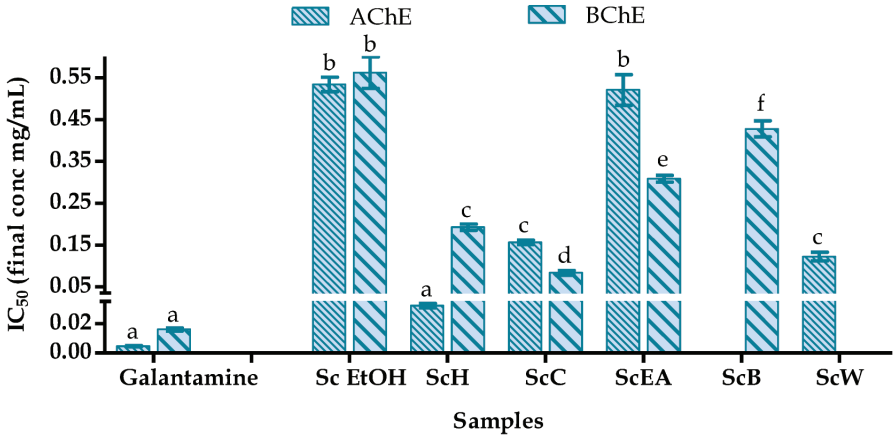

Figure 7.8. AChE and BChE inhibition by galantamine and *Senecio clivicolus* samples expressed as IC_{50} values in mg/mL

Samples are galantamine, crude ethanol extract (Sc EtOH), *n*-hexane fraction (ScH), chloroform fraction (ScC), ethyl acetate fraction (ScEA), *n*-butanol fraction (ScB) and water fraction (ScW). No enzymatic inhibition present for the missing samples. Data are means ± standard deviation from three experiments performed in triplicate. The concentration of the sample required to inhibit the activity of the enzyme by 50% (IC_{50}) in mg/mL was calculated by nonlinear regression analysis. In each test, the values with the same letter are not significant different at the $p < 0.05$ level, 95% confidence limit, according to one-way analysis of variance (ANOVA).

Once again, this is the first report on anticholinesterase activity of *S. clivicolus* samples. In conclusion, the best samples in AChE and BChE inhibition assays were the *n*-hexane and chloroform fractions, but their activities were lower than galantamine used as positive control.

Nevertheless, these results were good if compared with other reports. For example, the study on *S. abyssinicus* water extract showed as this *Senecio* specie

inhibited higher AChE (IC_{50} = 0.13 mg/mL) and BChE (IC_{50} = 0.16 mg/mL) activities and also exhibited antioxidant effect. Moreover, the researchers justified the inhibition of AChE and BChE enzymes, and antioxidant capacity of extract by the presence of gallic, ellagic and caffeic acids, quercetin, rutin, and catechin in the extract revealed by HPLC analysis. For them, these results could be among the mechanisms of actions related to *Senecio* use in folklore for the management of cognitive dysfunction (Odubanjo, Oboh *et al.* 2018).

Moreover, the 80% acetone extract of *S. biafrae* showed interesting inhibitory activities against acetylcholinesterase (IC_{50} = 347.22 µg/mL) and butyrylcholinesterase (IC_{50} = 378.79 µg/mL) enzymes. This study suggested that the leaves of *S. biafrae* may be useful in the management of Alzheimer's disease thanks to the presence of gallic, chlorogenic and caffeic acids, rutin, quercetin, and kaempferol revealed by HPLC (Ajiboye, Ojo *et al.* 2018).

6.6. Identification and quantification of compounds by mass spectrometry in *S. clivicolus* samples

The data shown below were presented in our paper (Faraone, Rai *et al.* 2018).

The compounds previously identified in aerial parts of *Senecio clivicolus* belong mainly to the class of alkaloids, eremophilanes and furanoeremophilanes (Pelser, Nordenstam *et al.* 2007; Dávila, Sterner *et al.* 2013). To evaluate the compounds responsible of the measured antioxidant and antidiabetic activities, the ethyl acetate fraction partitioned from ethanol extract of *S. clivicolus* aerial parts was subject to mass spectrometry analysis in negative ionization (Hossain, Rai *et al.* 2010).

The LC–MS profile of ScEA is show in **Fig. 6.9**. Several compounds (> 26) were detected and tentative identification of most of them have been reached through accurate mass and fragmentation pattern and aided by the existing literature (**Tab. 6.3**). As many as 19 of the compounds were of chlorogenic acid derivatives. Only eight phenolic compounds have been identified in the ethyl acetate fraction by comparing their retention times with those of the available commercial standards.

In particular, these compounds belong to the classes of:

- phenolic derivatives of benzoic acid (4-hydroxybenzoic acid (**1**));

- phenylpropanoids, and in particular cinnamic acid derivatives (chlorogenic acid methyl ester (**3**), 3,5-di-*O*-caffeoyl quinic acid (**7**), 3,4-di-*O*-caffeoyl quinic acid (**8**), caffeic acid (**10a**) and chlorogenic acid (**15a-16a**));
- flavonols (rutin (**4b**) and quercetin-3-*O*-glucoside (**5**)).

The most abundant was the 3,5-di-*O*-caffeoyl quinic acid (45.44 ± 0.91 mg/g DW), followed by 3,4-di-*O*-caffeoyl quinic acid (19.27 ± 0.68 mg/g DW). These phenolic compounds are known for their antioxidant properties (Wang, Nair *et al.* 1999; McDonald, Prenzler *et al.* 2001; Hung, Na *et al.* 2006; Yang, Guo *et al.* 2008; Razavi, Zahri *et al.* 2009; Naveed, Hejazi *et al.* 2018).

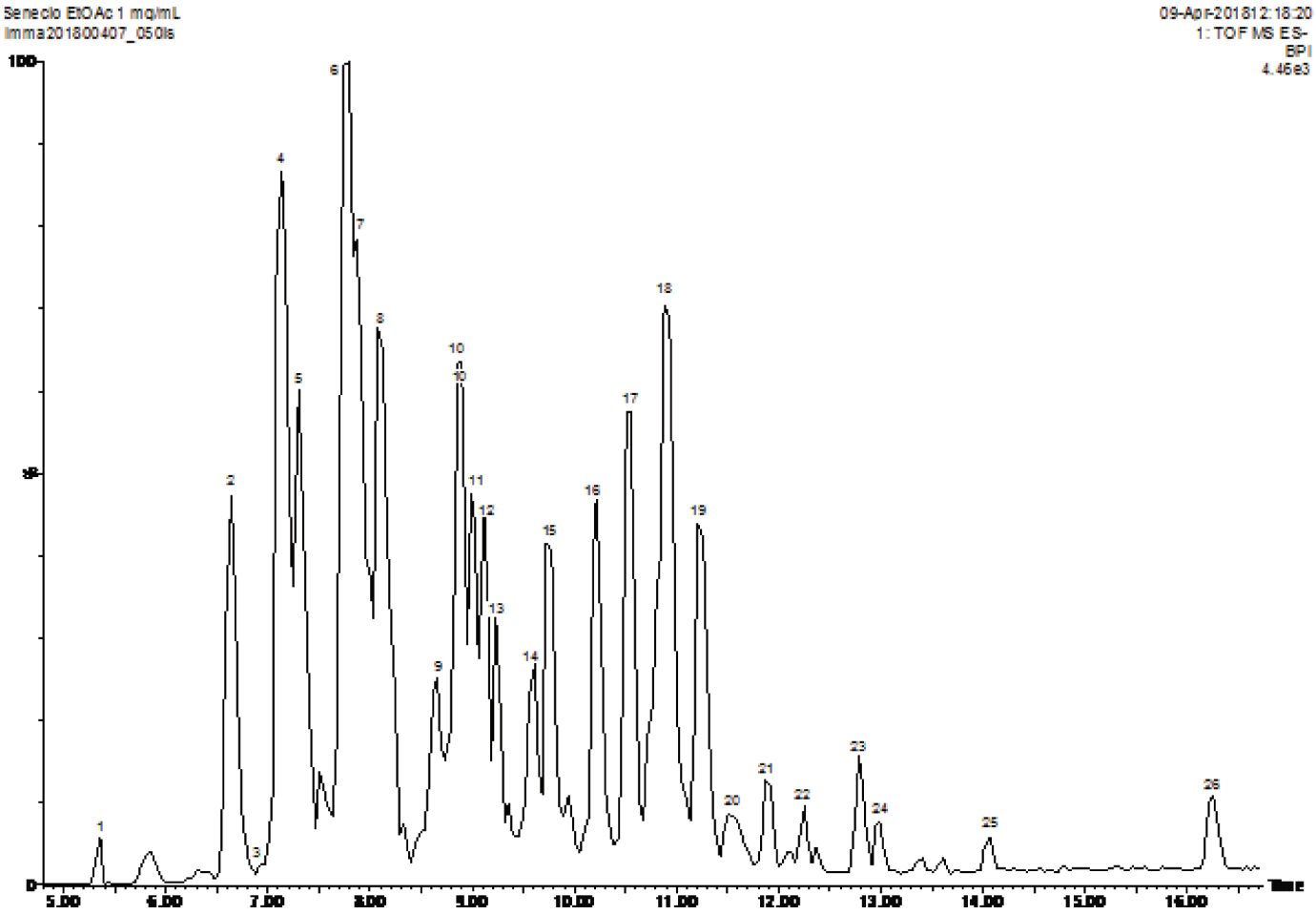

Figure 7.9. Ethyl acetate of *Senecio clivicolus* base peak intensity chromatogram (BPI)

As mentioned earlier, a number of tentatively identified compounds were chlorogenic acid derivatives; in particular, five of the compounds with *m/z* 529.13 tentatively identified as feruloyl-caffeoyl quinic acid isomers (**9**, **10b**, **12**, **13a** and **20a**). Upon fragmentation by CID, these compounds produced the ions at *m/z* 367, 353, 293, 193, 191, 179, 173, 161, 134 and 111 (Clifford, Johnston *et al.* 2003; Han, Ye *et al.* 2008). The signals at 9.23 (**13b**) and 11.87 (**21**) min *m/z* 793.40 indicating the presence of an extra hexose sugar unit with respect to *m/z* 529 and were tentatively identified as chlorogenic acid methylester hexoside derivative; they produced ions at *m/z* 529, 191, 179, 173 and 161 (Yépez, de Ugaz *et al.* 1991). The ESI-MS signals at *m/z* 601.22 (**15c**, **16c**), 617.23 (**15b**, **16b**), 779.23 (**17**), 763.23 (**18**, **19**), 819.26 (**22**), 807.30 (**20b**, **23**) and 735.32 (**24**) were tentatively identified as chlorogenic acid derivatives; they produced the ions at *m/z* 353, 191, 179, 161 and 135 (Jaiswal and Kuhnert 2011). The ESI-MS signal at *m/z* 479.07 (**2**) was tentatively identified as quercetagetin-*O*-glucoside because it produced the ion *m/z* 317 of quercetagetin, and the typical ions *m/z* 166 and 139 (Ibdah, Zhang *et al.* 2003). The ESI-MS signals at 7.17 (**4a**) and 9.61 (**14**) min *m/z* 493.09 were tentatively identified as mearnsetin-*O*-hexoside isomers and they gave dominant product ions *m/z* 478, 331 and 315 (Song, Desta *et al.* 2016). The ESI-MS signal at *m/z* 477.10 (**6**) was tentatively identified as isorhamnetin glycoside and it gave dominant product ions *m/z* 462, 315 and 299 (Schieber, Keller *et al.* 2002). Instead, the ESI-MS signal at *m/z* 519.10 (**11**) was tentatively identified as isorhamnetin-acetyl-glucoside because it produced the ion *m/z* 315 due to the loss of acetyl-glucose residue (Carazzone, Mascherpa *et al.* 2013).

Table 7.3. Liquid chromatography-tandem mass spectrometry (LC–MS/MS) of ethyl acetate fraction of *Senecio clivicolus*

Peak no.	RT (min)	ESI (-) MS observed	ESI (-) MS Calc.	Molecular Formula	MS/MS	Tentative Identity	mg/g DW	References
1	5.39	137.0242	137.0239	$C_7H_5O_3$	93	4-Hydroxybenzoic acid	2.25±1.31	(Hossain, Rai *et al.* 2010)
2	6.64	479.0779	479.0826	$C_{21}H_{19}O_{13}$	317, 166, 139	Quercetagetin-*O*-glucoside	nq	(Ibdah, Zhang *et al.* 2003)
3	6.92	367.1029	367.1029	$C_{17}H_{19}O_9$	161, 85	Chlorogenic acid methylester	2.57±0.07	(Hossain, Rai *et al.* 2010)
4	7.17	493.0982	493.0982	$C_{22}H_{21}O_{13}$	478, 331, 315, 287, 271, 244, 166	Mearnsetin-*O*-glucoside isomer	nq	(Song, Desta *et al.* 2016)
		609.1461	609.1456	$C_{27}H_{29}O_{16}$	300, 285, 271, 255, 179, 151	Rutin	0.16±0.02	(Hossain, Rai *et al.* 2010)
5	7.25	463.0894	463.0877	$C_{21}H_{19}O_{12}$	300, 271, 255, 179, 151	Quercetin-3-*O*-glucoside	0.84±0.05	(Hossain, Rai *et al.* 2010)
6	7.80	477.1067	477.1033	$C_{22}H_{21}O_{12}$	462, 315, 299, 271, 254, 243, 227, 151	Isorhamnetin glycoside	nq	(Schieber, Keller *et al.* 2002)
7	7.91	515.1174	515.1190	$C_{25}H_{23}O_{12}$	179, 135	3,5-Di-*O*-caffeoyl quinic acid	45.44±0.91	(Hossain, Rai *et al.* 2010)
8	8.13	515.1169	515.1190	$C_{25}H_{23}O_{12}$	179, 135	3,4-Di-*O*-caffeoyl quinic acid	19.27±0.68	(Hossain, Rai *et al.* 2010)
9	8.66	529.1370	529.1346	$C_{26}H_{25}O_{12}$	367, 349, 191, 179, 173, 161, 135, 133, 101, 93	Feruloyl-caffeoylquinic acid isomer	nq	(Clifford, Johnston *et al.* 2003;

								Han, Ye *et al.* 2008)
10	8.86	179.0353	179.0344	$C_9H_7O_4$	135, 79	Caffeic acid	1.88±0.13	(Hossain, Rai *et al.* 2010)
		529.1370	529.1346	$C_{26}H_{25}O_{12}$	367, 349, 191, 179, 173, 161, 135, 101	Feruloyl-caffeoylquinic acid isomer	nq	(Han, Ye *et al.* 2008)
11	8.99	519.1039	519.1139	$C_{24}H_{23}O_{13}$	504, 315, 299, 285, 271, 243, 191	Isorhamnetin-acetyl-glucoside	nq	(Carazzone, Mascherpa *et al.* 2013)
12	9.12	529.1370	529.1346	$C_{26}H_{25}O_{12}$	367, 349, 191, 179, 173, 161, 135, 101	Feruloyl-caffeoylquinic acid isomer	nq	(Han, Ye *et al.* 2008)
13	9.23	529.1370	529.1346	$C_{26}H_{25}O_{12}$	367, 349, 191, 179, 173, 161, 135, 101	Feruloyl-caffeoylquinic acid isomer	nq	(Han, Ye *et al.* 2008)
		793.4029	793.4046 or 793.4010	$C_{59}H_{53}O_2$ or $C_{41}H_{61}O_{15}$	529, 397, 353, 219, 191, 179, 173, 161, 101, 71	Chlorogenic acid methylester hexoside derivative	nq	(Yépez, de Ugaz *et al.* 1991)
14	9.61	493.0982	493.0982	$C_{22}H_{21}O_{13}$	331, 316, 179, 161, 135, 133, 101	Mearnsetin-*O*-glucoside isomer	nq	(Song, Desta *et al.* 2016)
15/ 16	9.72 10.21	353.0885	353.0873	$C_{16}H_{17}O_9$	191, 179, 173, 93, 85	Chlorogenic acid	2.33±0.45	(Hossain, Rai *et al.* 2010)
		617.2367	617.2387	$C_{35}H_{37}O_{10}$	353, 245, 191, 179, 173, 161, 135	Chlorogenic acid derivative	nq	(Jaiswal and Kuhnert 2011)
		601.2267	601.2285	$C_{31}H_{37}O_{12}$	439, 353, 263, 191, 179, 173, 161, 135, 85	Dicaffeoyl-methoxyoxaloylquinic acids	nq	(Jaiswal and Kuhnert 2011)
17	10.55	779.2360	779.2340	$C_{43}H_{39}O_{14}$	515, 375, 353, 335, 191, 179, 173, 161, 155, 135, 111, 93	Chlorogenic acid derivative	nq	(Jaiswal and Kuhnert 2011)
18/	10.88/	763.2333	763.2332	$C_{50}H_{35}O_8$	515, 353, 191, 179, 173, 161, 135, 110	Dicaffeoylquinic acid derivative	nq	(Jaiswal and

19	11.21							Kuhnert 2011)
20	11.50	529.1370	529.1346	$C_{26}H_{25}O_{12}$	367, 353, 293, 193, 191, 179, 173, 161, 134, 111	Feruloyl-caffeoylquinic acid isomer	nq	(Han, Ye *et al.* 2008)
		807.3002	807.3017	$C_{46}H_{47}O_{13}$	353, 335, 191, 179, 173, 161, 155, 135	Chlorogenic acid derivative	nq	(Jaiswal and Kuhnert 2011)
21	11.87	793.2888	793.2860	$C_{45}H_{45}O_{13}$	353, 191, 179, 173, 161, 155, 135	Chlorogenic acid derivative	nq	(Yépez, de Ugaz *et al.* 1991)
22	12.25	819.2629	819.2618	$C_{28}H_{51}O_{27}$	353, 335, 191, 179, 173, 161, 155, 135	Chlorogenic acid derivative	nq	(Jaiswal and Kuhnert 2011)
23	12.79	807.3002	807.3017	$C_{46}H_{47}O_{13}$	353, 335, 191, 179, 173, 161, 155, 135	Chlorogenic acid derivative	nq	(Jaiswal and Kuhnert 2011)
24	12.99	735.3240	735.3228	$C_{37}H_{51}O_{15}$	353, 335, 191, 179, 173, 161, 135	Chlorogenic acid derivative	nq	(Jaiswal and Kuhnert 2011)
25	14.70	675.3726	675.3744	$C_{37}H_{55}O_{11}$	415, 397, 277, 235, 161, 143, 125, 119, 113, 101, 89	Unknown	nq	
26	16.25	480.3110	480.3087	$C_{27}H_{44}O_{7}$	255, 242, 224, 168, 153, 79	Unknown	nq	

Identification of compounds based on *m/z*, fragmentation pattern and retention time of standards. Quantities of the detected phenolic compounds were determined using commercial standards; nq = not quantified

6.7. Biological activity on cell lines of *S. clivicolus* samples

The above presented results regarding ethyl acetate of *S. clivicolus* seemed very promising and this fraction was further investigated. As previously mentioned, the identified compounds have known antioxidant and anti-tumoral activities (Uma Devi, Ganasoundari *et al.* 2000; López-Lázaro 2009).

Moreover, Conforti *et al.* (Conforti F. 2006) reported the cytotoxic properties of different extracts of *S. vulgaris* and *S. inaequidens*. In particular, the *n*-hexane extract of *S. inaequidens* showed a highly significant and dose-dependent cytotoxic activity on cancer cell lines, while none of the extracts demonstrated activity on the normal cell line of human foetal lung MRC-5 at concentrations of less than 100 mg/mL. The most sensitive tumour cell line to the methanolic and CH_2Cl_2 extracts of *S. vulgaris* was colorectal adenocarcinoma Caco-2, with an IC_{50} of 34 mg/mL and 5 mg/mL, respectively. They tested also the samples on hepatocellular carcinoma HepG-2 cell line, with interesting values for *n*-hexane and CH_2Cl_2 extracts of both investigated *Senecio* species.

6.7.1. Viability analysis of HepG2 and healthy cells treated with ethyl acetate fraction of *S. clivicolus*

For these reasons, the cytotoxic effect of ethyl acetate of *Senecio clivicolus* was tested against hepatocellular carcinoma HepG2 cell line and normal human dermal fibroblast cells. The cells were treated with different concentrations of sample (100, 200, 300, 400, 500, 600, 800 and 1000 µg/mL) for 24 h, using the colorimetric method MTT assay.

Results exhibited a higher dose-dependent cytotoxic activity on human cancer cell lines (IC_{50} = 550 µg/mL) than on normal dermal fibroblast cells (IC_{50} = 716 µg/mL) (**Fig. 6.10**). These data suggest that this sample can act selectively towards tumour cells, with less effect on healthy cells.

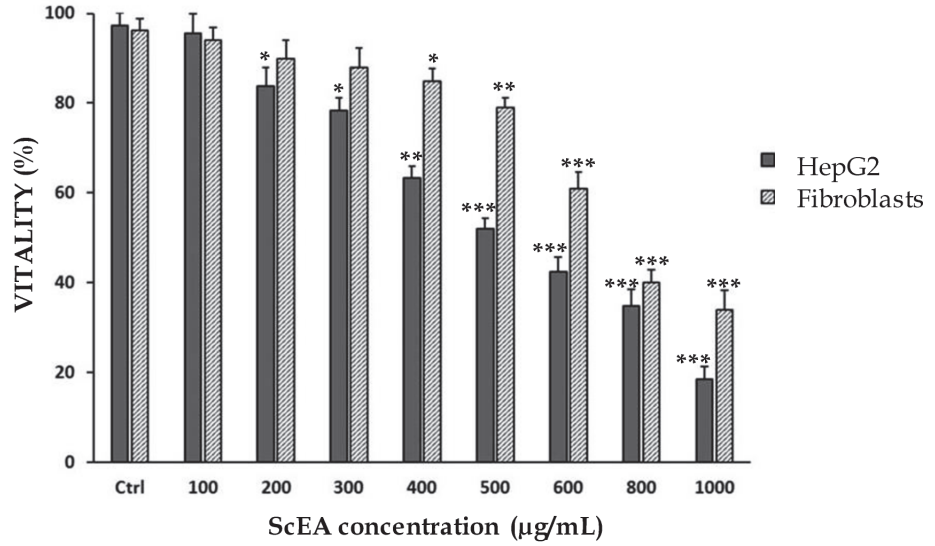

Figure 7.10. Cytotoxic effect of ethyl acetate fraction of *Senecio clivicolus* on HepG2 and human fibroblast cells

Cells were treated with the sample for 24 hours at different concentrations (100, 200, 300, 400, 500, 600, 800 and 1000 µg/mL). Data are expressed as the average percentage of three independent experiments performed in triplicate ± SD. Statistical analysis was performed with the Student test; significant differences between the control and the treated cells are indicated with ***($p < 0.001$), **($p < 0.01$), *($p < 0.05$), n=3.

6.7.2. Evaluation of apoptosis in HepG2 and healthy cells treated with ethyl acetate fraction of *S. clivicolus*

6.7.2.1. Annexin V/7-AAD staining assay

The percentage of cells undergoing apoptosis and necrosis after treatment with different concentrations of sample was quantified using FITC Annexin V-7-AAD kit (BD Pharmingen).

The onset of apoptosis was investigated by phosphoserine biomarker staining at the cell surface. HepG2 cells were incubated with different concentrations of ScEA and then stained with Annexin V-FITC/7-AAD to assess the apoptotic and necrotic cell populations.

Annexin V (or Annexin A5) is a member of the annexin family of intracellular proteins that binds to phosphatidylserine (PS) in a calcium-dependent manner. PS is normally only found on the intracellular leaflet of the plasma membrane in healthy cells, but during early apoptosis, membrane asymmetry is lost and PS translocates to

the external leaflet. Fluorochrome-labeled Annexin V can then be used to specifically target and identify apoptotic cells.

The cells were treated for 24 hours with the ScEA fraction at different concentrations (100, 200, 300, 600 and 900 µg/mL). The cytofluorimetric analysis showed that the increase in concentration of used sample, gave a decreased number of the percentage living cells.

Moreover, the percentage of non-viable cells was distributed in early apoptosis and in late apoptosis/necrosis. In particular, the treatment with the sample leads the cellular population to necrosis only at high concentrations (900 µg/mL) (**Fig. 6.11**). In contrast, at low or intermediate concentrations (100, 200, 300 and 600 µg/mL) was presented an apoptotic phenomenon.

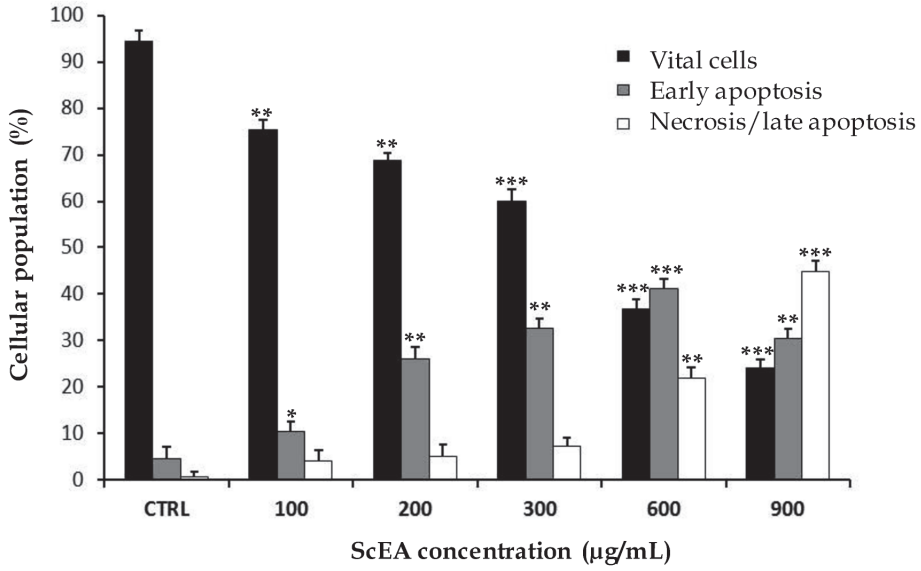

Figure 7.11. Annexin V/7-AAD staining assay in HepG2 cells with ethyl acetate fraction of *Senecio clivicolus*

The cells were treated for 24 hours with different concentrations of the ethyl acetate fraction of *S. clivicolus* (100, 200, 300, 600 and 900 µg/mL). The values were expressed as the average of three independent experiments ± standard deviation. Statistical analysis was performed with the Student test; significant differences between the control and the treated cells are indicated with ***($p < 0.001$), **($p < 0.01$), *($p < 0.05$), n = 3.

6.7.2.2. Observation of morphological changes

The morphological alterations of HepG2 cells were observed in two different modes.

At first, the HepG2 cells were treated for 24 h with *Senecio clivicolus* sample at different concentrations (100, 200, 300, 400, 500, 600, 800, 1000 μg/mL) and then observed using inverted phase contrast microscopy (Nikon Eclipse TS100) (Armentano, Bisaccia *et al.* 2015).

Treated cells showed dose-dependent morphological alterations:

- at low concentrations (100, 200 and 300 μg/mL) treated cells showed similar morphology (**Fig. 6.12 B-D**) to untreated cells (**Fig. 6.12 A**);

- at 400, 500 and 600 μg/mL concentrations the majority of cells lost their typical morphology and appeared round-shaped and translucent (**Fig. 6.12 E-G**);

- at 800 μg/mL and 1000 μg/mL the cells showed evident detachment and cell death (**Fig. 6.12 H-I**).

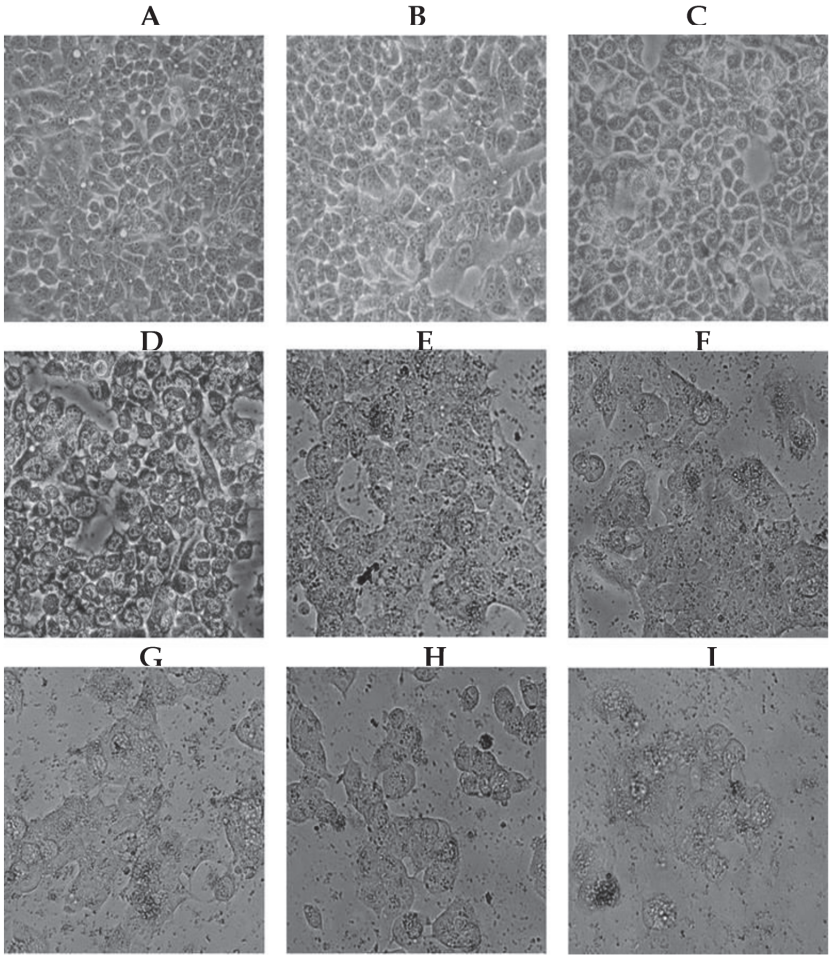

Figure 7.12. Morphological alterations of HepG2 cells treated for 24 h with the ethyl acetate fraction of *Senecio clivicolus* at different concentrations observed by inverted phase contrast microscopy

Concentrations of sample were: 0 μg/mL in control (**A**), 100 μg/mL (**B**), 200 μg/mL (**C**), 300 μg/mL (**D**), 400 μg/mL (**E**), 500 μg/mL (**F**), 600 μg/mL (**G**), 800 μg/mL (**H**) and 1000 μg/mL (**I**).

Apoptosis was also determined by the assessment of nuclear morphology using Hoechst 33258 DNA staining. The apoptotic cells most significant change is chromosome condensation. DNA cracking changes the shape of the nucleus.

Fluorescent dye Hoechst 33258 is a double benzene imidazole compound and it can be used to bind to the DNA molecule as a fluorescent probe. In apoptotic cell, the membrane's uptake in Hoechst 33258 increases combination enhances for highly condensed chromosomes and it shows strong blue. In normal cells, it shows only weak fluorescence.

The results of cells treated with ScEA fraction showed as the nuclei were regular, round shaped, and homogeneously stained in control cells (**Fig. 6.13 A**). The accumulation of fluorescent dye, due to morphological changes of cell apoptosis such as chromatin condensation (pyknosis), nuclear fragmentation (karyorrhexis), and cell shrinkage, instead, was detected in treated cells in a dose-dependent manner (**Fig. 6.13 B-E**). In detail, at the lowest concentrations of sample used (100 µg/mL and 200 µg/mL, **Fig. 6.13 B-C**), the cellular vitality aspect was comparable to that of control cells (**Fig. 6.13 A**); subsequently, the fluorescence intensity increases progressively with the increase in concentration used (300 µg/mL, 400 µg/mL, 500 µg/mL and 600 µg/mL), suggesting that the treatment gave a mechanism in the cells of apoptotic cell death through the condensation of chromatin (**Fig. 6.13 D-G**). Finally, with the highest concentrations of sample used (800 µg/mL and 1000 µg/mL), a clear decrease in fluorescence is evident in the few remaining cells (**Fig. 6.13 H- I**); in this case, the lack of aggregation of the chromatin is an aspect that strongly supports the hypothesis that at high concentrations of sample used the cells go to a cell death by necrosis.

These data findings suggest that treatment kills HepG2 cells via apoptotic mechanism in according with other study on aqueous extracts of *S. latifolius* (10 mg/mL) that induced apoptosis on HepG2 cells by caspase activation (Neuman, Jia *et al.* 2007).

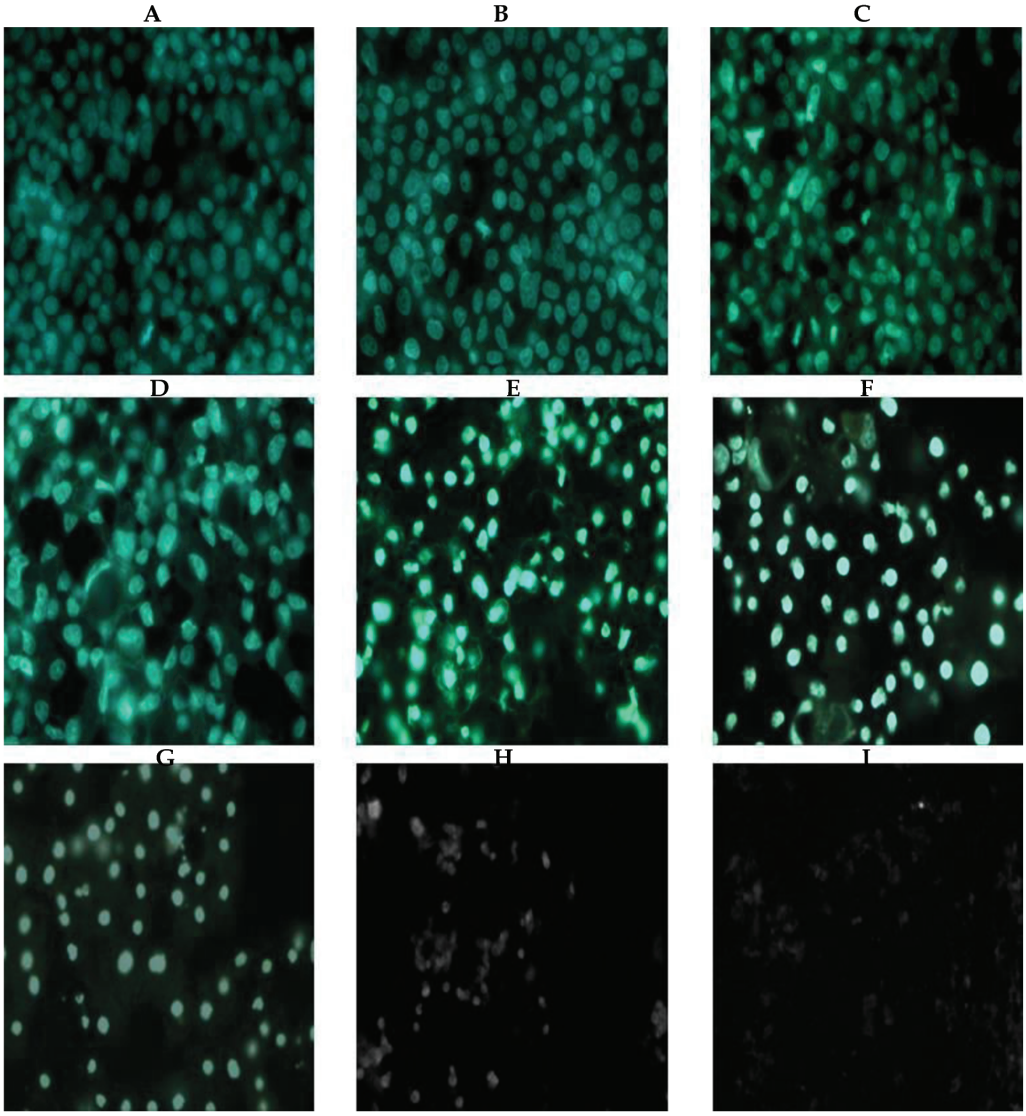

Figure 7.13. Morphological alterations of HepG2 cells treated for 24 hours with different concentrations of the ethyl acetate fraction of *S. clivicolus* labelled with the Hoechst33258 dye The images are representative of three independent experiments. Concentrations of sample were: 0 µg/mL in control (**A**), 100 µg/mL (**B**), 200 µg/mL (**C**), 300 µg/mL (**D**), 400 µg/mL (**E**), 500 µg/mL (**F**), 600 µg/mL (**G**), 800 µg/mL (**H**) and 1000 µg/mL (**I**).

6.7.3. Measurement of Reactive Oxygen Species (ROS) generation and of mitochondrial membrane potential ($\Delta\Psi_m$)

6.7.3.1. ROS generation

The Reactive Oxygen Species (ROS) and the resulting oxidative stress play a pivotal role in apoptosis. The level of intracellular ROS was determined following the

method reported by Armentano *et al.* with slight modification (Armentano, Bisaccia *et al.* 2015). In particular, the intracellular level of ROS was determined using a cell permeable fluorogenic probe, 2',7'-dichlorofluorescein diacetate (DCFH-DA). This molecule is deacetylated by intracellular esterases and converted to non fluorescent dichlorodihydrofluorescein (DCFH), which is oxidized rapidly to the highly fluorescent compound dichlorofluorescein (DCF) in the presence of ROS. HepG2 and fibroblast cells were treated with different concentrations of *S. clivicolus* sample (100, 200, 300, 400, 500, 600, 800, 1000 μg/mL).

At low concentration, ROS level is similar to the endogenous level of the control cells. Instead, when the concentration of ScEA increases, ROS level increases in dose-dependent manner.

On the other hand, pre-treatment of cells with *N*-Acetyl-*L*-cysteine (NAC) blocks the increase in DCF fluorescence. The different concentrations of the ethyl acetate of *S. clivicolus* used for 24 hour treatment (200, 300, 400, 600 and 1000 µg/mL) stimulate ROS formation in dose mode dependent, compared to control cells (**Fig. 6.14**). In particular, at the lowest concentration of the sample of 200 µg/mL, the level of ROS produced was very similar to the level of endogenous ROS present in the control cells; while increasing the concentration of the sample (300, 400, 600 and 1000 µg/mL) there was a proportional increase in the level of ROS. Characteristic is also the trend of the level of ROS produced in the presence of NAC, an important quencher of ROS. In fact, at lower concentrations of the sample (200, 300 and 400 µg/mL), there was a significant quenching of ROS; while the same effect, there was not at the highest concentrations (600 and 1000 µg/mL).

A high production of ROS is a common event both in apoptosis and in necrosis. These data evidence that, the different quenching activity exerted by NAC depending on the concentrations of sample used, depends on the different fate to which the cells are after treatment, apoptosis at lower concentrations, and necrosis at higher concentrations.

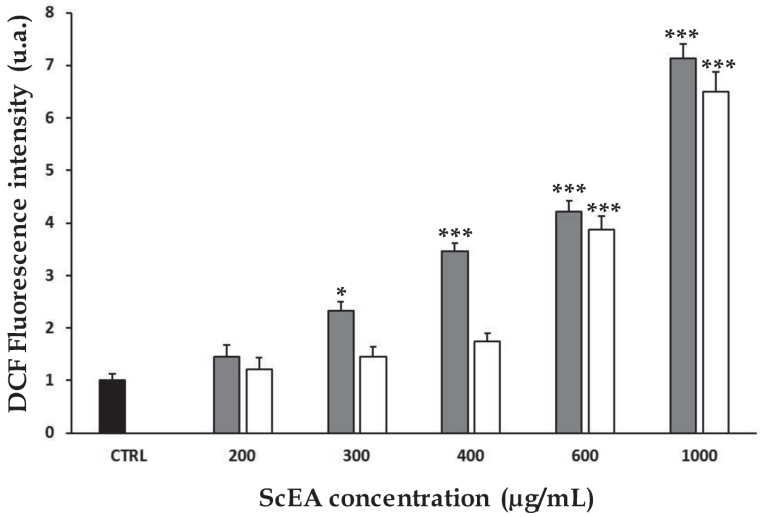

Figure 7.14. Dose-dependent production of intracellular ROS in HepG2 cells.
The cells were treated for 24 hours with different concentrations of the ethyl acetate fraction of *S. clivicolus* (200, 300, 400, 600 and 1000 µg/mL). Control (CTRL) was set equal to 1 (endogenous ROS) in arbitrary fluorescence intensity. The values were expressed as an average percentage of three independent experiments ± standard deviation. Statistical analysis was performed with the Student test; significant differences between the control and the treated cells are indicated with ***($p < 0.001$), **($p < 0.01$), *($p < 0.05$), n = 3.

6.7.3.2. $\Delta\Psi_m$ measurement

Since excessive oxidative stress could lead to mitochondrial damage, causing a loss of mitochondrial membrane potential ($\Delta\Psi_m$) and mitochondria-mediated apoptosis. For this reason, the mitochondrial membrane polarization of HepG2 cells treated with different concentrations of sample was analyzed using a cationic fluorescent probe tetramethyl rhodamine methy (TMRM), a cell-permeant, cationic, red-orange fluorescent dye that is readily sequestered by active mitochondria. The fluorescence intensity decreases when sample concentration increases.

The integrity of mitochondrial cell membranes was estimated after 24 hours of treatment of HepG2 cells with different sample concentrations (100, 200, 300, 600 and 900 µg/mL). Then, the variations in $\Delta\Psi_m$ were evaluated using a fluorescence microscope and a 100X magnification by measuring of the fluorescence intensity of TMRM in cells.

In detail, in the control cells (**Fig. 6.15 A**) the intense fluorescence signals correspond to a physiological mitochondrial membrane potential, characteristic of healthy cells; this data was also found in the cells treated with low concentrations of

ScEA (100, 200 and 300 µg/mL, **Fig. 6.15 B-D**). At higher concentrations (600 and 900 µg/mL) the treated cells emitted a low-intensity fluorescence signal (**Fig. 6.15 E-F**), related to the permeabilization of the mitochondrial membrane; the loss of the TMRM signal is in fact an event that can characterize both apoptotic and necrotic cells.

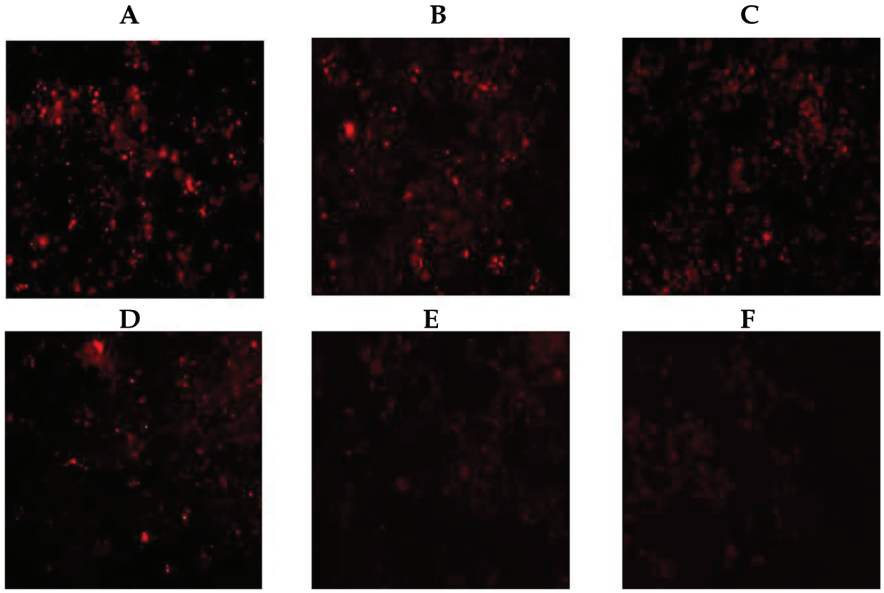

Figure 7.15. Evaluation of mitochondrial membrane potential variation in HepG2 cells treated with ethyl acetate fraction of *S. clivicolus*
The images are representative of three independent experiments. Concentrations of the sample were: 0 µg/mL in control (**A**), 100 µg/mL (**B**), 200 µg/mL (**C**), 300 µg/mL (**D**), 600 µg/mL (**E**) and 900 µg/mL (**F**).

The following **figure 6.16**, highlights the data obtained through an image analysis of the cells treated with the fluorescence sample of the TMRM probe, for the evaluation of the variations in the $\Delta\Psi_m$. In fact, the fluorescence intensity decreases when ScEA concentration increases.

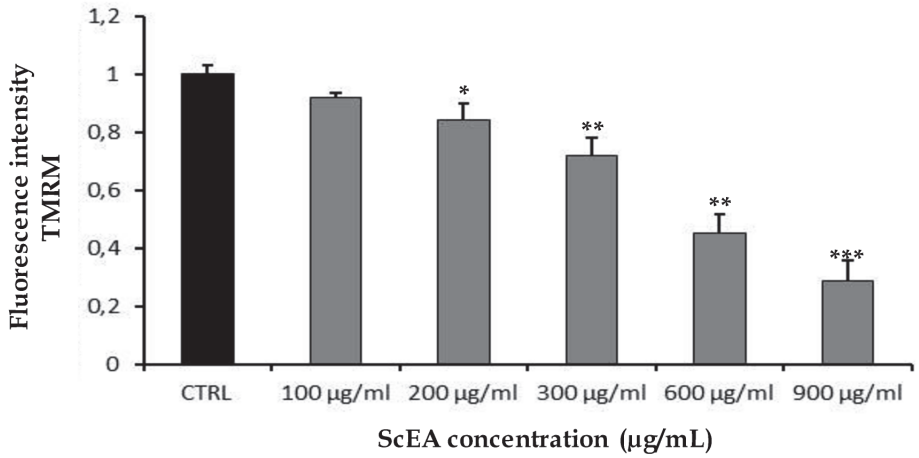

Figure 7.16. Fluorescence intensity of TMRM in the treated cells with ethyl acetate fraction of *S. clivicolus*

Concentrations of the sample were: 0 µg/mL in control (CTRL), 100 µg/mL, 200 µg/mL, 300 µg/mL, 600 µg/mL and 900 µg/mL. The values were expressed as an average percentage of three independent experiments ± standard deviation. Statistical analysis was performed with the Student test; significant differences between the control and the treated cells are indicated with ***($p < 0.001$), **($p < 0.01$), *($p < 0.05$), n = 3.

6.7.4. Western blot analysis

Mitochondria play a key role in apoptosis by releasing cytochrome *c* into the cytosol where it participates in caspase activation.

Changes in mitochondrial membrane potential and mitochondrial permeability transition result in the release of cytochrome *c* from the mitochondria into the cytosol; this process is blocked by Bcl-2, an anti-apoptotic protein localized on the outer mitochondrial membrane.

The previously discussed data shown an increase in ROS produced in HepG2 cells treated with ethyl acetate fraction of *Senecio clivicolus*. For this reason, the possible release of cytochrome *c* from the mitochondrial intermembrane space (IMS) to the cytosol was evaluated. The release of this protein, in fact, involves an interaction with the IP3 receptor on the endoplasmic reticulum, causing the release of calcium ions; the total increase in intracellular calcium triggers a positive feedback mechanism that leads to a further increase in the concentration of this ion, with subsequent activation of the procaspase 9 to caspase 9, which can then activate caspases 3 and 7, responsible for cell death.

Western blotting analysis shows that cytochrome *c* was released into the cytosol in the HepG2 treated with the *Senecio clivicolus* sample at the concentration

corresponding to the IC_{50} (550 µg/mL). This release increased with time (3 hours - 6 hours - 24 hours of treatment) compared to control cells (**Fig. 6.17**). At the same time, the presence of cytochrome *c* tended to disappear into the mitochondria with the passage of time.

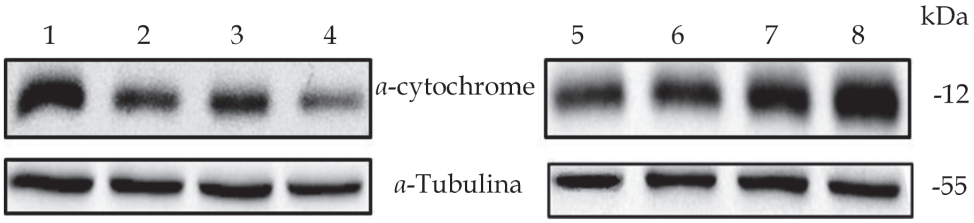

Figure 7.17. Western blotting of HepG2 cells treated with the sample at the concentration of 550 µg/mL
Lane 1 and 5: Untreated HepG2 cells; **lane 2, 3** and **4**: mitochondria; **lane 6, 7** and **8**: cytosol of HepG2 treated with the ethyl acetate fraction of *S. clivicolus* sample at the concentration of 550 µg/mL, respectively for 3h, 6h and 24h.

The densitometric analysis performed on the blots (**Fig. 6.18**) allowed highlighting the result obtained. In conclusion, it is possible that there is an effective activation of the intrinsic pathway of apoptosis, probably mediated by ROS.

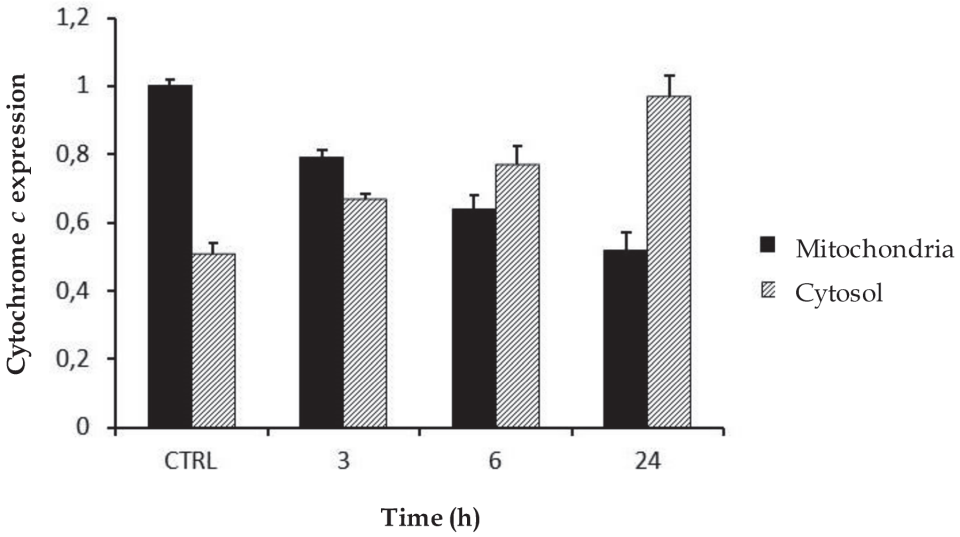

Figure 7.18. Densitometric analysis of cytochrome *c* expression in HepG2 cells treated with ethyl acetate fraction of *S. clivicolus* at the concentration of 550 µg/mL
The values obtained express the average of three independent experiments performed in triplicate ± standard deviation.

The family of Bcl-2 proteins controls the various metabolic pathways by directing cells to death or cell survival. In particular, the anti-apoptotic Bcl-2 protein was monitored in this work. This protein, together with the Bcl-XL protein, is sequestered in the mitochondria and inhibits the release of pro-apoptotic factors, thus inhibiting apoptosis. However, if pro-apoptotic stimuli increase, these proteins lose their inhibitory capacity and promote cell death.

The Bcl-2 protein expression was verified in HepG2 cells treated for 3h, 6h and 24h with the sample at the concentration corresponding to the IC_{50} (550 µg/mL), compared to the untreated cells (**Fig. 6.19)**.

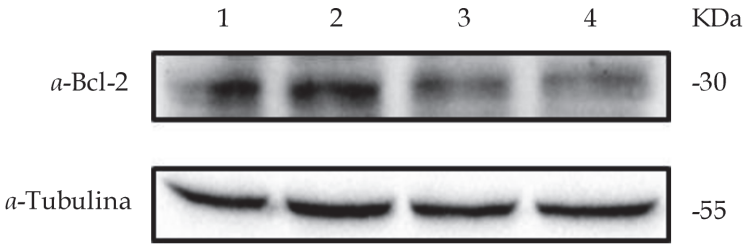

Figure 7.19. Western blotting of HepG2 cells treated with the ethyl acetate fraction of *S. clivicolus* at the concentration of 550 µg/mL
Lane 1: untreated HepG2 cells; **lane 2**, **3** and **4**: cells treated with the sample at the concentration of 550 µg/mL, respectively for 3, 6 and 24 h.

There is a down-regulation of Bcl-2 expression, thus suggesting that the apoptosis induced by the sample is modulated through the Bcl-2 family of proteins; the densitometric analysis performed on the blots (**Fig. 6.20**) highlights the result obtained.

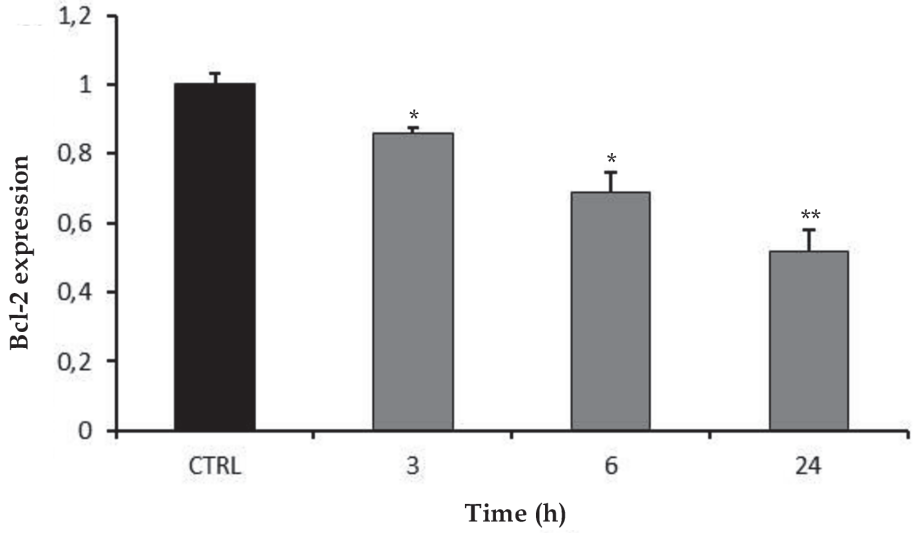

Figure 7.20. Densitometric analysis of Bcl-2 protein expression in HepG2 cells treated with ethyl acetate fraction of *S. clivicolus* at the concentration of 550 µg/mL
The values obtained express the average of three independent experiments performed in triplicate ± standard deviation. Statistical analysis was performed with the Student test; significant differences between the control and the treated cells are indicated with ***($p < 0.001$), **($p < 0.01$), *($p < 0.05$), n = 3.

6.7.5. Conclusions to biological activity on cells of *S. clivicolus*

In conclusion, an inhibitory effect on the proliferation of HepG2 cells by the ethyl acetate fraction of *S. clivicolus* sample is evident. The sample has a cytotoxic action on fibroblasts only at the highest concentrations. These data suggest that this sample is selective towards cancer cells.

The treated cells show an altered morphology compared to the untreated cells, which could make one think of a cell death by apoptosis; however, at the highest concentration used, the characteristic values of cell death due to necrosis are present.

Then, we proceeded to evaluate whether an increase in the intracellular level of ROS could explain the cell death induced by the sample, since ROS are known biochemical mediators of apoptosis. In the treated HepG2 cells, the sample causes an increase in ROS production.

Therefore a qualitative and quantitative analysis of apoptosis was performed. At the highest concentrations there was a lack of aggregation of chromatin, an aspect that supports the hypothesis that at high concentrations the cells go to a cell death due to necrosis.

To be sure of the ability of the ethyl acetate fraction of *S. clivicolus* to induce a different mechanism of cell death based on the concentration used, we proceeded with a quantitative evaluation of the induced cell death mechanisms: the result obtained leads to the conclusion that the tumour cells treated with the sample are brought to cell death by apoptosis or necrosis depending on whether low/intermediate or high concentrations are used.

A high level of intracellular ROS induces cell death through interactions with the mitochondrial permeability transition complex (PTPC) proteins. For this reason, the loss of mitochondrial membrane potential was evaluated. In fact, the treated cells show a loss of mitochondrial membrane potential and therefore *Senecio clivicolus* sample has cytotoxic activity because it activates a pro-apoptotic mechanism that involves the mitochondria.

Therefore the proteins involved in this process were evaluated. In particular, the expression of the anti-apoptotic Bcl-2 protein and the release of cytochrome c from the mitochondria to the cytosol were evaluated.

The results confirm that this fraction of *S. clivicolus* is actually capable of inducing cell death via the mitochondrial apoptotic pathway.

It is possible explain these results also on the basis of major compounds present in the tested sample; in fact the chlorogenic acid and derivatives have the capability to inhibit the HepG2 cancer cell growth through apoptosis induction (Sukohar and Muhartono 2015).

6.8. *Senecio clivicolus* study conclusions

The ethanol extract of *S. clivicolus* aerial parts was subjected to liquid/liquid fractionation using solvent with increasing polarity.

The antioxidant activity, determined by six complementary *in vitro* assays, showed different values among fractions. Relative Antioxidant Capacity Index (RACI) evidenced *S. clivicolus* ethyl acetate fraction as the most active. More in detail, fraction reported activity was: *n*-hexane < water < chloroform < *n*-butanol < ethyl acetate.

Moreover, this study reports the profile of the phenolic compounds in *S. clivicolus* ethyl acetate fraction. The phytochemical investigation allowed the

identification or tentative identification of 30 compounds and confirms that the LC-MS-based profiling is a powerful technique for the phenolic characterization.

Furthermore, the cytotoxicity of ethyl acetate fraction of *S. clivicolus* on HepG2 cell was evaluated and the results suggest that this sample is selective towards cancer cells. The treated cells showed a loss of mitochondrial membrane potential. Then, the cytotoxic activity of the *Senecio clivicolus* sample depended from the activation of a pro-apoptotic mechanism that involves the mitochondria. The results confirm that this sample of *S. clivicolus* is actually capable of inducing cell death via the mitochondrial apoptotic pathway.

In conclusion, this first report on *S. clivicolus* phenolic characterization and biological activity demonstrated as it could be considered a rich source of health promoting compounds, particularly chlorogenic acid, and flavonoid derivatives.

Especially its polar fractions might be used for mitigating human and animal diseases. The presence of potential nutraceuticals is suitable and promising for the development of safe food products, natural additives and cosmetics.

CHAPTER 7.

CONCLUSIONS

The antioxidant, antidiabetic and anticholinesterase activities and the phytochemical profiles on the aerial parts of *Azorella glabra*, *Minthostachys diffusa* and *Senecio clivicolus* were here performed for the first time.

In particular, the dried aerial parts of *A. glabra*, *M. diffusa* and *S. clivicolus* were subjected to dynamic maceration using 96% ethanol. The obtained ethanol extracts were fractionated on the basis on the affinity solvent by liquid/liquid extraction using an increasing solvent polarity obtaining the *n*-hexane, chloroform, ethyl acetate, *n*-butanol and water fractions.

The total polyphenolic (TPC), flavonoid (TFC) and terpenoid (TTeC) content were determined by three different *in vitro* colorimetric assays. Instead, to determine the antioxidant activity six complementary *in vitro* assays were used.

The results of the antioxidant activity were obtained by ABTS, DPPH, SO, NO, FRAP, BCB and TPC i*n vitro* assays and, subsequently have been integrated by calculating the Relative Antioxidant Capacity Index (RACI). The RACI values obtained are in agreement with those obtained so far evidencing as the three ethyl acetate fractions presented the highest value, followed by butanol fractions.

Oxidative stress is involved in several diseases, such as inflammation, diabetes, neurodegenerative diseases and cancer. These confirm the antioxidant activity of investigating plant species and might partially justify their uses in Bolivian populations, in particular, the ethnobotanical use as a tea or infusion of plant species as antirheumatic or anti-inflammatory (Floegel, Kim *et al.* 2011; Sung, Kwon *et al.* 2015; Gayathiri, Sangeetha *et al.* 2016).

Moreover, the inhibitory ability of samples against enzymes involved in diabetes (*e.g. a*-amylase and *a*-glucosidase enzymes) and Parkinson's or Alzheimer's diseases (*e.g.* acetylcholinesterase and butyrylcholinesterase enzymes) was investigated.

In particular, the inhibition of *a*-amylase and *a*-glucosidase enzymes is a strategy in the treatment of diabetes and/or obese patients. For these reasons, different concentrations of samples were assayed for both enzyme inhibitory activities. Among samples, in both inhibition tests, the *n*-hexane and ethyl acetate fractions of *Minthostachys diffusa* showed the highest potential antidiabetic activity with IC_{50} values lower than acarbose. The inhibitory activity of *Azorella glabra* samples was also interesting and these results supported the ethnobotanical use of *A. glabra* as antidiabetic remedy (Fuentes, Sagua *et al.* 2005).

The inhibition of acetylcholinesterase and butyrylcholinesterase enzymes are considered as a strategy for the treatment of Parkinson's and Alzheimer's diseases, senile dementia, ataxia, and myasthenia gravis (Areche, Cejas *et al.* 2009; Fidelis, Faraone *et al.* 2018). The three Bolivian plant species had a concentration-dependent activity on both enzymes and the ability of samples to inhibit the AChE and BChE enzymes was expressed as IC_{50} and results were compared with galantamine. Among all, *M. diffusa* samples showed the highest anticholinesterase activity. For these reasons, the AChE and BChE inhibition *in vitro* assays were performed to test the activities of identified terpenes (betulinic, corosolic, maslinic, oleanolic and ursolic acids) from aerial parts of *M. diffusa.* Then, molecular modelling studies on AChE and BChE enzymes were performed for the first time with the lead triterpene. The promising results showed that terpenoids derived from *M. diffusa* could be potential leads for the development of cholinesterase inhibitors.

To evaluate the compounds responsible of the measured biological activities, the phytochemical profiles of the three Bolivian plant species were achieved by using mass spectrometry analysis in negative ionization. Several compounds were detected and tentative identification of most of them have been reached through accurate mass and fragmentation pattern and aided by the existing literature. In particular, we have been identified for the first time six cinnamic acid derivatives, 4 flavones, 4 flavonols and a triterpene in *A. glabra*, a phenolic acid, 6 flavonols, 4 flavones, 2 flavanones, 4 cinnamic acid derivatives and 5 triterpenes in *M. diffusa* and a phenolic derivative of benzoic acid, 5 cinnamic acid derivatives and 2 flavonols in *S. clivicolus.*

Moreover, *A. glabra* samples were tested on Multiple Myeloma (MM) cell lines using several assays for the first time and the chloroform fraction was the sample with highest activity; in particular, it reduced the cell viability, induced the apoptosis, and arrested the cell cycle arrest on MM cells in G0/G1 phase.

Instead, the ethyl acetate fraction of *Senecio clivicolus* was tested on hepatocellular carcinoma HepG2 cell line for the first time. The results of cytotoxic assays suggest that the ethyl acetate fraction was selective towards cancer cells and it was capable to induct cell death via the mitochondrial apoptotic pathway.

In conclusion, this first report on *Azorella glabra*, *Minthostachys diffusa* and *Senecio clivicolus* phytochemical characterization and biological activity evaluation, demonstrates as these Bolivian plant species could be considered a source of health

promoting compounds. Some of the results obtained during this study might partially explain their ethnobotanical use, evidencing a potential economic added value for extract or pure compound future use in the field of biotechnology applied to environmental, agricultural, health, pharmaceutical and cosmeceutical development.

REFERENCES

Agostini-Costa, T. d. S., R. F. Vieira, *et al.* (2012). Secondary metabolites. Chromatography and its applications, InTech.

Ajiboye, B. O., O. A. Ojo, *et al.* (2018). *In vitro* antioxidant activities and inhibitory effects of phenolic extract of *Senecio biafrae* (Oliv and Hiern) against key enzymes linked with type II diabetes mellitus and Alzheimer's disease. Food Science & Nutrition.

Ali, M., S. Muhammad, *et al.* (2017). Neurologically potent molecules from *Crataegus oxyacantha*; isolation, anticholinesterase inhibition, and molecular docking. Frontiers in pharmacology 8: 327.

Alkire, B. H., A. O. Tucker, *et al.* (1994). Tipo, *Minthostachys mollis* (lamiaceae): an Ecuadorian mint. Economic Botany 48(1): 60-64.

Andrade-Cetto, A. and M. Heinrich (2005). Mexican plants with hypoglycaemic effect used in the treatment of diabetes. Journal of Ethnopharmacology 99(3): 325-348.

Araujo, N., R. Mü Ller, *et al.* (2005). Análisis de vacíos de representatividad del Sistema Nacional de Áreas Protegidas. FAN, Santa Cruz.

Areche, C., P. Cejas, *et al.* (2009). Triterpenoids from *Azorella trifurcata* (Gaertn.) Pers and their effect against the enzyme acetylcholinesterase. Química Nova 32(8): 2023-2025.

Armentano, M. F., F. Bisaccia, *et al.* (2015). Antioxidant and proapoptotic activities of *Sclerocarya birrea* [(A. Rich.) Hochst.] methanolic root extract on the hepatocellular carcinoma cell line HepG2. BioMed research international 2015.

Babu, M., M. Johnson, *et al.* (2014). Chemical constituents and their biological activity of *Ulva lactuca* Linn. International Journal of Pharmaceutics and Drug Analysis 2(7): 595-600.

Bahadori, M. B., L. Dinparast, *et al.* (2016). Bioactive constituents from roots of *Salvia syriaca* L.: acetylcholinesterase inhibitory activity and molecular docking studies. South African Journal of Botany 106: 1-4.

Barros, L., M. Dueñas, *et al.* (2013). Phenolic profiles of cultivated, *in vitro* cultured and commercial samples of *Melissa officinalis* L. infusions. Food Chemistry 136(1): 1-8.

Bonaccorsi, P., C. Caristi, *et al.* (2008). Flavonol glucosides in *Allium* species: A comparative study by means of HPLC–DAD–ESI-MS–MS. Food Chemistry 107(4): 1668-1673.

Bórquez, J., N. L. Bartolucci, *et al.* (2016). Isolation of cytotoxic diterpenoids from the Chilean medicinal plant *Azorella compacta* Phil from the Atacama Desert by high-speed counter-current chromatography. Journal of the Science of Food and Agriculture 96(8): 2832-2838.

Bórquez, J., E. J. Kennelly, *et al.* (2013). Activity guided isolation of isoflavones and hyphenated HPLC-PDA-ESI-ToF-MS metabolome profiling of *Azorella madreporica* Clos. from northern Chile. Food research international 52(1): 288-297.

Bourdy, G., P. Oporto, *et al.* (2004). A search for natural bioactive compounds in Bolivia through a multidisciplinary approach: part VI. Evaluation of the antimalarial activity of plants used by Isoceno-Guaranı Indians. Journal of Ethnopharmacology 93(2): 269-277.

Bourgaud, F., A. Gravot, *et al.* (2001). Production of plant secondary metabolites: a historical perspective. Plant science 161(5): 839-851.

Bouyahya, A., Y. Bakri, *et al.* (2017). Antibacterial, antioxidant and antitumor properties of Moroccan medicinal plants: a review. Asian Pac J Trop Dis 7: 57-64.

Buchanan, B. B., W. Gruissem, *et al.* (2000). Biochemistry & molecular biology of plants, American Society of Plant Physiologists Rockville, MD.

Bustamante, G., L. Escalante, *et al.* (2001). Estudio etnobotánico y actividad antimicrobiana de las plantas medicinales de los valles bajos de Cochabamba, Universidad Mayor de San Simón, Cochabamba-Bolivia.

Carazzone, C., D. Mascherpa, *et al.* (2013). Identification of phenolic constituents in red chicory salads (*Cichorium intybus*) by high-performance liquid chromatography with diode array detection and electrospray ionisation tandem mass spectrometry. Food Chemistry 138(2-3): 1062-1071.

Carpinella, M. C., D. G. Andrione, *et al.* (2010). Screening for acetylcholinesterase inhibitory activity in plant extracts from Argentina. Phytotherapy Research: An International Journal Devoted to Pharmacological and Toxicological Evaluation of Natural Product Derivatives 24(2): 259-263.

Cha, S., H. Zhang, *et al.* (2008). Direct profiling and imaging of plant metabolites in intact tissues by using colloidal graphite-assisted laser desorption ionization mass spectrometry. The Plant Journal 55(2): 348-360.

Chen, J., Y. Wu, *et al.* (2016). *a*-Glucosidase inhibition and antihyperglycemic activity of flavonoids from *Ampelopsis grossedentata* and the flavonoid derivatives. Bioorganic & medicinal chemistry 24(7): 1488-1494.

Chun, O. K. and D. O. Kim (2004). Consideration on equivalent chemicals in total phenolic assay of chlorogenic acid-rich plums. Food research international 37(4): 337-342.

Clifford, M. N., K. L. Johnston, *et al.* (2003). Hierarchical scheme for LC-MS n identification of chlorogenic acids. Journal of agricultural and food chemistry 51(10): 2900-2911.

Conforti, F., M. R. Loizzo, *et al.* (2006). Biological properties of different extracts of two *Senecio* species. International Journal of Food Sciences and Nutrition 57(1-2): 1-8.

Conforti, F., Marrelli M., *et al.* (2006). Antioxidant and cytotoxic activities of methanolic extract and fractions from *Senecio gibbosus subsp. gibbosus* (GUSS) DC. Natural product research 20(9): 805-812.

Conforti F., L. M. R., Statti G.A., Houghton P.J. & Menichini F. (2006). Biological properties of different extracts of two *Senecio* species. International Journal of Food Sciences and Nutrition 57(1-2): 1-8.

Cotton, C. M. and P. Wilkie (1996). Ethnobotany: principles and applications, John Wiley & Sons Chichester.

Dalar, A., Y. Uzun, *et al.* (2015). *Centaurea karduchorum* Boiss. from Eastern Anatolia: Phenolic composition, antioxidant and enzyme inhibitory activities. Journal of Herbal Medicine 5(4): 211-216.

Dávila, M., O. Sterner, *et al.* (2013). Furanoeremophillanes from *Senecio clivicolus* Weddell. Revista Boliviana de Química 30(1): 80-83.

Deharo, E., G. Bourdy, *et al.* (2001). A search for natural bioactive compounds in Bolivia through a multidisciplinary approach. Part V. Evaluation of the antimalarial activity of plants used by the Tacana Indians. Journal of Ethnopharmacology 77(1): 91-98.

Dekdouk, N., N. Malafronte, *et al.* (2015). Phenolic compounds from *Olea europaea* L. possess antioxidant activity and inhibit carbohydrate metabolizing enzymes in vitro. Evidence-Based Complementary and Alternative Medicine 2015.

Downey, M. O. and S. Rochfort (2008). Simultaneous separation by reversed-phase high-performance liquid chromatography and mass spectral identification of anthocyanins and flavonols in Shiraz grape skin. Journal of Chromatography A 1201(1): 43-47.

Faraone, I., D. Rai, *et al.* (2018). Antioxidant Activity and Phytochemical Characterization of *Senecio clivicolus* Wedd. Molecules 23(10): 2497.

Ferracane, R., G. Graziani, *et al.* (2010). Metabolic profile of the bioactive compounds of burdock (*Arctium lappa*) seeds, roots and leaves. Journal of pharmaceutical and biomedical analysis 51(2): 399-404.

Fidelis, Q. C., I. Faraone, *et al.* (2018). Chemical and Biological insights of *Ouratea hexasperma* (A. St.-Hil.) Baill.: a source of bioactive compounds with multifunctional properties. Natural product research: 1-4.

Floegel, A., D.-O. Kim, *et al.* (2011). Comparison of ABTS/DPPH assays to measure antioxidant capacity in popular antioxidant-rich US foods. Journal of food composition and analysis 24(7): 1043-1048.

Fournet, A., A. A. Barrios, *et al.* (1994). Leishmanicidal and trypanocidal activities of Bolivian medicinal plants. Journal of Ethnopharmacology 41(1-2): 19-37.

Fuentes, N. L., H. Sagua, *et al.* (2005). Experimental antihyperglycemic effect of diterpenoids of llareta *Azorella compacta* (Umbelliferae) Phil in rats. Phytotherapy Research: An International Journal Devoted to Pharmacological and Toxicological Evaluation of Natural Product Derivatives 19(8): 713-716.

Garnatje, T., J. Peñuelas, *et al.* (2017). Ethnobotany, phylogeny, and 'omics' for human health and food security. Trends in plant science 22(3): 187-191.

Gayathiri, K., M. Sangeetha, *et al.* (2016). Review: Potential pharmacological uses of natural products from Laminaceae. Int J Pharma Res Rev [Internet]: 21-34.

Geromichalos, G. D., F. N. Lamari, *et al.* (2012). Saffron as a source of novel acetylcholinesterase inhibitors: molecular docking and *in vitro* enzymatic studies. Journal of agricultural and food chemistry 60(24): 6131-6138.

Ghorai, N., S. Chakraborty, *et al.* (2012). Estimation of total terpenoids concentration in plant tissues using a monoterpene, Linalool as standard reagent. Protocol Exchange 5.

Gruz, J., O. Novák, *et al.* (2008). Rapid analysis of phenolic acids in beverages by UPLC–MS/MS. Food Chemistry 111(3): 789-794.

Gülçin, I., I. G. Sat, *et al.* (2004). Comparison of antioxidant activity of clove (*Eugenia caryophylata* Thunb) buds and lavender (*Lavandula stoechas* L.). Food Chem. 87: 393-400.

Hajdu, Z. and J. Hohmann (2012). An ethnopharmacological survey of the traditional medicine utilized in the community of Porvenir, Bajo Paraguá Indian Reservation, Bolivia. Journal of Ethnopharmacology 139(3): 838-857.

Halliwell, B. (2007). Biochemistry of oxidative stress, Portland Press Limited.

Han, J., M. Ye, *et al.* (2008). Characterization of phenolic compounds in the Chinese herbal drug *Artemisia annua* by liquid chromatography coupled to electrospray ionization mass spectrometry. Journal of pharmaceutical and biomedical analysis 47(3): 516-525.

Hariprasath, L., J. Raman, *et al.* (2012). Gastroprotective effect of *Senecio candicans* DC on experimental ulcer models. Journal of Ethnopharmacology 140(1): 145-150.

Hassan, W., A. Gendy, *et al.* (2012). Chemical constituents and biological activities of *Senecio aegyptius* var. discoideus Boiss. Zeitschrift für Naturforschung C 67(3-4): 144-150.

Hilgert, N. I. (2001). Plants used in home medicine in the Zenta River basin, Northwest Argentina. Journal of Ethnopharmacology 76(1): 11-34.

Hossain, M. B., D. K. Rai, *et al.* (2010). Characterization of phenolic composition in Lamiaceae spices by LC-ESI-MS/MS. Journal of agricultural and food chemistry 58(19): 10576-10581.

Hung, T. M., M. Na, *et al.* (2006). Antioxidant activity of caffeoyl quinic acid derivatives from the roots of *Dipsacus asper* Wall. Journal of Ethnopharmacology 108(2): 188-192.

Ibdah, M., X.-H. Zhang, *et al.* (2003). A novel Mg^{2+}-dependent *O*-methyltransferase in the phenylpropanoid metabolism of *Mesembryanthemum crystallinum*. Journal of Biological Chemistry 278(45): 43961-43972.

Ibrahim, R. M., A. M. El-Halawany, *et al.* (2015). HPLC-DAD-MS/MS profiling of phenolics from *Securigera securidaca* flowers and its anti-hyperglycemic and anti-hyperlipidemic activities. Revista Brasileira de Farmacognosia 25(2): 134-141.

Iswaldi, I., D. Arráez-Román, *et al.* (2011). Identification of phenolic compounds in aqueous and ethanolic rooibos extracts (*Aspalathus linearis*) by HPLC-ESI-MS (TOF/IT). Analytical and bioanalytical chemistry 400(10): 3643-3654.

Jaiswal, R. and N. Kuhnert (2011). Identification and characterization of two new derivatives of chlorogenic acids in Arnica (*Arnica montana* L.) flowers by high-performance liquid chromatography/tandem mass spectrometry. Journal of agricultural and food chemistry 59(8): 4033-4039.

Jamila, N., M. Khairuddean, *et al.* (2015). Cholinesterase inhibitory triterpenoids from the bark of *Garcinia hombroniana*. Journal of enzyme inhibition and medicinal chemistry 30(1): 133-139.

Justus, C. R., N. Leffler, *et al.* (2014). *In vitro* cell migration and invasion assays. Journal of visualized experiments: JoVE(88).

Kontogianni, V. G., G. Tomic, *et al.* (2013). Phytochemical profile of *Rosmarinus officinalis* and *Salvia officinalis* extracts and correlation to their antioxidant and anti-proliferative activity. Food Chemistry 136(1): 120-129.

Krasovskaya, N., N. Kulesh, *et al.* (1989). Natural antioxidants. Furanoeremophilanes from *Cacalia roots*. Chemistry of Natural Compounds 25(5): 545.

Krzyzanowska-Kowalczyk, J., Ł. Pecio, *et al.* (2018). Novel Phenolic Constituents of *Pulmonaria officinalis* L. LC-MS/MS Comparison of Spring and Autumn Metabolite Profiles. Molecules 23(9): 2277.

Lahlou, M. (2013). The success of natural products in drug discovery. Pharmacol Pharm 4(3A): 17-31.

Lamorte, D., I. Faraone, *et al.* (2018). Future in the Past: *Azorella glabra* Wedd. as a source of new natural compounds with antiproliferative and cytotoxic activity on Multiple Myeloma cells. International journal of molecular sciences 19(11): 3348.

Laurenzana, I., A. Caivano, *et al.* (2016). A Pyrazolo [3, 4-d] pyrimidine compound reduces cell viability and induces apoptosis in different hematological malignancies. Frontiers in pharmacology 7: 416.

Laurenzana, I., A. Caivano, *et al.* (2016). "A Pyrazolo [3, 4-d] pyrimidine compound inhibits Fyn phosphorylation and induces apoptosis in natural killer cell leukemia. Oncotarget 7(40): 65171.

Lawal, I., N. Uzokwe, *et al.* (2010). Ethno medicinal information on collation and identification of some medicinal plants in Research Institutes of South-west Nigeria. African Journal of Pharmacy and Pharmacology 4(1): 001-007.

Leal, A. S. M. (2012). Preparation and biological evaluation of new triterpene derivates of ursolic and oleanolic acid.
Lienou, L. L., P. B. Telefo, *et al.* (2010). Article original Pharmacology Effect of ethanolic extract of *Senecio biafrae* on puberty onset and fertility in immature female rat. Cameroon Journal of Experimental Biology 6(02): 101-109.
López-Lázaro, M. (2009). Distribution and biological activities of the flavonoid luteolin. Mini reviews in medicinal chemistry 9(1): 31-59.
Loyola, L. A., J. Bórquez, *et al.* (2004). Mulinane-type diterpenoids from *Azorella compacta* display antiplasmodial activity. Phytochemistry 65(13): 1931-1935.
Macía, M. J., E. García, *et al.* (2005). An ethnobotanical survey of medicinal plants commercialized in the markets of La Paz and El Alto, Bolivia. Journal of Ethnopharmacology 97(2): 337-350.
Mahmood, T. and P.-C. Yang (2012). Western blot: technique, theory, and trouble shooting. North American journal of medical sciences 4(9): 429.
Mariod, A. and B. Matthaeus (2008). Fatty acids, tocopherols, sterols, phenolic profiles and oxidative stability of *Cucumis melo* var. agrestis oil. Journal of food lipids 15(1): 56-67.
Markesbery, W. R. (1997). Oxidative stress hypothesis in Alzheimer's disease. Free Radical Biology and Medicine 23(1): 134-147.
Markesbery, W. R. (1999). The role of oxidative stress in Alzheimer disease. Archives of neurology 56(12): 1449-1452.
McDonald, S., P. D. Prenzler, *et al.* (2001). Phenolic content and antioxidant activity of olive extracts. Food Chemistry 73(1): 73-84.
Melo, A., L. Monteiro, *et al.* (2011). Oxidative stress in neurodegenerative diseases: mechanisms and therapeutic perspectives. Oxidative medicine and cellular longevity 2011.
Meng, X.-Y., H.-X. Zhang, *et al.* (2011). Molecular docking: a powerful approach for structure-based drug discovery. Current computer-aided drug design 7(2): 146-157.
MikaMi, I., M. YaMaguChi, *et al.* (2009). Development and validation of a microplate-based *β*-carotene bleaching assay and comparison of antioxidant activity (AOA) in several crops measured by β-carotene bleaching, DPPH and ORAC assays. Food science and technology research 15(2): 171-178.
Milella, L., A. Bader, *et al.* (2014). Antioxidant and free radical-scavenging activity of constituents from two *Scorzonera* species. Food Chemistry 160: 298-304.
Milella, L., M. Caruso, *et al.* (2011). Role of the cultivar in choosing *Clementine* fruits with a high level of health-promoting compounds. Journal of agricultural and food chemistry 59(10): 5293-5298.
Milella, L., S. Milazzo, *et al.* (2016). *a*-Glucosidase and *a*-amylase inhibitors from *Arcytophyllum thymifolium*. Journal of natural products 79(8): 2104-2112.
Mishra, B. B. and V. K. Tiwari (2011). Natural products: an evolving role in future drug discovery. European journal of medicinal chemistry 46(10): 4769-4807.
Mukherjee, P. K., V. Kumar, *et al.* (2007). Acetylcholinesterase inhibitors from plants. Phytomedicine 14(4): 289-300.
Müller, V., C. Lankes, *et al.* (2013). Centelloside accumulation in leaves of *Centella asiatica* is determined by resource partitioning between primary and secondary metabolism while influenced by supply levels of either nitrogen, phosphorus or potassium. Journal of plant physiology 170(13): 1165-1175.
Muñoz, V., M. Sauvain, *et al.* (2000). A search for natural bioactive compounds in Bolivia through a multidisciplinary approach: Part I. Evaluation of the

antimalarial activity of plants used by the Chacobo Indians. Journal of Ethnopharmacology 69(2): 127-137.
Nakamura, M., J.-H. Ra, *et al.* (2017). Impact of different partitioned solvents on chemical composition and bioavailability of *Sasa quelpaertensis* Nakai leaf extract. journal of food and drug analysis 25(2): 316-326.
Naveed, M., V. Hejazi, et al. (2018). Chlorogenic acid (CGA): A pharmacological review and call for further research. Biomedicine & Pharmacotherapy 97: 67-74.
Neuman, M. G., A. Y. Jia, *et al.* (2007). *Senecio latifolius* induces *in vitro* hepatocytotoxicity in a human cell line. Canadian journal of physiology and pharmacology 85(11): 1063-1075.
Oancea, M., S. Mazumder, *et al.* (2006). Apoptosis assays. Cardiovascular Disease, Springer: 279-290.
Odubanjo, V. O., G. Oboh, *et al.* (2018). Anticholinesterase activity and phenolic profile of two medicinal plants (*Quassia undulata* and *Senecio abyssinicus*) used in managing cognitive dysfunction in Nigeria. Journal of Food Biochemistry 42(4): e12497.
Ovesna, Z., A. Vachalkova, *et al.* (2004). Pentacyclic triterpenoic acids: new chemoprotective compounds Minireview. Neoplasma 51(5): 327-333.
Palacios, S. M., S. del Corral, *et al.* (2010). Screening for natural inhibitors of germination and seedling growth in native plants from Central Argentina. Industrial Crops and Products 32(3): 674-677.
Panda, P., P. Dash, *et al.* (2018). Chemometric profile, antioxidant and tyrosinase inhibitory activity of Camel's foot creeper leaves (*Bauhinia vahlii*). Natural product research 32(5): 596-599.
Parejo, I., E. Caprai, *et al.* (2004). Investigation of *Lepechinia graveolens* for its antioxidant activity and phenolic composition. Journal of Ethnopharmacology 94(1): 175-184.
Patel Rajesh, M. and J. Patel Natvar (2011). *In vitro* antioxidant activity of coumarin compounds by DPPH, Super oxide and nitric oxide free radical scavenging methods. Journal of Advanced Pharmacy Education & Research 1: 52-68.
Pelser, P. B., B. Nordenstam, *et al.* (2007). An ITS phylogeny of tribe *Senecioneae* (Asteraceae) and a new delimitation of *Senecio* L. Taxon 56(4): 1077-1077.
Pereira, O. R., A. M. Peres, *et al.* (2013). Simultaneous characterization and quantification of phenolic compounds in *Thymus x citriodorus* using a validated HPLC–UV and ESI–MS combined method. Food research international 54(2): 1773-1780.
Petkovskaa, A., V. Gjamovskic, et al. NPC Natural Product Communications 2017. NPC Natural Product Communications: 35.
Phillipson, J. D. (2007). Phytochemistry and pharmacognosy. Phytochemistry 68(22-24): 2960-2972.
Prabhakar, P. and M. Doble (2008). Mechanism of action of medicinal plants towards diabetes mellitus-a review. Recent progress in medicinal plants 22: 181-204.
Rahman, I. U., A. Afzal, *et al.* (2018). Historical perspectives of Ethnobotany. Clinics in Dermatology.
Rajanandh, M. and J. Kavitha (2010). Quantitative estimation of β-sitosterol, total phenolic and flavonoid compounds in the leaves of *Moringa oleifera*. International Journal of PharmTech Research 2(2): 1409-1414.
Razavi, S. M., S. Zahri, *et al.* (2009). Biological activity of quercetin-3-*O*-glucoside, a known plant flavonoid. Russian Journal of Bioorganic Chemistry 35(3): 376-378.

Ren, Y., P. J. Houghton, *et al.* (2004). Novel diterpenoid acetylcholinesterase inhibitors from *Salvia miltiorhiza*. Planta medica 70(03): 201-204.

Rico, D., A. B. M. Diana, *et al.* (2018). Characterization and *in vitro* evaluation of seaweed species as potential functional ingredients to ameliorate metabolic syndrome. Journal of Functional Foods 46: 185-194.

Riss Terry L., M. R. A., Niles Andrew L., *et al.* (2013). Cell Viability Assays. Assay Guidance Manual.

Rout, S. P., K. Choudary, *et al.* (2009). Plants in traditional medicinal system-future source of new drugs. Int J Pharm Pharm Sci 1(1): 1-23.

Ruhal, P. and D. Dhingra (2018). Ameliorative effect of Betulinic acid on ageing and Scopolamine-induced learning and memory impairment in rats. Asian Journal of Pharmacy and Pharmacology 4(6): 825-841.

Russo, D., N. Malafronte, *et al.* (2015). Antioxidant activities and quali-quantitative analysis of different *Smallanthus sonchifolius* [(Poepp. and Endl.) H. Robinson] landrace extracts. Natural product research 29(17): 1673-1677.

Russo, D., P. Valentão, *et al.* (2015). Evaluation of antioxidant, antidiabetic and anticholinesterase activities of *Smallanthus sonchifolius* landraces and correlation with their phytochemical profiles. International journal of molecular sciences 16(8): 17696-17718.

Saeed, N., M. R. Khan, *et al.* (2012). Antioxidant activity, total phenolic and total flavonoid contents of whole plant extracts *Torilis leptophylla* L. BMC complementary and alternative medicine 12(1): 221.

Salgado, F., C. Areche, *et al.* (2014). A new mulinane diterpenoid from the cushion shrub *Azorella compacta* growing in Perú. Pharmacognosy magazine 10(Suppl 3): S543.

Saltos, M. B. V., B. F. N. Puente, *et al.* (2015). Inhibitors of *a*-amylase and *a*-glucosidase from *Andromachia igniaria* Humb. & Bonpl. Phytochemistry Letters 14: 45-50.

Sánchez-Rabaneda, F., O. Jáuregui, *et al.* (2003). Liquid chromatographic/electrospray ionization tandem mass spectrometric study of the phenolic composition of cocoa (*Theobroma cacao*). Journal of mass spectrometry 38(1): 35-42.

Savelev, S. U., E. J. Okello, *et al.* (2004). Butyryl-and acetyl-cholinesterase inhibitory activities in essential oils of *Salvia* species and their constituents. Phytotherapy Research: An International Journal Devoted to Pharmacological and Toxicological Evaluation of Natural Product Derivatives 18(4): 315-324.

Schieber, A., P. Keller, *et al.* (2002). Detection of isorhamnetin glycosides in extracts of apples (*Malus domestica* cv. "*Brettacher*") by HPLC-PDA and HPLC-APCI-MS/MS. Phytochemical Analysis 13(2): 87-94.

Schmidt-Lebuhn, A. (2008). Ethnobotany, biochemistry and pharmacology of *Minthostachys* (Lamiaceae). Journal of Ethnopharmacology 118(3): 343-353.

Schofield, P., D. M. Mbugua, *et al.* (2001). Analysis of condensed tannins A review. Anim. Feed Sci. Tech. 91: 21-40.

Senatore, F. (1995). Composition of the essential oil of *Minthostachys spicata* (Benth.) Epl. Flavour and fragrance journal 10(1): 43-45.

Shaikh, S. A., T. Jain, *et al.* (2007). From drug target to leads-sketching a physicochemical pathway for lead molecule design *in silico*. Current pharmaceutical design 13(34): 3454-3470.

Shi, P., Q. He, *et al.* (2007). Characterization and identification of isomeric flavonoid *O*-diglycosides from genus *Citrus* in negative electrospray ionization by ion trap mass spectrometry and time-of-flight mass spectrometry. Analytica chimica acta 598(1): 110-118.

Singleton, V. L. and J. A. Rossi (1965). Colorimetry of total phenolics with phosphomolybdic-phosphotungstic acid reagents. American Journal of Enology and Viticulture 163(3): 144-158.

Solis-Quispe, L., C. Tomaylla-Cruz, *et al.* (2016). Chemical composition, antioxidant and antiproliferative activities of essential oil from *Schinus areira* L. and *Minthostachys spicata* (Benth.) Epl. grown in Cuzco, Peru. Journal of EssEntial oil rEsEarch 28(3): 234-240.

Song, Y., K. T. Desta, *et al.* (2016). Polyphenolic profile and antioxidant effects of various parts of *Artemisia annua* L. Biomedical Chromatography 30(4): 588-595.

Sukohar, A. and M. Muhartono (2015). Comparative effects of chlorogenic acid and doxorubic in against expression of caspase-3 in cell lines HepG2. Journal of Chemical and Pharmaceutical Research 7(1): 187-192.

Sultana, N. (2011). Clinically useful anticancer, antitumor, and antiwrinkle agent, ursolic acid and related derivatives as medicinally important natural product. Journal of enzyme inhibition and medicinal chemistry 26(5): 616-642.

Sung, M. H., O.-K. Kwon, *et al.* (2015). *Azorella compacta* methanolic extract induces apoptosis via activation of mitogen-activated protein kinase. Molecular medicine reports 12(5): 6821-6828.

Tchivounda, H. P., B. Koudogbo, *et al.* (1991). Triterpene saponins from *Cylicodiscus gabunensis*. Phytochemistry 30(8): 2711-2716.

Thomas, E., L. Semo, *et al.* (2011). Ethnomedicinal practices and medicinal plant knowledge of the Yuracarés and Trinitarios from indigenous territory and national park Isiboro-Sécure, Bolivian Amazon. Journal of Ethnopharmacology 133(1): 153-163.

Todaro, L., D. Russo, *et al.* (2017). Effects of thermo-vacuum treatment on secondary metabolite content and antioxidant activity of poplar (*Populus nigra* L.) wood extracts. Industrial Crops and Products 109: 384-390.

Trino, S., I. Iacobucci, *et al.* (2016). Targeting the p53-MDM2 interaction by the small-molecule MDM2 antagonist Nutlin-3a: a new challenged target therapy in adult Philadelphia positive acute lymphoblastic leukemia patients. Oncotarget 7(11): 12951.

Tripathi, R. K. and S. R. Ayyannan (2018). Evaluation of 2-amino-6-nitrobenzothiazole derived hydrazones as acetylcholinesterase inhibitors: *in vitro* assays, molecular docking and theoretical ADMET prediction. Medicinal Chemistry Research 27(3): 709-725.

Tůmová, L., Z. Dučaiová, *et al.* (2017). *Azorella compacta* infusion activates human immune cells and scavenges free radicals *in vitro*. Pharmacognosy magazine 13(50): 260.

Tundis, R., M. Loizzo, *et al.* (2007). *In vitro* hypoglycemic and antimicrobial activities of *Senecio leucanthemifolius* Poiret. Natural product research 21(5): 396-400.

Uma Devi, P., A. Ganasoundari, *et al.* (2000). Radiation protection by the *Ocimum* flavonoids orientin and vicenin: mechanisms of action. Radiation research 154(4): 455-460.

Vaquero, M. R., L. T. Serravalle, *et al.* (2010). Antioxidant capacity and antibacterial activity of phenolic compounds from argentinean herbs infusions. Food Control 21(5): 779-785.

Wang, H., M. G. Nair, *et al.* (1999). Novel antioxidant compounds from tart cherries (*Prunus c erasus*). Journal of natural products 62(1): 86-88.

Willcox, J. K., S. L. Ash, *et al.* (2004). Antioxidants and prevention of chronic disease. Critical reviews in food science and nutrition 44(4): 275-295.

Wong, F. C., C. C. Woo, *et al.* (2013). The anti-cancer activities of *Vernonia amygdalina* extract in human breast cancer cell lines are mediated through caspase-dependent and p53-independent pathways. PLoS One 8(10): e78021.

Wu, J., K. Liu, *et al.* (2016). The anti-inflammatory activity of several flavonoids isolated from *Murraya paniculata* on murine macrophage cell line and gastric epithelial cell (GES-1). Pharmaceutical biology 54(5): 868-881.

Yang, J., J. Guo, *et al.* (2008). *In vitro* antioxidant properties of rutin. LWT-Food Science and Technology 41(6): 1060-1066.

Yépez, A. M., O. L. de Ugaz, *et al.* (1991). Quinovic acid glycosides from *Uncaria guianensis*. Phytochemistry 30(5): 1635-1637.

Zhu, M.-Z., W. Wu, *et al.* (2015). Analysis of flavonoids in lotus (*Nelumbo nucifera*) leaves and their antioxidant activity using macroporous resin chromatography coupled with LC-MS/MS and antioxidant biochemical assays. Molecules 20(6): 10553-10565.

Zoete, V., A. Grosdidier, *et al.* (2009). Docking, virtual high throughput screening and in silico fragment-based drug design. Journal of cellular and molecular medicine 13(2): 238-248.

Zorova, L. D., V. A. Popkov, *et al.* (2018). Mitochondrial membrane potential. Analytical biochemistry 552: 50-59.